Reserve of strength in prefabricated reinforced concrete slab of bridge decks and RC culverts

Author:
Moradi, Masoud

Publication Date:
2019

DOI:
https://doi.org/10.26190/unsworks/21532

Reserve of strength in prefabricated reinforced concrete slab of bridge decks and RC culverts

Masoud Moradi

Supervisor:

A/Prof Hamid Vali Pour

Co-supervisor:

Prof Stephen Foster

A thesis in fulfilment of the requirements for the degree of

Doctor of Philosophy

School of Civil and Environmental Engineering

Faculty of Engineering

June 2018

THE UNIVERSITY OF NEW SOUTH WALES
Thesis/Dissertation Sheet

Surname	:	**Moradi**
Given Name	:	**Masoud**
Abbreviation for degree as give in the University calendar	:	**PhD**
Faculty	:	**Engineering**
School	:	**School of Civil and Environmental Engineering**
Thesis Title	:	**Reserve of strength in prefabricated reinforced concrete slab of bridge decks and RC culverts**

Abstract 350 words maximum:

This study intends to develop a deconstructable steel-concrete composite deck with external restraining system to mobilise the arch action and accordingly increase the cracking load, ultimate load carrying capacity and fatigue life and durability of the bridge decks. The possibility for partial replacement of reinforcing steel bars with dispersed fibres is considered and application of bolted shear connectors for connecting the precast concrete slabs to steel beams and developing composite action in the longitudinal and arching action in the transverse direction is studied. It is shown that the bolt connectors can facilitate the dismantling, repairing and upgrading of the bridge deck in future. The structural efficiency and feasibility of this novel bridge deck subject to static and cyclic fatigue loads is investigated experimentally. Moreover, the reserve of strength provided by arch action in the deconstructable concrete decks and buried RC culverts are investigated numerically.

In the first two series of experiments, structural behaviour of the transversely restrained deck slabs subjected to static load is evaluated and in the third series of specimens, fatigue behaviour of reinforced concrete slabs (with or without fibres) subjected to high range cyclic loading is studied. In addition to proof of feasibility of proposed construction method, the experimental results indicate that, development of arching action not only increases the ultimate load capacity of deconstructable precast deck slabs but also enhances the fatigue life of specimens significantly. Furthermore, it is shown that adding certain amount of steel fibres can improve the behaviour of the deck slabs under service and ultimate loading conditions.

The numerical study of this thesis comprises of two parts. In the first part, 3D continuum based finite element models of the deconstructable deck slabs with transverse restraining systems are developed, analysed and validated against the experimental data. In the second part, 2D nonlinear continuum-based FE models of RC culverts in conjunction with surrounding soils are developed and analysed to assess the enhancing effect of arching action on the strength and fatigue life of slabs in buried RC culvert. A parametric study is also conducted using validated finite element models.

ORIGINALITY STATEMENT

‘I hereby declare that this submission is my own work and to the best of my knowledge it contains no materials previously published or written by another person, or substantial proportions of material which have been accepted for the award of any other degree or diploma at UNSW or any other educational institution, except where due acknowledgement is made in the thesis. Any contribution made to the research by others, with whom I have worked at UNSW or elsewhere, is explicitly acknowledged in the thesis. I also declare that the intellectual content of this thesis is the product of my own work, except to the extent that assistance from others in the project's design and conception or in style, presentation and linguistic expression is acknowledged.’

Signed ……………………………………

Date ………………………………………

COPYRIGHT STATEMENT

Signed ……………………………………

Date ………………………………………

AUTHENTICITY STATEMENT

'I certify that the Library deposit digital copy is a direct equivalent of the final officially approved version of my thesis. No emendation of content has occurred and if there are any minor variations in formatting, they are the result of the conversion to digital format.'

Signed ……………………………………

Date ………………………………………

INCLUSION OF PUBLICATIONS STATEMENT

UNSW is supportive of candidates publishing their research results during their candidature as detailed in the UNSW Thesis Examination Procedure.

Publications can be used in their thesis in lieu of a Chapter if:

- The student contributed greater than 50% of the content in the publication and is the "primary author", ie. the student was responsible primarily for the planning, execution and preparation of the work for publication
- The student has approval to include the publication in their thesis in lieu of a Chapter from their supervisor and Postgraduate Coordinator.
- The publication is not subject to any obligations or contractual agreements with a third party that would constrain its inclusion in the thesis

Please indicate whether this thesis contains published material or not.

☐ *This thesis contains no publications, either published or submitted for publication*

☐ *Some of the work described in this thesis has been published and it has been documented in the relevant Chapters with acknowledgement*

☒ *This thesis has publications (either published or submitted for publication) incorporated into it in lieu of a chapter and the details are presented below*

CANDIDATE'S DECLARATION

I declare that:

- I have complied with the Thesis Examination Procedure
- where I have used a publication in lieu of a Chapter, the listed publication(s) below meet(s) the requirements to be included in the thesis.

Name	**Signature**	**Date**
Masoud Moradi		

Postgraduate Coordinator's Declaration

I declare that:

- the information below is accurate
- where listed publication(s) have been used in lieu of Chapter(s), their use complies with the Thesis Examination Procedure
- the minimum requirements for the format of the thesis have been met.

PGC's Name	**PGC's Signature**	**Date**
Mitchell Harley		

For each publication incorporated into the thesis in lieu of a Chapter, provide all of the requested details and signatures required

Details of publication #1:

Full title: *Behaviour of precast concrete deck slabs with transverse confining systems*

Authors: *Masoud Moradi, Hamid Valipour, Stephen Foster*

Journal or book *name: Magazine of Concrete Research*

Volume/page numbers: *Volume 68 Issue 17, pp. 863-876*

Date accepted/ published: *September, 2016*

Status	*Published*	×	*Accepted and In press*		*In progress (submitted)*	

The Candidate's Contribution to the Work

The candidate has been the major contributor in this published paper with more than 75% contribution.The experimental work, data analysis and writing the paper have been carried out by candidate. The paper has been finalized under supervision of supervisors by candidate.

Location of the work in the thesis and/or how the work is incorporated in the thesis:

The paper is the main framework of chapter three. There is more explanation in preparation, fabrication of specimens and data analysis in this chapter in compare with the relevant paper.

Primary Supervisor's Declaration

I declare that:

- the information above is accurate
- this has been discussed with the PGC and it is agreed that this publication can be included in this thesis in lieu of a Chapter
- All of the co-authors of the publication have reviewed the above information and have agreed to its veracity by signing a 'Co-Author Authorisation' form.

Supervisor's name *Hamid Valipour*	*Supervisor's signature*	*Date :*

Details of publication #2:

Full title: *Deconstructable steel–fibre reinforced concrete deck slabs with a transverse confining system*

Authors: *Masoud Moradi, Hamid Valipour, Stephen Foster, Mark Bradford*

Journal or book name: *Materials & Design Elsevier*

Volume/page numbers: *Volume 89 Pages 1007-1019*

Date accepted/ published: *5 January 2016,*

Status	*Published*	×	*Accepted and In press*		*In progress (submitted)*	

The Candidate's Contribution to the Work

The candidate has been the major contributor in this published paper with more than 75% contribution.The experimental work, data analysis and writing the paper have been carried out by candidate. The paper has been finalized under supervision of supervisors by candidate.

Location of the work in the thesis and/or how the work is incorporated in the thesis:

The paper is the main framework of chapter four. There is more explanation in preparation, fabrication of specimens and data analysis in this chapter in compare with the relevant paper.

Primary Supervisor's Declaration

I declare that:

- the information above is accurate
- this has been discussed with the PGC and it is agreed that this publication can be included in this thesis in lieu of a Chapter
- All of the co-authors of the publication have reviewed the above information and have agreed to its veracity by signing a 'Co-Author Authorisation' form.

Supervisor's name	*Supervisor's signature*	*Date:*
Hamid Valipour		

Details of publication #3:

Full title: *Fatigue behaviour of transversely restrained precast steel fibre reinforced concrete slabs in a deconstructable composite deck*

Authors: *Masoud Moradi Hamid Valipour Stephen Foster*

Journal or book name: *Construction and Building Materials Elsevier*

Volume/page numbers: *Volume 132, Pages 516-528*

Date accepted/ published: *1 February 2017,*

Status	*Published*	×	*Accepted and In press*		*In progress (submitted)*	

The Candidate's Contribution to the Work

The candidate has been the major contributor in this published paper with more than 75% contribution.The experimental work, data analysis and writing the paper have been carried out by candidate. The paper has been finalized under supervision of supervisors by candidate.

Location of the work in the thesis and/or how the work is incorporated in the thesis: The paper is the main framework of chapter five. There is more explanation in preparation, fabrication of specimens and data analysis in this chapter in compare with the relevant paper.
Primary Supervisor's Declaration I declare that: • the information above is accurate • this has been discussed with the PGC and it is agreed that this publication can be included in this thesis in lieu of a Chapter • All of the co-authors of the publication have reviewed the above information and have agreed to its veracity by signing a 'Co-Author Authorisation' form.

Supervisor's name *Hamid Valipour*	*Supervisor's signature*	*Date :*

Details of publication #4: ***Full title***: *Finite element modelling of demountable precast reinforced concrete deck slabs with external confining system* ***Authors***: *Abdolreza Ataei, Masoud Moradi, Hamid Valipour, Mark Bradford* ***Journal or book name***: *Journal of Constructional Steel Research Elsevier* ***Volume/page numbers:*** *Volume 151, Pages 204-215* ***Date accepted/ published***: *December 2018*						
Status	*Published*	×	*Accepted and In press*		*In progress (submitted)*	
The Candidate's Contribution to the Work The candidate has been the second major contributor in this published paper with major contribution. The finite element model, validation of model, data analysis and writing the paper have been carried out by candidate. The parametric study has been carried out by A. Ataei .The paper has been finalized under supervision of supervisors by candidate.						
Location of the work in the thesis and/or how the work is incorporated in the thesis: The paper is the main framework of chapter six and the materials of paper and chapter are entirely matched.						
Primary Supervisor's Declaration I declare that: • the information above is accurate						

- this has been discussed with the PGC and it is agreed that this publication can be included in this thesis in lieu of a Chapter
- All of the co-authors of the publication have reviewed the above information and have agreed to its veracity by signing a ‘Co-Author Authorisation’ form.

Supervisor’s name	*Supervisor’s signature*	*Date :*
Hamid Valipour		

Details of publication #5:

Full title: *Reserve of Strength in Inverted U-Shaped RC Culverts: Effect of Backfill on Ultimate Load Capacity and Fatigue Life*

Authors*: Masoud Moradi; Hamid Valipour; and Stephen Foster*

Journal or book name*: Journal of Bridge Engineering*

Volume/page numbers*: Vol. 21, Issue 2*

Date accepted/ published*: February 2016*

Status	*Published*	×	*Accepted and In press*		*In progress*	

The Candidate’s Contribution to the Work

The candidate has been the major contributor in this published paper with more than 75% contribution.The finite element model, validation of the model, data analysis and writing the paper have been carried out by candidate. The paper has been finalized under supervision of supervisors by candidate.

Location of the work in the thesis and/or how the work is incorporated in the thesis:

The paper is the main framework of chapter six and the materials of paper and chapter are entirely matched.

Primary Supervisor’s Declaration

I declare that:

- the information above is accurate
- this has been discussed with the PGC and it is agreed that this publication can be included in this thesis in lieu of a Chapter
- All of the co-authors of the publication have reviewed the above information and have agreed to its veracity by signing a ‘Co-Author Authorisation’ form.

Supervisor’s name	*Supervisor’s signature*	*Date :*
Hamid Valipour		

PUBLICATION DECLARATION

The list of publications based on this research including the authors, title and publication detail are presented in page iii. I hereby declare that I have been the major contributor in all of the published papers with more than 75% contribution. Table below summerises the main chapters in this thises and the correspocnding publication.

Chapter No	**Publication title**
Chapter 3	Behaviour of precast concrete deck slabs with transverse confining systems.
Chapter 4	Deconstructable steel–fibre reinforced concrete deck slabs with a transverse confining system.
Chapter 5	Fatigue behaviour of transversely restrained precast steel fibre reinforced concrete slabs in a deconstructable composite deck.
Chapter 6	Finite element model of deconstructable bridge deck concrete slabs with transvers confining systems.
Chapter 7	Reserve of strength in inverted u-shaped rc culverts: effect of backfill on ultimate load capacity and fatigue life.

Sincerely Dedicated to My

Wife

&

Parents

ACKNOWLEDGEMENTS

I would like to express my sincere gratitude and appreciation to the individuals who supported me during my PhD studies. This research work could have not been possible without their support and guidance. I am immensely grateful to my principal supervisor, A/Prof Hamid Vali Pour, who has provided me with intellectual guidance, encouragement, limitless support, and was always available to discuss this work. I greatly appreciate my co-supervisor, Prof Stephen Foster, for his mentorship and unfailing assistance and support throughout the course of this research.

The author gratefully acknowledges the financial and technical support provided by the University of New South Wales (UNSW), the University of Technology Sydney (UTS) and BOSFA for providing 5D steel fibers.

I am appreciative to all my friends and colleagues, particularly Dr Mohammadreza Hassani, Dr Reza Ataei and Mr Peter Brown for their invaluable friendships and emotional and technical support.

I wish to take this opportunity to express my heartfelt gratitude to my family for their priceless support and confidence in me without which I would never have achieved this moment. At the end I would like to express appreciation to my beloved wife, Dr Shamila Salek, for her support, encouragement and patience.

LIST OF PUBLICATIONS BASED ON THIS RESEARCH

- Moradi, M., Valipour H., & Foster, S. 2016, 'Behaviour of precast concrete deck slabs with transverse confining systems', *Magazine of concrete research,* vol. 68, no. 17, pp. 863-876.
- Moradi, M., Valipour H., & Foster, S. 2016, 'Reserve of Strength in Inverted U-Shaped RC Culverts: Effect of Backfill on Ultimate Load Capacity and Fatigue Life', *Journal of Bridge Engineering*, vol. 21, no. 2.
- Moradi, M., Valipour H., Foster, S. & Bradford, M.A. 2016, 'Deconstructable steel–fibre reinforced concrete deck slabs with a transverse confining system', *Materials & Design*, vol. 89, pp. 1007-1019.
- Moradi, M., Valipour H. & Foster, S. 2017, 'Fatigue behaviour of transversely restrained precast steel fibre reinforced concrete slabs in a deconstructable composite deck', *Construction and Building Materials*, vol 132, pp. 516-528.
- Ataei, R., Moradi, M., Valipour H. & Bradford, M. 2018, 'Finite element model of deconstructable bridge deck concrete slabs with transvers confining systems', *Construction Steel Research,*.Vol 151, pp 204-215.

TABLE OF CONTENTS

LIST OF FIGURES AND ILLUSTRATIONS

LIST OF TABLES

NOMENCLATURE

A	Cross-sectional area of a rectangular concrete section
A_b	Equivalent area of support beam
A_s	Cross-sectional area of reinforcement
A'_s	Cross-sectional area of compressive reinforcement
b	Width of a rectangular cross-section (width of slab)
B_{eff}	Effective width of the slab subjected to arching action
c	Depth of neutral axis
C	Membrane force
C_c	Compressive force carried by concrete
C_s	Compressive force carried by tensile
d	Effective depth (the distance from the extreme fibre to the centroid of the tensile steels)
D	Diameter of high strength bolt
d_b	Diameter of steel reinforcement
d_1	Half of the arching depth
d'	Distance from the extreme compressive fibre to the centroid of the compression steels
e	Distance from neutral axis
E	Modulus of elasticity of steel reinforcement
E_c	Modulus of elasticity of concrete
f_c	Compressive strength of concrete – stress in concrete
f'_c	Characteristic compressive (cylinder) strength of concrete
f_{cu}	Compressive (cube) strength of concrete
f_{cyl}	Compressive (cylinder) strength of concrete
f_{cm}	Mean compressive strength of concrete
F_t	Post tensioning force induced in high strength bolt
f_u	Specified ultimate strength of steel reinforcement
f_{uf}	Tensile strength of 8·8 bolts

f_y	Specified yield strength of steel reinforcement
h	Overall height of a rectangular cross-section
h_a	Height of the arch in three-hinged arch theory
h_1	Distance between membrane force at hogging and sagging
k	The ratio of the outward movement of the support to elastic shortening of the beam
k	Lateral stiffness in a laterally restrained RC member
K_b	Equivalent stiffness of support beam
K_d	Stiffness of diaphragm and slab
K_r	Combined stiffness of restraint
K_{tor}	Restraint stiffness from the torsional effects
l	RC member's span length
L	RC member's span length
L_e	Half of span length in elastically restrained arch
L_r	Half of span length in rigidly restrained arch
M_a	Arching moment of resistance
M_{ar}	Arching moment of resistance of rigidly of rigidly restrained slab strip
M_r	Moment ratio (non-dimensional)
n_u	Difference between compressive and tensile forces in a yielded section
P	Applied load
P_a	Predicted ultimate arching capacity
P_b	Predicted ultimate flexural capacity
P_j	Johansen's loads (i.e. flexural capacity using yield line analysis)
pL	Length of the end portions of a strip
P_m	Load due to compressive membrane action
P_p	Predicted ultimate capacity under Park's method
P_{test}	Maximum total load on the slab
P_{vf}	Flexural punching strength
P_{vs}	Shear punching strength
R	McDowell's non-dimensional parameter (elastic deformation)
R	Robustness index

t	Thickness of slab
T	Tensile force carried by tensile reinforcement
u	Arching deflection parameter
w	Load⁄(unit area carried by arching action)
w	Deflection under the point load
ψ	Curvature of section
ε_{av}	Average axial strain in a section
ε_0	Concrete compressive plastic strain
ε_u	Concrete maximum compressive strain
ξ	Axial strain
ε	Strain
ε	Sum of elastic, creep and shrinkage axial strains shortening
ε_c	Plastic strain of idealised elastic-plastic concrete
φ	Width of circular patch load
ρ	Longitudinal tension reinforcement ratio in a section (A_s/bd)
ρ^-	Negative reinforcement ratio
ρ_a	Effective arching reinforcement ratio at principal section
ρ_e	Effective reinforcement ratio at principal section
μ	Ductility index (general definition)
$\mu_\emptyset$	Ductility index in term of curvature
μ_θ	Ductility index in term of rotation
μ_Δ	Ductility index in term of deflection
μ_E	Energy ductility index
$\emptyset$	Curvature
θ	Rotation
β_1	Ratio of depth of rectangular stress block, *a*, to depth to neutral axis, *c*
δ	Deflection under the load point
Δ	Deflection at centre of structure member
Δ_e	Mid-span elastic deformation
Δ_u	Ultimate deflection
Δ_p	Mid-span plastic deformation
Δ_y	Yielding deflection

ABBREVIATIONS

1D	One Dimensional
2D	Two Dimensional
3D	Three Dimensional
AASHTO	American Association of State Highway and Transportation Officials
ACI	American Concrete Institute
AS	Australian Standard
ASTM	American Society For Testing And Materials
BFRP	Basalt Fibre Reinforced Plastic
BS	British Standard
CAA	Compressive Arching Action
CFRP	Carbon Fibre Reinforced Plastic
CIP	Cast In Place
CMA	Compressive Membrane Action
C-SG	Concrete Stain Gauge
EA	Equal Leg Angel
FE	Finite Element
FEA	Finite Element Analysis
FGBSCs	Friction Grip Bolted Shear Connectors
Fib	Federation Internationale du Beton
FIP	Federation Internationale de la Precontrainte
FRC	Fibre Reinforced Concrete
FRP	Fibre Reinforced Plastic
GFRP	Glass Fibre Reinforced Plastic
kN	Kilo Newton
LBTF	Large Building Test Facility
LVDT	Linear Variable Displacement Transducer,

MPa	Mega Pascal
NFEA	Nonlinear Finite Element Analysis
NLFEM	Nonlinear Finite Element Model
NSW	New South Wales
OHBDC	Ontario Highway Bridge Design Code
PBSCs	Post-Installed Shear Connectors
PFBSCs	Post-Installed Bolted Shear Connectors
PFGB	Post-Installed Friction Grip Bolted
PVC	Polyvinyl Chloride
QUB	Queen University Belfast
RC	Reinforced Concrete
SBETA	Stahlbeton Analyse
SFRC	Steel Fibre Reinforced Concrete
SG	Strain Gauge
S-N	Curve Plot Of Stress (S) Against The Number Of Cycles To Failure
St-SG	Steel Strain Gauge
UB	Universal Beam
UK	United Kingdom

Abstract

This study intends to develop a deconstructable steel-concrete composite deck with external restraining system to mobilise the arch action and accordingly increase the cracking load, ultimate load carrying capacity and fatigue life and durability of the bridge decks. The possibility for partial replacement of reinforcing steel bars with dispersed fibres is considered and application of bolted shear connectors for connecting the precast concrete slabs to steel beams and developing composite action in the longitudinal and arching action in the transverse direction is studied. It is shown that the bolt connectors can facilitate the dismantling, repairing and upgrading of the bridge deck in future. The structural efficiency and feasibility of this novel bridge deck subject to static and cyclic fatigue loads is investigated experimentally. Moreover, the reserve of strength provided by arch action in the deconstructable concrete decks and buried RC culverts are investigated numerically.

In the first two series of experiments, structural behaviour of the transversely restrained deck slabs subjected to static load is evaluated and in the third series of specimens, fatigue behaviour of reinforced concrete slabs (with or without fibres) subjected to high range cyclic loading is studied. In addition to proof of feasibility of proposed construction method, the experimental results indicate that, development of arching action not only increases the ultimate load capacity of deconstructable precast deck slabs but also enhances the fatigue life of specimens significantly. Furthermore, it is shown that adding certain amount of steel fibres can improve the behaviour of the deck slabs under service and ultimate loading conditions.

The numerical study of this thesis comprises of two parts. In the first part, 3D continuum based finite element models of the deconstructable deck slabs with transverse restraining systems are developed, analysed and validated against the experimental data. In the second part, 2D nonlinear continuum-based FE models of RC culverts in conjunction with surrounding soils are developed and analysed to assess the enhancing effect of arching action on the strength and fatigue life of slabs in buried RC culvert. A parametric study is also conducted using validated finite element models.

CHAPTER 1

INTRODUCTION

1. Introduction

1.1. Overview

Bridges and culverts are critical infrastructures that play a significant role in the transport network and economic development of societies. Consequently, increasing the capacity of bridges and culverts as well as extending their serviceable life without the need for costly repair will be of vital importance for protecting nation’s economy and transport as well as development of local communities.

Most of the existing bridges and culverts require ongoing maintenance and development that comprise rehabilitation of defective bridges/culverts and construction of new ones, due to the deterioration of old bridges and increase of the axle loads and traffic volume. Steel-concrete composite is one of the most common types of bridges that consist of reinforced concrete (RC) slab, steel girders, and the shear connectors (Ghani Razaqpur, Shedid & Nofal 2013). Prefabricated RC culverts can be considered as communal small bridges that have been extensively utilised in transport network. The RC deck slab of bridges and culverts are susceptible to damage and degradation due to combined effect of variable cyclic wheel loads and harsh environmental conditions. Accordingly, precise structural assessment of existing deck slabs including the exact loading capacity and remaining fatigue life of bridge decks and culverts are critical in improving the service life and economy of transport network. Also, developing novel construction methods that can facilitate rehabilitation/repair of faulty slabs and upgrading of the existing bridge decks is very important to prevent and reduce economic losses associated with traffic disruptions.

Cracking of RC members subject to vertical load is associated with a change of the neutral axis position in the section that results in horizontal elongation of the member. If this lateral extension restrained by adjacent span, edge girders and transverse diaphragm or cross-bracings, arching or compressive membrane action would occur in restrained RC deck slab (Taylor & Mullin 2006; Valipour, Farhangvesali & Foster 2013; Yu Zheng 2010; Zheng et al. 2008). The degree of arching action depends on the stiffness of lateral restraint which is not easy to characterise, though taking advantage of this effect can lead to improved serviceability, load carrying capacity and reduction of steel reinforcement in bridge decks (Mufti et al. 1993; Mufti & Newhook

1999; Taylor et al. 2007; Taylor, Rankin & Cleland 2005). Enhancement of the ultimate capacity and post-cracking stiffness of laterally restrained RC bridge decks, due to development of arching action has been fully recognised, (Brotchie & Holley 1971; Eyre 1997; Guice & Rhomberg 1988; Hayes 1968; Hon, Taplin & Al-Mahaidi 2005; Kirkpatrick, Rankin & Long 1984; Lahlouh & Waldron 1992; Ockleston 1958; Park & Gamble 1980; Rankin & Long 1997; Ruddle, Rankin & Long 2002; Taylor, Rankin & Cleland 2001) and implemented in a few design codes (BD 81/02 2002; CHBDC 2006; Department of Regional Development for Northern Ireland 1986).

Use of prefabricated RC culverts and precast concrete slabs in transport network and bridge deck construction has gained popularity over the past decades owing to advantages of prefabricated slabs compared to cast in situ slabs. Mass production of RC slabs and culverts with the possibility for close monitoring of the quality of the slabs, reusing of the formworks, enhancing of safety in work place, reduced construction time and labour cost and less disruption on traffic flow in big cities, are some of the advantages of prefabricated/precast slab decks. The precast/prefabricated slab decks can be used for repairing or strengthening of the existing bridge decks and also, they are easy to replace in the future, which is an effective strategy for reducing time of reconstruction and bridge lanes closure (Ryua et al. 2005; Shah et al. 2007; Shim et al. 2006; Shim & Chang 2003; Shim, Lee & Chang 2001). To gain benefit from enhancing effect of arching action and use of prefabricated RC slabs simultaneously, a practical and efficient construction method for steel-concrete composite bridge deck slabs, is proposed and evaluated. Furthermore, developing the arching action due to lateral stiffness of backfill in buried RC culverts is investigated numerically to demonstrate the enhancing effect of arching action on the load carrying capacity and fatigue life of the RC culverts. The main challenges for developing arching action is that the existing lateral confining systems rely on welded and/or permanently connected members to the bridge girders and the concrete deck slabs and these permanent connection can significantly hinder the future repair, rehabilitation, dismantling of the structural components and recycling and reusing of the construction materials. Furthermore, identifying the sources of lateral stiffness for mobilising arching action in reinforced concrete culverts have remained a challenge and whether the backfill soil in culverts can mobilise arching action remains unanswered. This project is an attempt to address these challenges.

1.2. Outline of the research

This thesis deals with structural behaviour, load carrying capacity and fatigue life of a novel deconstructable composite bridge deck with precast concrete slab and external transverse restraining/confining system that mobilise arching action and accordingly enhance the performance of precast deck slabs under service and ultimate loading conditions. Furthermore, the enhancing effect of arching action on structural behaviour of deck slabs in buried RC culverts is studied. This research project comprises an experimental program and a numerical study that involves developing nonlinear continuum-based finite element models for analysis of transversely restrained deconstructable deck slabs and buried RC culverts.

In the experimental program, two series of static tests and one series of fatigue experiments are conducted on thirty-four transversely restrained deconstructable precast RC and steel fibre reinforced concrete (SFRC) deck slabs attached to steel girders using post-installed friction grip bolted (PFGB) shear connectors. In the first stage of the laboratory experiments, structural performance of transversely restrained prefabricated RC slab is evaluated and in the second stage, partial replacement of conventional steel bars with disperse steel fibres in the precast slabs is investigated. In the third stage, fatigue behaviour of the transversely restrained RC and SFRC precast deck slabs is studied by performing low magnitude high cycle fatigue tests on the specimens. The confining system, reinforcing bar arrangement, the reinforcement ratio, concrete compressive strength and dosage of steel fibres are the main variables considered in the experimental program. The data acquired during the tests include the mode of failure, load-deflection response, fatigue life, strain of concrete and steel bars, strain in transverse confining systems, axial elongation and rotation of slabs at the end supports and crack width under cyclic fatigue loads.

At the final stage of this research, 2D and 3D continuum based finite element (FE) models of the deconstructable deck slabs with transverse restraining systems are developed, analysed and calibrated against experimental data. The verified 3D FE models are used to conduct a parametric study considering more factors that can influence structural performance of the transversely restrained RC deck slabs. In addition to the FE models of precast RC deck slabs, 2D nonlinear continuum-based models of RC culverts in conjunction with surrounding soils are developed and analysed to investigate the possible enhancing effect of arching action on the peak load capacity and fatigue life of top slabs in the buried RC culverts. Using developed FE models, a parametric study is carried out to quantify influence of different parameters on the peak load capacity and fatigue life (represented by magnitude and range of stress in steel bars) of the inverted U-shape RC culverts.

1.3. Research objectives

The main focus of this study is to investigate the enhancing effect of arching action in precast RC/SFRC deck slabs and buried RC culverts. The existing lateral restraints provided for bridge deck and culvert slabs are identified and characterise to obtain a more accurate estimation of loading capacity and structural behaviour of the deck and culvert slabs that develop arch action. Furthermore, the possibility of inducing arch action in the concrete slabs of a novel deconstructable steel-concrete composite deck that takes advantage of PFGB as shear connectors is explored. The main objectives of this project are as below;

- Identifying the lateral restraints that can provide arch action in the slabs of existing culverts and steel-concrete composite bridge decks. The source and effects of lateral restraints in conjunction with other parameters such as reinforcing proportion and concrete compressive strength on the arch action and structural behaviour of the culverts have been introduced and evaluated in Chapter 3 and Chapter 7, respectively.
- Characterising the arch action for accurate load capacity assessment of existing bridge deck slabs/buried RC culverts and using the strength enhancement provided by arch action for rehabilitation and strengthening of the concrete deck slabs/buried culverts. This is studied in Chapter 3, Chapter 5 and Chapter 7.
- Proposing a novel and efficient deconstructable steel-concrete composite deck slab with precast/prefabricated RC and SFRC decks and PFGB shear connectors. The proposed system facilitates future repair and replacing of the deck slabs. This objective has been addressed mainly in Chapter 3 and Chapter 4 and 5.
- Inducing the arch action and exploiting the enhancing effect of the arch action in the proposed deconstructable deck slabs. Furthermore, fatigue behaviour of

deconstructable deck slabs that develop arch action is investigated. The enhancing effects of arch action on the structural behaviour of the proposed deconstructable bridge deck slabs has been studied in Chapter 3 to Chapter 6.

– Investigate the effect of steel fibres in flexural and fatigue life of prefabricated slabs with arch action. This has been evaluated in Chapter 4 and Chapter 5.

1.4. Significance and innovation

The outcomes of this research project provide the benchmark data on structural performance of prefabricated deconstructable transversely restrained concrete deck slabs. Furthermore, the superior performance and efficiency of the proposed structural system is demonstrated through this research project. The proposed construction system can immensely facilitate deconstruction and future reuse and/or recycling of materials. Moreover, with regard to constant increase in volume and weight of heavy vehicles in the transport network and also much attention focused on assessment and load rating of the infrastructures, the results of this study can be used for structural assessment of steel concrete composite bridge deck slabs as well as buried RC culverts by taking into account the effect of arching action on loading capacity and serviceability level. In addition to environmental benefits of the deconstructable structural systems, the economic efficiency of deconstructable systems have been thoroughly investigated by Tingley and Davison (2012), and it has been demonstrated that the deconstructable systems, particularly the steel composite systems, similar to the one proposed in this study, have the potential reduce the total cost of the construction. However, the cost efficiency of the deconstructable systems is significantly influenced by the connections and construction details proposed to facilitate dismantling of the structure.

1.5. Lay out of the dissertation

This thesis consists of eight chapters. After the introduction in Chapter 1, a comprehensive literature review is presented in Chapter 2. The experimental and numerical investigations about enhancing effects of arching action on the loading capacity and fatigue life of RC slabs with respect to different contributing factors are covered in the review of literature. Furthermore, the main studies which led to implementation of arching action in bridge design codes are discussed in Chapter 2.

Chapter 3 deals with evaluation of structural performance of novel deconstructable precast concrete deck slabs with confining system. In this chapter the results of static tests on twelve one-half scaled precast RC slab will be explained and discussed. The configuration and proportion of the reinforcing steel bars and types of transverse confining system (cross-bracings or ties) are the main test variables. In addition to the load deflection response, mode of failure, rotation and elongation of precast slab at its ends (supports), strain in reinforcement, concrete and confining members (i.e. straps or cross bracings) are monitored and recorded during the experiments to investigate the efficiency of proposed bridge deck system. Chapter 4 presents the results of static tests on fourteen SFRC precast slabs to provide the benchmark data on structural behaviour of transversely restrained precast SFRC deck slabs. The dosage of steel fibres, proportion of conventional reinforcing steel bars, concrete compressive strength and the type, location and stiffness of restraining system (i.e. cross-bracings and straps) in the transverse direction are the main variables in the experimental program. Similar to chapter 4, load deflection relationship, mode of failure, rotation and elongation of precast slab at the supports and strains in different components are monitored during the tests presented in this chapter.

Fatigue behaviour of transversely restrained precast RC deck slabs with and without steel fibres (SF) in a novel deconstructable composite deck system is studied Chapter 5. Eight slabs are tested under cyclic loads with the type of lateral restraint, reinforcing configuration and steel fibre dosage (i.e. 0.25% and 0.5%) being the main variables. The mid-span deflection, failure mode, level of strains/stress range in the reinforcing bars and transverse ties/bracings and crack width and patterns are measured and reported. In Chapter 6, structural behaviour of the precast RC deck slabs with transverse confining system in a deconstructable composite deck is numerically studied using nonlinear 3D FE models. Commercial software ABAQUS is used to develop and analyse detailed FE models of the transversely restrained deck slabs. In the first step, the 3D finite element models of a one-span precast concrete deck slab with transverse ties and/or cross-bracings is developed and validated with experimental data from Chapter 3. The validated model is used to conduct a parametric study and elucidate various aspects of the structural behaviour of the precast RC deck slabs with external confining ties/straps. In the parametric study, effect of size of clearance between the PFGB shear connectors and holes, magnitude of post-tensioning force in the PFGB shear connectors, reinforcing bar yield strength, concrete compressive strength, thickness of slab/haunch, effective depth of the reinforcing bars on the structural behaviour of the precast RC slabs with external transverse ties in a deconstructable composite deck are evaluated. The load vs mid-span deflection are evaluated and the key performance attributes of the precast deck slab with transverse confining system are also assessed with respect to the results of parametric study.

In chapter 7, the effect of lateral stiffness of backfill that can potentially increase the ultimate load capacity and fatigue life of invert U-shape RC culverts due to development of arching action is studied in detail. The 2D nonlinear continuum-based finite element models of culverts in conjunction with surrounding soils are developed and verified using ATENA software. By using validated FE models, a parametric study is undertaken to quantify the influence of culvert geometry, compressive strength of concrete, reinforcing proportion and stiffness of backfill on the peak load capacity and fatigue life of the inverted U-shape RC culverts. Lastly, in Chapter 8 conclusions are drawn with respect to experimental data and finite element model predictions and some recommendations for future studies are made.

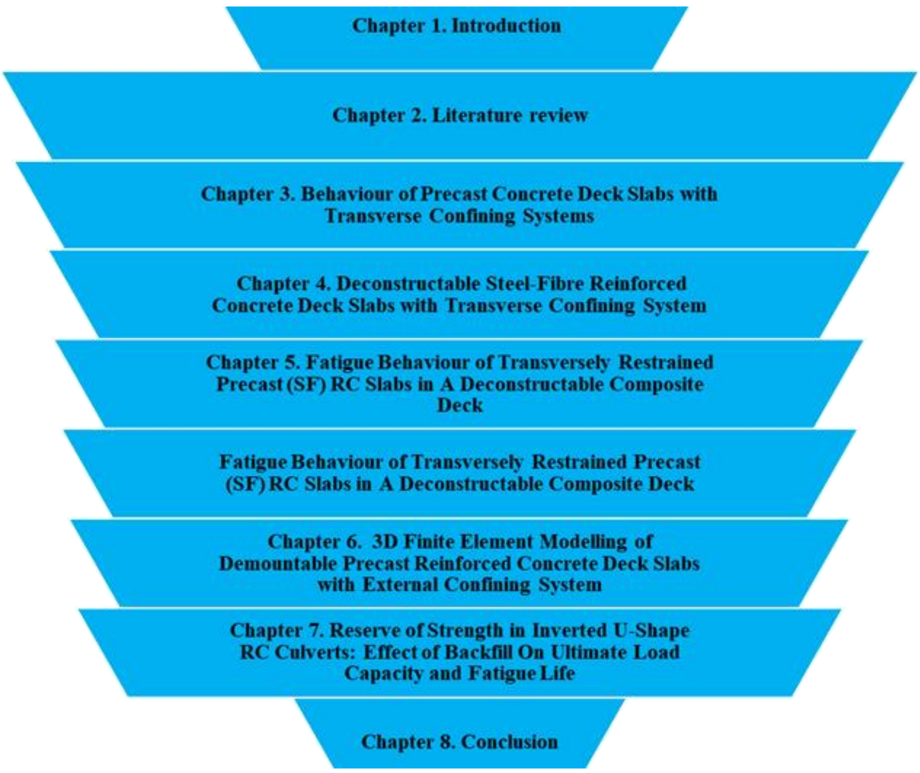

Figure 1.1 Graphical form of thesis layout.

CHAPTER 2

Literature Review

2. Literature Review

2.1. Introduction

It has been observed that the bridge deck slabs have inherent reserve of strength, in excess of flexural strength, due to development of compressive membrane action (CMA) when sufficient restraints are provided along the edges/boundaries. This phenomenon occurs due to significant difference between the tensile and compressive strength of concrete. Cracking of reinforced concrete (RC) slab subject to vertical load is associated with a change of the neutral axis position in the section that leads to elongation of the slab. If this tendency for expansion/elongation is restrained, a compressive force (arching force) is developed that leads to enhancement of strength and post-cracking stiffness of the RC members/slabs. The terms compressive arching action (CAA) and compressive membrane action (CMA) are used to describe the arching phenomenon in one-way and two-way slabs, respectively. But, these terms are used interchangeably in this dissertation.

The enhancement effects of arching/compressive membrane action on serviceability state and ultimate strength of slabs has been recognised and studied for more than five decades. Furthermore, the enhancing effect of arching action has been implemented in a few bridge design codes (ACI ITG-3-04 2004; BD 81/02 2002; CHBDC 2006; Department of Regional Development for Northern Ireland 1986).

Effect of different factors such as geometry, size of slab, type of reinforcement, reinforcement ratio and configuration, strength of concrete as well as different types of boundary conditions on the arching action have been investigated experimentally. Furthermore, different analytical methods based on simplifying assumptions such as rigid-plastic and elastic-plastic behaviour of materials have been proposed to take into account the effect of arching action on the ultimate strength of RC members. In addition to these hand calculation approaches, nonlinear finite element analysis has been used to capture the effect of CMA/CAA on the behaviour of restrained RC slabs and beams. In addition to strength enhancement under ultimate limit state conditions, the effect of CMA/CAA on serviceability of the slab, particularly on fatigue performance of bridge deck slab has been evaluated.

At the first part of this chapter, background and major researches on arching action up until the end of the twentieth century are discussed briefly. Afterwards, the significant studies that led to considering the effect of compressive membrane action on bridge design code in United Kingdom and North America are explained separately. Then after, more recent studies (after year 2000) are described and the outcomes of the research on the membrane action to date are summarised at the end of this chapter.

2.2. Background

The enhancing effect of arching action was observed for the first time during several full-scale slab panel tests, where the ultimate load of the slabs supported on all edges was much higher than ultimate strength of identical slabs without edge supports (Westergaard & Slater 1921). However, no reasonable explanation for this unexpected high ultimate strength was provided. The more thoughtful investigation on membrane action was carried out by Gvozdev that led to considering the effect of arching action in the Russian code in 1930s (Gvozdev 1939). In spite of these first steps, the enhancing effect of arching action on slab ultimate strength was not of interest to researchers until full-scale destructive load tests on Old Dental Hospital in Johannesburg carried out by Ockleston (1958). The destructive test results, showed that ultimate load capacity of lightly reinforced slabs was much higher than that calculated by conventional or plastic design theory of Johansen (Johansen 1943). Ockleston re-examined the test results to justify this discrepancy and found that strain hardening of reinforcement or concrete tensile strength cannot be the reason for this behaviour and arching action due to the development of compressive membrane stresses could be the only rational explanation for this unexpectedly higher ultimate loads in the tested slabs. However, the extension and degree of arching action effect on ultimate load needed more investigation (Ockleston 1958). Almost at the same time, Powell conducted experimental program by testing fifteen fully restrained small scale isotopically reinforced concrete slabs under uniformly distributed load (Powell 1956). It was observed that the ratio of failure load to theoretical ultimate load obtained from the yield-line method was about 1.60 to 8.25.

In addition to experimental studies, some researchers at 1960s have attempted to evaluate the effect of membrane action on behaviour of RC slabs by means of simplified numerical analysis. Two main approaches with regard to material behaviour adopted for concrete as well as analysis method have been developed, i.e. rigid-plastic models and elastic-plastic models. Different parameters that could influence behaviour of restrained slabs including support conditions, geometry of the slab and reinforcing arrangement and ratio were also considered in different studies.

A rigid-plastic material behaviour in conjunction with equilibrium equations of plate and collapse mechanism was used by Wood (1961) to analyse restrained circular RC slab (Wood 1961). The load-deflection relationship of restrained circular slab under the uniform distributed load was determined. In rigid-plastic approach, the maximum load capacity of slab occurred at zero deflection which contradicted with experimental results, since in reality, the maximum load took place at a noticeable deflection (see Figure 2.1). This behaviour was related to rigid-plastic behaviour of material adopted in plastic analysis. Wood also proposed an empirical correction factor to calculate ultimate load capacity of restrained slabs by adjusting the results of his own tests on square slab and other available experimental data.

Arching action in one-way slab was analysed and a method based on elastic-plastic approach was developed to estimate the ultimate strength of the interior RC slabs by Christiansen (1963). Christiansen separated arching effect from bending effect and considered a unit width of slab strip between support and mid-span where the plastic hinges fully developed. The available depth of section for arching action was calculated by taking into account the outward movement of the support, the elastic shortening of the slab strip due to axial forces and the elongation of the strips due to rotation of the supports.

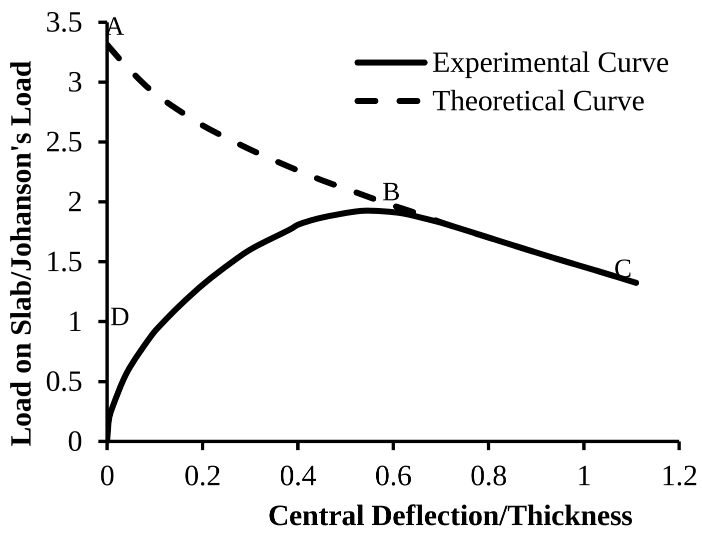

Figure 2.1 Typical theoretical and experimental load-deflection curves for a slab restrained along the edges (Wood 1961).

The arching action induced in the strip was resultant of compressive forces at the support and mid-span. To validate the method, four laterally restrained RC beams were tested subjected to concentrated load at mid span. Four simply supported identical beams were also built and tested to determine pure flexural capacity of the beams. A good agreement between experimental results and proposed numerical method was observed. However, the method was limited to one-way slab. Two decades later, Christiansen's research was further extended by conducting laboratory experiments on rectangular restrained RC slabs (Christiansen & Fredriksen 1983). The experimental program included two full scale tests on slabs of a building in Copenhagen and eleven tests on scaled slab panel in the laboratory. The effect of different variables including, reinforcing ratio, aspect ratio (i.e. length over width, l / b) of the rectangular slab as well as slenderness ratio (i.e. span length over slab thickness) on the arching action were examined. The load carrying capacity due to membrane action was again separated from the flexural strength determined based on Johansen yield line theory. From the experimental results, it was concluded that load due to membrane action, was reasonably independent of the reinforcing ratio and proportion of the length and width of the slab. However, the arching action was depended on the slab slenderness. Furthermore, by evaluating available test results, it was shown that, the proposed factor for calculation of effect of membrane action can vary between 1 and 3 depending on rigidity of the boundary conditions (edge restraints) of the slabs. One of the major researches on membrane action was carried out by Park in 1960s. Park was the first researcher who analysed compressive membrane action in restrained rectangular two-way RC slabs (Park 1964 -b). A modified yield line theory was developed to calculate ultimate load capacity of the laterally restrained rectangular concrete slabs by taking into account the effect of CMA (Park 1964 -b), and subdividing slabs into strips running along both direction (see Figure 2.2). The tensile strength of the concrete, as well as the effects of the torsional moments and the shear force was neglected along the yield lines. By assuming a rigid-plastic model for slab strips (see Figure 2.3) the compressive actions at the yield lines were calculated from the geometry and the equilibrium of rigid portions. The ultimate load for short term uniform loading condition was then obtained from the virtual work method for different boundary conditions, including four-edge restrained, one of the short edges unrestrained and one of the long edge unrestrained. The proposed formula for the ultimate load capacity depended on the slab deflection. Therefore, tests were carried out to directly obtain the deflection (Park 1964 -b). Apart from using the deflections obtained from experiments, an empirical formula was proposed for estimating the slab deflection. The developed method with empirical value of deflection also showed good accuracy to determine the ultimate short-term strength of slabs considering membrane forces in one or two directions.

In Park (1964 -b) experimental program, twelve RC slabs with different reinforcement ratio and boundary conditions as well as five unreinforced concrete slabs with different thicknesses were tested under a uniform distributed load. The cube compressive strength of concrete was 30-45 MPa. The bottom bars were continuous while, the top bars were discontinuous and were extended to the supports (with a ratio of 50% of the bottom bars). Test results showed that Johansen’s yield-line theory was a very conservative method for estimating the ultimate load carrying capacity of the restrained RC slabs because of ignoring the effect of compressive membrane action.

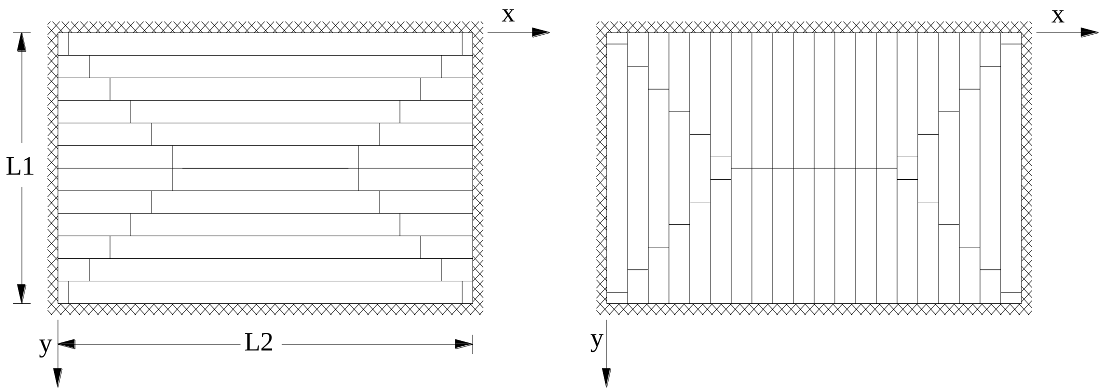

Figure 2.2 Idealised rectangular slab strips in Park model (Park 1964 -b).

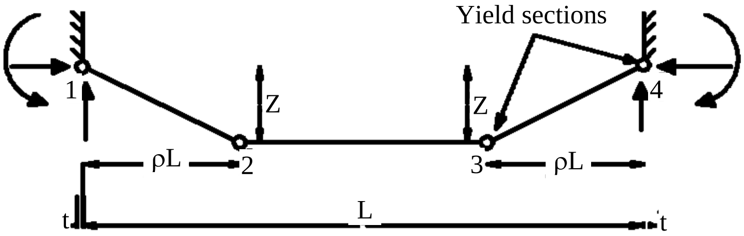

Figure 2.3 collapse mechanism of plastic rigid strip (Park 1964 -b).

Effect of shrinkage and creep on the ultimate strength of two-way RC slab with partially restrained edges was considered in a later study by Park (1964 -a). Also, Park's original analytical model was modified by considering lateral displacement of support due to partial edge restraint and incorporating the elastic, shrinkage and creep components of the axial strains into the model (see Figure 2.4). Since the predicted load was dependant on the deflection of slab, eight unreinforced concrete slabs, primarily subjected to a 42 days sustained load, reloaded and tested until the failure. The developed theory indicated a significant reduction in strength due to partial lateral restraint at the boundaries and axial strains in the plane of the slab, particularly for thin slabs. However, the ultimate load was still noticeably larger than that obtained from yield-line theory. To improve efficiency of the analytical method and reduce the demanding calculations, a reduction factor in conjunction with fully restrained boundary conditions was introduced to take account of the axial strains and lateral displacements at the partially restrained edges. A good agreement was observed between the calculated load and the test results.

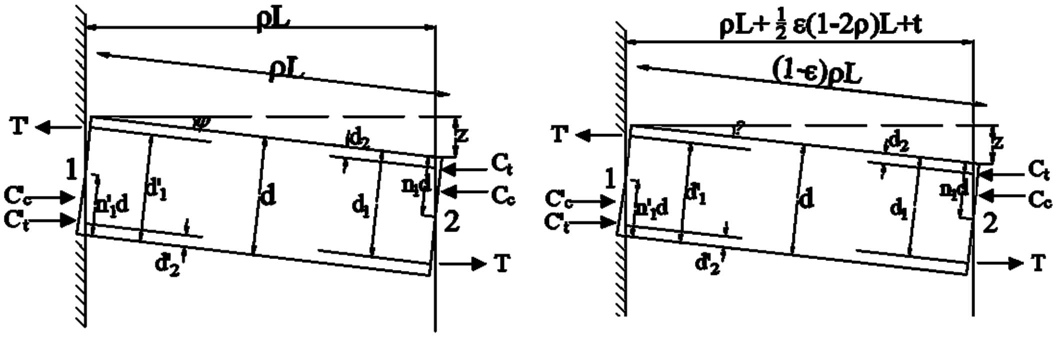

(a) Initial model **(b) Modified model**

Figure 2.4 Portion of strip between yield section with internal action (a) initial model (Park 1964 -b) and (b) Modified model (Park 1964 -a).

The experimental results revealed that elastic and shrinkage axial strains need to be considered in the calculation of ultimate load capacity, but, creep strains occurred at the mid-depth of the slabs were small. The research was extended to determine required lateral stiffness and strength to ensure development of CMA in RC slab-and-beam floor system (Park 1964 -a). For this purpose, twenty small scaled slabs with different span-to-depth ratio, exterior slabs geometry and the reinforcing arrangements at the supports were tested. The interior slab was unreinforced and the steel reinforcement placed with different configuration around the edges to simulate the ties reinforcement in the edge beams. The slabs were tested mainly to investigate the modes of failure of exterior panels and the effect of the extension of the tie reinforcement on the membrane action. The adjacent beams were modelled by roller supports along the lines of the edges of the interior panel and along the outside edges of the floors (see Figure 2.5). The experimental results revealed that the tie reinforcement had to be placed continuously around the adjacent beams to prevent failure of exterior panel and induce membrane action in the interior panel. Moreover, outward movement of the edges of the panels due to stretching of the reinforcing ties had to be considered in ultimate strength prediction.

The analytical model developed in previous study of (Park 1964 -a), that consider the axial strain in the panel and the lateral movement of the edges, can predict the ultimate load carrying capacity of the interior slabs in which the tie reinforcement are continuous.

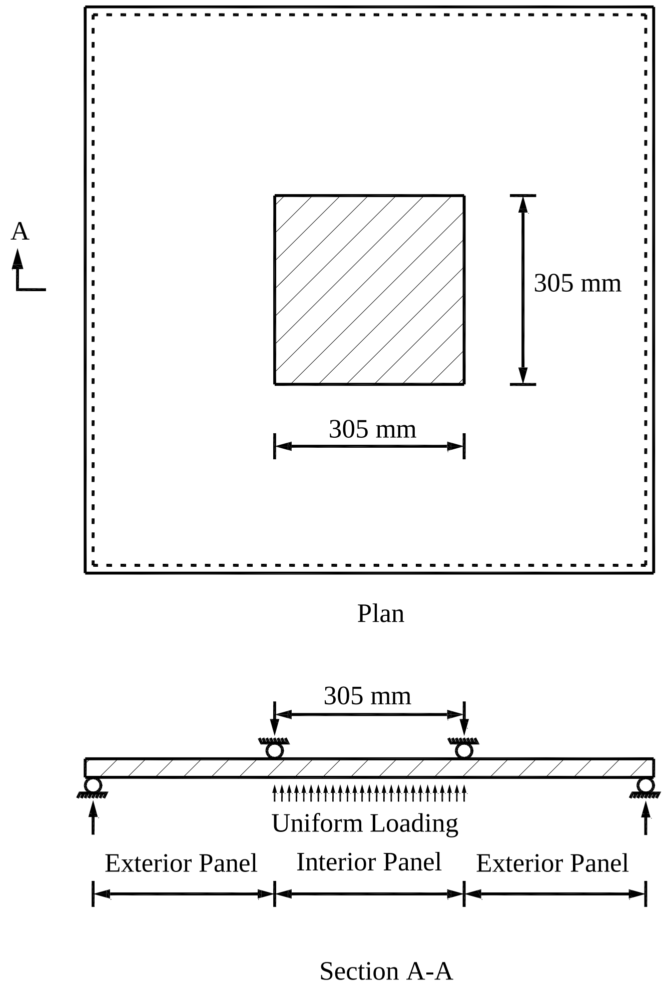

Figure 2.5 Details of loading and supports for slabs tested by Park (1965).

Two 1/4th scale RC slabs and beam floor systems were tested to evaluate the behaviour of the floor under service loading condition (Park 1971). The slabs had been designed according to yield-line theory and the beams designed by considering the collapse mechanisms that encompassed both the beams and the panels. The slabs were loaded in two phases. At the first stage, the slab was loaded to a level slightly higher than the service load and then unloaded to zero. At the second stage, the slabs were reloaded up to failure. The results proved that the behaviour of the slabs designed by the limit state procedure was acceptable in terms of serviceability limit state requirements including crack width and deflection limit. Furthermore, the ultimate load measured at the test was much higher than theoretical load due to membrane action effect and the reserve of strength was available where failure was limited to parts of the slab. The detailed procedure can be found in Chapter 12 of Park and Gamble (Park & Gamble 1980).

In addition to the restrained RC slabs, membrane action has been studied in simply supported RC slabs by Sawczuk (1965). A plastic analysis method was employed to evaluate membrane action in isotopically reinforced simply supported slabs in the way that the slab was restrained against lateral movement but the slabs were free to rotation along the edges. Nonlinear strain-displacement relation was used to determine compressive and tensile action in the slabs. It was concluded that in early stage of the loading, the compressive action governed the behaviour of the slab. However, post yield behaviour of the simply supported slabs at large deflections was influenced by the tensile membrane action (Sawczuk & Winnicki 1965). The load-deflection relationships for different yield patterns were obtained and a good agreement with experimental results was observed.

An upper bound solution including the effect of membrane action on simply support square RC slab has been proposed by Kemp (1967). The method was similar to Wood’s (1961) method by assuming rigid plastic material for the slab. The yield load of slab was calculated by taking into account the in-plane force due to development of arching action. The results revealed that enhancement of yield load become more substantial for slab with lower reinforcing ratio.

The membrane action on simply supported rectangular RC slabs has been studied also by Hayes (1968). His analysis method was similar to the Sawczuk & Winnicki (1965), but Hayes used equilibrium approach instead of energy method. The model was capable of considering the formation of in-plane plastic hinges on the long side as well as in-plane shear forces along the yield lines. The magnitudes of axial and shear force were calculated by using the in-plane equilibrium of the rigid portions between the yield line. The membrane forces were found to be independent of deflection that does not seem to be right. However, calculated load-deflection curves were in good agreement with that of previous studies (Kemp 1967; Sawczuk & Winnicki 1965) and also the experimental results. It was also observed that the strength enhancement reduces with increasing rectangularity of the slab as well as increasing the differential of reinforcing ratio in both discretions.

The conventional yield line theory was modified by Morley (1967) to consider the effect of membrane action in RC slabs (Morley 1967). The membrane forces acting on the yield lines were calculated by using the equilibrium approach and considering the displacement rates. The load-deflection relationship was then determined in accordance with principle of virtual work and assumption of rigid-plastic material for the concrete slab. To calculate the ultimate strength, an estimation of the slab deflection was required similar to Park's (1964-b) method. The results from Morley's method exhibited good agreement with the Park's (1964-b) results if value of the ultimate deflection was taken as half of the slab thickness. However, Morley's method was still limited to isotropic slabs and was not capable of considering either lateral movement of the support or the elastic shortening of the slab properly.

Since the rigid-plastic analysis methods provide an upper-bound solution (Jacobson 1967), rigorous elastic-plastic analysis based on flow rule theory was employed by Massonet (1968) to take account of the effect of membrane action in plates. Furthermore, the governing equations for large deflection considering the effect of yielding were used in Massonet's method. By assuming elastic-perfectly plastic behaviour for concrete, the partial differential equations were derived for a general condition of the yield criterion and the general boundary conditions. No specific yield pattern was assumed in deriving the governing equations, so, the analysis was a lower-bound solution of two-way RC slabs; however, no closed form analytical solution for either applied load or the axial membrane force vs. slab deflection was proposed.

In order to provide benchmark test data on the behaviour of thick plates and also propose simplified method for predicting the load carried by membrane action and the corresponding deflection, forty five small scale square RC slabs subjected to uniform load were tested by Brotchie & Holley (1971). The variables in the experimental program were span-to-depth ratio, reinforcing ratio and boundary conditions including restrained against elongation at the bottom of the slabs edges, simply supported on rollers and clamped at the edges to provide fixed conditions. A simple expression based on equilibrium equations, strain, and displacement has been developed to calculate compressive and tensile membrane actions. It was shown that the lateral restraints increase the load capacity and stiffness of the slabs and reduce the crack width in slab during the compressive membrane action phase. It was also shown that collapse load resistance of slab increased by increasing the reinforcement ratio, due to development of tensile membrane action. However, in unreinforced slabs, tensile membrane action could not develop. Moreover, it was evident that compressive membrane action was higher in thick slabs while the tensile membrane action was more significant in thin slabs. A good correlation between calculated membrane load and the experimental arching action was observed, despite discrepancy between the experimental and analytical deflections.

Since yield-line analysis is not capable of predicting the slab deflections, Moy & Mayfield (1972) proposed a method for calculating the load-deflection curve from zero load to failure (Moy & Mayfield 1972). The Massonet's formulation was extended along with the proper yield criterion to determine the membrane action effect on RC slabs. The RC slab was assumed to be an elastic-fully-plastic. This involved plastic flow without strain-hardening and allowed other regions of the slab to become plastic, instead of limiting all plastic deformation to yield lines. The finite difference technique was employed to solve equilibrium equations in conjunction with the yield criterion. The method could create a complete load-deflection curve for a RC slab. To validate the theoretical solution, twenty-two scaled slabs were tested subjected to different types of loading (i.e. central concentrated load and distributed load). The boundary conditions (i.e. simple support and fix support) and the aspect ratio of the slabs were other variables considered in the experimental program. Although, the analysis results were in close agreement with the experimental results in terms of trend and shape for load-deflection curve, there were noticeable discrepancies between the experiments and theoretical curves. This was attributed to the fact that, reduction in stiffness due to cracking of concrete and the also strain hardening of steel was not considered in the analysis.

To investigate the effect of arching action on behaviour of damaged concrete structure, a number of precast slab strips and cast-in-place slab strips with 51 mm thickness, 5486 mm length and with a central joint between two strips at 2743 mm (simulating lost support) were tested under a concentrated load at mid-span (Regan 1975). The failure mode of precast slabs was mainly associated with bottom reinforcing bars fracture, near the support, however, in some of the slabs, the failure was related to rapture of the end ties due to limited rotational capacity provided at the end supports. With regard to test results, it was concluded that both tensile strength and ductility of the reinforcing bars have significant roles in development of tensile membrane action.

In addition, a simple model was developed to capture the behaviour of slab based on equilibrium and the load extension characteristics of the member. Good correlation between theoretical and experimental load-deflection curves was observed, but the predicted ultimate load was not accurate.

Experimental tests on nineteen single-panel square slab-beam models were carried out by Datta & Ramesh (1975) to evaluate the enhancement of load capacity of slab-beam panels (Datta & Ramesh 1975). In the experimental program effect of degree of edge restraint and reinforcing ratio were considered. The edge restraint condition was depended on the size of the edge beam as well as end connection of the beams at the slab corners. Moreover, to investigate the effect of T-beam action on the enhancement of the load bearing capacity, the slab was connected to the edge beams in two different ways. Nine slabs were connected in the way that the centre of slab was at the same level of beam centre and for the rest, the top of the slabs was level with top of the beam. It was observed that, for partial restraint within a certain range of stiffness, the ultimate strength increased, while the deflection corresponding to the ultimate load increased by reducing the edge restraint. Beyond the upper limit of the edge stiffness, the slabs were completely restrained with full development of the compressive membrane action whereas, below that edge stiffness limit, the tensile membrane action dominated the slab behaviour. It was concluded that T-action increased the ultimate load capacity of slab by 20% compared to the slab-beam floors without T-action. A method was proposed for predicting the ultimate load by modifying the Park’s strip approach and considering the lateral displacement of the edge beam due to in-plane compressive force in the slab and the proposed analytical method showed good agreement with the test results.

A review of literature on the effect of membrane action on the ultimate load capacity and serviceability state of two-way slabs has been carried out by Desayi & Kulkarni (1977) and a semi-empirical analysis method for predicting load-deflection behaviour of restrained slab was proposed (Desayi & Kulkarni 1977). The main focus of this study was serviceability (deflection and maximum crack widths) of the restrained RC slab.

The rigid plastic analysis for slabs with fully fixed or simple edge supports provided reasonable description of membrane force reduction and a lower bound for peak load carrying capacity. But, the slightest flexibility of the edge supports and in-plane flexibility of slabs (which are not considered in rigid plastic analysis) can significantly affect the behaviour of slabs. To predict the load-deflection relationship more precisely, Al-Hassani (1978) considered slab strip with elastoplastic materials applying the deformation theory for the loading branch and the flow rule theory for the unloading part of the load-deflection curve (Al-Hassani 1978). The reason for this action attributed to existence of physical gap at the boundaries of slab in real structure due to shrinkage, surface irregularity etc. A similar research was carried out to take into account the influence of elastic deformation of supports and slabs and to predict the initial part of the load-deflection curve by use of flow rule theory (Braestrup & Morley 1980). Braestrup & Morley (1980) combined the support flexibility and in-plane flexibility of slab into a single spring for a partially restrained circular slab. The membrane action was assumed to induce an initial elastic deflection. The result for the initial part of the load-deflection curve showed a good agreement with the experimental results. Also a comparative study has been conducted by Braestrup (1980) to evaluate the difference between results of two plastic analysis approaches, i.e. flow rule theory and deformation theory. The main difference between the two methods is that the deformation theory uses the total strains in the materials, whereas, the flow rule theory is based on the strain increment. To evaluate the difference between two methods, the slab strip with rigid supports was subjected to a uniform load. The concrete in compression zone was assumed as a rigid perfectly plastic material while tensile strength of concrete was ignored. The load-deflection response obtained from deformation theory, displayed unrealistic behaviour, because the material was assumed to maintain its ultimate compressive stress even during softening. Although the total strain was still compressive, the total stress could be zero and this behaviour could be captured by the flow rule theory. Furthermore, from load-deflection curve, it was clear that the deterioration of the membrane force in deformation theory was very slow compared to experiments. This trend was also observed for the flow rule theory however; it was closer to experimental results in comparison to deformation theory result. This behaviour was attributed to the strain softening of concrete in the compressive zone.

Twenty-five one-way slab strips, fully restrained at the supports were tested under monotonically increasing uniform load to investigate the effect of various configuration and amount of stirrups on the behaviour of restrained slab (Woodson 1985) and the influence of main longitudinal reinforcing ratio and configuration on the ultimate capacity of the slabs (Woodson & Garner 1985). Ten slab strips with different number and configuration of stirrups and fifteen slabs with various longitudinal reinforcing configurations were built and tested with the identical geometry. The load carrying capacity of the slab was also calculated using the yield line theory and compared to the experimental results. In addition to compressive membrane action, tensile membrane force was also developed as both the top and bottom reinforcements of the slabs were in tension, when, the slab was close to failure.

Further investigation on one-way slabs with imperfect boundary conditions, i.e. partial lateral and rotation restraint has been carried out by testing sixteen RC slab strips under monotonically increasing uniform load (Guice 1986; Guice & Rhomberg 1988; Guice, Slawson & Rhomberg 1986). The variables in these experimental program included span to thickness ratio, reinforcing proportion and the partial restraint against rotation along two edge supports. The main objective of these series of tests was to investigate the influence of partial edge restraint on the strength, ductility and failure mechanism of the slabs (Guice 1986; Guice & Rhomberg 1988). It was concluded that the small rotational freedom at supports had negligible effect on compressive membrane action, but it enhanced the tensile membrane capacity as well as the incipient collapse deflection. Increasing the slab thickness, enhanced the compressive membrane action of the slab, as long as rotational freedom did not lead to loss of restraining arching forces developed. Furthermore, thin slabs carried much higher percentage of the load by tensile membrane action, regardless of the rotational freedom at edges. Also, sufficiently ductile reinforcement had to be provided in the slabs to allow for development of any tensile membrane action. The experimental program was extended to study the membrane action on flat slabs (Guice, Slawson & Rhomberg 1989). Thirty-one RC slabs with rigid supports were tested with different reinforcement ratio and configuration. A theoretical method was also proposed based on previous studies to predict the ultimate flexural capacity of the slabs. In the majority of the previous analytical methods, a suitable assumption for the deflection corresponding to the ultimate load capacity (as a portion of the depth of the specimen) was required (Datta & Ramesh 1975; Morley 1967; Park 1964 -b; Sawczuk 1965). However, in this approach by using equilibrium equations and the geometry of deformation for a rigid-plastic strip and a reasonable approximation for the support stiffness, the deflection corresponding to the peak load could be determined. This method eliminated the empirical nature of determining deflection corresponding to the peak load capacity of the slab. However, this method was limited only to ultimate strength of slabs with fixed edges.

A comprehensive study regarding the behaviour of RC slab bridge deck composites with steel girder has been conducted to evaluate the effect of membrane action on static and fatigue performance of cast in situ and precast slab under service load and over load condition (Fang 1990; I.K. Fang 1986; Tsui 1986). For this purpose, a full-scale bridge deck detailed in accordance with the Texas State Department of Highways provisions (AASHTO 1983) was constructed and tested. However, the deck slabs were designed and reinforced isotopically in accordance with existing Ontario High Bridge Design Code (OHBDC 1983) requirements that included beneficial effect of arching action. This Standard (OHBDC 1983) permitted use of less flexural steel reinforcement than required according to AASHTO (1983) specifications. Moreover, the deck slab had been divided into two parts in the way that the northern part of the deck was made of cast-in-place (CIP) concrete and the southern part was built of precast prestressed panels that integrated together by cast-in-place concrete on top of the precast panels. The slabs were sitting on three steel girders by means of shear stud connectors to provide two span bridge decks in transverse direction. The steel girders were connected to each other by X cross bracing at mid spans and the beam type diaphragms at the ends of the girders. The bridge was tested statically that reached three times higher than the existing AASHTO service live load. These loads were applied at four locations, simulating four-wheel loads in the way that the worst possible scenario in terms of total moment induced on the bridge. Afterwards, the slabs were subjected to 5,000,000 cycles load applied at each point. The range of the loading was between 25% and 125% of service live load. Finally, after the fatigue test, the bridge deck slabs were tested statically under a monotonically increasing load that reached twice the service live load (including the dynamic amplification factors). Before, during and after fatigue test, the parameters including the deflection of the slabs, crack pattern and width, strain in reinforcing bars, strain in concrete surface and strain in transverse diaphragms and cross bracings were monitored and recorded. In addition to experimental program, detailed finite element models of the slab were created and analysed using SAP IV Software. To consider in-plane restraint at the boundaries of a cracked concrete segment, the deck slab was modelled using two layers of three-dimensional finite elements. The composite action was modelled by combining thick shell elements and three-dimensional beam elements. The steel girder was modelled using a series of separate three-dimensional beam elements with the same properties as girders. To model concrete behaviour, smeared cracking model and Kupfer's biaxial failure criterion were used. A reduced shear modulus was also used parallel to the crack plane, to represent the effects of aggregate interlock and dowel action. A sequence of linear elastic analyses were used to deal with nonlinear behaviour due to crack formation (Fang 1986). The diaphragms were created by three-dimensional beam elements by considering real flexural and axial stiffness of cross bracing diaphragms. The precast prestressed panel also modelled with different moduli of elasticity, representing different stiffness between cast-in-place and precast panels. From experimental observation and numerical modelling, it was concluded that, the slab decks designed in accordance with OHBDC (1983), behaved satisfactorily under current AASHTO design load levels, in terms of deflection, local stiffness, crack widths and bending moments. Even under overloading conditions, the behaviour of slabs was nearly linear except for some minor tensile cracks in concrete. Furthermore, before formation of cracks in the slab, the compressive membrane action did not significantly influence the behaviour of slabs, however, after cracking, notable membrane forces remarkably enhanced the flexural capacity of the slabs. The results also indicated that, the fatigue loading did not notably affect the slab performance as it was observed in static tests before and after cyclic loadings. The developed analytical model showed good correlation with the experimental results. The research was extended in the following years to investigate the effect of material properties and slab geometry on the compressive membrane action in partially restrained slabs (Fang , Lee & Chen 1994). Eighteen 1000 x 2300 mm RC slabs with thicknesses of 115 mm and 75 mm, which supported edge beams with 300 x 245 mm dimension, were built and tested under incremental concentrated load up to failure. The concrete compressive strength varied from 28.8 to 49.0 MPa and reinforcement grade was between f_y= 310 MPa and 469 MPa. In addition to experimental works, analytical models for punching shear strength of partially restrained slabs was developed by Nielsen (1984) and Braestrup (1979). It was shown that the slab thickness has a significant effect on increasing load carrying capacity of the restrained slabs. In thick slabs, compressive strength of concrete had a more pronounced influence on the peak load capacity, whereas, in thin slabs, effect of flexural reinforcement on peak load capacity was more pronounced. Moreover, load capacity of partially restrained slabs was predicted reasonably by developed punching shear model, provided that the tensile strength of concrete was ignored.

The fatigue strength of RC bridge deck slab has been investigated extensively by conducting the experimental test on small scale deck slabs (Perdikaris & Beim 1986; Perdikaris & Beim 1988; Perdikaris, Beim & Bousias 1989). The experimental program included static test under concentrate load, cyclic test under pulsating fixed-point load and fatigue test under moving constant wheel load. The slab panels were reinforced isotropically and orthotropically in accordance with current OHBDC (1983) and AASHTO (1983) requirements. Some panels were also unreinforced to compare the results and develop better understanding regarding the effect of reinforcement. In addition to loading conditions (i.e. pulsating and moving load) and reinforcement ratio and arrangement, concrete strength and boundary conditions (slab continuity) were other main variables in the experimental program. After determining the ultimate load capacity of the specimens by carrying out the static tests, the new specimens were subjected to cyclic load equal to 60% of ultimate static load in both conditions, i.e. pulsating and moving loads. It was observed that the moving wheel-load caused more severe damage than the fixed pulsating load, as effect of one pass of the moving wheel-load was equivalent to about 34 and 1,800 cycles for the isotropically and orthotropically reinforced slab, respectively. The results also indicated that fatigue life of isotropically reinforced slab was much higher than the orthotropic reinforced slabs, however, the fatigue life of orthotropic reinforced concrete slab still was higher than the code requirements. It was also found that the deck continuity increased the fatigue life of slabs under the pulsating load, regardless of reinforcement pattern. However, the fatigue life of continues slab under moving loads were directly related to reinforcement pattern. In continuous slabs, the fatigue life of isotropically reinforced slab enhanced in contrast to orthotropically reinforced slab where its fatigue life reduced under the moving load. The ultimate loads obtained in static tests were much higher than the design load for the reinforced slabs. The ultimate load of unreinforced slab was also greater than design load. However, the failure mode of reinforced slab was punching shear and unreinforced slab failed in flexural mode. It was concluded that the reinforcement requirements of existing design Code, i.e. AASHTO, could be reduced significantly and the slabs were still able to meet the serviceability and strength limit state design requirements.

Most of the analytical methods were not sufficiently accurate for predicting the load-deflection of the restrained slabs with flexibility edge restraints and capturing strain softening of concrete. An analytical model was proposed by Ouyang (1987) to predict load-deflection of the edge-restrained rectangular RC slabs more accurately (Ouyang 1987). The model developed based on plastic-flow theory by considering the compatibility condition in conjunction with a yield criterion and equilibrium equations. A nonlinear differential equation developed by combining compatibility condition, the flow rule and the axial equilibrium condition to determine the membrane force in the slab. The model was obtained by assuming the interactive curves between the axial force and the bending moment and the allowance for the in-plane deformations of the slab. The tensile strength and stiffness of concrete was neglected in the calculation. Moreover, the load-deflection curve was assumed to have a linear trend up to the peak load with a deflection corresponding to the yield load of 5% of the depth of slab that seemed to be a reasonable assumption according to several test results. The results, showed a good correlation with experiments up to the peak load and beyond that the result was improved by using an approximate analysis that incorporated the effect of strain softening into the analysis.

After proposing a simplified graphical method for easy calculation of the effect of membrane action on the loading capacity of RC slabs (Eyre and Kemp 1984), Eyre extended his study to examine the use of plastic theories, i.e. deformation theory and flow rules, in collapse-load predictions of elastic-plastic slab model (Eyre 1990). The equations for both theories were derived and compared for the one-way strip spanning between fully plastic yielding hinges to show the conditions for the correct use of each method and also to define the circumstances at the point of transition from one theory to another. Since the peak load always occurred before maximum membrane force was reached, using a total strain flow rule was correct to predict the peak load, whereas, in flow rule, the predicted peak load was higher and overestimated. Therefore, it was concluded that to predict the peak load by using deformation theory, total strain flow rule, was more accurate and suitable than the differential formulation in incremental strain flow rule. Furthermore, it was shown that the transition from total strain flow rule to incremental strain flow rule should occur at the maximum membrane force as, the neutral axis was at its closest location to mid depth of the section and both flow rules were permissible. The theoretical prediction of the peak load capacity of laterally restrained RC slab were not completely successful due to sensitivity of the load capacity of such slabs with respect to in-plane stiffness of slab and surrounding areas (Eyre & Kemp 1994). An assessment of experimental work conducted by Eyre & Kemp (1994) showed that the assumption of an elastic full depth of element, which was commonly used for the slab self-stiffness in the theoretical load prediction of compressive membrane slabs, was an overestimating assumption. The experimental programme on elements under the combination of bending moment and axial force were carried out to reflect the stress state and its effect on axial stiffness. The column element was chosen to make direct measurements of shortening under various combinations of moment and axial force, in a way that the specimen was representing a one-quarter span element of a centrally loaded one-way slab with equal reinforcement. In total, fifteen specimens in four different categories of RC section, by variation in concrete strength and reinforcement ratio, were designed, built and tested under various ratios of moment to axial force. The main conclusion was that the effective shortening, i.e. combination of elastic axial shortening and elastic curvature, was considerably bigger than shortening of the member under pure axial load. Therefore, the stiffness of slab could not be calculated based on full depth of concrete section and stiffness of slab would reduce significantly depending on the ratio of yield moment to the axial force. The research has been continued to determine the strength of RC slab due to development of membrane action with proper and simple model (Eyre 1997). The RC slab with specific materials, geometric properties and certain in-plane elastic stiffness were considered. In accordance with Eyre (1990) that the maximum membrane force in a strip always lies on the strain rate rigid-plastic membrane force-deflection graph, an analytical model was developed. The model safely predicted the peak load capacity of the one-way and square isotropic slabs, however, for rectangular and orthotropic slab, further research was recommended and importance of the reliable information particularly the in-plane stiffness of supports was underlined. In the following studies, complexity regarding determination of lateral stiffness of supports that prevented use of membrane action in practical design of RC slabs was addressed (Eyre 2007). To address this problem, only the surrounding slab was considered as restrained boundaries where, a failure mechanism took place entirely within the overall slab area. This solution only required the slab properties and since it did not take into account other sources of restraint, it provided a lower bound solution to consider the membrane action enhancement. By applying this solution for idealised circular isotropic slab and considering the interaction between in-plane and rotational stiffness of the slab, the slab system was analysed where, an interior slab sector was restrained only by the surrounding area. The analytical results were much closer to real behaviour of slab in comparison with previous methods and it was recommended that the new approach could provide the benchmark for future design and study regarding the effect of various support system. In most recent study, the enhancement effect of membrane action on ultimate strength of slab on ground has been investigated by Eyre which is out of the scope of this literature (Eyre 2006).

In addition to previous analytical studies that had been carried out by Morley (1967), an experimental programme was conducted to evaluate the effect of compressive membrane action on the structural behaviour and punching shear capacity of restrained RC slab (Kuang & Morley 1992). Twelve one-fifth scale square RC slabs restrained by the edge beams on all four sides were tested under the concentrated load at mid span. Different variables including the degree of edge restraint, steel reinforcement ratio and span to slab thickness ratio were considered. It was observed that the punching shear capacity of restrained slabs were much higher than predicted strength by yield line theory and existing design codes (ACI 318 1989; BS 8110 1985) due to development of compressive membrane forces. This strength enhancement depends on the degree of edge restraint and stiffness. Moreover, an upper-bound plastic model was developed to determine the ultimate punching shear capacity of laterally confined RC slabs (Kuang & Morley 1993). A modified flexural theory of elasto-plasticity, developed previously by Braestrup & Morley (1980), was utilised to determine the compressive membrane actions. The concrete was assumed to be a rigid-plastic material and a parabolic Mohr failure criterion controlled the yielding of the section. This approach allowed for prediction of the punching shear strength enhancement as a result of compressive membrane action. The results of analytical model were compared with a wide range of experimental data from 86-specimens and showed a good correlation. In the following study by Morley, a computer program based on Galerkin method was developed to establish rapid response for load-deflection curve of axial symmetric and one-way slab strips, subjected to symmetrical loading (Morley & Olonisakin 1995). The geometry, material and non-linearity of slabs as well as several shape functions for deflection of slab were considered in Morley's computer program.

Many analytical methods have been proposed to capture load-deflection response of the restrained slabs, but only a few of these methods can predict the early stage elastic deformation of the slabs with mediocre accuracy (Braestrup & Morley 1980; Desayi & Kulkarni 1977). Furthermore, most of the analytical methods were only applicable for slabs with idealised edge restraints and simple geometries. Accordingly, nonlinear finite element analysis was employed to capture the behaviour of laterally restrained slab strip from the initial elastic stage up to collapse by accounting for the material and geometrical nonlinearities (Lahlouh & Waldron 1992). To validate the results of finite element models, three H-shaped subassemblies, consisted of a horizontal slab strip between two vertical side walls, were constructed and tested and a 3D non-linear finite element model was developed using ANSYS Software package. An eight-node solid element was used to create the model, capable of modelling material nonlinearities such as creep, shrinkage and plastic deformation. The concrete was idealised as an elasto-plastic material under uniaxial compression and its tensile behaviour was assumed to be linear up to tensile strength with the slope equal to the initial elastic modulus in compression. Longitudinal reinforcement was modelled directly by use of truss elements with elastic material and mild hardening after yield point. After validation of model with the experimental results, the parametric study was conducted to study effect of concrete compressive strength, reinforcement ratio, span to depth ratio and the degree of end restraint. It was evident from experiments and numerical results that the load-carrying capacity of axially restrained slabs increase with enhancement of lateral stiffness (provided by the sidewalls). It was also observed that the crack formation delayed and deflections reduced by increasing the boundary stiffness. Moreover, it was observed that arching action increased by enhancement of compressive strength of concrete and the arching action reduce by increasing the reinforcing ratio and span to depth ratio.

A parametric model was developed by means of finite element analysis to produce the design charts for fully restrained reinforced concrete slabs under uniformly distributed load (Famiyesin 1998). The comprehensive parametric study was conducted to consider the effect of various variables on computational process, including convergence criteria, nonlinear solution techniques, ultimate compressive strain of concrete and tension stiffening (Hossain & Famiyesin 1996b), and the effect of numerous combination of geometric and material properties on slab model was investigated (Hossain & Famiyesin 1996a). A 3D degenerated layered shell element with eight or nine nodes were used to model the slab. The reinforcement was modelled as a smeared layer of equivalent thickness with uniaxial strength and rigidity. The compressive behaviour of concrete was modelled by either a perfectly plastic or a strain hardening plasticity approach whereas, the tensile behaviour of concrete was assumed to be linear elastic until the fracture surface was reached and then, it was governed by a maximum tensile strength criterion. This process involved 864 finite element slab models that generated a database to develop the charts for prediction of the strength and displacement of fully restrained rectangular slabs. A comparative study consisted of 36 experimental slabs with similar boundary conditions showed that the charts predict the strength and displacement within a mean value of 2% and 4% difference, respectively. The charts were also capable of meeting the serviceability limit states in design approach and could be used for design engineers to estimate the global load factor in their design practice.

An extensive study was carried out to increase the knowledge about fatigue behaviour of RC bridge and propose a logical approach to evaluate the fatigue performance of existing bridge deck slabs, considering the relevant fatigue models and existing code provisions (Schlafli & Bruhwiler 1998). In total, 27 slab models were tested under cyclic load in four-point and three-point bending test set up. The slab reinforcement ratio and steel configuration as well as load range, were the main variables in their experiments. The crack pattern and width, strain in reinforcement and deflection of the slabs were monitored and recorded during the fatigue tests. The results indicated that the existing design requirements were conservative. It was also observed that fatigue failure of concrete for slender flexural element in such slabs was unexpected to occur. However, additional bending stress for reinforcement had to be considered, where the reinforcement ratio was low or large size rebar was used in thin RC slab. It was also claimed that developing a proper approach for accurate evaluation of fatigue performance of existing bridge decks is highly necessary.

2.3. Research led to implementation of CMA in British bridge design code

Four full scale tests on bridge deck slabs on North Ireland were conducted to investigate the load distribution within bridge decks with M-beams and develop simplified economic design procedure and address concerns regarding the strength of the deck slab (Kirkpatrick 1982). In addition, an experimental program and analytical study were conducted by Kirkpatrick, Rankin & Long (1984). Due to possibility of damage to bridge deck slab because of high level of loading, one-third-scale model of the prototype bridge deck slab was built and tested. In addition to experimental work, an analytical model was proposed to develop a rational method for calculation of ultimate load capacity of slabs spanning between the M-beams and developing membrane action. In the experimental phase, twenty scaled panels representative of a prototype real bridge deck slab were tested under the concentrated load, simulating the wheel load of the UK abnormal vehicle. The main variables in the experimental program were reinforcing ratio and spacing of the M-beams. The results showed that all panels failed in punching shear despite being designed with respect to flexural design requirements. The test results were compared to the punching shear capacity that obtained from the existing bridge Codes (BS 5400 1978; Highway bridge design code 1979; Transportation Officials 1977) and it was concluded that these standards did not correctly predict the punching shear capacity of the bridge deck slabs and hence a suitable method, capable of considering the in-plane action, was required for calculating the punching shear capacity of the bridge deck slabs. Accordingly, the method based on the two-phase approach for predicting punching shear capacity of the slabs was developed (Long 1975). The key concept of the two-phase approach was related to two main modes of failure on slabs, i.e. yielding of steel reinforcement before concrete crushing that led to flexural failure and concrete failure prior to yielding the reinforcement that causes the shear failure. The bridge slabs were also assumed to be fully restrained by presence of the M-beam and diaphragm. Therefore, the maximum arching moment in a rigidly restrained concrete slab, developed in member section, could be calculated by **Equation 2.1** (see Figure 2.6).

$$M_{ar} = \kappa f_c' h^2$$
$$\text{where, } \kappa = \frac{0.21 M_r}{4}$$
Equation 2.1

Since concrete does not follow the assumption of rigid plastic behaviour, the bending moment resistance corresponding to maximum arching action could not be obtained from **Equation 2.1**. This effect has been considered and the arching moment as a function of the stress-strain relationship for laterally restrained concrete slab had been derived by idealising elastic plastic material for concrete (Rankin 1982). The approach was based on McDowell, McKee and Sevin's method, developed for considering the effect of arching action on restrained masonry walls (McDowell, Mckee & Sevin 1956). Modified design chart was proposed by Kirkpatrick for any combination of span to depth ratio (L/h) and compressive strength of concrete (f_c) assuming rigid-plastic material behaviour, i.e. plastic strain= 0. Accordingly, punching shear capacity of the restrained slab was determined at critical section at $d/2$ distance from the perimeter of the loaded area by means of the graphs shown in Figure 2.7 and **Equation 2.2** and Equation **2.3** including arch action. The effect of arching action was incorporated into calculation of punching shear capacity by an effective reinforcement ratio (see **Equation 2.2**) and total punching strength was **Equation 2.3**. A good correlation has been observed between the predicted load and experimental failure loads for the experimental data on bridge deck slabs. This study has been continued by investigating the effect of compressive membrane action on the serviceability of beam and slab bridge decks (Kirkpatrick, Long & Rankin 1986). It was previously concluded that the scaled slabs were not proper model for serviceability state evaluation of bridge deck slabs. Therefore, a series of full scale tests on bridge decks (Clinghan's Bridge) were conducted by applying a simulated single-wheel load on slabs, supported by beams to investigate the effect of CMA on the serviceability of the bridge decks.

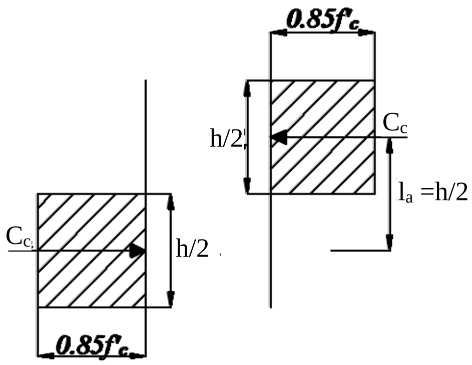

Figure 2.6 Equilibrium of forces corresponding to maximum possible arch action (Kirkpatrick , Long & Thompson 1984).

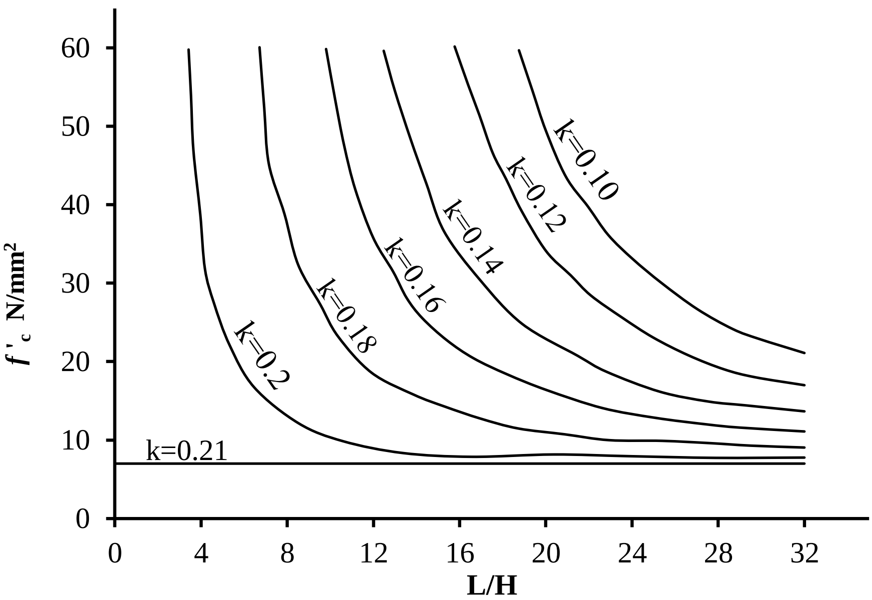

Figure 2.7 Coefficient k for arching action moment (Kirkpatrick , Long & Thompson 1984).

$$\rho_e = k\left[\frac{f_c'}{240}\right]\left[\frac{h}{d}\right]^2$$ **Equation 2.2**

$$p_{ps} = 1.52\left(\phi + d\right)d\sqrt{f_c'}\left(100\rho_e\right)^2$$ **Equation 2.3**

Deflection profiles, initial cracking loads and crack width were accurately recorded during the test (Kirkpatrick, Long & Rankin 1986). It was observed that even at relatively low levels of load, compressive membrane force had significant influence on cracking of the slabs and crack width calculation for restrained bridge deck slabs. Accordingly, new provisions for economic design of M-beam and slab bridge decks in Northern Ireland by taking into account the effect of membrane action was developed (Department of Regional Development for Northern Ireland 1986). The concept and method were later incorporated, by the United Kingdom Highways Agency, into the UK design manual for roads and bridges (BD 81/02 2002). The Kirkpatrick approach slightly overestimated the capacity of slab, where a flexural failure took place, for instance, lightly reinforced slab with moderate degree of lateral restraint. Accordingly, Rankin & Long (1997) used deformation theory to modify Kirkpatrick's approach for slabs with less rigid in-plane restraints (Rankin & Long 1997). The assumptions made by Ranking and Long are; the maximum arching moment occurred after yielding the reinforcement and the required bending deformation for yielding reinforcement was neglected. By this idealisation, the total capacity of section was obtained by summing up the bending and arching loads. The deformed geometry of the slab was obtained from analytical method proposed by McDowell, Mckee & Sevin (1956) for laterally restrained masonry walls. Two main geometrical parameters were utilised to describe the deformations, i.e. R which was a measure of the elastic deformation and u which was non-dimensional measure of the deflection,

$$R = \frac{\varepsilon_c L_r^{\ 2}}{4d_1^{\ 2}}$$ **Equation 2.4a**

and

$$u = \frac{w}{2d_1}$$ **Equation 2.4b**

and to derive the arch moment ratio M_r as

(i) $R > 0.26$

$$M_r = \frac{0.3615}{R}$$ **Equation 2.5**

(ii) $0 < R < 0.26$

$$M_r = 4.3 - 16.1\sqrt{\left(3.3\times10^{-4} + 0.1243R\right)}$$ **Equation 2.6**

Then, the maximum arching moment resistance in slab section is obtained from,

$$M_a = \frac{M_r\, 0.85 f_c' d_1^{\,2}}{4}$$ **Equation 2.7**

To calculate *R*, the plastic strain of the concrete ε_c and the depth of the arching section $2d_1$ are required. By converting the parabolic stress–strain curve for concrete to an equivalent trapezoidal (elastic-plastic) stress–strain relationship as shown in Figure 2.8, the magnitude of plastic strain can be obtained from **Equation 2.8** and **Equation 2.9**,

$$\varepsilon_c = 2\varepsilon_u\left(1-\beta_1\right)$$ **Equation 2.8**

$$\varepsilon_c = \left(-400 + 60f' - 0.33f_c^{\,2}\right)\times10^{-6}$$ **Equation 2.9**

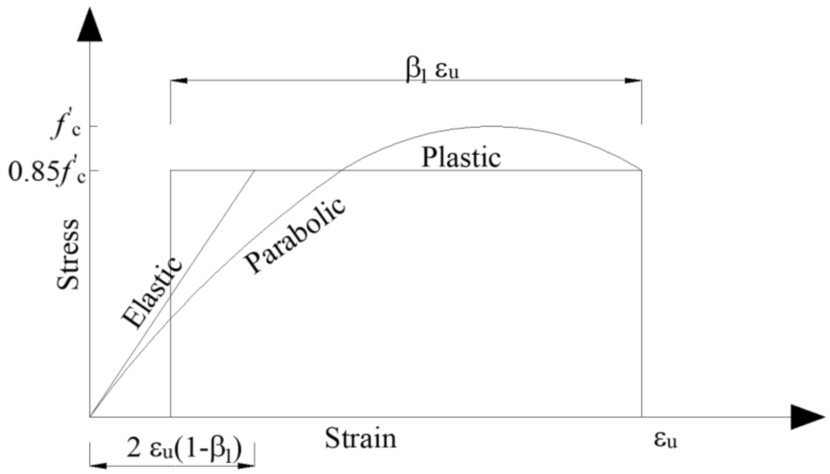

Figure 2.8 Idealised stress-strain relationship for concrete in compression (Rankin & Long 1997).

The depth of section available for arching was set equal to depth of section after subtraction of the compression zone depth required for yielding of reinforcement, (similar to the Christiansen's approach) as follows

$$2d_1 = h - (\rho + \rho')\frac{f_y d}{0.85 f_c'}$$ **Equation 2.10**

A simple analogy based on three-hinged arch with linear elastic spring with finite restraint stiffness was used (see Figure 2.9) to determine the degree of lateral restraint. By solving the equilibrium equation for this arch, an analytical solution for the model with infinite restraint stiffness could be derived (see Figure 2.9b). The equivalent length of the rigid model (arch) was obtained from

$$L_r = L_e\left[\frac{E_c A}{K L_e} + 1\right]^{\frac{1}{3}}$$ **Equation 2.11**

After knowing the required parameters, arching moment ratio could be determined that leads to calculation of resistant arching moment and ultimate loading capacity of the restrained slab. This lower bound approach was validated for a wide range of available experimental data and the accuracy of the method to determine the stiffness of the lateral restrained slab was also demonstrated.

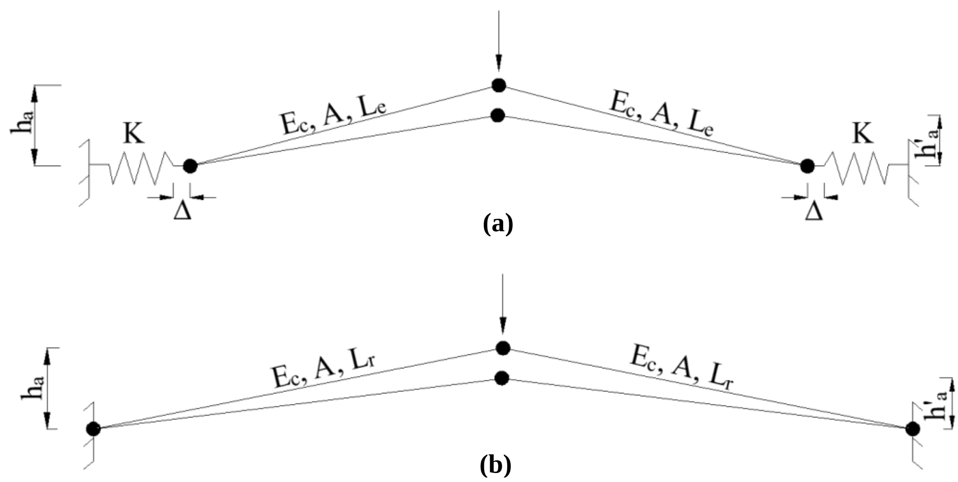

Figure 2.9 Equivalent three-hinged arches (a) elastically restrained arch (b) rigidly-restrained arch (Rankin & Long 1997).

Most of the studies on arching behaviour of RC beams and slabs were limited to concrete with compressive strength below 70 MPa that could not cover the strain-stress relationship for high strength concrete with failure and mechanical properties different from the normal strength concrete (Karr, Hanson & Capell 1987). Concrete Society (1999) published a report to amend the standard and incorporate the characteristic of high strength concrete into the standard. Accordingly, development of arching action in high-strength concrete slabs of bridge deck was examined and a new formulation was proposed to refine the material behaviour of concrete, where, high strength concrete was used (Taylor, Rankin & Cleland 2001). Fifteen RC slab strips, representative of a typical bridge deck slab were built and tested under the knife edge line load at mid span except for one slab that was loaded at the quarter spans. The variables including boundary conditions, reinforcing type, ratio and arrangement and a wide range of concrete compressive strength (30 to 100 MPa) were considered in the experimental program. The test results indicated that enhanced strength of the laterally restrained slab due to development of arch action could increase by use of high strength concrete, however, the failure mode of high strength slabs was very brittle and associated with concrete crushing. In an analytical study, Rankin and Long's (1997) method was modified by considering the stress-strain characteristics of normal and high strength concrete. Equations were proposed for ultimate strain ε_u and stress block coefficient β as shown in Figure 2.10 and **Equation 2.12** and **Equation 2.13**,

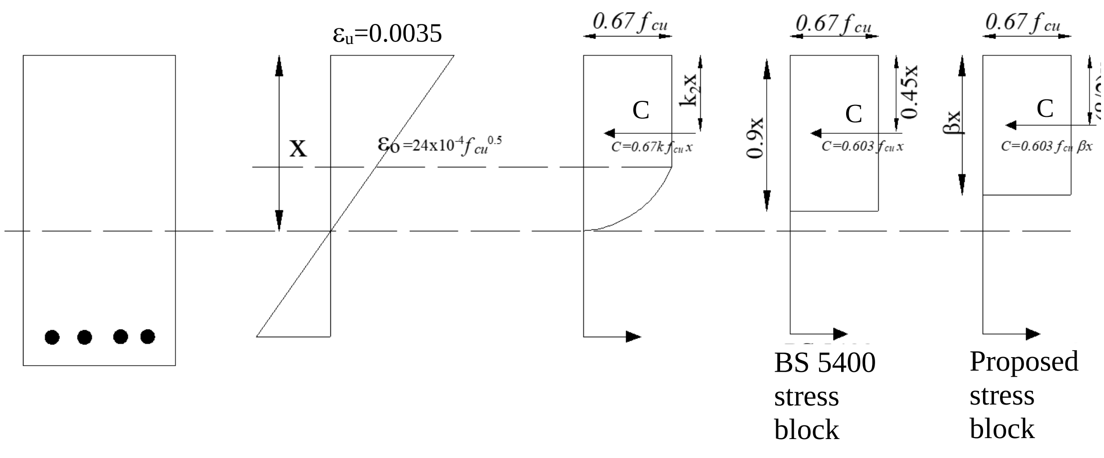

Figure 2.10 BS5400 model for normal strength concrete (f_{cu}<60 MPa) at ultimate state and proposed stress block (Taylor, Rankin & Cleland 2001).

$$\varepsilon_u = 0.0043 - \left[\left(f_{cu} - 60 \right) \times 25 \times 10^{-5} \right]$$ **Equation 2.12**

$$\beta = 1 - 0.003 f_{cu} \;\; (< 0.9)$$ **Equation 2.13**

Determination of the degree of lateral restraint in bridge deck slabs has been a challenge for accurate arching action analysis of bridge deck slabs. Furthermore, the method proposed by Rankin & Long (1997) was not directly applicable to predict punching shear strength of bridge deck slabs as it only calculated flexural capacity of the restrained slabs. Therefore, a study was carried out by testing eight one-third scaled bridge deck slabs with different range of boundary conditions (representing the real boundary conditions of bridge decks) under the knife edge load at mid span (Taylor S.E 2003). In addition to the boundary conditions, different types of reinforcement, reinforcement ratio and configuration were considered in the experimental program. Polypropylene fibre was used in two of the specimens, instead of conventional reinforcement. The fibres reduced the thermal shrinkage cracks and also fibres were found to be advantageous in slabs with high strength concrete. Furthermore, an analytical model was proposed to calculate the lateral stiffness of restrained slab more accurately. The stiffness used in the analytical model was related to the stiffness of the edge beams, diaphragm and surrounding area of the loaded slab. The equivalent stiffness of edge beam was obtained from the following equations,

$$K_b = EA_b / L_e$$ **Equation 2.14**

$$A_b = 985 \frac{L_e L_{yb}}{L^3} \quad \text{for fixed end condition}$$ **Equation 2.15**

$$A_b = 114.6 \frac{L_e L_{yb}}{L^3} \quad \text{for simply supported condition}$$ **Equation 2.16**

The contribution of unloaded slab outside the effective width and end diaphragms in the equivalent edge stiffness was cumulative and obtained from,

A_d = area of diaphragms + area of slab outside effective width

$$\Rightarrow K_d = \sum \frac{A_d E}{L_e}$$ **Equation 2.17**

and the total equivalent stiffness of the system could be determined by

$$\frac{1}{K_r} = \frac{1}{K_b} + \frac{1}{K_d}$$

Equation 2.18

or $$K_r = \frac{1}{(1/K_b) + (1/K_d)}$$

A more rigorous approach for calculation of the lateral stiffness of restrained slab considering the ductility of the slab have been conducted by Taylor (2000). In the proposed method, the punching strength was interpolated, using the moment factors obtained from finite-element analysis and yield line analysis under the fully elastic and the plastic modes of failure, respectively. However, the model was not easy to use in practice. Accordingly, after estimation of the total stiffness, a simplified model, based on two phase approach (Long 1975) for punching strength calculation was proposed. The enhanced punching shear strength p_{pv} was determined in terms of equivalent reinforcement ratio ρ_e and considering the effect of bending and arching action, similar to the Kirkpatrick's (1984) method

$$\rho_e = (\rho_a + \rho)\left(\frac{f_y}{320}\right) = \left(\frac{M_a + M_b}{M_b}\right)\left(\frac{f_y}{320}\right)\rho$$ **Equation 2.19**

$$p_{pv} = \frac{0.43}{r_f}\sqrt{f_{cu}} \times (\text{critical perimeter}) \times d\ (100\rho_e)^{0.25}$$ **Equation 2.20**

In the two-phase approach, ultimate strength is estimated based on the lesser of the flexural punching or shear punching strength of the slab obtained from **Equation 2.21**;

If $p_{pf} < p_{pv} \Rightarrow p_p = p_{pf}$

If $p_{pf} > p_{pv} \Rightarrow p_p = p_{pv}$

Equation 2.21

A comparative study showed that Taylor's method gives a better prediction of the punching capacity of the restrained slab compared to the British Standard and Kirkpatrick, Rankin & Long (1984) approach. The research was extended further to investigate the serviceability behaviour of bridge deck slabs by taking into account the effect of arching action (Taylor et al. 2007). Full-scale tests were carried out on Corick Bridge in North Ireland, which was representative of a typical modern short span bridge deck system in the UK, Europe and Asia. The bridge deck was divided to twelve panels with different properties including reinforcing ratio, configuration and type and various concrete compressive strength. The slab panels were subjected to concentrated load at the mid span. Amount of the applied load was at least three times of the maximum service wheel load according to British Standards (BS 8110 1985; Standard 1978). One of the main criteria for the test program was to evaluate the effect of the reinforcement type and position on serviceability behaviour of the bridge deck slab. Therefore, four panels were reinforced with 0.6% reinforcement in the top and bottom layer configuration as per the Code. The rest were reinforced with one layer at mid-depth with 0.5% and 0.25% reinforcement. Polypropylene fibres were added in four panels with 0.5% and 0.25% dosage to reduce thermal shrinkage cracks. The deflections along the centre line of panels and crack width on the edge panels were measured to compare with the current Code requirements. The results indicated that under the service load the deflections of panels were independent of the amount of tensile reinforcement and all panels were uncracked. Panels with one-layer of reinforcement showed much higher ultimate strength than strength predicted by design codes and behaved similar to the specimens with two layers of reinforcement up to a load twice as high that of the standard wheel load. The results were promising in terms of saving cost and increasing the overall durability of the bridge deck slabs by providing more concrete covers for one-layer reinforcement slab. Moreover, it was observed that the crack width, predicted by Standards, were more conservative for the specimens reinforced centrally in comparison to the panels with double-layer reinforcement. Lastly, it was shown that by taking advantage of arching action, slabs with low reinforcement can be used in practice that led to reduction of corrosion effect and improvement in service life of the deck slabs.

The performance of steel reinforced and FRP reinforced concrete slabs with edge restraints and potential for developing arch action have been also investigated (Taylor & Mullin 2006). The possibility of replacing steel bars with FRP bars to address the durability issues associated with corrosion of steel bars have been studied by fabrication and testing of six full-scale one-way concrete slab strips, reinforced with either steel or glass fibre reinforced polymer (GFRP). Apart from type of reinforcement, concrete compressive strength and boundary conditions were also considered in Taylor and Mullin's experimental program. Ultimate load, deflection, crack propagation and reinforcement strains were recorded and compared to evaluate the performance of GFRP reinforced slab. The peak load, was also compared to ultimate load, obtained from theory developed at Queen's University of Belfast (Taylor, Rankin & Cleland 2002). It was observed that the deflection of FRP reinforced simply supported slabs was significantly higher than steel reinforced slabs owing to lower modulus of elasticity of GFRP bars compared to the steel ones. However, in laterally restrained slab, the mid span deflection of GFRP reinforced slab reduced remarkably and showed better service behaviour than steel reinforced slab with similar edge restraint condition. It was also indicated concrete compressive strength had more influence on ultimate capacity of the laterally restrained slabs than reinforcement type. Lastly, it was concluded that use of GFRP bars could be a practical option in laterally restrained concrete slabs.

The research regarding compressive action on bridge deck slab has been continued by use of nonlinear finite element (FE) analysis to capture in-plane action of the slab more accurately (Zheng et al. 2008). ABAQUS Software was used to create the 2D and 3D models with concrete damage plasticity model to take into account nonlinear behaviour of concrete properly. For concrete in compression, elasto-plastic with strain hardening relationship was considered, while, tensile behaviour of concrete was modelled by a simple linear elastic relationship with linear softening. The elastic-perfect plastic behaviour was used for reinforcing bars. The FE model of slabs were validated by previous experimental results, carried out by Taylor, Rankin & Cleland (2001). The distribution of stress in sections at mid span and supports were extracted from FE model to assess the development of arching action in the model. The nonlinear finite element model (NLFEM) were used for a wide range of analysis (Birke 1975; Lahlouh & Waldron 1992) to demonstrate the capability of NLFEM for predicting the load carrying capacity and structural behaviour of concrete slabs with in-plane restraints. It was concluded that the NLFEM can capture the effect of membrane action on structural behaviour of reinforced concrete slabs with in-plane restraints. The ultimate load obtained from NLFEM for a wide range of lateral restraint (in-plane) stiffness had excellent correlation with the experimental results. It was also observed that the nonlinear material models could capture the behaviour of reinforced concrete in laterally restrained slabs and the distribution of stress and strain through the depth of slab could be also captured with reasonable accuracy. This was not simple to achieve by other analytical methods.

In current research, the effect of arching action on composite concrete steel bridge decks, with various boundary condition by use of different size of steel girders has been investigated (Zheng et al. 2010). The QUB model (Taylor, Rankin & Cleland 2002) was also extended to predict the ultimate load capacity of such system. Six one-third scaled models, representing lower levels of external restraint in real bridge, were designed, built and tested. In addition to the steel girder size, effect of compressive strength of concrete and reinforcement ratio was also considered in the experimental program. The steel reinforcement was placed at the mid depth of section with the reinforcement ratio of 0.5% and 1%. Slabs were connected to the steel girders by means of welded shear stud on top flange of girders to achieve. The steel girders were connected by end diaphragms consisting of parallel flange channel sections. The models were loaded under knife-edge load at the mid span up to the service load and then up to the failure. From the experimental results, it was clear that development of compressive membrane action, which was directly related to lateral stiffness and concrete strength, increased the ultimate load capacity of slabs, while, the reinforcement ratio had less significant effect. In numerical part, the QUB model modified to take to account of the effect of torsional stiffness of the supporting beam. The main components of external restraint stiffness were horizontal bending stiffness of the supporting beams about the minor axis, axial stiffness of the unloaded concrete slab and torsional stiffness of the supporting edge beams. Therefore, lateral stiffness could be calculated by the following equation,

$$\frac{1}{K_r} = \frac{1}{K_b} + \frac{1}{K_d} + \frac{1}{K_{tor}} \qquad \text{or}$$

$$K_r = \frac{1}{\left(1/K_b\right) + \left(1/K_d\right) + \left(1/K_{tor}\right)}$$ **Equation 2.22**

Another refinement was related to effective width of the slab subjected to arching action, and it was formulated as presented in **Equation 2.23**,

$$b_{eff} = C_y + L\left(1 - r_{cp}\right) \times \tan\left(\phi\right);$$ **Equation 2.23**

$$\phi = 23 \times r_{cp} + 35.10$$

when r_{cp} > 0.4; take r_{cp} = 0.4

where r_{cp} is the ratio of C_x to the span of the bridge deck, C_x and C_y are the transverse and longitudinal length of the patch loads.

The refined model, with the incorporation of the torsional stiffness of steel beam, did not notably improve the estimated ultimate strength. This was justified by the fact that the restraint stiffness was more influenced by bending stiffness of the beam which was much lower than torsional stiffness. However, the proposed method still gave an accurate estimation of the ultimate capacity of a wide range of laterally restrained bridge deck slabs, whereas current design standards (AASHTO 1996; European Committee for Standardization 2004) were highly conservative in predicting the ultimate strength of such slabs.

In addition to the above-mentioned research which led to implementation of compressive membrane action on British bridge design code (BD 81/02 2002; Bridge design code Northern Ireland 1986), there were some other studies by these researchers, concerning membrane action on RC slabs that the main ones have been summarised in following.

The enhancing effect of arching action on punching shear capacity of interior slab panels, has been investigated by Rankin & Long (1987) and a simple method was developed base on two-phase approach (Rankin & Long 1987; Rankin & Long 1987). In another study, the ultimate strength and reserve of strength in uniformly loaded restrained slab was studied by conducting laboratory tests and numerical modelling (Rankin et al. 1991). The contribution of compressive membrane action on load carrying capacity of composite metal decking with concrete floor slabs, as typical floor systems in building, has been investigated by Peel–Cross et al. (2001). Full-scale in situ testing of composite floor slabs was conducted on Building Research Establishment's Large Building Test Facility (LBTF) at Cardington. The ultimate load capacity obtained from conventional yield analysis and developed method at QUB were compared with the experimental results. In addition to the enhancement effect of arching action on slabs, the influence of this phenomena on rectangular and Tee beam sections have been evaluated by Ruddle, Rankin & Long (2002) and the proposed flexural method for restrained slab strips was extended to calculate the capacity of the restrained beams with Tee sections.

2.4. Research led to implementation of CMA in Canadian bridge design code

In North America, the main pragmatic approach and research regarding compressive membrane action on bridge deck slabs were conducted by Tong (1971), Hewitt & Batchelor (1975), Batchelor & Tissington (1976) and finally Batchelor et al. (1978) in the 1970s. An extensive experimental programme including field tests and laboratory tests on bridge deck slabs led to introduction of an empirical design approach into the Highway bridge design code (1979). Thereafter, various researches were conducted to examine and refine the Bridge Design Code as well as implementing the new design concept, i.e. steel–free deck slab, in the Bridge Design Standards by taking advantage of the enhancing effect of the arching action. These studies are discussed in the following paragraphs.

The ultimate punching shear strength of isotopically reinforced two-way bridge slabs subjected to concentrated load were investigated through experimental work on two sets of bridge deck slabs, i.e. continuous three-span and single-span panel (Tong 1971). Moreover, a model based on relationship between the flexural and shear strength, was proposed to predict the ultimate strength of slabs enhanced by compressive membrane action. The model predicted the ultimate strength of the restrained slabs with acceptable accuracy. Use of low percentage of reinforcement, was also recommended for two-way bridge slabs to change the failure mode of slabs from brittle punching failure to ductile flexural failure. In a supplementary study, a rational theory was developed based on the method established by Kinnunen & Nylander (1960), to estimate the ultimate punching strength of restrained slab more effectively for certain boundary conditions (Hewitt & Batchelor 1975). To simplify the design procedure in situations where the accurate amount of in-plane restraint provided for the slab was unknown, an empirical factor was introduced to approximate the effect of restrained boundary condition for a number of confined slab systems. Later, the previous experimental results conducted on scaled bridge deck slabs were used to develop a new model for calculating the flexural and arching moment separately (Christiansen 1963), and also for calculating the shear strength of two-way slabs (Batchelor & Tissington 1976). Furthermore, the effect of different variables including boundary conditions, reinforcement ratio and concrete properties as well as dead load stresses was studied. In late 70’s, extensive experimental program on five one-eighth scaled model deck slabs composite with steel girder was performed by Batchelor et al. (1978). The slabs were reinforced orthotropically and isotropically with different reinforcing ratio and tested under the concentrated load at mid-span. The model developed with respect to Kinnunen and Nylander’s work, was used to calculate the punching shear capacity of slabs. It was observed that the restraint system due to presence of diaphragms, steel girder, shear connectors and the neighbouring slab areas induced in-plane force in the slab that led to increase of punching strength. Furthermore, it was shown that conventionally reinforced slabs had significantly higher punching shear capacity than required ones, and the reinforcement ratio could be reduced significantly from 0.5 percent to 0.2 percent for isotopically reinforced concrete slab. This reinforcement ratio was recommended as adequate reinforcement for slab deck by considering the requirements for ultimate strength, shrinkage and temperature reinforcement. Despite this large reduction in reinforcing bars, high factor of safety could be achieved. These promising tests results, led to extensive series of field tests on actual bridge structure, funded by the Ontario Ministry of Transport. Consequently, an empirical design method was implemented in the Highway bridge design code (1979) that allowed only minimum isotropic reinforcement of 0.3% in the bridge deck slabs, provided certain conditions for edge supports were met.

Although, the effect of membrane action was implemented in the Highway bridge design code (1979), the corrosion of embedded steel reinforcing bars associated with concrete degradation, still imposed very high cost of maintenance and repair of RC slab deck. In the 1990s Mufti, Bakht and Jaeger extended the research about behaviour of bridge deck slabs to investigate the feasibility of fibre-reinforced concrete slab decks that were entirely devoid of steel reinforcement. Several experimental and analytical studies carried out by Mufti, Bakht et al during 1990s and 2000s led to construction and rehabilitation of several bridge decks devoid of steel reinforcement. It was expected that significant enhancements in the durability of laterally restrained

FRC slabs could be achieved by deck slabs devoid of reinforcements. The results of research conducted by Mufti, Bakht et al during 1990s and 2000s in Canada are summarised in the following paragraphs.

Primarily, an experimental work was conducted to evaluate the practicality of using polypropylene fibre reinforced concrete with no steel reinforcement in bridge deck slab construction (Mufti, Bakht & Jaeger 1991). Two half scale models consisted of fibre reinforced slabs connected by shear connectors to steel girders and steel channel diaphragms to tie the steel girders were tested under concentrated load. One model had three intermediate diaphragms at mid span and one at each end of the quarter span while, the other model had two diaphragms, added at the supports, in addition to the intermediate diaphragms. The first specimen failed under a load around 177 kN whereas, the second one failed at about 222 kN and this load carrying capacity enhancement was attributed to presence of the diaphragm at the supports. The failure mode of slabs was similar and they failed mainly in bending. Although, there was an increase in the ultimate strength of specimens, it was realised that the transverse diaphragms were not sufficiently effective for mobilising the arching action in the slabs. In the next step, similar bridge deck slab systems were constructed and tested. In the new model, the top flanges of steel girders were interconnected by welded steel straps just under the deck to improve lateral confinement (Mufti et al. 1993). The results showed that the deck slab carried much higher load and it failed in punching shear mode. To evaluate effect of the adjacent concentrated load on the peak load capacity of the continuous FRC deck slab, slab deck specimen supported by three steel girders, connected with the transvers straps were constructed (Mufti et al. 1993). The specimen was tested under two concentrated loads which applied at the middle of each span simultaneously. A concurrent punching shear failure under the loads proved that the negative moments due to loads over the internal girder did not have influence on load capacity of the deck slab and the ultimate strength of slab under the concentrated load was not affected significantly by the concentrated loads applied on the adjacent slabs (Mufti, Bakht & Jaeger 1993). The straps and shear connectors together showed sufficient capacity to provide sufficient transverse confinement in the system. Furthermore, it was concluded that, the bottom reinforcement in the conventionally reinforced slab decks performed similar to straps in providing transverse restraint.

Finally, adding fibres adequately controlled the shrinkage cracks and cracking due to temperature in the concrete deck slab. Additionally, behaviour of the cantilever deck slabs and negative bending moments on the interior supporting girders were investigated by Mufti, Bakht & Jaeger (1993). It was shown that the hogging moments in the overhang deck slabs (due to presence of the load on slab) were transmitted to interior slab panel adjacent to the overhangs. Therefore, to resist against this hogging moment over the supports, the tensile reinforcement must be provided in the overhangs as well as interior panels in the vicinity of the overhangs. To preserve the deck slab against the corrosion of steel bars, it was recommended that the tensile reinforcement could be in the form of fibre reinforced plastic (FRP) i.e. carbon, aramid and/or glass fibre reinforced polymer.

Apart from laboratory experiments, non-linear finite element model (NLFEM) was utilised to model and predict the ultimate strength and load-deflection behaviour of the tested FRC bridge deck slabs (Wegner & Mufti 1994). The ultimate load predicted by NLFEM was in a good agreement with the experimental peak load, but considerable modification of the modelling parameters was needed to validate the NLFEM. Moreover, the numerically predicted load-deflection curves were overly stiff compared to experimental load-deflection plots.

Bakht & Agarwal (1995), conducted research by testing one third scaled two-span model of a composite skew bridge where the skew angle was 45 degrees. The aim of this study was to investigate the effect of deck skewness on load carrying capacity of restrained deck slab and also determine whether the additional reinforcement required in accordance with the Canadian Code OHBDC (1995) could be avoided (Bakht & Agarwal 1995). The girders of the specimens with skewed decks were connected by steel straps and end diaphragms and the deck slabs were reinforced with synthetic fibre. The FRC deck slab devoid of tensile reinforcement was used in this recent study, because the failure mode of such slab was extremely dependent on stiffness of lateral restraint. If there was not sufficient confinement, the slab would have failed in bending instead of punching failure. The results showed that restriction of code for skew bridge deck could be removed, if high level of lateral restraints is provided for the deck. Accordingly, an appendix was issued to OHBDC that removed the limitations on skew deck slabs, provided high level of confinement is provided for the deck slab (OHBDC

1995). The minimum amount of required reinforcement (i.e. 0.3%) was doubled for the end zones near the skew supports, where the angle of skew was greater than 20°.

Thorburn & Mufti (1995) carried out some tests on full-scale model of FRC deck slab to optimise the amount of required lateral in-plane stiffness (Thorburn & Mufti 1995). A twelve-meter-long deck slab connected to steel girders by means of shear connectors was constructed. The equally spaced straps welded to the top flange of the girders provided the in-plane stiffness, but the cross sectional area of straps (along the girder) varied in such a way that, four distinctive amounts of lateral stiffness were provided along the deck slab. All segments of the deck slabs were tested under a concentrated load to failure. The area of load path was equal to a dual tire of typical commercial vehicle. The panels along the deck slab failed in punching failure at different load levels. The results of experiments provided valuable information regarding the optimised amount of lateral restraint stiffness along the FRC deck slabs devoid of reinforcing steel bars.

To evaluate the fatigue behaviour of FRC deck slab system devoid of steel bars, in a comprehensive study, a full-scale model with the cross section shown in Figure 2.11 was constructed and tested under the moving loads (Selvadurai & Bakht 1995). The cyclic loads were applied on a number of loading pads at certain locations to simulate the rolling wheel loads. The actuators employed were able to apply loads up to 100 KN at speed of about 40 km/hr. The maximum permitted wheel load on commercial vehicles in Ontario was less than 60 KN and the heaviest wheel load of OHBDC design truck was 100 KN. The slab deck had been firstly subjected to eight million passes of loads at different levels, i.e. 53, 71, 89, and 98 KN (two million cycles at each load level). After this series of tests, the transvers stiffness of restraint slab reduced to a quarter of initial stiffness by replacing the straps with smaller strap sizes. The slabs were subjected to additional four million moving loads of 98 KN. No deterioration was observed during this stage. To examine durability of slab due to water penetration similar to Matsui (1994) research, the slab was saturated under a layer of water and experienced another four million passes of 98 KN. The FRC slab showed no noticeable damage even after this stage. Afterwards, all straps were removed and the lateral confinement only provided by the flexural rigidity of the girder flanges and axial rigidity of diaphragm. Again, the slabs tolerated four million cycles

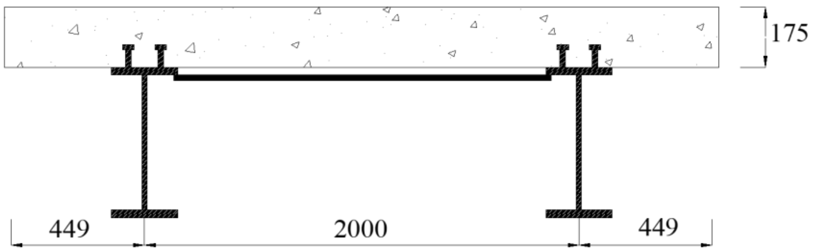

Figure 2.11 Cross section of the full scale model (Selvadurai & Bakht 1995).

of 98 KN without significant damage and finally, after this phase, the slab was subjected to gradual increasing load until failure at around 400 KN. In accordance with the existing OHBDC code requirements, the bridge component should be able to safely withstand two million cycles of a 75 KN wheel. By comparison of the results, it was clear that the FRC deck slabs were capable of bearing the several million cycles of 98 KN wheel load under different conditions and with even minimal lateral restraint. In another study, a numerical model was developed by Newhook & Mufti (1995) to predict the ultimate load capacity of FRC deck slab (Newhook & Mufti 1995). All the parameters which influence the load carrying capacity of such slabs under concentrated load were taken into account and the model was verified against the results obtained from various experiments. A series of charts which determine the ultimate load carrying capacity of FRC deck slabs under the dual-tire wheel load of commercial vehicles were provided. All the research on FRC bridge deck slabs have been summarised in Bakht & Mufti (1996).

Bakht & Mufti (1996) have emphasised that the steel free deck slabs, not only were capable of showing very high static and fatigue strength (provided that sufficient transverse confinement delivered) but also, they could display higher level of durability than conventionally reinforced concrete slabs. Moreover, where tensile reinforcement was required like cantilever overhangs of deck slab, fibre reinforced polymer (FRP) reinforcement could be used. A primary cost analysis for the deck slab of such system showed an increase of only about 8 percent (in the initial cost) compared to the conventional system, however, this system would be more economical and durable over the time. With respect to extensive research conducted on FRC deck slabs devoid of steel bars, a new section dealing with fibre reinforced concrete deck slabs was added to CHBDC (1996). This amendment, provided requirements (such as girder spacing, minimum transverse stiffness, slab depth to span ratio, strap spacing and etc) that should be satisfied for laterally restrained fibre reinforced slab bridge decks. Using new provisions of CHBDC (1996) for FRC bridge decks, five bridges with steel free deck slabs have been designed and constructed in Canada (Bakht & Mufti 1998; Bakht, Mufti & Jaeger 1998). The deck slabs contained fibres to control cracking due to shrinkage, creep and temperature variation effects. The deck slabs have been either cast in situ or precast slab panel which have been attached to the steel or precast concrete girders by flexible shear connectors. The girders have been transversely tied together by steel straps and cross frames. The details of each bridge described in Newhook, Jaeger & Mufti (1996); Newhook, John & Mufti (1996); Newhook, Mufti & Jaeger (1996) for Salmon River bridge, Mufti, Jaeger & Bakht (1997) for Chatham bridge, Tadros, Tromposch & Mufti (1998) for Crowchild Trail bridge, Mufti, Newhook & Jalali (1999) for Waterloo Creek bridge and Sargant, Mufti & Bakht (1999) for Lindquist bridge.

The research on restrained concrete bridge deck slabs was continued by developing an analytical model that could predict the behaviour of laterally restrained fibre reinforced concrete bridge deck slabs (Mufti & Newhook 1998). The proposed model for prediction of punching shear strength of FRC deck slabs (devoid of steel) could take into account the lateral stiffness of lateral restraining system in a clear and detailed manner. The main parameters in the developed model were, slab thickness, spacing and cross sectional area of straps, spacing of support girders and dimensions of loaded area beside material properties (including modulus of elasticity of the transverse straps, yield strain of the straps and compressive strength of the concrete). The model was also used to determine the punching shear capacity of conventional reinforced concrete deck slab. The analytical model predictions were compared with the experimental results and it was shown that the model can determine the ultimate strength and load-deflection of the restrained slabs with a good accuracy, even for conventionally reinforced slabs.

Since the welded straps could not be used for confinement of the slab in all the situation, the performance of two other types of transverse restraining system (i.e. cruciform straps and threaded rods) which met the CHBDC requirements, were investigated by performing laboratory tests (Bakht & Lam 2000). In accordance with

CHBDC (1996) requirements, the minimum cross section area of the straps to provide transverse confining system in steel-free deck slabs, was calculated by **Equation 2.24**:

$$A = \frac{F_s S^2 S_1}{E_t} \times 10^9 \qquad \textbf{Equation 2.24}$$

where F_S is a factor equals to 5.0 for internal panels and 6.0 for external panels, S is the spacing between the girders in m, S_1 is the spacing between the straps in m, E is the modulus of elasticity in MPa and t is the thickness of the deck slab in mm.

In the cruciform straps, steel straps are connected to the girders by crossbars welded in a cruciform pattern to the top flange of the steel girders. In this approach, the crossbars and a small portion of the transverse straps are embedded in haunches of concrete slab. However, threaded rods passed through plastic tubes embedded in the deck slab haunches and the threaded rods were anchored to the other side of the haunch by a washer and nut. Four specimens, one small-scale with three continuous spans and three full-scale single span steel free deck slab were constructed with the abovementioned restraining systems and the specimens were subjected to a pair of concentrated loads (simulating the dual tires of a typical commercial vehicle) until failure. The results indicated that ultimate load capacity of the restrained steel free deck slabs with these new methods were more than 10 times that of theoretical bending peak load and this significant difference was demonstrative of the effectiveness of the confining systems. Furthermore, it was seen that restrained deck slabs exhibit different failure modes including failure of haunches in addition to the punching shear failure of the slab. However, in all models, the failure occurred at much higher level of the load, predicted by the Ontario highway bridge design code. Finally, the cost analysis of construction, demonstrated that even the short-term cost of a steel-free deck slab could be lower than that of conventional deck slabs.

A paper summarising the design provisions of the Canadian Highway Bridge Design Code for fibre reinforced structure was published by Bakht et al. (2000). However, the provisions were limited to only certain applications of fibre reinforced concrete and it mainly included concrete beams, slabs, FRC deck slabs as well as fully, or partially prestressed concrete beams and slabs and barrier walls (Bakht et al. 2000). Additionally, Thorburn & Mufti (2001) developed a design method for externally restrained bridge deck slab with respect to the existing Canadian design concept. Moreover, the governing maximum vehicle loads in both service and ultimate loading conditions were considered to meet the code requirements. It was shown that, if the lateral restraining system meet the ultimate condition requirements, the serviceability limits of deflection and fatigue would be fulfilled automatically.

The steel free deck slab concept, as an innovative method has been used to rehabilitate several bridges and one marine structure in North America and these projects have been summarised in a report prepared by Newhook et al. (2002). Furthermore, the potential applications of this new concept in strengthening of the existing bridge decks have been discussed in Newhook et al. (2002).

Although, laboratory fatigue test on bridge deck slabs is usually carried out under the constant magnitude loads, bridge deck slabs are subjected to various numbers of wheels with different magnitudes of load. Therefore, to establish the equivalence between number of the actual wheel passes on a bridge and number of fatigue test cycles, an analytical method was developed using equivalent damage concept (Mufti et al. 2002). The method was initially developed for steel free deck slabs, but it could be used for all types of bridge deck slabs. The proposed method was also applicable to formulate specific fatigue load requirements for bridge deck slabs and the results of two sets of experiments on full scale steel free deck slab (one precast slab and one cast in situ slab) were used to verify the model. The results of tests showed that both types of steel-free deck slabs could tolerate more damage than what was expected to happen by the projected population of wheels during the bridge lifetime.

The application of stay-in-place metallic forms as a lateral confining systems, was investigated analytically (Bakht, Mufti & Tadros 2002). The metal sheet could act the same way as steel straps if the steel sheets were bonded adequately to the flanges of steel girders. It was shown that the deflection requirements governed the thickness of the steel sheet instead of the lateral confining system.

A precast steel-free deck slab acting compositely with steel girders was developed and tested by Mufti, Bakht & Newhook (2004). The experimental program also involved investigation of structural performance of slab panel at the construction stage, when it was not connected to steel girders and there was no composite action. The precast panel was restrained laterally by external transverse steel straps anchored in the edge of the concrete panels and eliminate the need for filed connection of straps to the steel girders. The panel then connected to the girders by clusters shear studs, which were installed beforehand on the top flanges of the girders, passed through the pocket on panels and grouted at the final stage of the installation. It was shown that precast deck slabs devoid of steel bars are able to withstand loads much higher than the construction load and design load in both stages of non-composite and composite action, respectively. However, it was recommended to provide a nominal crack control reinforcement for the laterally restrained precast deck slabs.

The static and fatigue behaviour of steel free deck slabs reinforced with CFRP and GFRP bars were studied by Klowak, Memon & Mufti (2006). In the Klowak's experiment, a full-scale slab was divided into three segments; in the first segment only conventional reinforcing steel bars were used, while the second and third segments were reinforced with CFRP/GFRP crack control grids, respectively and restrained laterally with steel straps. In order to have better understanding and comparison between the segments under fatigue loadings, all segments were designed nearly with equal ultimate load carrying capacity. The overall dimension of the first bridge deck specimen was 9000 mm (in length) and 3000 mm (in width) and 175 mm (in thickness) and the slab was supported by two steel girders 2000 mm far apart. The segments were first tested under the concentrated load of 25 tons for one million cycles and then the load level increased up to 60 tons in which the segments failed at different cycles. A second full-scale bridge deck slab (9000 mm long, 5000 mm wide and 200 mm thick) supported on steel girders was also tested. The girders were spaced in 2500 mm distance to provide 1250 mm cantilever slabs at each side of the main span. The interior span was reinforced with GFRP crack control grid and restrained by steel straps. The three different types of tensile reinforcements over the supports were considered in three segments to compare the performance of GFRP, CFRP and steel reinforcement under the fatigue tests. Each of the three segments was designed in the way that the nominal capacity of sections became almost equal. The interior panel was tested under a monotonically increasing concentrated load up to failure. The test results demonstrated that either the CFRP or GFRP crack control grids with external steel straps effectively prevented the propagation of cracks over the cross section depth.

Moreover, it was found that the overall area of CFRP and GFRP bars could be reduced by up to 40%. No significant damage was seen in under one million cycles of 25-ton load. The conventional steel reinforced slab, failed after 23162 cycles under 60-ton load, while the number of cycles up to failure, were 198863 cycles and 420648 cycles for CFRP and GFRP reinforced slabs at the same level of fatigue load. It was concluded the steel free deck slab reinforced with GFRP and restrained externally with the straps, had the best fatigue performance and it could be effective and economic solution for eliminating the steel corrosion problem in bridge deck slabs. The results of these studies led to some modification in CHBDC (2006).

The behaviour of non-composite precast concrete slab with external restraining/confining system has been investigated by fabricating and testing five full scale slab panels (Edalatmanesh & Newhook 2012). The slabs had identical sizes but the concrete strength and restraining systems were different. All slabs were tested under monotonically increasing concentrated load until failure. The load-deflection curve, crack width and strap strain were monitored and recorded during the tests. The results showed that by providing sufficient confinement in both in-plane directions, the precast slab failed in punching shear similar to that observed for cast-in-place composite deck slabs. Furthermore, the PUNCH Software model was used to predict the ultimate load and corresponding deflection of panels. It was observed that the model was able to predict the ultimate strength of precast panel with a good accuracy, where, two-way restraint/confinement was provided for the slab panels. Use of precast deck slabs for rapid construction and repair of the bridge decks was also recommended. Edalatmanesh & Newhook (2013) also investigated fatigue behaviour of the externally restrained non-composite steel-free deck slabs by testing ten full scale precast slabs restrained in both directions, with identical geometry in two sets of specimens. All specimens were constructed using two concrete compressive strength and tested under various load conditions, including fatigue load range and number of cycles. The range of fatigue loading was from 10% to 60% and/or 90% of the ultimate load. The crack pattern, crack width, strain in straps and deflection were measured and documented during the cyclic test to monitor the damage accumulative of specimens, under fatigue loading. Different modes of failure were observed during the test, including punching shear failure and straps failure. Moreover, three distinguished phases of damage accumulation were identified including initiation phase, stable damage accumulation phase and final rapid damage propagation phase. Accordingly, an idealised damage accumulation model was proposed. It was found that there was solid correlation between the amount of ultimate displacement of the same slab under cyclic test and under the static load test. Finally, by means of experimental results, an S-N curve was developed for precast steel-free deck slabs.

In a recent study, it was shown that the cantilever bridge deck slabs could develop internal arching action to some extent under the concentrated load (Mufti, Bakht & Jaeger 2008). Laboratory experiments were carried out to evaluate development of arching action in edge stiffened bridge deck cantilever slabs as shown in Figure 2.12 (Klowak, Mufti & Bakht 2014). The full-scale bridge decks with 9150 mm length, 6500 mm width and 200 mm thickness having 75 mm thick haunches over the supports was constructed and tested under static and fatigue load. The steel girders were 2500 mm apart provided the cantilevers with 2000 mm span. The traffic barrier walls that provided the edge stiffening was designed and detailed in accordance with CHBDC (2006). The slab was cast monolithically in such a way that it could be divided into halves after the concrete set. The northern segment of the deck slab was steel free deck reinforced with bottom GFRP reinforcement for crack control and top GFRP reinforcement over the supports for the cantilever slab. The southern segment of the deck slab was reinforced with conventional steel reinforcement in accordance with the Code. The outline of the cross section of the specimen and the configuration of reinforcements in each segment are illustrated in Figure 2.13 and Figure 2.14.

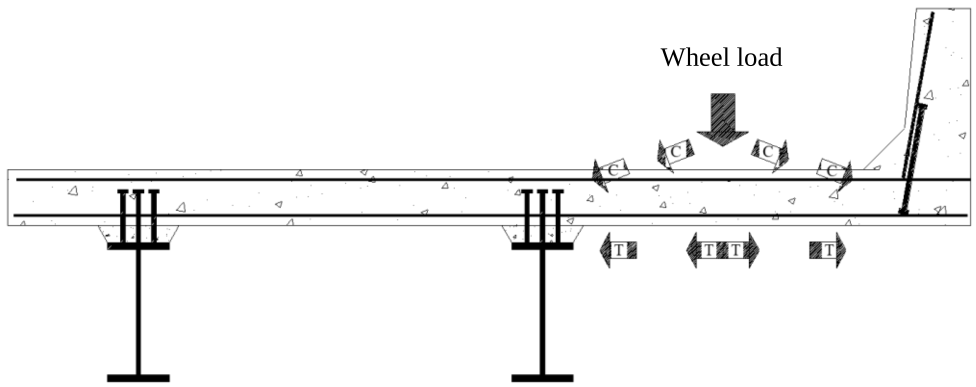

Figure 2.12 Hypothesis of arching action present in bridge deck cantilever overhangs (Klowak, Mufti & Bakht 2014).

Six destructive tests were carried out on the bridge deck cantilever slabs. Firstly, two static tests were performed on the cantilever parts, to determine the ultimate load carrying capacity of the segments in one side of the main span. Then two fatigue tests were conducted on the opposite side on cantilever slab with the range of up to 70% of the static peak load, to evaluate fatigue performance of the cantilever slabs. Two fatigue tests were also carried out in the north and south part of the internal span.

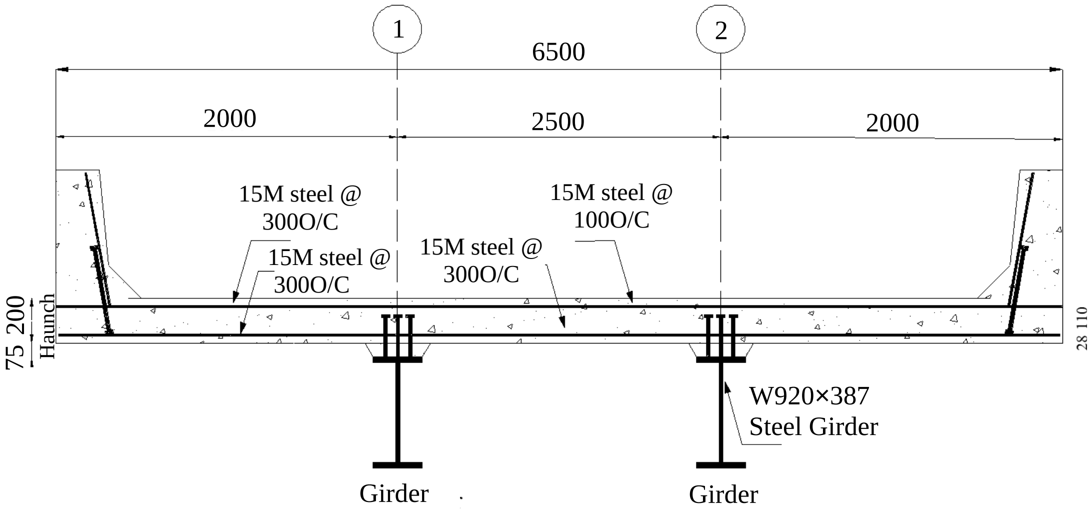

Figure 2.13 Typical transverse cross section of corrosion/steel-free section of the bridge deck with GFRP reinforcement (Klowak, Mufti & Bakht 2014).

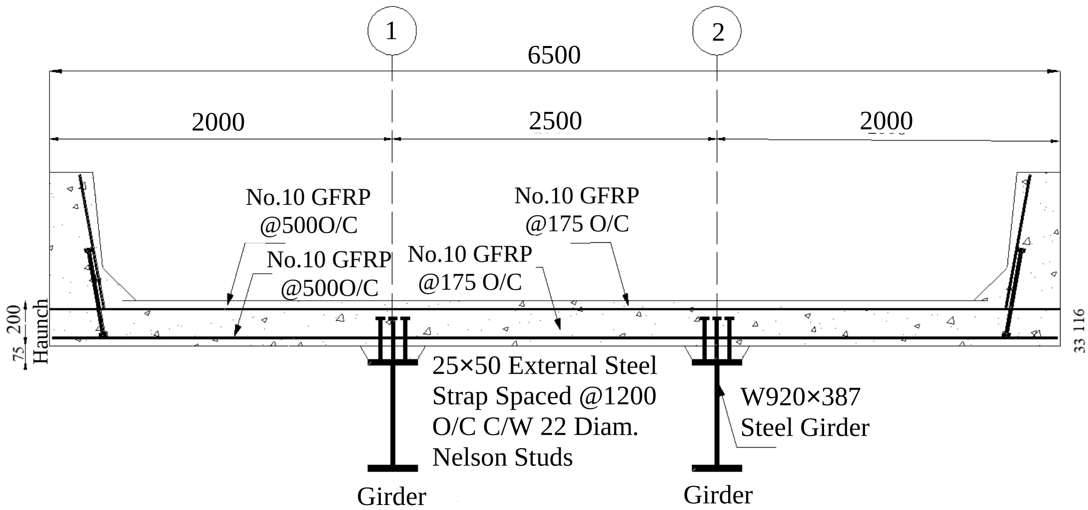

Figure 2.14 Typical transverse cross section of the conventional steel reinforced section of bridge deck (Klowak, Mufti & Bakht 2014).

The limited data obtained from static tests showed that a significant component of the arching action in the edge-stiffened bridge deck cantilever slab is developed that increase the ultimate load carrying capacity of the cantilever sections well beyond the flexural failure load. Furthermore, presence of compressive strain on the top surface of the cantilever and the tensile strain on the bottom transverse bars disproved classical flexural behaviour in cantilever slab. The bending strain was developed in the barrier wall because the wall acted like an upstand girder supporting the deck slab.

2.5. Others research after 2000

The most significant research on compressive membrane action of slabs and fatigue performance of the shear connectors and steel-concrete composite bridge deck slabs, carried out recently (after year 2000) is discussed briefly in this section.

Due to effectiveness and popularity of precast slabs, fatigue tests were carried out to develop methods for designing shear connectors (including grouted pockets) in steel-concrete composite decks with precast slabs (Shim, Lee & Chang 2001). Two full-depth models of composite bridge decks were constructed and tested under two-point concentrated loads, simulating the truck load at the mid span. The specimens, tolerated two million cycles of load. Then, they were loaded statically up to failure. The experimental results demonstrated the acceptable fatigue performance of the shear connectors in pockets of grout in precast composite deck slabs.

Bailey (2001) developed a new analytical procedure for capturing the behaviour of lightly reinforced concrete subject to large deflection by taking into account the effect of membrane action. The Bailey's model which was based on equilibrium approach, showed a good agreement with the large as well as the small-scaled experimental data. Moreover, a simplified design equation was proposed to predict the ultimate failure load of unrestrained slabs, considering the tensile membrane action. This equation was based on the fracture of the reinforcement, across the shorter span of the slab. However, it was always conservative in predicting of the ultimate load. This simple approach, was based on limited experimental results, so, Bailey, Toh & Chan (2008) continued their research on analysis of membrane action by conducting fourteen tests on small-scale unrestrained reinforced concrete slabs. In addition to the simple approach, an advanced nonlinear finite element model was developed to validate the accuracy of the simplified method. In nonlinear finite element model, an eight-node quadrilateral isoparametric curved layered shell element with ten integration points over the thickness was used to capture the membrane action in the RC slab and reinforcing mesh was modelled by plane grid reinforcement, embedded in the shell element. The uniaxial stress-strain relationship of Eurocode 2, Part 1.1 (EN 1992-1-1 2004) was considered for concrete in compression behaviour and for the tensile behaviour of concrete, the fixed smeared crack model with linear tension softening after cracking was adopted. Comparison of the results form experiments, simple method and FEM analysis, demonstrated that the simple method was as accurate as the FEA for predicting the load-deflection response. The FEA showed that the formation of compressive membrane action around the perimeter and tensile membrane action in the middle of slab was rationally characterised in the simplified approach. The FEA was almost capable of capturing the load-displacement response up to the failure load, but predicting the actual failure load required calibration of the finite element models.

Huang, Burgess & Plank (2003a) conducted an extensive research regarding the effect of membrane action on the behaviour of reinforced concrete slabs in steel-concrete composite frames subjected to fire (Abu, Burgess & Plank 2013; Huang, Burgess & Plank 2003a, 2003b).

A comparative study was carried out to investigate the effect of strength of confining system instead of stiffness of confining system on the behaviour of laterally restrained steel free deck slabs (Hassan et al. 2002). The strength of restraining members, concrete compressive strength and steel ratio of confining systems were the main variables considered in Ammar Hassan’s research. Seven large-scale steel-free deck slabs were constructed and restrained by unbounded prestressed bars (see Figure 2.15). Two levels of prestressing and two concrete compressive strength (i.e. normal and high strength) were used in the fabrication of specimens. All specimens were tested under the monotonically increasing static load applied at mid span up to failure. Initial cracking load, crack pattern and failure mode of specimens were examined during the tests. It was observed that global performance of these restrained prestressed slabs was similar to slabs confined with straps and punching shear was dominant failure mode in all slabs. Furthermore, the prestressed confining system did not prevent the occurrence of longitudinal cracks in steel free slabs, however, it delayed formation of cracks that in turn led to serviceability performance improvements. Test results showed that high strength concrete increased the ultimate load carrying capacity of the restrained slabs, but the high strength concrete was not effective in preventing the onset of the longitudinal cracks. The test results revealed that after onset of longitudinal cracks, the steel free deck slabs rely only on the confining system and there was no alternative redistribution of the internal load if the restrained system would have failed.

Twelve full-scale model of bridge deck slabs were tested under static and cyclic load to investigate effect of arching action on punching shear behaviour of bridge deck slab subjected to fatigue load (Graddy et al. 2002). Two types of slabs, i.e. cast in place and precast prestress slabs were fabricated and tested under different ranges of the pulsating fatigue loads. A method was also developed for predicting the punching shear capacity and the fatigue life of the slabs. The behaviour of specimens during the test, failure mode, fatigue life and ultimate load carrying capacity of the slabs were recorded.

The results showed that the punching shear capacity of the slabs were much higher than the predicted load by AASHTO (1996) and ACI 318 (1989) codes, due to ignoring the effect of arching action. Moreover, the developed models captured the ultimate load of slabs with a good accuracy and it was found that finite element model was capable of predicting the membrane action distribution throughout a cracked deck. A good correlation between fatigue life and applied stress range was observed under pulsating loads. The results of experiments revealed that loss of composite action between the precast slab and girders was more prominent than the composite decks with cast-in-situ slabs.

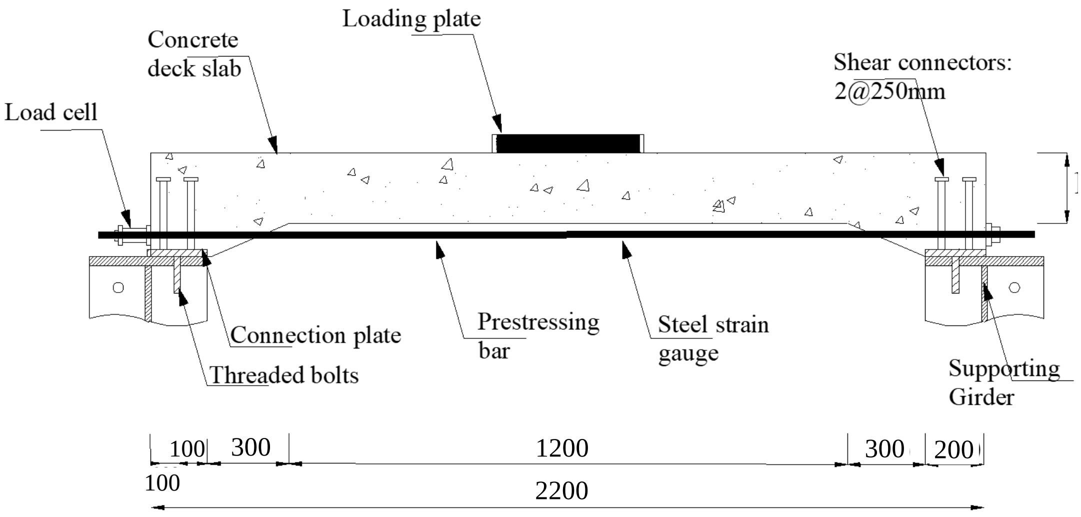

Figure 2.15 Section of prestressed steel free slab (Hassan et al. 2002).

The effect of degree of confinement on structural behaviour and punching shear capacity of RC slabs was examined experimentally by Salim & Sebastian (2003) and a model was also developed using plasticity theory to predict the ultimate punching strength of the restrained deck slabs. In the model proposed, rigid-plastic material was used for concrete with a parabolic Mohr failure criterion. The enhancing effect of compressive membrane action on punching shear capacity was taken into account, and the compressive membrane forces were determined by a modified flexural theory (Braestrup & Morley 1980). In the experimental program, four square RC slabs 1200x1200x150 mm, supported on four corners, were subjected to monotonically increasing concentrated load, applied at the mid span up to failure. The specimens were restrained by means of internal hoop reinforcement. The three different amounts of layers of hoop reinforcement were used to provide different levels of in-plane lateral restraints for the slabs. The beneficial effect of compressive membrane action on ultimate load capacity and on the serviceability performance of the slabs, i.e. crack width and crack propagation, was clear. The developed model not only was capable of predicting the peak loads of the four tested specimens accurately, but also showed a good agreement with other experimental results.

To evaluate the enhancing effect of compressive membrane action on the strength of existing RC beam-and-slab bridge decks and also develop a design method for RC beam-and-slab bridge decks, experimental and analytical studied were carried out by

Hon, Taplin & Al-Mahaidi (2005). Eight imposed punching shear failure tests and fifteen imposed flexural failure tests were conducted on one-way slabs with 600 mm span and 75 mm depth with different boundary conditions, provided by changing the width of edge beam. The crack patterns, load-deflection curve of the slabs and horizontal expansion of edge beam were monitored and recorded. The developed model by Rankin & Long (1997) was used to calculate the ultimate load capacity of restrained slab. However, to determine the horizontal stiffness of restrained system properly, a beam model of the slab and beam system was generated separately. In this model, the horizontal confining stiffness attributed to axial stiffness of the surrounding slab area, horizontal bending stiffness of the edge beam and the location of the loaded area were considered. Since, the uncracked gross section properties are often used in structural design, a linear elastic behaviour was assumed for analysis of the beam models. After calculating the lateral stiffness, the strength of the slab influenced by the compressive membrane action could be calculated. Moreover, a nonlinear finite element model was also employed to predict the slab strips' behaviour in flexural mode and examine accuracy of the proposed model. It was demonstrated that the developed model based on Rankin & Long (1997) approach and the FE model are capable of predicting the ultimate strength of the restrained slab, provided the stiffness of the lateral restraints can be estimated with reasonable accuracy. Furthermore, it was found that the developed beam model was able to predict the rotational and translational stiffness of the in-plane restraints with sufficient accuracy.

Six full-scale laterally confined bridge deck slabs (3000 mm long, 2500 mm wide and 200 mm thick) reinforced with FRP bars were built and tested to investigate the behaviour of restrained edge slabs (El-Gamal, El-Salakawy & Benmokrane 2005). Empirical equations were also proposed to determine the punching shear capacity of the restrained slab reinforced with FRP bars. Three deck slabs were reinforced with glass fibre reinforced polymer (GFRP) bars and two deck slabs were reinforced with carbon fibre reinforced polymer (CFRP) bars and the last specimen was reinforced with conventional steel bars as a reference test to compare the results. In addition to reinforcement type, the reinforcement ratio was another variable considered. The slabs were connected and restrained to steel girders by steel bolts and steel channels on top of the flange (see Figure 2.16). The specimens were subjected to monotonically increasing concentrated load, applied at the mid span with the contact area of 600x250 mm to simulate the footprint of a truck wheel load (87.5 kN CL-625 truck) according to CHBDC (2000). The ultimate load capacity of the slabs were more than three times larger than design factored load obtained from CHBDC (2000) provisions. All specimens failed in punching shear mode that confirmed the development of compressive membrane action, otherwise the specimens should have failed in flexural mode. It was also observed that, the crack width and deflection at service load level were lower than permissible code restrictions. Finally, the proposed model was capable of predicting the punching failure load of restrained FRP-reinforced deck slabs with good accuracy.

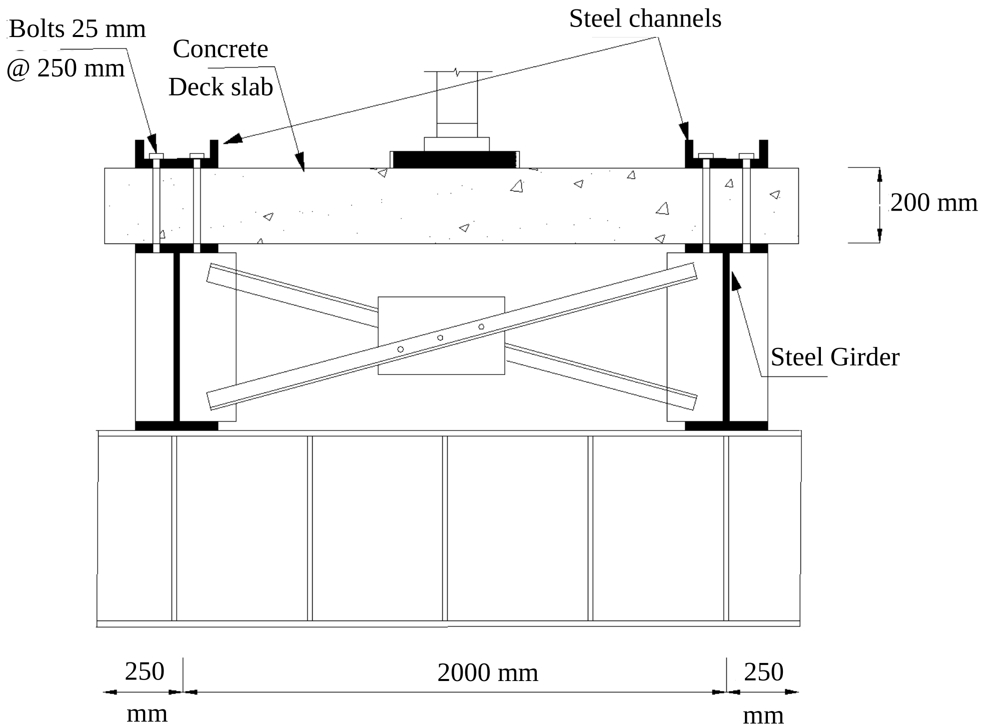

Figure 2.16 Cross section of specimen (El-Gamal, El-Salakawy & Benmokrane 2005).

The research has been extended to evaluate fatigue behaviour and fatigue life of concrete bridge deck slabs reinforced with GFRP bars (El-Ragaby, El-Salakawy & Benmokrane 2007). Five full-scale deck slabs similar to previous research in terms of the geometry and confinement system were constructed. Four of the specimens were reinforced with GFRP bars and one specimen was reinforced with steel reinforcement, as control sample. The reinforcement ratio and configuration were other variables. All slabs were tested under cyclic concentrated load, applied at mid span. Two patterns of fatigue loading were used, i.e. accelerated fatigue loading with variable amplitude (scheme-I) and constant amplitude fatigue loading (scheme-II) as shown in Figure 2.17. Deflections at mid span, strains in the concrete, strain in FRP bars and crack widths at different levels of cyclic loading were recorded. All specimens failed in punching shear mode. The GFRP reinforced concrete slabs displayed superior fatigue performance and fatigue life compared to steel reinforced slab. This behaviour was attributed to close value of modulus of elasticity for GFRP composite bars and concrete that produced a close to uniform stress distribution between the reinforcement and concrete. It was concluded that the provisions for FRP-reinforcement ratio in CHBDC (2006) was adequate to meet the fatigue strength, serviceability and fatigue life requirements of the concrete bridge decks.

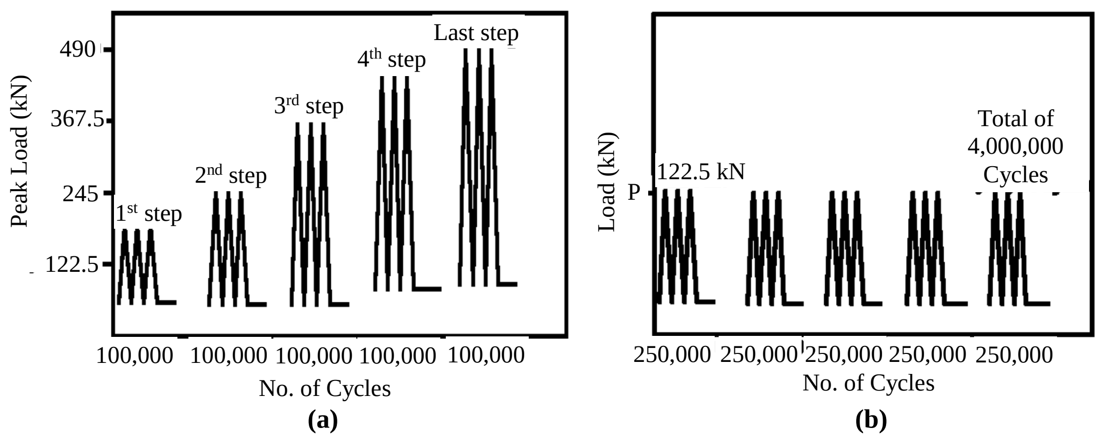

Figure 2.17 Fatigue loading schemes (a) scheme-I, variable amplitude fatigue loading pattern and (b) scheme-II, constant amplitude fatigue loading pattern (El-Ragaby, El-Salakawy & Benmokrane 2007).

The finite element model for analysing fatigue life of RC bridge deck slabs subjected to moving wheel loads was developed using crack bridging degradation concept (Suthiwarapirak & Matsumoto 2006). Degradation of bridging stress over the crack in concrete slab lead to continuing crack formation/propagation under fatigue load that ultimately causes slab failure. To represent the real moving load effect, three-dimensional FEM was considered by Suthiwarapirak & Matsumoto (2006). The model took advantage of smeared crack concept for concrete and 1D truss elements for reinforcing steel bars. The fatigue analysis was conducted on slabs with 2500 x 3750 x 180 mm dimension that contained 1.3% and 0.5% reinforcement in the longitudinal and transverse directions, respectively. The specimens were subjected to two different loading conditions, i.e. fixed cyclic load and moving load. Moreover, two retrofitting methods were applied on the specimens to evaluate the effectiveness of strengthening methods for improving the fatigue life of the deck slabs. It was concluded that slabs under moving loads display much lower fatigue life and had severe damage with more deflection at mid-span in comparison with slabs subjected to pulsating load. Furthermore, it was found that both repairing methods were effective in enhancing the fatigue life and reducing the mid-span deflection compared to original slab.

An analytical study was conducted by Welch, Hall & Gamble (2008) to examine Park's compressive membrane theory and to predict the capacity of restrained RC slab. In the proposed method, the ultimate load capacity of the confined slab was determined with respect to the peak point of thrust instead of mid span deflection. Accordingly, the proposed approach resolved the difficulty associated with estimation of ultimate deflection in Park & Gamble (1980) method and the loading capacity of the restrained RC slab could be calculated even if the experimental data was not available. The new approach was as accurate as the formulations that required deflection for predicting the strength of restrained one-way slabs.

To evaluate the effect of edge restrained condition on ultimate load capacity of the RC slabs, nine rectangular orthotropic reinforced concrete slabs with various boundary conditions were constructed and tested under uniform distributed load (AL-Hassani , Husain & AL-Badri 2009).The restraint conditions of slabs varied in all specimens from simply supported to all four edges fully fixed. The orthotropic reinforcement was placed in both directions in such a way that bottom reinforcement was 50% of the top reinforcement. The experimental results were compared to the theoretical results obtained from elastic-plastic models developed by Abdul-Qader (2008). It was concluded that the edge restraining increased the load carrying capacity of the slabs significantly compared to the peak load calculated by Johansson’s theory. In addition, the strength enhancement increases by the number of the restrained edges.

The three-dimensional nonlinear finite element analysis was employed to investigate the damage mechanism of RC slab decks under high cyclic moving loads (Fujiyama & Maekawa 2009). To capture the cumulative fatigue damage, three basic models including compression, tension and crack shear model were considered separately to simulate microscopic behaviour of material at each stage. Two types of model i.e. simply supported RC slab and steel concrete composite slab, were modelled and subjected to both pulsating and moving loads. The fatigue performance of models including fatigue life, mode of failures and the mid-span deflection was studied and S-N curve model was proposed based on the results. The FE model predictions exhibited a good agreement with the available experimental results in both types of the loadings and slabs.

The modified strut-and-tie model was developed to predict the ultimate load capacity of the restrained steel-free bridge deck slabs supported by concrete wide-flange girders (Bae, Oliva & Bank 2011). The model was capable of capturing punching and flexural failure of the restrained deck slabs. Two main assumptions were considered in the modified strut and tie model, i.e. 2D axisymmetric model was assumed to adequately represent the behaviour of a restrained 3D bridge deck slab, and to capture the effect of geometrical nonlinearity, a second order method was utilised to analyse the struts. The model was verified against results obtained from nonlinear finite element analysis (NFEA). The results showed that the proposed 2D model was sufficiently accurate to predict the behaviour of 3D restrained slab decks, provided certain limitations regarding the thickness of the slabs and spacing of the girders are met. The ultimate capacity estimated by the modified strut-and-tie model was sufficiently close to the NFEA predictions, however, the strut and tie model was computationally more efficient than the time consuming NFEA.

An experimental program was carried out on half-scale specimens to evaluate fatigue performance of top slabs in typical box-girder rail-way bridges (Zanuy et al. 2011). The top slabs in this system are usually lightly reinforced and are prone to huge number of cyclic loads that could lead to fatigue damage accumulation. Three identical specimens were constructed and then, one of the specimens was tested statically to produce benchmark results and the other two specimens were tested under cyclic loads with different ranges of loading. Furthermore, a finite element software was employed to simulate the static behaviour of samples. Ductile flexural failure was observed in the static test, whereas brittle fracture of the reinforcing bars was the governing mode of failure in fatigue tests. This brittle failure was predictable by available S-N curves (CEB-FIP 1993). It was also observed that, the lightly reinforced slabs show significant tension stiffening capacity under service loading conditions, but the effect of tension stiffening significantly reduce by increasing the number of loading cycles. It was concluded that the negative tension stiffening (developed at minimum level of cyclic loads) affect the permanent crack expansion and deflections.

One-third scaled concrete bridge deck slabs, reinforced with GFRP bars was tested to investigate the effect of compressive action on ultimate strength of the slabs (Zheng, Yu & Pan 2012).The main variables in the Zheng et al. experimental program were reinforcement ratio, reinforcement types and the size of supporting beams. Moreover, a new model was also developed for predicting the ultimate strength of GFRP reinforced slab (Zheng et al. 2010). The model was validated through experimental results and was used to carry out a parametric study in which effect of a wide range of parameters including reinforcement ratio, concrete strength and magnitude of lateral restraint stiffness were considered. It was shown that compressive membrane action had a great influence on ultimate load capacity as well as serviceability performance of the laterally restrained GFRP reinforced concrete slab. Moreover, GFRP bar was assumed to be a proper alternative for steel reinforcement to overcome corrosion problem associated with steel bars. The research extended on the behaviour of laterally restrained GFRP reinforced concrete slab by carrying out more tests on one-way concrete slabs considering different variables such as boundary conditions, compressive strength of concrete, reinforcement ratio and configuration (Zheng, Li & Yu 2012). Furthermore, a nonlinear finite element analysis was conducted by means of commercial Software, ABAQUS, to simulate arching effects on such structures. In

FE analysis, concrete damaged plasticity model, was used to capture material behaviour of concrete, a bilinear stress-strain model considered for steel materials and because of substantial discrepancy of compressive and tensile behaviour of GFRP bars, Hashin Damage model (Hashin 1980) was used to simulate the material properties of GFRP bars. The test results indicated that due to development of compressive membrane action, the effect of GFRP bars in ultimate load capacity and serviceability of laterally restrained slab were insignificant and compressive strength of concrete and lateral restraint stiffness played an important role. Furthermore, NLFEM not only was capable of predicting the ultimate strength of slabs with excellent accuracy, but also the behaviour of restrained GFRP reinforced concrete slab was simulated accurately. Further numerical Simulations were carried out and the structural behaviour of GFRP reinforced concrete bridge deck slabs under static and dynamic loads were investigated (Zheng et al. 2013). The validated FE from previous research was used to carry out a parametric study for the slab under the static load. Moreover, model of an existing bridge, Cookshire-Eaton Bridge in Canada, was created and utilised to investigate the dynamic behaviour of GFRP reinforced concrete deck slabs under traffic loads. It was observed that proposed nonlinear finite element analysis can capture the behaviour of slab under static and dynamic loads with a good accuracy while providing stress distribution through the depth of slabs and stress distribution at the deck surfaces during the whole process of moving truck loads. Finally, it was recommended that NLFEM could be a good alternative to laboratory experimentation (owing to lower cost and efficiency) for assessing structural performance of the FRP reinforced concrete bridge decks.

The fatigue behaviour of cantilever bridge deck slabs due to shear was investigated by construction and testing of ten full scale slabs (Natário, Ruiz & Muttoni 2015). In total four static tests as reference and eleven fatigue tests were conducted. All specimens were tested under concentrated load, applied at two different loading locations corresponding to a clear distance from the line support. For each load location, four different levels of maximum loads were applied and the results were compared to the strength predictions of FIB-Model Code (2010) and the critical shear crack theory. The majority of slabs failed in shear fatigue mode, however, the experimental results also showed that cantilever deck slabs were much less sensitive to shear failure, compared to the beams/slabs without shear reinforcement. Some the specimens also failed due to fracture of reinforcing bars, however, they showed notable remaining fatigue life after failure of first reinforcement. Comparison of the results with the strength, predicted by FIB-Model Code (2010) and critical shear crack theory, showed that both models provide safe predictions of the fatigue shear failure, particularly, FIB-Model Code (2010) that estimated shear strength of slab in very conservative manner which was attributed to underestimation of the arching action.

Since there was no established deterioration model available for reliability assessment of externally restrained steel free deck slabs, an analytical research has been carried out to evaluate the structural behaviour of this bridge decks by means of the reliability approach and FE modelling (Ghodoosi, Bagchiand & Zayed 2016). The main purpose of reliability assessment was to take into account the uncertainties associated with loads and strength of the materials. The developed model was used for assessment of an existing steel-free bridge deck slab, Crowchild Trail Bridge, that had been constructed and instrumented in Canada. The finite element model of the bridge deck was also created and calibrated with respect to static deflections, vibration characteristics, load distribution and crack patterns of the Crowchild Trail Bridge obtained from the field experiments. The results showed that the modification of the deck behaviour from flexural to arching action lead to a great improvement in the structural strength of the slab. Furthermore, the design approach for this system was found to be conservative in terms of reliability as the difference between reliability indices for one year and seventy-five years was negligible. The reason for this behaviour could be attributed to the use of stainless steel for the girders and straps instead of conventional internal steel reinforcements in the concrete deck. It was recommended that the current design approach (for externally restrained deck slab) could be modified, however, the serviceability state of bridge deck slab should be considered to avoid extensive crack propagations in the deck slab.

In the most recent research, the application of new fibre reinforced polymer bars i.e. basalt-fibre-reinforced-polymer BFRP in edge restrained concrete bridge deck slabs has been investigated (Elgabbas, Ahmed & Benmokrane 2016). The BFRP bars has higher strength and modulus of elasticity compared to E-glass FRP with no extra cost (Wu, Wang & Wu 2012). An experimental program was carried out including construction and testing of seven full-scale concrete deck slabs simulating the commonly used slab-on-girder bridges in North America. The size of deck slabs was 3000 mm × 2500 mm with the thickness of 200 mm. The variables in the specimens were, reinforcement type (i.e. steel and BFRP), reinforcing bar size (i.e. 12 and 16 mm), reinforcement ratio in each direction (i.e. 0.4 up to 1.2%) and edge restraints (i.e. six restrained and one unrestrained slab deck). All slabs were loaded under monotonic concentrated load at mid-span with contact area 600 × 250 mm to simulate the footprint of a sustained truck wheel load (87.5- kN CL-625 truck) as specified by CHBDC (2010).

From the experimental results, it was concluded that, the structural behaviour of BFRP-RC slab was similar to other type of reinforcements (e.g. steel, GFRP and CFRP) and all restrained slabs were failed in punching failure mode. The load capacity of restrained slab was higher than the design factored load in Canadian Standards and the deflection, crack width and strain in reinforcement in the restrained slab was much lower than the unrestrained slabs. These results, confirmed the beneficial effects of compressive membrane action in transversally confined slab decks. Furthermore, in contract with the top reinforcement, bottom reinforcement, affected the structural performance of the specimens such as reducing deflection, crack width and strains, significantly.

Development of arching and catenary action in reinforced concrete sub-assemblies

In addition to research on slabs, development of arching and catenary action in reinforced concrete subassemblies has been of interest since collapse of World Trade Centre towers on 11 September 2001 due to terrorist attacks. The effect of arching/compressive and catenary action on progressive collapse response of the reinforced concrete subassemblies has been investigated experimentally. Moreover, simplified models and advanced nonlinear finite element models have been developed to capture the arching and catenary behaviour of RC subassemblies following critical member loss. These studies are out of the scope of this research project, however, more details regarding arching and catenary behaviour of RC subassemblies following column loss scenarios can be found in Beeby & Fathibitaraf (2001), Orton (2007), Choi & Kim (2011); Sasani & Kropelnicki (2008); Su, Tian & Song (2009); Yi et al.

(2008); Yu & Tan (2013a, 2013b); Yu & Tan (2014).

2.6. Summary

The review of the existing literatures shows that strength and stiffness enhancement due to development of membrane/arching action in the concrete slabs has been well-recognised for many decades and experimentally studied by different research groups throughout the world. Furthermore, simplified models and advanced nonlinear numerical models have been proposed and successfully used to consider the effect of arching action on peak load carrying capacity and stiffness of slabs. These methods can be mainly categorised into two groups, i.e. hand calculation methods which includes elastic plastic approach (Brotchie & Holley 1971; Christiansen 1963; Kirkpatrick, Rankin & Long 1984; Rankin & Long 1997; Taylor, Rankin & Cleland 2002) and plastic approach (Braestrup 1980; Eyre & Kemp 1994; Park 1965; Park & Gamble 1980; Wood 1961) and computer-based method which consisted of nonlinear finite element analysis based on elastic- plastic material modellings (Fang , Lee & Chen 1994; Klowak, Memon & Mufti 2006; Lahlouh & Waldron 1992; Morley & Olonisakin 1995; Mufti et al. 2002; Newhook & Mufti 1995; Perdikaris & Beim 1986; Thorburn & Mufti 1995; Zheng et al. 2008). In spite of numerous studies on arching action and its contribution to structural performance of the slabs, the enhancing effect of arching action has been implemented only in a few bridge design standards (ACI ITG-3-04 2004; CHBDC 2006). By taking advantage of arching action, practical application of the steel-free concrete decks with or without polymeric fibres/bars for developing more durable construction and rehabilitation systems in several projects has been studied (Bakht & Mufti 1998; Newhook et al. 2002). However, in current construction practice for composite bridge deck slabs, the slab-to-girder and slab-to-confining system connections (e.g. welded studs buried in concrete or pockets filled with grout) are typically permanent and these connections immensely hinder the speedy and cost-effective replacement of defective slabs and/or the transverse confining system. Moreover, the existing composite decks are not conducive to deconstruction and/or recycling of the construction materials. Accordingly, there is a need for developing structurally efficient bridge decks that allow for easy deconstruction and recycling as well as rehabilitation and replacing of the concrete decks. To address these shortcomings and to gain benefit from enhancing effect of arching action and use of prefabricated concrete slab simultaneously, a practical and efficient construction method for steel-concrete composite bridge deck slabs, has been proposed. In this method, by taking advantage of post-installed bolted shear connectors (PFBSCs) composite action between the precast (SF)RC slabs and girders will be developed. The superior composite efficiency and fatigue life of PBSCs, as compared to conventional shear studs, is evident from three-point bending tests conducted on composite beams and push-out tests conducted on composite connections (Kwon, Engelhardt & Klinger 2011; Liu, Bradford & Lee 2014; Rowe & Bradford 2013).

Therefore, the focus of this study is to explore the possibility of inducing arch action in concrete slabs of a novel deconstructable steel-concrete composite deck that takes advantage of friction grip bolted shear connectors (FGBSCs). Furthermore, enhancement effect of arching action on RC deck slabs and buried RC culverts due to existing lateral restraints is investigated to obtain a more accurate estimation of loading capacity and structural behaviour of the deck and culvert slabs influenced by developing arch action. The major objectives of this project are as below;

- Proposing a novel and efficient deconstructable steel-concrete composite deck slab with precast/prefabricated RC and SFRC decks and fiction grip bolted shear connectors (FGBSCs). The proposed system facilitates future repair and replacing of the deck slabs.
- Inducing the arch action and exploiting the enhancing effect of the arch action in the proposed deconstructable deck slabs. Furthermore, the fatigue behaviour of deck slabs that develop arch action is investigated.
- Investigate the effect of steel fibres in flexural and fatigue behaviour of prefabricated slabs that develop arch action. In particular, assess the peak load carrying capacity, serviceability and fatigue life of deconstructable steel-fibre reinforced concrete decks slabs devoid of conventional reinforcing steel bars.
- Identifying the lateral restraints that can provide arch action in the slabs of existing culverts and steel-concrete composite bridge decks.
- Characterising the arch action for accurate load capacity assessment of existing bridge deck slabs/buried RC culverts and considering the level of strength

enhancement provided by arch action for rehabilitation and strengthening of the concrete deck slabs/buried culverts.

CHAPTER 3

BEHAVIOUR OF PRECAST CONCRETE DECK SLABS WITH TRANSVERSE CONFINING SYSTEMS

3. Behaviour of Precast Concrete Deck Slabs with Transverse Confining Systems

3.1. Introduction

As discussed in the literature review, the enhanced loading capacity of the transversely confined concrete deck slabs has been demonstrated through different studies. However, in current construction practice for bridge deck slabs, the slab-to-girder and slab-to-confining system connections (e.g. welded studs buried in concrete or pockets filled with grout) are typically permanent and these connections immensely hinder the speedy and cost-effective replacement of defective slabs and/or the transverse confining system. Moreover, the existing composite decks are not conducive to deconstruction and/or recycling of the construction materials. Accordingly, there is a need for developing structurally efficient bridge decks that allow for easy deconstruction and recycling as well as rehabilitation and replacing of the concrete decks. Therefore, laboratory experiments on thirty-four half-scaled transversely restrained precast slabs, attached to the girders using bolted shear connectors, are carried out to investigate the effects of various parameters on structural behaviour of this novel system. Precast slabs are tested under monotonically increasing static load and also fatigue load applied at the mid-span. The configuration and proportion of the reinforcing steel bars, dosage of steel fibres and types of the transverse confining system i.e. cross-bracings, straps (ties) and combination of cross bracings with ties are the main test variables. The efficiency of the proposed system for mobilising arching action in the precast concrete deck slabs is also evaluated in both static and fatigue tests.

In the first part of experimental program, the static behaviour of twelve conventionally reinforced precast concrete deck slab with transverse confining system is evaluated and the results are discussed in this chapter. In the second stage, the structural performance of fourteen transversely confined steel fibre reinforced (SFRC) precast slabs is explored and the results are reported in Chapter 4. The last part of the experimental program that involve fatigue behaviour of the transversely restrained RC/SFRC precast slab is reported in Chapter 5.

The experimental results of twelve half-scaled transversely confined precast slabs subject to monotonically increasing static load is reported in the following section.

3.2. Experimental program

To study the behaviour of precast concrete deck slabs with transvers confining system, a real (prototype) precast slab which was part of a 12 m long simply supported steel-concrete composite bridge deck in NSW, Australia has been considered. The bridge deck is 7.0 m wide with no cantilever and it is supported by four steel girders 2.2 m c/c apart (Figure 3.1).

. The bridge can accommodate two standard lanes, each lane being 3.2 m wide according to Australian Standard AS5100 (2004) specifications. The concrete deck slab in the transverse direction was designed as simply supported (i.e. spanning between two adjacent girders,) and the slabs complied with the minimum design requirements of Australian Standard AS5100 (2004). In the experimental program, behaviour of a one-half scale precast slab from the middle module of the real bridge deck was studied (Figure 3.1).

3.2.1. Geometry and preparation of precast slabs and steel girders

All half-scale precast concrete deck slabs were 1100 mm long with a thickness of 100 mm and width of 600 mm. At each end, the slabs had a 25 mm thick haunch where it was connected to steel girders. The slabs reinforced with 10 mm diameter cold-rolled ribbed bars with different reinforcement arrangement i.e. reinforcement at bottom, middle and top. In addition to reinforcement arrangement, the reinforcement ratio, confining system and concrete compressive strength were other parameters. Overall view of the slab with its hunches is illustrated in Figure 3.2 (a) Outline of the geometry and dimensions and (b) cross-section.

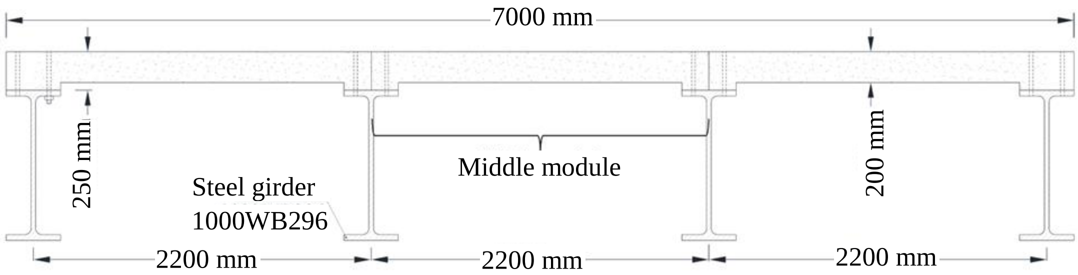

Figure 3.1 Outline of the geometry cross-section of real composite bridge deck.

Formwork

The formworks with 1100×600×100 mm dimensions were made using plywood sheets which was cut in specific dimensions in the way that after assembly of parts each formwork had a 25 mm thick haunch at each end. Two holes with 20 mm diameter were drilled at each end of moulds and a 20-mm PVC pipe was fixed in these holes before pouring the concrete for easy connection of precast slab to steel girders by using 16 mm diameter high strength bolts. Furthermore, to avoid the leakage of cement paste during concrete placement, joints of formwork walls were sealed with silicon glue.

Reinforcing mesh and bars arrangement

To build reinforcing mesh, N10 deformed steel bars were cut, bent and assembled. Different number of bars i.e. 3, 4 and 6 bars were used to fabricate each slab mesh depending on the reinforcing bar proportion. The reinforcement mesh was placed at different height in slab section i.e. bottom, middle or top, by using of different size bar chairs, to provide different reinforcing proportions with different effective depth *d* according to minimum requirements of AS5100 (2004). For main longitudinal bars, 90° bend was provided at the end of each N10 bar according to AS3600 (2009), while transverse bars which was only used for assembly of the reinforcement mesh were straight. Before placing the steel mesh in the formwork, 6 mm long steel strain gauges were mounted at mid-span of mesh and were covered by silicon and electrical tape to prevent any damage during concrete placement.

Concrete casting and curing

The concrete was supplied as a ready mix with Grade 50 MPa and 60 MPa concrete with maximum 10 mm aggregate size and 80 mm slump (Figure 3.3). A portable vibrator was used to vibrate and place concrete properly in the formworks. In addition to the main slabs, eighteen cylindrical specimens were cast to measure compressive strength of concrete at different ages when testing the slabs. After concrete placement and surface levelling, curing of slabs started by covering them with thick plastic sheet and keeping them wet by use of soaked sponge foam up to 7 days. Six cylinders were also cured with the same conditions of slab and the remaining (twelve) cylinders were demoulded 24 hours after casting and cured in a water basin.

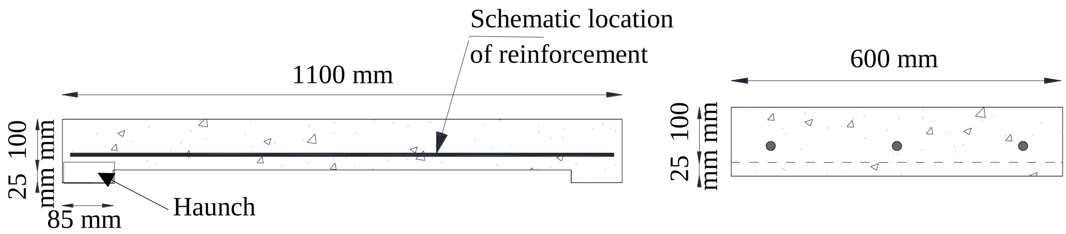

(a) (b)

Figure 3.2 (a) Outline of the geometry and dimensions and (b) cross-section.

(a) (b)

Figure 3.3 Concrete casting and curing (a) ready mix concrete and (b) slump test.

Steel girders, bracings and straps

Alongside of preparation of slabs, a universal beam 310UB32 was cut to the specified length to provide steel girders (see Figure 3.4).

a) supporting the precast slabs in a composite bridge deck. The top flanges of steel girders were drilled to provide holes with 20 mm diameter to connect the precast slabs to steel girder by means of high strength M16 bolts. In addition to the holes drilled for connecting the slabs to girders, some holes were drilled in top flange for connecting lateral restraining straps to steel girders. Furthermore, 12 mm thick steel plates welded inside of the beams (to the web and flanges) as stiffeners to prevent web crippling. The stiffeners were also drilled to prepare holes for connecting the cross bracings (lateral restraining members) to steel girders by high strength bolts (see Figure 3.4).

b). The cross-bracings and straps were made of equal leg angle section, L45×45×5EA and L45×45×3EA of Grade 300PLUS steel, respectively (see Figure 3.4).

c). For easy installation of M16, 18 mm-diameter holes were predrilled in all transverse straps and cross bracings.

High strength bolts

The proposed composite deck was designed in such a way that can allow for easy deconstruction and recycling as well as replacing of defective precast slab panels. This requirement was achieved by use of high strength post-installed bolt shear connectors (PBSC). The superior composite efficiency and fatigue life of post-installed bolted shear connectors (PBSCs) compared to conventional shear studs, has been demonstrated previously through push-out and three-point bending tests conducted on composite connections and beams (Kwon, Engelhardt & Klinger 2011; Liu, Bradford & Lee 2014; Rowe & Bradford 2013).

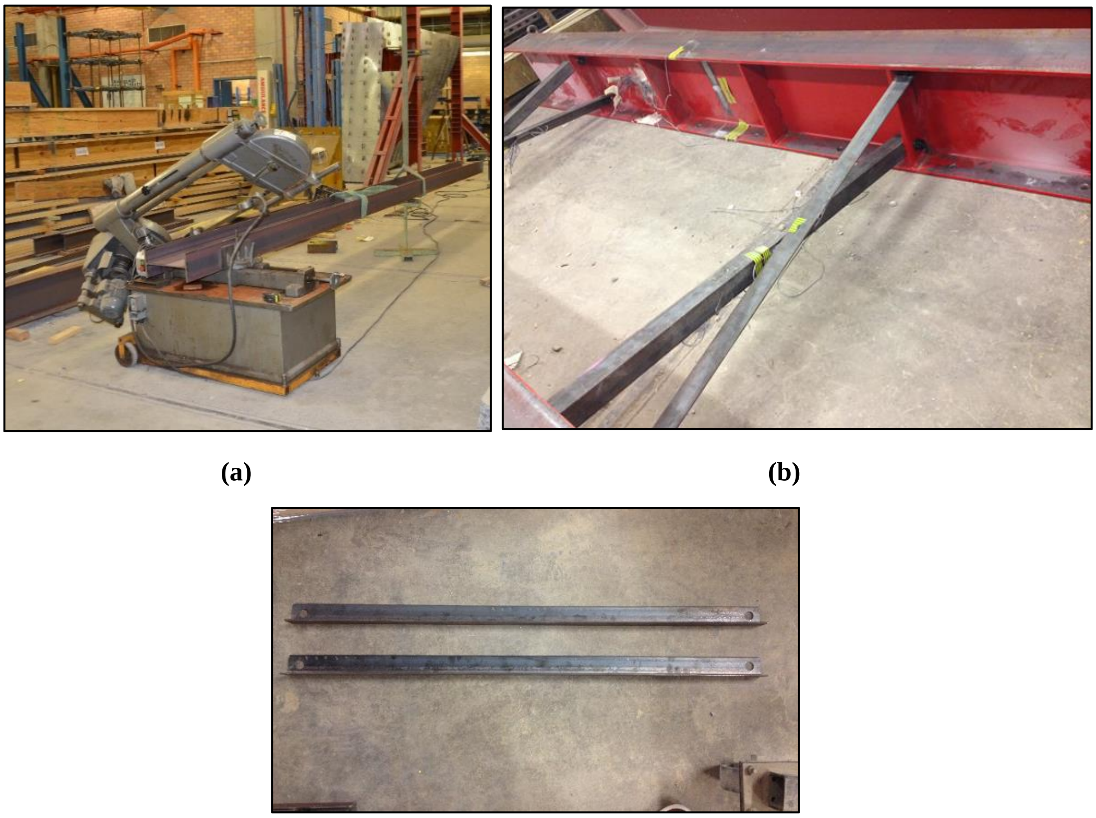

(a) **(b)**

(c)

Figure 3.4 Preparation of steel girder, bracing and straps, (a) cutting steel beam, (b) welded stiffeners and (c) equal leg angle straps/bracings.

The push-out tests carried out by Liu, Bradford & Lee (2014) have shown that PBSCs, can promote deconstruction at structural life-end and facilitate reusing of construction materials. In addition, the ability of PBSCs for preventing relative slip between normal strength concrete slabs and girders in a transversely confined deck slabs with cross-bracings was investigated by Valipour et al. (2015). Therefore, high strength 8.8/FT bolts were used in this study with an ultimate strength of f_u = 800 MPa and the yield strength of $f_y = 0.8 \times 800 = 640$ MPa. In addition to precast slab, straps and cross bracing as restraining members were also attached to steel girders by use of high strength bolts to ensure that the entire composite deck can be easily dismantled at the end of each test. A torque meter wrench with torque control method was used for tightening the bolts (Figure 3.5).

Figure 3.5 Torque meter wrench and M16 bolt shear connectors with steel strain gauges attached.

3.2.2. Test setup

After fabrication of twelve half-scale precast RC slab panel, they were connected to top flange of the 310UB32 supporting steel girders by high-strength Grade 8.8 bolts of 16 mm diameter. The outline of geometry, test setup and configuration of transverse ties and cross-bracings are shown in Figure 3.6 and Figure 3.7.

The transverse restraining systems employed to mobilise arch action, were cross-bracings (four specimens), straps (six specimens) and combination of straps and cross bracings (two specimens). The cross-bracings were bolted to the web stiffeners using high-strength M16, 8.8/TF bolts tightened to a shank tension of $0.6 f_{uf} = 495$ MPa (f_{uf} being the tensile strength of class 8.8 bolts) (see Figure 3.7), whereas, the transverse straps were connected to the bottom surface of the top flange of the supporting steel girders by the high-strength M16, 8.8 PFBSCs tightened to a shank tension of $0.4 f_{uf} = 330$ MPa . Two different arrangements were considered for the straps, i.e. straps under the slab and straps away from the slabs. The latter arrangement was when straps were used in conjunction with cross bracings (see Figure 3.7).

(a)

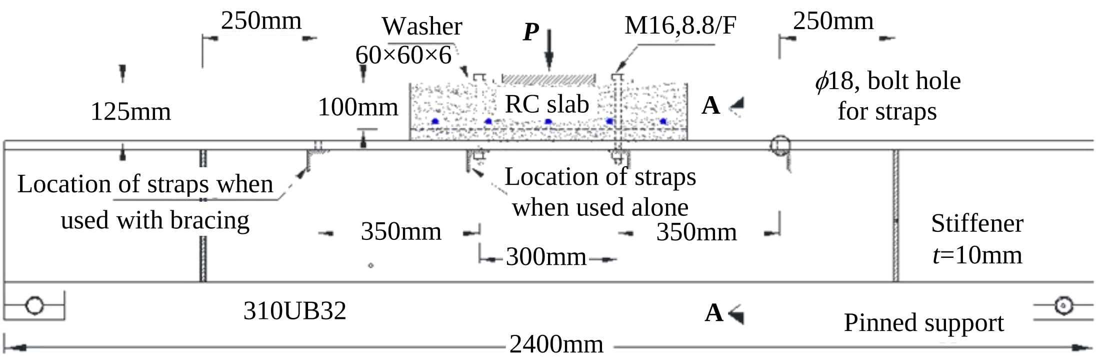

(b)

Figure 3.6 Outline of the (a) test set up and (b) geometry and dimensions of the deconstructable composite deck with precast slab mounted on steel beams.

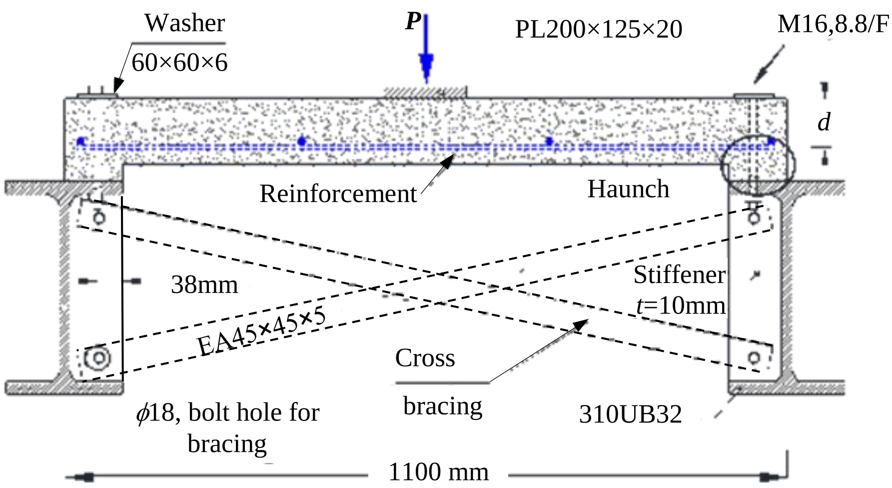

(a)

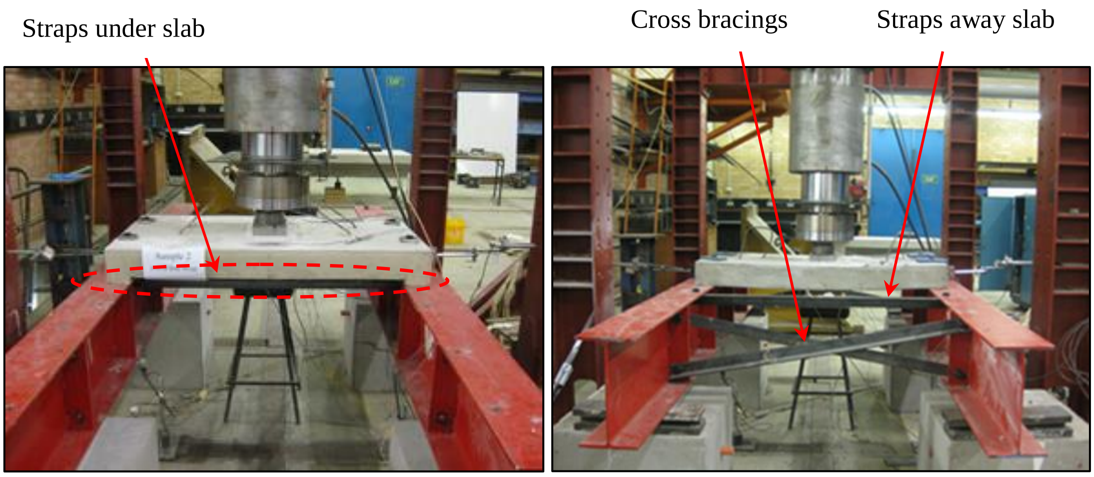

(b) **(c)**

Figure 3.7 (a) Cross-section view of the deconstructable deck with (b) straps and (c) straps plus cross bracings.

The designation and details of the specimens, including proportion and effective depth (see Figure 3.7) of reinforcing steel bars are given in Table 3.1. In Table 3.1, the designation Ln-R for specimens was made with respect to L the location (T: top, M: middle and B: bottom layer), n number of reinforcing bars and -R the type of transverse restraining/confining system (-C: cross-bracing and -S: strap-BS combination of cross-bracing and straps away from slab).

Table 3.1 Designation, concrete compressive strength and reinforcing details of the specimens.

Specimen No.	Designation of specimens	Numbers & Location of reinforcing bars	d (mm)	$\rho=A_{st}/bd$ (%)	f_{cm} (MPa)	Confining system in the transverse direction # (see Figure 3.1)
1	M4	4N10 (middle)	55	0.97	60	Straps
2	M0-S	Unreinforced	---	0.00	60	
3	M3-S	3N10 (middle)	55	0.73	60	
4	M4-S	4N10 (middle)	55	0.97	60	
5	B4-S	4N10 (bottom)	75	0.71	60	
6	T4-S	4N10 (top)	25	2.10	60	
7	M3-B	3N10 (middle)	55	0.73	70	Cross-bracings
8	B3-B	3N10 (bottom)	75	0.53	70	
9	BT3-B	3N10 (bottom & top)	75	0.53	70	
10	M6-B	6N10 (middle)	55	1.46	70	
11	B3-BS	3N10 (bottom)	75	0.53	70	Cross-bracings &Straps
12	M6-BS	6N10 (middle)	55	1.46	70	

The cross-bracings and straps were made of Equal Leg Angle, 45X45X5EA and 45X45X3EA-Grade 300PLUS, respectively

3.2.3. Instrumentation

A 500 kN flat load cell and a 100 mm-stroke LVDT was used to respectively measure the load and displacement at the mid-span. Moreover, an inclinometer and LVDT were mounted at each end of the slab to measure the rotation and horizontal displacement, respectively (Figure 3.8). The compressive strains in the slabs and tensile strains in reinforcing bars were measured respectively by two 60 mm long concrete strain gauges and two 6 mm long steel strain gauges at the mid- and end-spans (Figure 3.8). Moreover, the strain in the cross-bracings was measured by four strain gauges St-B-SG1 to 4 and the strain in ties/straps was measured by two strain gauges St-S-SG1 and 2. All slabs were tested under a monotonically increasing force applied at the mid-span via a hydraulic actuator operated in displacement control at a rate of 0.1 mm/s while forces, deformations and strains were recorded and monitored. All tests were continued until the compressive concrete on top of the slabs was partially/entirely crushed, fracture of reinforcing bars occurred or wide cracks developed between the bolts in supports. The tests were terminated to avoid any damage to the instruments.

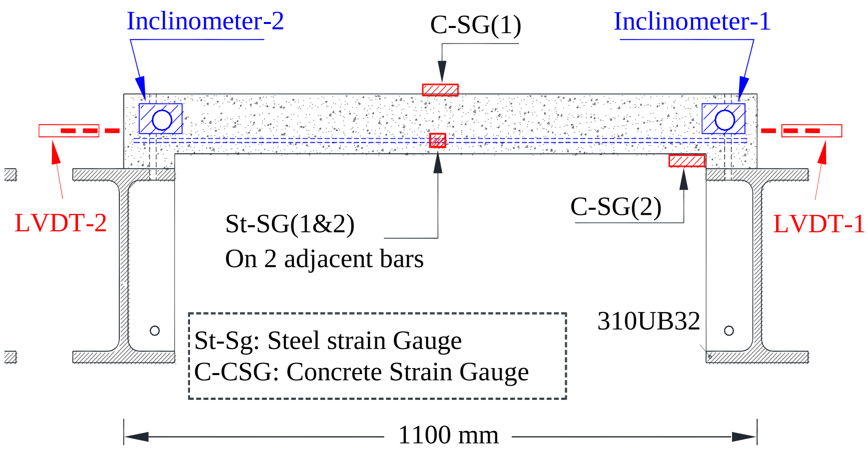

(a)

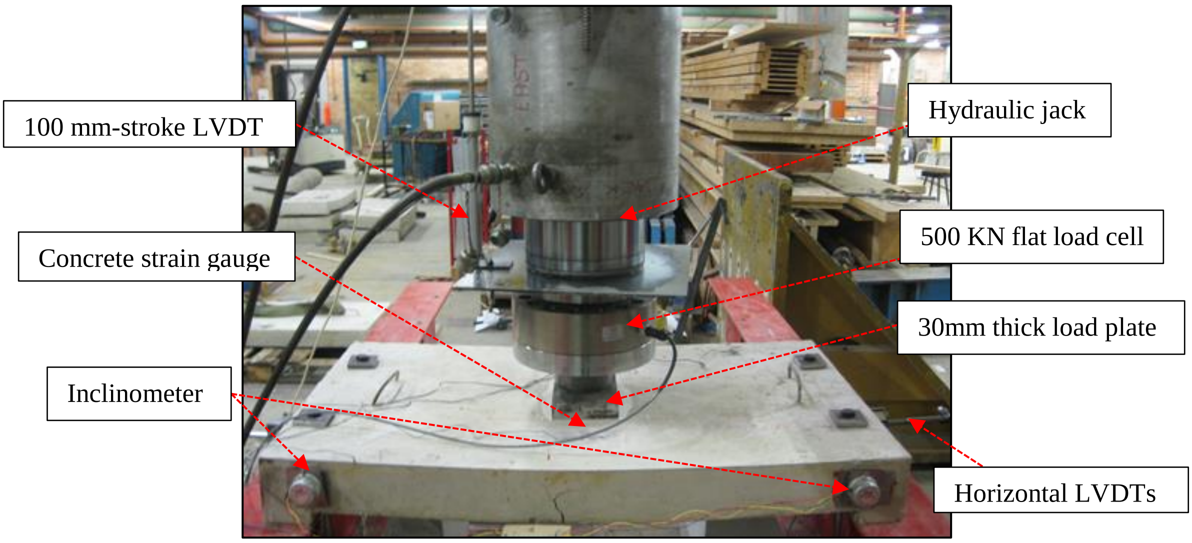

(b)

Figure 3.8 (a) Locations of the LVDTs, inclinometers and strain gauges and (b) overview of the actuator and instrumentations.

3.2.4. Material

The precast slabs were reinforced with N10 ribbed bars of Grade 500 MPa. The mean yield and ultimate strength of the steel bars (obtained from direct tension test on three specimens) were $f_y = 575$ MPa and $f_u = 680$ MPa , respectively and the uniform elongation of the bars at ultimate strength was about 8%. The strain- stress curve for average of these three tests is plotted in Figure 3.9.

The slabs were cast with Grade 50 and 60 MPa concrete (AS3600 2009), respectively.

The mean compressive strength of concrete f_{cm} after 28 days and on the testing day were obtained from the average of three cylinders tested, in accordance with AS1012.9 (1999) the average compressive strength of the concrete in the specimens is given in Table 3.1and strain-stress curve is illustrated in Figure 3.10. The standard deviation for 60 MPa concrete grade was 2.5 MPa and for 70 MPa concrete grade the standard deviation was 3.5. The standard deviation of the tested reinforcing bars was 9 MPa. It is noteworthy that the stress-strain plots in Figure 3.10 are just one sample results and slightly lower stiffness of the 70 MPa concrete compared to 60 MPa concrete should be attributed to the age of the concrete and effect of shrinkage at the time of testing.

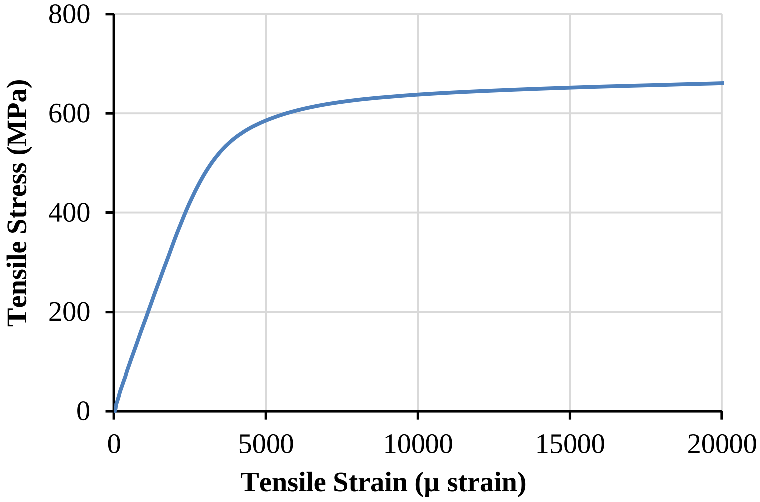

Figure 3.9 Uniaxial stress-strain diagram of reinforcing steel bars.

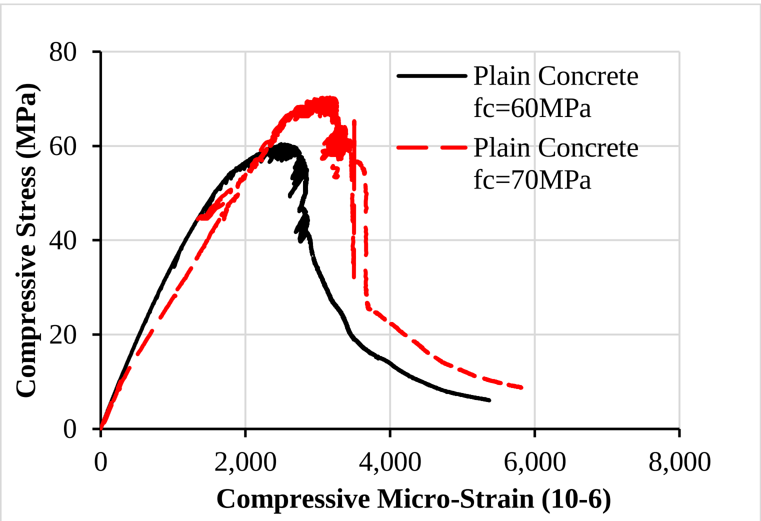

Figure 3.10 uniaxial stress-strain diagram of plain concrete.

3.3. Experimental results

To investigate the structural behaviour of transversely restrained precast bridge deck slabs and evaluate the enhancing effect of arch action,

- Mode of failure
- Global response including load vs deflection and load vs end rotation
- Local response including load vs strain in concrete and steel bars and
- Deformability/ductility and robustness of precast slab

are reported and discussed in the following sections.

3.3.1. Modes of failure

Three distinctive failure modes were identified in the tested precast slabs. The first mode of failure (Mode I) was a ductile mode and it was associated with development of large cracks in the soffit of the slab, yielding of the reinforcing steel bars at mid-span and partial crushing of the concrete on the top surface of slabs at the mid-span. Only specimen M4 with no transverse confining system failed in this mode (i.e. Mode I). The second mode of failure (Mode II) was rather brittle and it was characterised by development of cracks and yielding of steel bars in the soffit of the slab at mid-span, followed by crushing of concrete on the top surface of slabs at the mid-span and development of cracks at the supported edges of the slab (between the bolted shear connectors). The second mode of failure (Mode II) was observed in all the transversely confined precast slabs except for specimens T4-S. The third mode of failure (Mode III) was brittle and it was observed in specimens T4-S. The third failure mode was associated with development of cracks in the soffit and crushing of concrete on the top surface of the slabs at the mid-span. The failure mode of each specimen is reported in Table 3.2. Furthermore, the extent of damage and pattern of cracks for each one of the failure modes are shown in Figure 3.11

The deconstructability of the proposed system was examined after each test by untightening and removing of the bolted shear connectors. It is noteworthy that no sign of damage or excessive (or plastic) deformation was observed in the PFBSCs (see(a) (b)

Figure 3.12a). Furthermore, the damaged slab after the test has been removed without the difficulties and the concrete material of slab can be recycled easily (see Figure 3.12b).

Table 3.2 Test results and observations.

Specimen No.	Designation of specimens	Experiment				Plastic analysis P_u (kN)	R Index	μ_ψ Index	Mode of failure (see Figure 3.11)
		Ultimate		$\varepsilon_C = 0.001^{\#}$					
		P_u (kN)	Δ_u (mm)	$P_{0.001}$ (kN)	$\Delta_{0.001}$ (mm)				
1	M4	55.8	28.9	16.2	2.6	46.0	38.3	12.8	Mode I
2	M0-S	43.7	13.6	42.2	12.2	00.0	1.2	------	Mode II
3	M3-S	81.5	19.0	34.7	3.1	35.0	14.4	9.5	Mode I & II
4	M4-S	84.5	18.0	34.5	3.6	46.0	12.2	6.8	Mode II
5	B4-S	111.8	21.2	40.0	4.0	63.0	14.8	12.8	Mode II
6	T4-S	44.9	22.5	27.1	7.7	18.0	4.8	4.7	Mode III
7	M3-B	73.6	33.1	36.3	7.8	35.0	8.6	10.0	Mode II
8	B3-B	91.3	20.7	47.1	5.8	47.5	6.9	6.9	Mode II
9	BT3-B	92.7	35.2	37.8	6.7	47.5	12.9	14.4	Mode II
10	M6-B	102.9	28.7	41.4	6.7	67.0	10.6	7.7	Mode II
11	B3-BS	105.2	34.65	57.0	8.6	47.5	7.4	7.3	Mode II
12	M6-BS	104.8	28.33	39.5	5.1	67.0	14.7	6.12	Mode II

Compressive strain of concrete at mid-span on the top surface of the slab.

One of the failure modes of the transversely confined deck slabs (particularly under cyclic loading scenarios) is characterised by loss of transverse confinement due to development of horizontal cracks along the haunches and on the faces of slabs (Edalatmanesh & Newhook 2012; Klowak, Memon & Mufti 2006). However, in the proposed deconstructable bridge deck slab, no sign of cracking was seen along the haunches even after slabs had undergone large deflections and rotations. With regard to this observation it can be argued that the clamping force of post-tensioned bolted shear connectors can potentially improve the loading capacity of the transversely confined deck slabs (with haunched edges) by preventing/controlling the horizontal cracks along the haunches.

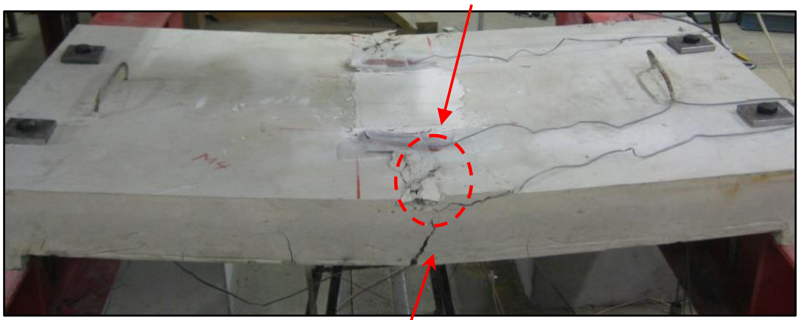

(a) Failure Mode I

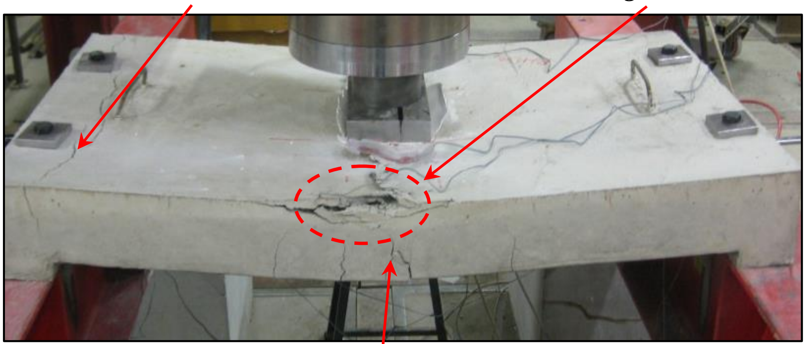

(b) Failure Mode II

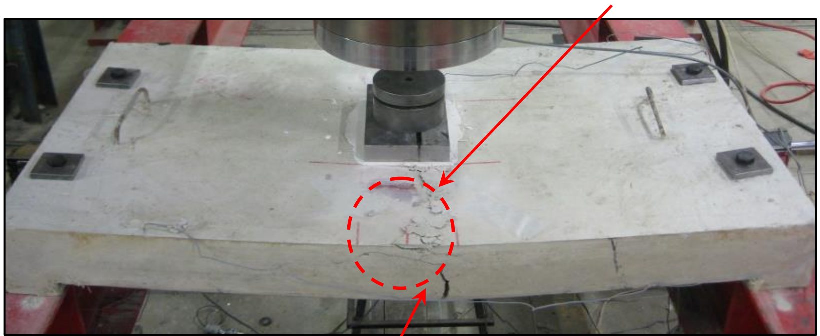

(c) Failure Mode III

Figure 3.11 The pattern, type and extent of cracking/damage in different modes of failure.

(a) **(b)**

Figure 3.12 (a) Bolted shear connectors taken out of their sleeves after the test and (b) the specimens easily removed after the test.

3.3.2. Global response

The applied load versus mid-span deflection plots of the slabs are shown in Figure 3.13 to Figure 3.16. The key events (i.e. yielding of steel bars, crushing of concrete, development of crack on the supported edge of the slabs) associated with failure of the specimens are shown on the load-deflection plots. It is noteworthy that the small dips following the first peak in the load versus mid-span deflection plots are due to development of cracks at the supported edges of the slabs and between the PBSCs (see Figure 3.11b).

The peak load capacity and the mid-span deflection corresponding to the peak load capacity of the slabs are reported in Table 3.2. It is observable that the transverse confining system can significantly increase the loading capacity of the precast slabs. For example, the load carrying capacity of specimens M4-S (with straps) is about 53% more than that of specimen M4 (no strap/bracing). Comparing the peak load capacity of the specimens T4-S, M4-S and B4-S shows that the location of reinforcing steel bars in the slab has a significant influence on the peak load capacity of the single span transversely confined slabs. However, the top bars have negligible influence on the peak load carrying capacity of the slabs with straps; for example, the peak load carrying capacity of the specimens T4-S and M0-S are approximately equal.

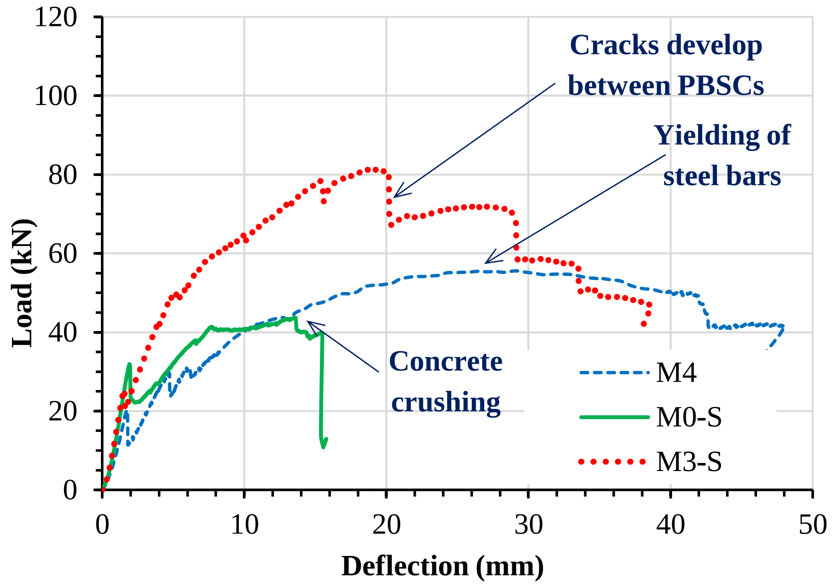

Figure 3.13 Load versus vertical displacement at mid-span of the slabs.

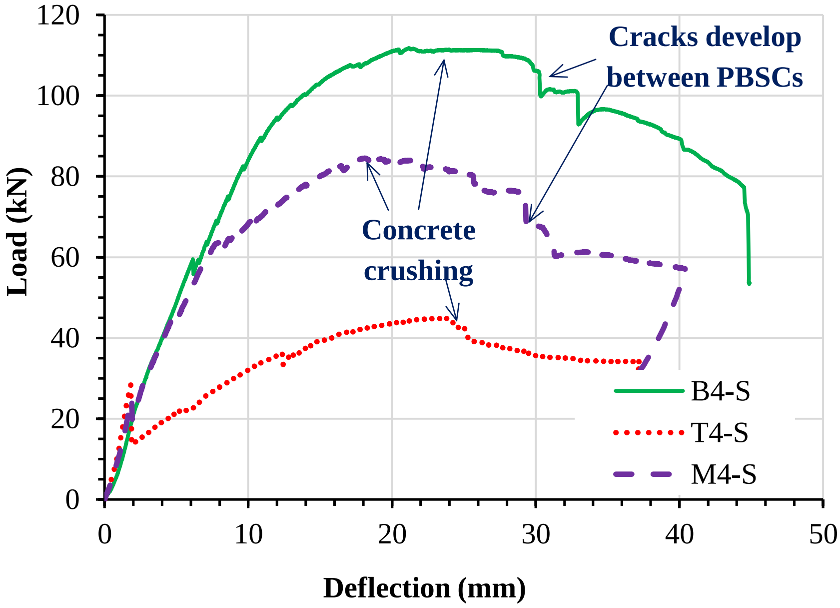

Figure 3.14 Load versus vertical displacement at mid-span of the slabs.

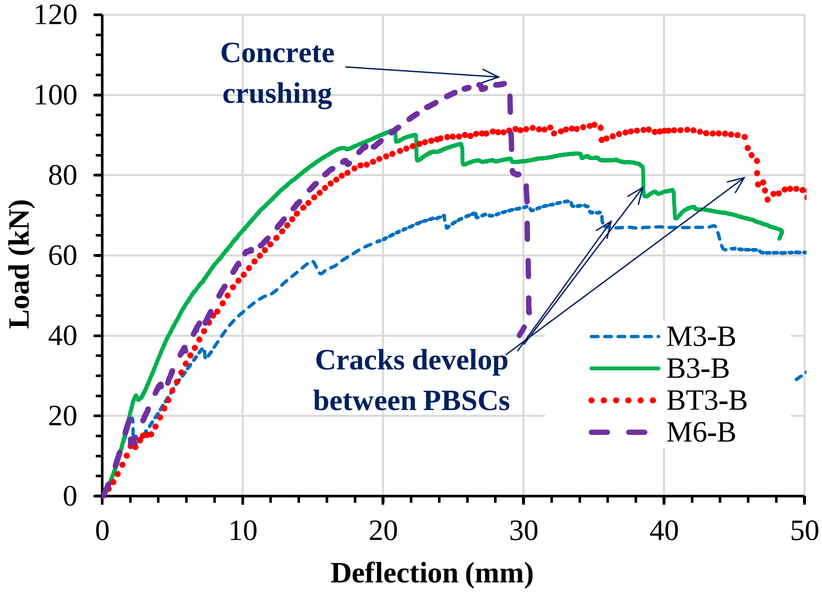

Figure 3.15 Load versus vertical displacement at mid-span of the slabs.

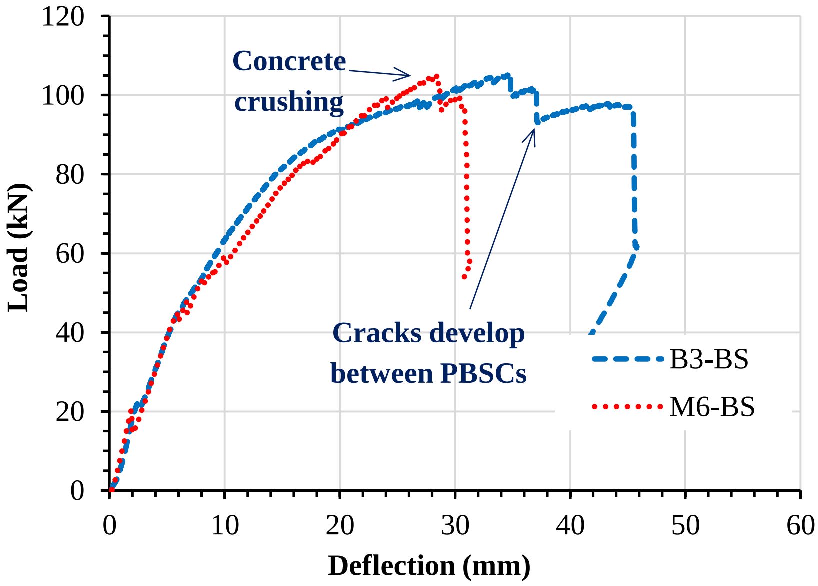

Figure 3.16 Load versus vertical displacement at mid-span of the slabs.

The plots of applied load at mid-span versus average rotation at end span for the tested slabs are shown in Figure 3.17to Figure 3.20 and a nonlinear relationship between the applied load and average rotations at the supporting points is observable. Accordingly, it is concluded that the transverse confining system (i.e. cross-bracings, straps only and combination of cross-bracings and straps) can provide some rotational fixity for the single-span precast slabs that, in turn, leads to the development of a hogging bending moment and cracks on the top edge of the slabs (see Failure Mode II in Figure 3.11b).

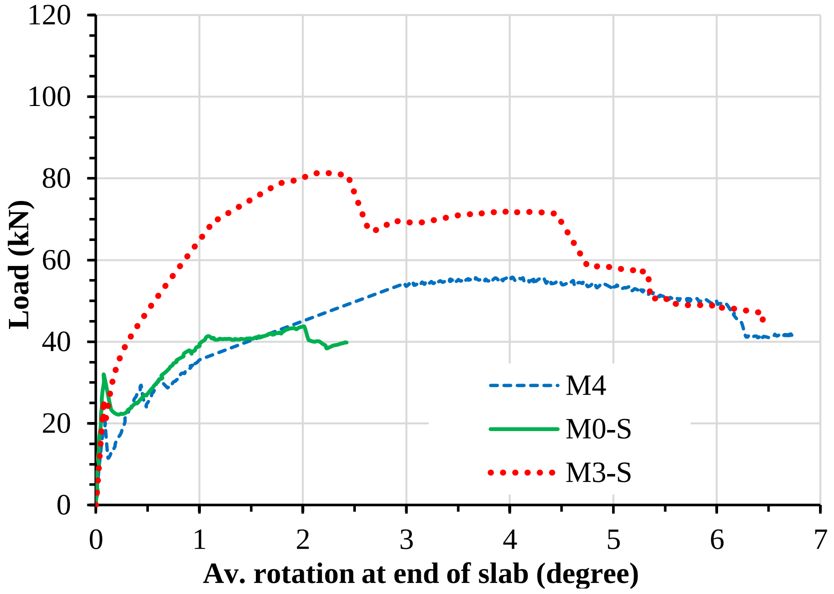

Figure 3.17 Load versus average rotation at the end of slabs no. 1-3.

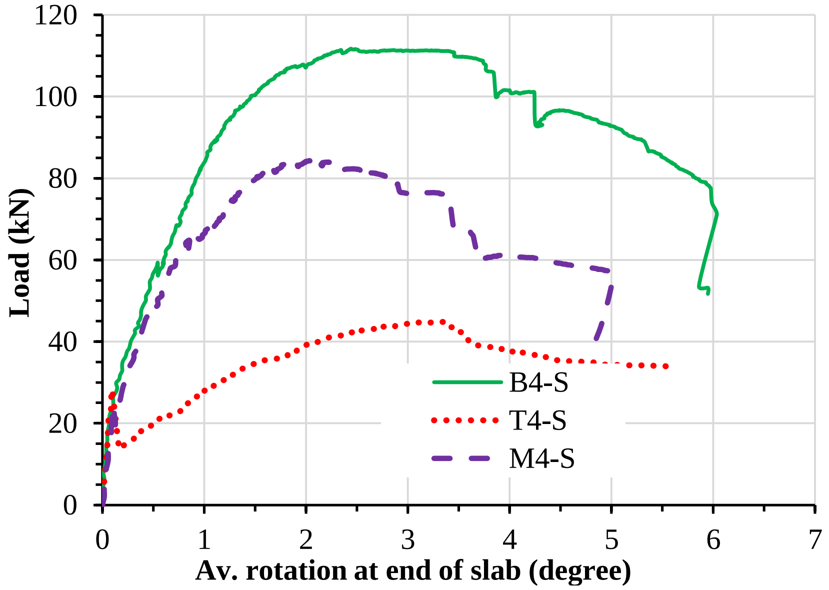

Figure 3.18 Load versus average rotation at the end of slabs no. 4-6.

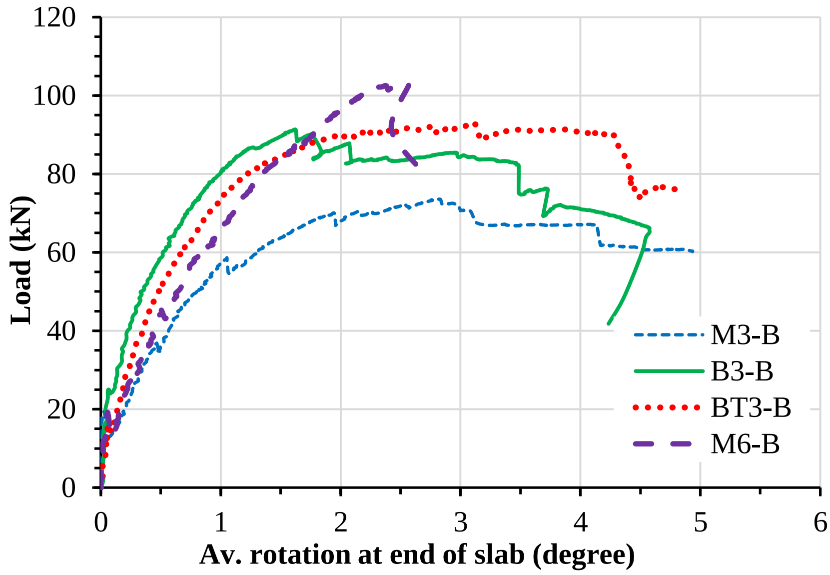

Figure 3.19 Load vs average rotation at the end of slabs no. 7-10.

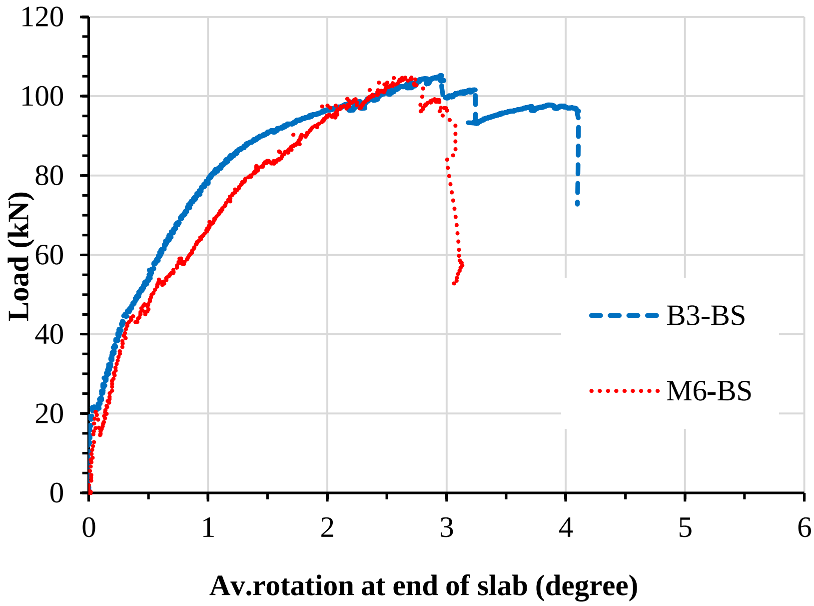

Figure 3.20 Load vs average rotation at the end of slabs no. 11-12.

The elongation of the slabs in the transverse direction was obtained from the LVDT-1 and LVDT-2 attached to the sides of slabs (see Figure 3.8a and b) and the applied load versus elongation of the slabs is shown in Figure 3.21 to Figure 3.24.

.

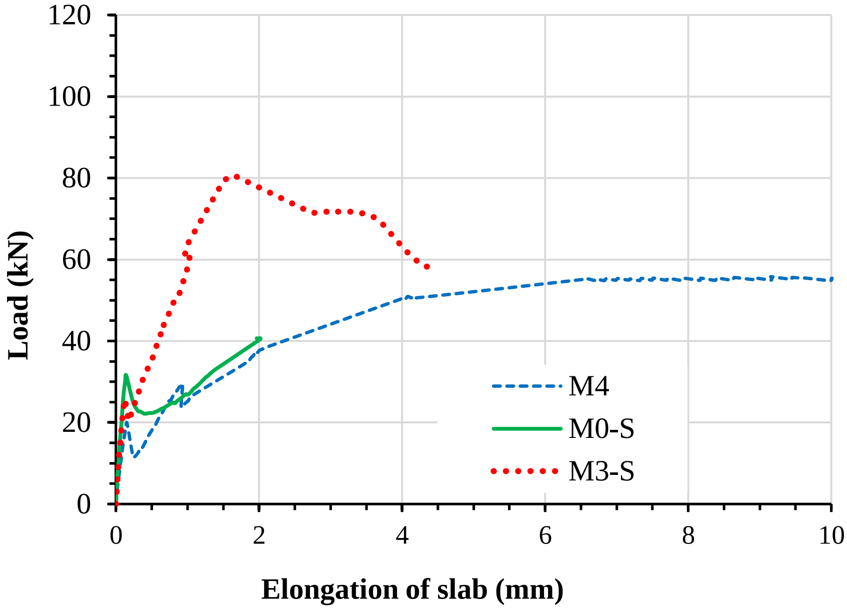

Figure 3.21 Load versus total elongation of the slabs measured by horizontal LVDTs mounted at the end of slabs no. 1-3.

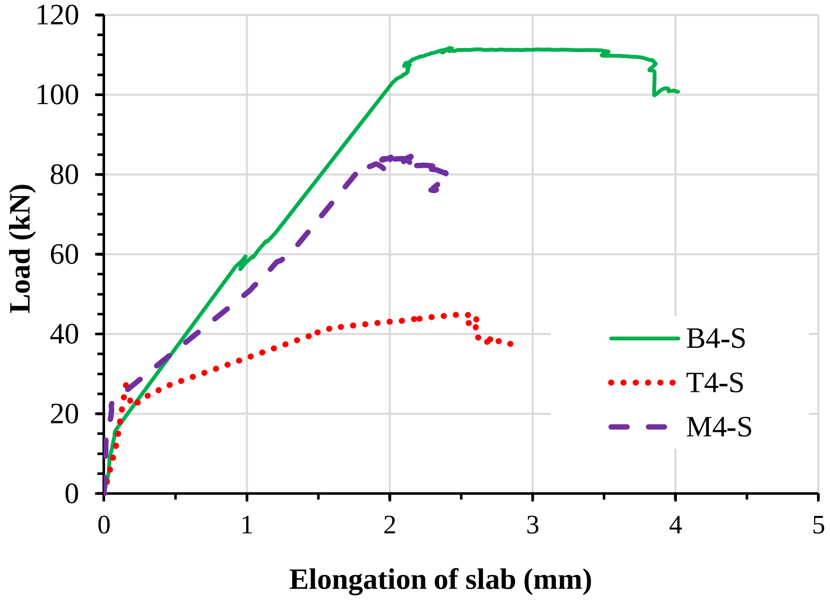

Figure 3.22 Load versus total elongation of the slabs measured by horizontal LVDTs mounted at the end of slabs no. 4-6.

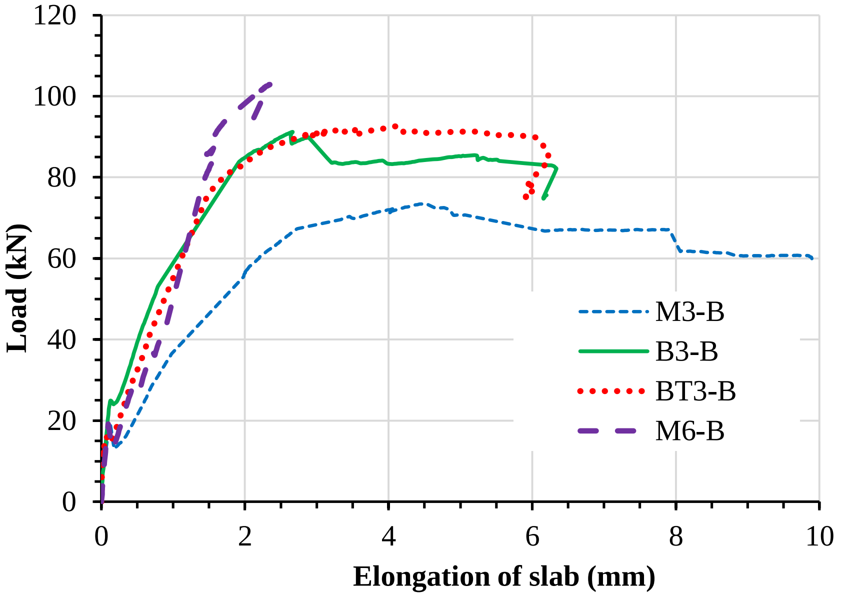

Figure 3.23 Load versus total elongation of the slabs measured by horizontal LVDTs mounted at the end of slabs no.7-10.

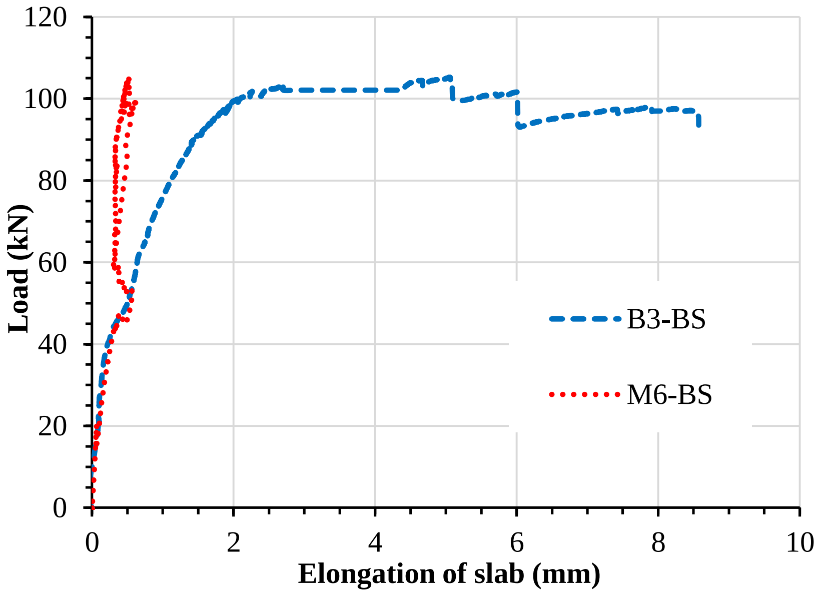

Figure 3.24 Load versus total elongation of the slabs measured by horizontal LVDTs mounted at the end of slabs no.11-12.

3.3.3. Local response (Load vs strain)

Plots of applied load versus the average tensile strain in the reinforcing bars (average of strain gauge St-SG(1) and St-SG(2) at mid-span, see Figure 3.8a) are shown in Figure 3.25 to Figure 3.28. It is observed that in all specimens except for T4-S, yielding of steel bars has occurred before the peak load capacity of the slabs is reached. Moreover, curves of applied load versus concrete compressive strain at mid-span of slabs (results of concrete strain gauge C-SG(1), see Figure 3.8a) are shown in Figure 3.29 to Figure 3.32. It is seen that in all specimens except for M0-S, the strain in the farthest compressive fibre of the concrete section at mid-span has reached values greater than the ultimate strain of concrete (i.e. $\varepsilon_{cu} = 0.003$) adopted in design codes. With regard to plots of strain in Figure 3.25 to Figure 3.32, it can be concluded that the failure mode of the tested precast slabs (except T4-S and M0-S) is not fully brittle and some level of ductility is available in the transversely confined slabs. The brittle failure mode of M0-S can be attributed to lack of conventional reinforcement in the slabs, whereas the brittle failure mode of T4-S is due to the over reinforcement (ρ= 2.1%) in the slab.

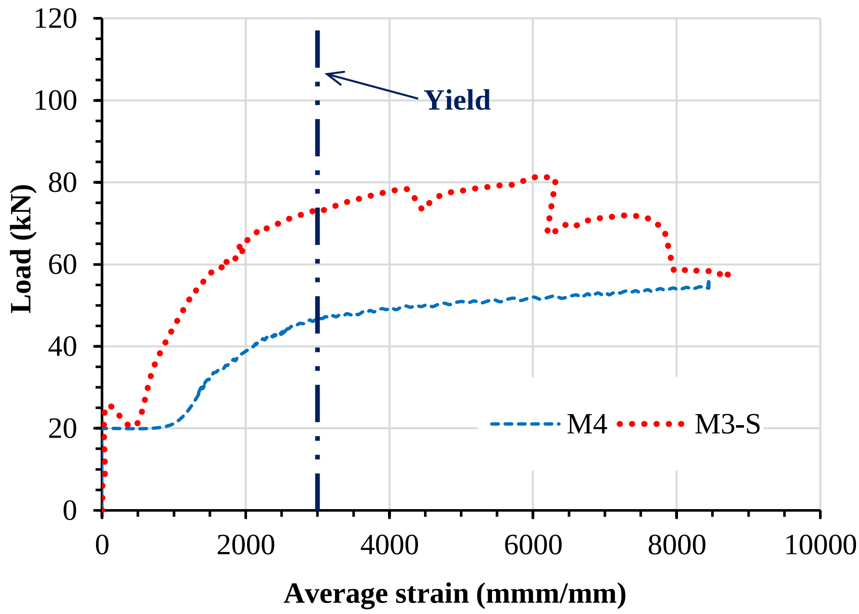

Figure 3.25 Load versus tensile strain in reinforcing steel bars (St-SG1) at mid-span of slabs no. 1 and 3.

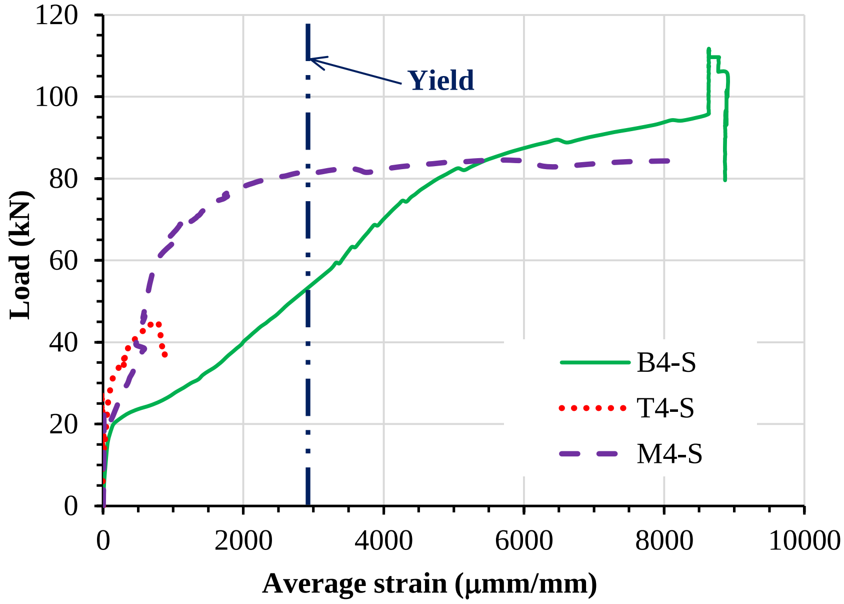

Figure 3.26 Load versus tensile strain in reinforcing steel bars (St-SG1) at mid-span of slabs no. 4-6.

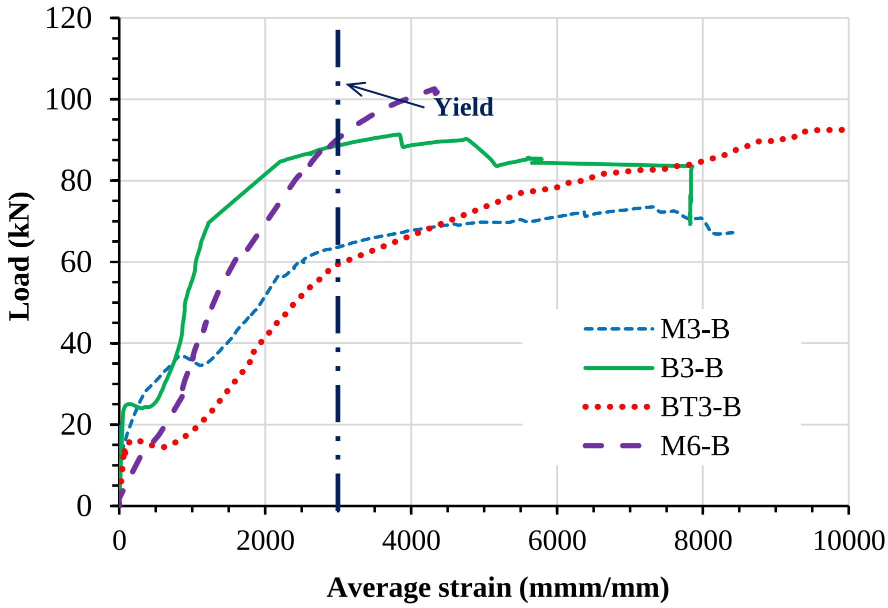

Figure 3.27 Load versus tensile strain in reinforcing steel bars (St-SG1) at mid-span of slabs no. 7-10.

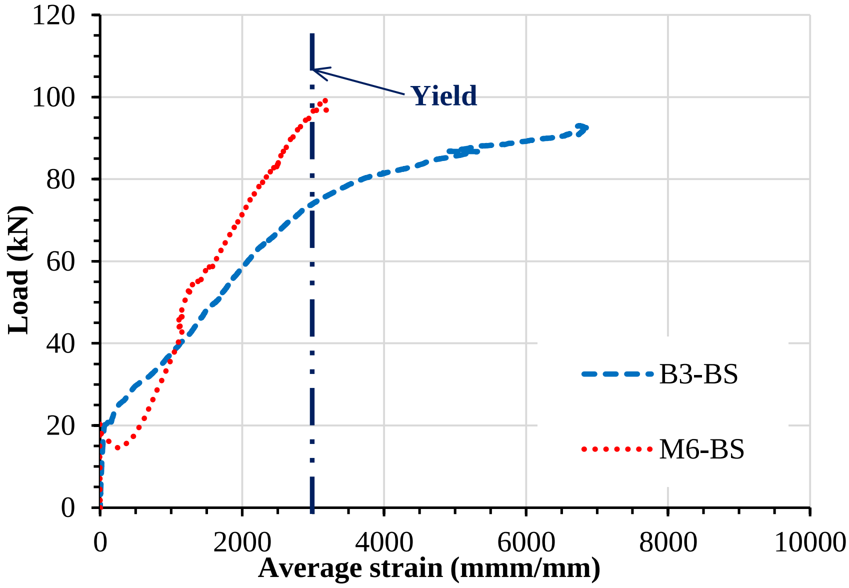

Figure 3.28 Load versus tensile strain in reinforcing steel bars (St-SG1) at mid-span of slabs no. 11-12.

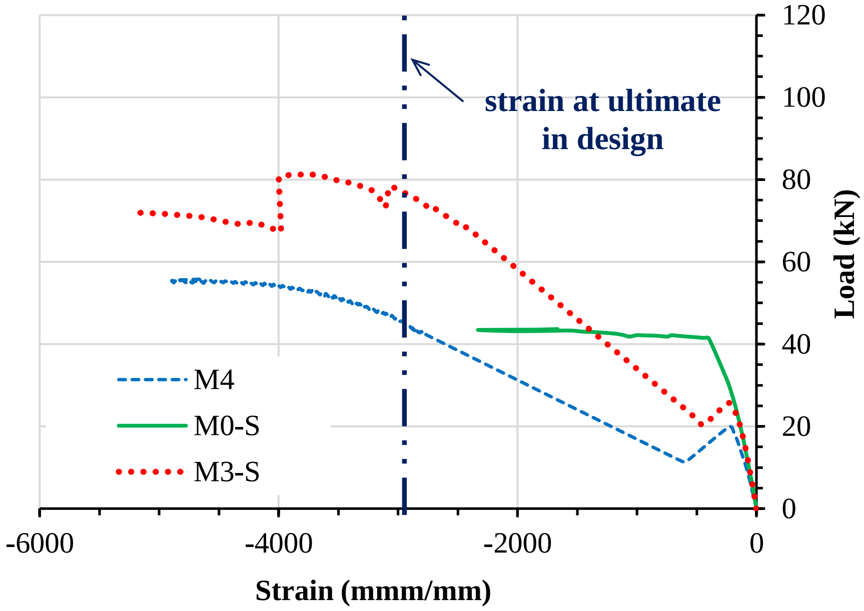

Figure 3.29 Load versus concrete compressive strain at mid-span on the top surface of the slabs no. 1-3.

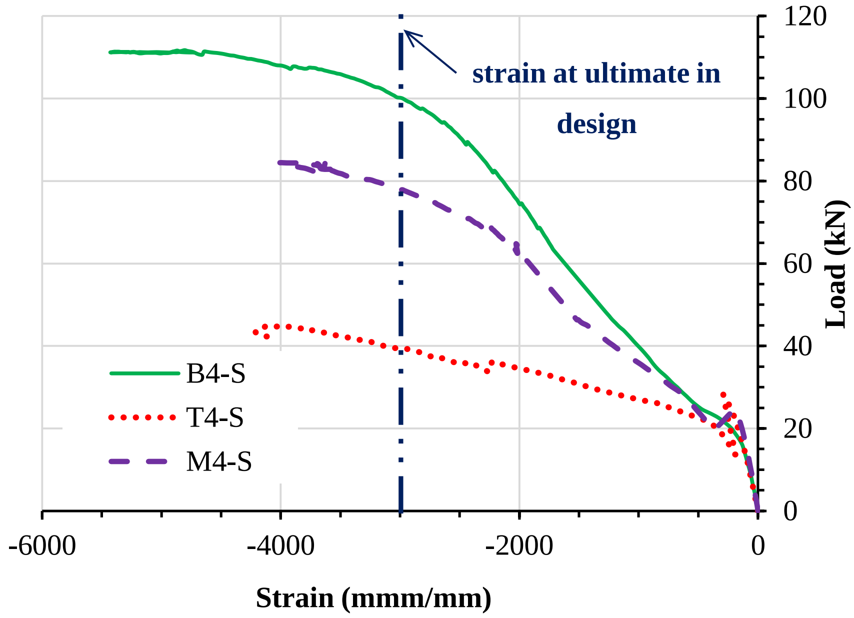

Figure 3.30 Load versus concrete compressive strain at mid-span on the top surface of the slabs no. 4-6.

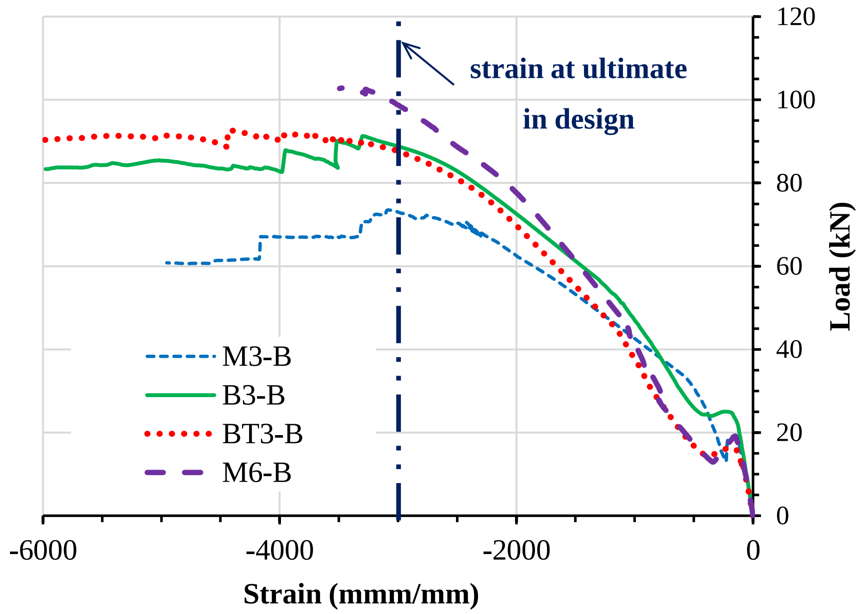

Figure 3.31 Load versus concrete compressive strain at mid-span on the top surface of the slabs no. 7-10.

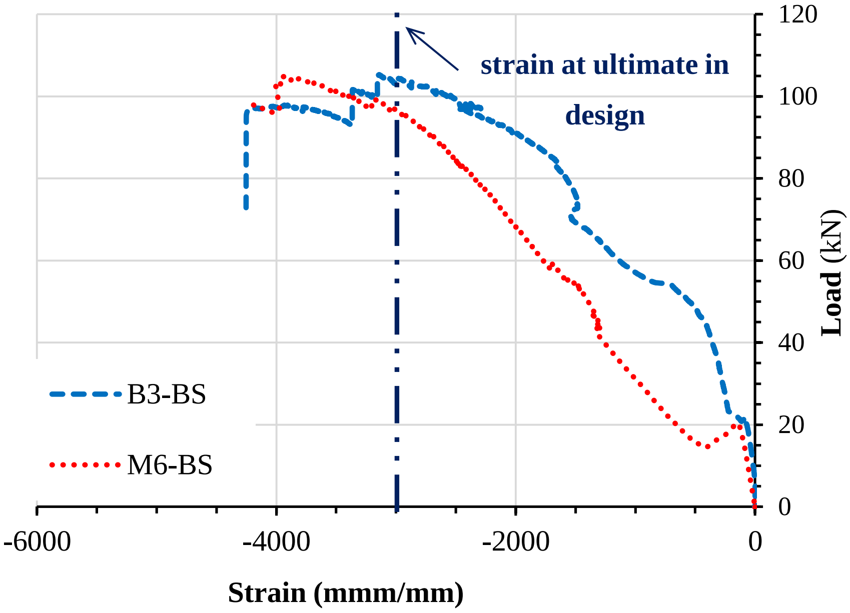

Figure 3.32 Load versus concrete compressive strain at mid-span on the top surface of the slabs no. 11-12.

Plots of applied load versus average tensile strain in the cross-bracings (average results of strain gauges St-B-SG 1 to 4) and in the straps (average results of strain gauges St-S-SG1 and 2) are shown in Figure 3.33 to Figure 3.37. It is seen that the cross-bracings and straps remain within their elastic range of behaviour (i.e. strain in cross-bracings and straps is below $\varepsilon_y = 0.0016$, yield strain of the 300PLUS grade steel). Furthermore, it can be concluded that the friction grip bolted connections employed in the deconstructable deck slabs have been effective in preventing the relative slip between different structural components (i.e. precast slab, transverse confining system and steel girders). This is evident from the strains (in the transverse confining system) that continuously increase/decrease as the applied load increase/decrease. Furthermore, it can be seen from comparing Figure 3.35 and Figure 3.37 that strain in bracing members of specimens confined with combination of cross bracing and straps reduced significantly in comparison with strain in bracings of specimens confined only by cross bracings and it can be concluded the straps has more prominent role to provide confinement for the combined system (i.e., cross bracings plus straps).

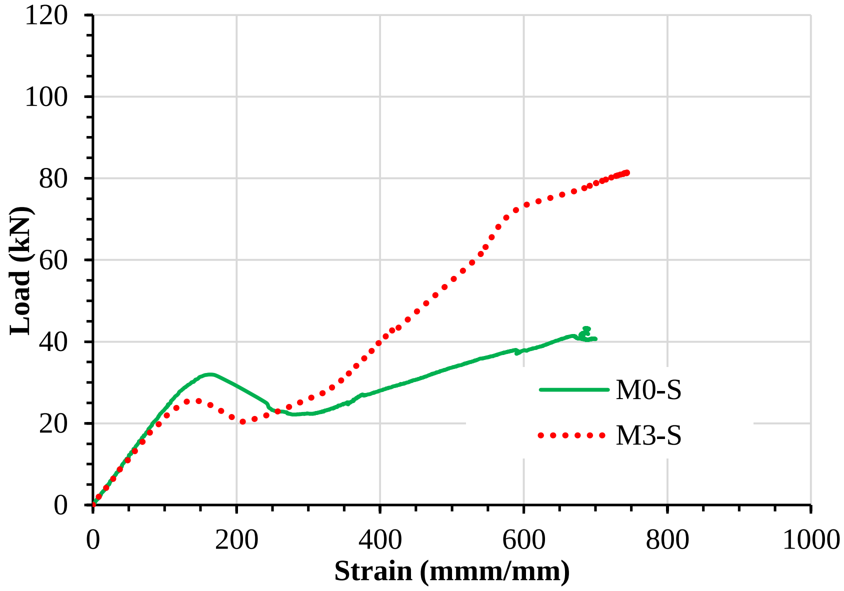

Figure 3.33 Load versus tensile strain in the straps of the transversely confined slabs no. 1-3.

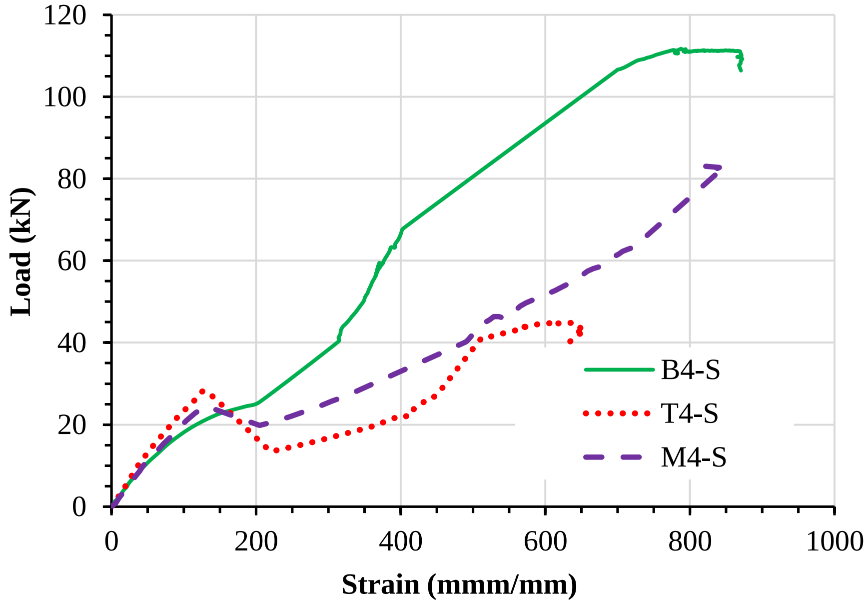

Figure 3.34 Load versus tensile strain in straps of the transversely confined slabs no. 4-6.

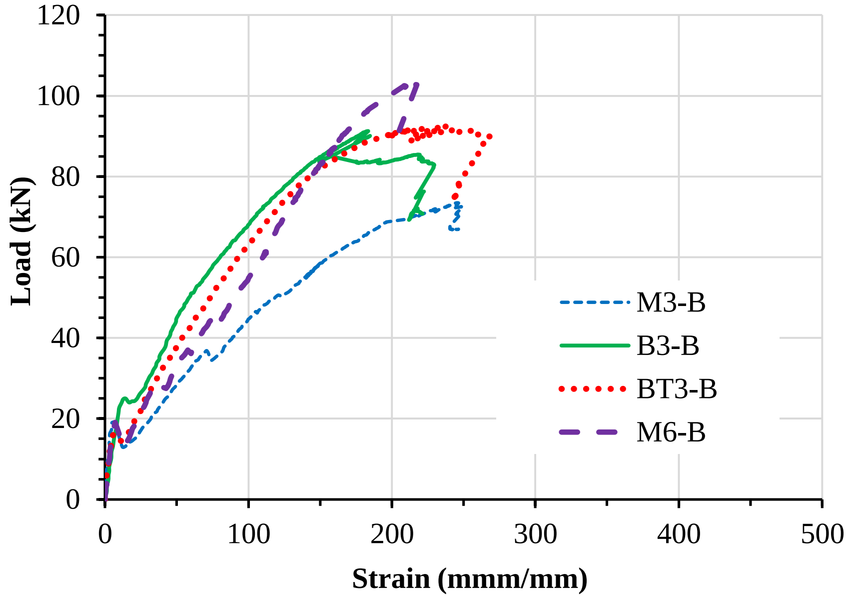

Figure 3.35 Load versus tensile strain in the cross bracings of the transversely confined slabs no. 7-10.

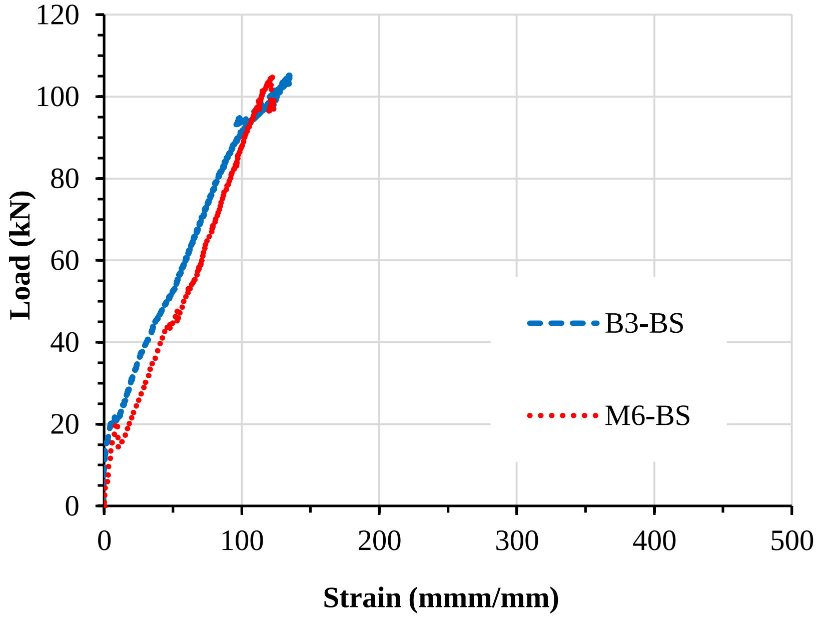

Figure 3.36 Load versus tensile strain in the cross bracings and straps of the transversely confined slabs no. 11-12, (strain in cross bracing).

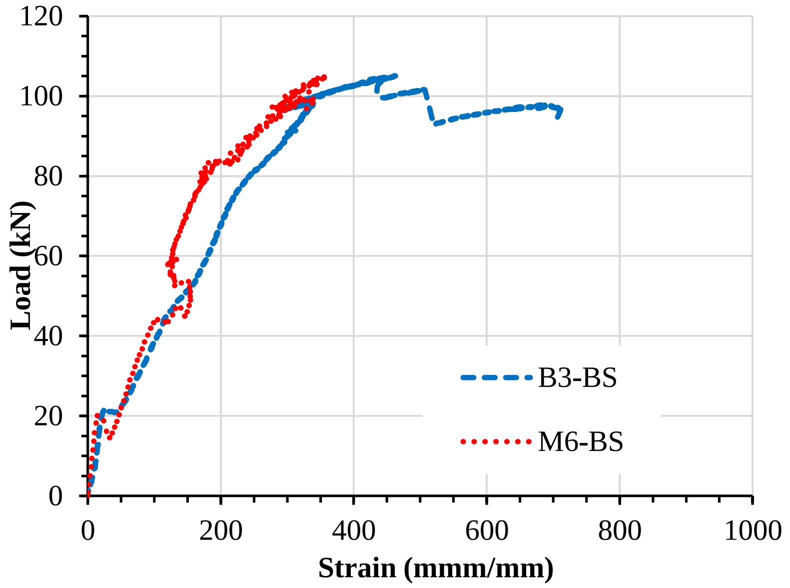

Figure 3.37 Load versus tensile strain in the cross bracings and straps of the transversely confined slabs no. 11-12, (strain in straps).

3.3.4. Deformability and robustness of precast slabs

The strength enhancement provided by development of arching action in the transversely confined concrete slabs is usually associated with a reduction in the ductility and deformability of the slabs. In this section, the curvature ductility/deformability μ_{ψ} is used to evaluate the structural ductility/deformability of the proposed deconstructable deck slabs with transverse confining system. The μ_{ψ} is defined as

$$\mu_{\psi} = \left(\frac{\psi_{u}}{\psi_{0.001}} \right) \qquad \textbf{Equation 3.1}$$

where ψ_u and $\psi_{0.001}$ are the curvature at ultimate load and at the load corresponding to compressive strain of 0.001 in the concrete, respectively. It is noteworthy that the strain of 0.001 is assumed to be the beginning of inelastic deformation in concrete and accordingly $\psi_{0.001}$ denotes the curvature under service load condition (Van Erp 2001). In this study, the curvature ψ is obtained from

$$\psi = \frac{|\varepsilon_S - \varepsilon_C|}{d}$$ **Equation 3.2**

where ε_S is the tensile strain in steel bars, ε_C is the compressive strain in concrete (see Figure 3.8) and *d* is the effective depth of section given in Table 3.1.

In addition to μ_ψ, the robustness index *R* is also calculated for the slabs (Van Erp 2001). The robustness index *R* is defined as

$$R = \left(\frac{\Delta_u}{\Delta_{0.001}}\right) \times \left(\frac{P_u}{P_{0.001}}\right)$$ **Equation 3.3**

where $\Delta_u / \Delta_{0.001}$ is the mid-span displacement at ultimate relative to the value at concrete compressive strain of 0.001 and $P_u / P_{0.001}$ is the load at ultimate relative to the value at a concrete compressive strain of 0.001. It is noteworthy that the *R* index is similar to the *J* factor introduced by Mufti, Newhook & Tadros (1996) and adopted by Canadian Highway Bridge Design Code (2006) for evaluating the ductility/deformability of the FRP reinforced/strengthened concrete members. Accordingly, in this study the *R* index and *J* factor are used interchangeably.

The deformability index μ_ψ and the robustness index *R* of the precast slabs in the transversely confined system are given in Table 3.2. It is observable that specimen M4 without transverse confining system has the highest robustness/deformability indices (R = 38.3 and μ_ψ= 12.8), whereas the lowest robustness/deformability indices belong to specimens M0-S (R = 1.2) and T4-S (R = 4.8 and μ_ψ= 4.7). As discussed before, the specimens M0-S and T4-S failed in a brittle mode and this is also evident from the robustness/deformability indices. The brittle failure of specimens M0-S and T4-S can be attributed to lack of reinforcement (ρ= 0%) and over reinforcement (ρ= 2.1%), respectively. The variation of the *R* index with respect to the ratio of confining system stiffness $K_{\text{Confining system}}$ (in the transverse direction) divided by the axial stiffness of slab K_{Slab} is shown in Figure 3.38. It is seen that the *R* index of all slabs, except for specimen M0-S, is above the minimum requirement of *J*= 4.0 specified in CHBDC code (2006) for rectangular sections with FRP reinforcements.

The normalised experimental peak load capacity of the specimens versus the relative stiffness of the transverse confining system (i.e. $K_{\text{Confining system}}/K_{\text{Slab}}$) is shown in Figure 3.39. It is noteworthy that the experimental peak load capacities were normalised with respect to peak load capacity obtained from an elementary plastic hinge analysis and assuming pinned conditions for the supported edges of the slab. The peak load carrying capacities of the specimens obtained from plastic analysis are given in Table 3.2. With regard to Figure 3.39, it can be concluded that ignoring the strength enhancement provided by arching action in the transversely confined deck slabs can lead to overly conservative design; for example, the failure load of specimens M6-B and B4-S, is underestimated by 54% and 77%, respectively. Despite lower stiffness of straps/ties compared to cross-bracings, it is observable that the strength enhancement provided by the transverse ties/straps under the slabs is larger than that provided by the cross-bracings away from the slabs (see Figure 3.39). This can be attributed to formation of a closed force loop, when the transverse confining system (ties) are right under the RC slabs and directly connected to the slabs.

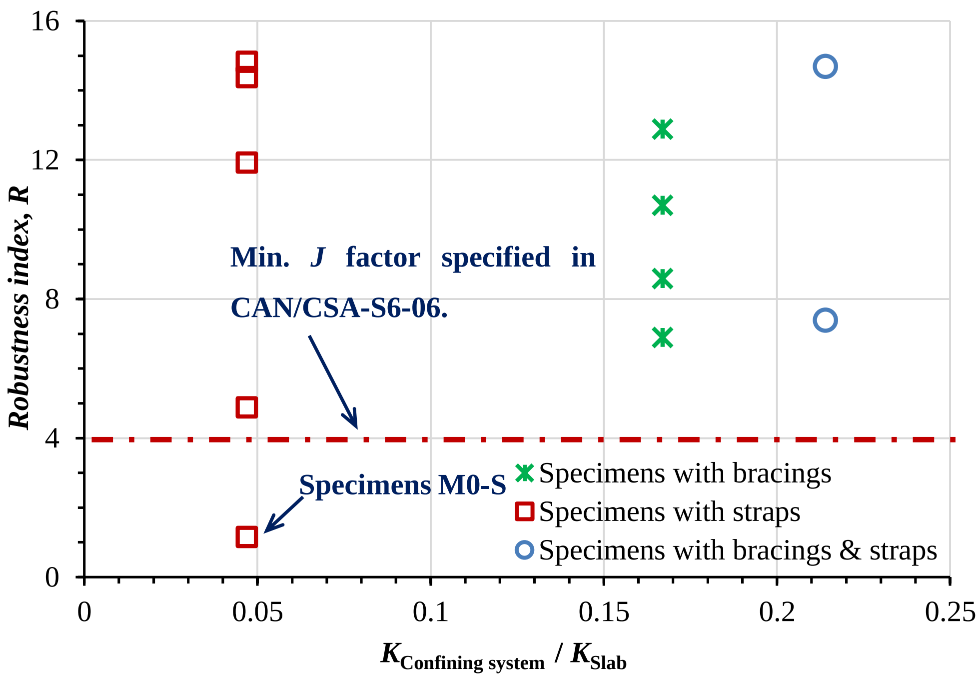

Figure 3.38 Variation of the robustness index R of slabs with respect to the relative stiffness of the transverse confining system.

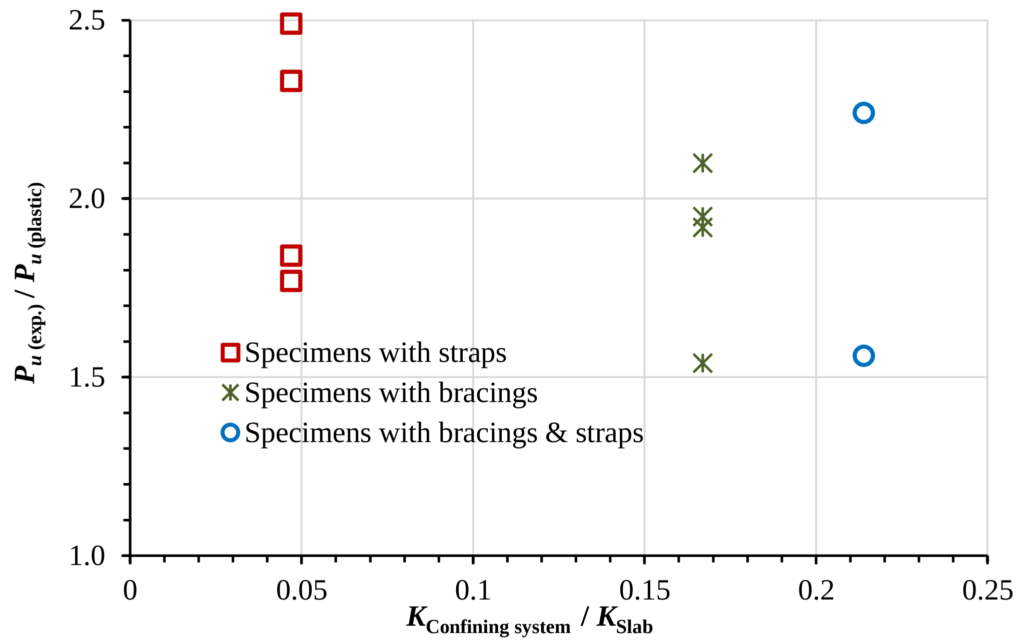

Figure 3.39 Normalised experimental peak load capacity of the transversely confined slabs with respect to the peak load capacity obtained from an elementary plastic analysis versus relative stiffness of the transverse confining system.

3.4. Conclusions and discussions

The enhancing effect of arching action in the transversely confined concrete deck slabs has been well established in the literature. However, the existing bridge decks use cast-in-situ concrete slabs with permanent connection to the girders and transverse confining system that can hinder deconstruction and repair of the concrete deck slabs. Accordingly, this chapter aims to propose and experimentally investigate the structural behaviour of transversely confined precast deck slabs in a deconstructable bridge deck. The proposed concept of deconstructable deck slabs with bolted shear connectors and transverse confining system is not only applicable for constructing new bridge decks, but also the concept can be used for strengthening existing concrete decks by externally mobilising the arch action mechanism in the concrete deck slabs.

Twelve precast deck slabs with either cross-bracings or ties/straps as transverse confining system are fabricated and tested under a monotonically increasing force applied at the mid-span and benchmark experimental results for future validation of numerical/analytical models are provided. Also, the following conclusions are drawn from the laboratory test results;

- The strain in transverse ties/straps and cross-bracings continuously increased as the load increased. This demonstrated the efficiency of the bolted shear connectors in preventing relative slip between the precast slab and the transverse confining system. It should be noted this full interaction has a vital role for mobilising arch action in the precast slabs of the proposed deconstructable system. Accordingly, the transverse ties (straps) and cross-bracings can be used in conjunction with post-installed bolted connections to mobilise the arch action and improve the loading capacity of the existing bridge decks with cast-in-situ as well as precast concrete slabs. However, in terms of ability to mobilise arch action, the transverse ties are much more effective than cross-bracings.

- The strength enhancement (due to development of arch action) observed in the transversely confined decks would have significant implications for strength assessment of existing RC deck slabs, where transverse bracings are typically provided for the steel–concrete composite decks in order to prevent overturning and lateral torsional buckling of steel girders during the construction. However, the effect of these transverse bracings on the ultimate load-carrying capacity of the concrete decks is not taken into account in the current strength assessment practices. In this study, the experimental peak load capacity of the concrete deck slabs ($\rho<1{\cdot}5\%$) with transverse cross-bracings was around 60–70% more than the peak load predicted by the plastic hinge analysis (see Table 3.2), which is demonstrative of the level of conservatism in the current strength assessment practices for concrete deck slabs.

- With regard to Figure 3.39 and $P_{u(Plastic)}/P_{u(Exp.)}$ reported in Table 3.2, it can be concluded that ignoring the strength enhancement provided by arching action in the transversely confined deck slabs can lead to overly conservative design. Accordingly, it is recommended that for accurate strength assessment of existing concrete decks with transverse cross-bracings, the effect of arch action is taken into account by using a non-linear FE model or a simplified model such as the one described by Yu and Tan (Yu & Tan 2014).

- Except for slab T4-S that was overly-reinforced ($\rho = 2.1\%$), in all the other transversely confined slabs ($\rho < 1.5\%$), the failure was associated with development of cracks and yielding of steel bars in the soffit of the slab at mid-span, followed by crushing of concrete on the top surface of slabs at the mid-span and onset of cracks at the supported edges of the slab. In slab T4-S, yielding of the flexural reinforcements did not take place.

– The curvature-based ductility/deformability index μ_{ψ} and the robustness index *R* for all transversely confined precast slabs were calculated. Except for specimens T4-S (overly-reinforced) and specimen M0-S (no reinforcement), in all other specimens the μ_{ψ} index was greater than 6.0 and *R* index was greater than 4.0. With regard to the similarity between *J* factor used in CHBDC (2006) and *R* index adopted in this study, it can concluded that all specimens (except for T4-S and M0-S) comply with minimum ductility/deformability requirement of *J*= 4.0 specified in CHBDC (2006). This observation confirms the brittle failure mode of specimens T4-S and M0-S. Accordingly; a maximum reinforcing ratio of 1.5% is recommended to avoid brittle failure (concrete crushing) in the transversely confined concrete deck slabs with cross-bracings or ties.

CHAPTER 4

DECONSTRUCTABLE STEEL-FIBRE REINFORCED CONCRETE DECK SLABS WITH TRANSVERSE CONFINING SYSTEM

4. Deconstructable Steel-Fibre Reinforced Concrete Deck Slabs with Transverse Confining System

4.1. Introduction

As stated in literature review, the idea of mobilizing arching action to develop slab decks totally or partially devoid of conventional reinforcing steel have been investigated in various studies (Bakht & Lam 2000; Klowak, Memon & Mufti 2006; Mufti, Bakht & Newhook 2004). However, less attention has been paid to development of compressive membrane action and its beneficial effect on the ultimate load capacity and structural behaviour of steel fibre reinforced concrete (SFRC) slabs and bridge decks (Bednář et al. 2013; Belletti, Vitulli & Walraven 2014).

In general, over the past two decades, the application of fibre reinforced concrete (FRC), particularly steel fibre reinforced concrete (SFRC), has gained popularity in the construction industry (Alberti et al. 2014; Amin, Foster & Watts 2015; Foster 2009), and a significant body of experimental and analytical studies have been conducted to characterise mechanical properties and behaviour of SFRC at the materials and structural level (Amin, Foster & Muttoni 2014; Trapko 2014; Yap et al. 2014). The studies undertaken by different research groups cover various aspects of steel fibre reinforced concrete members, such as punching shear capacity of SFRC slabs (Maya et al. 2012), development of high performance concrete with fibres (Kaïkea et al. 2014; Yap et al. 2014), energy absorption and blast/impact resistance of fibre reinforced panels and slabs (Haido et al. 2011; Hao & Hao 2013; Mohammadi et al. 2009; Pantelides et al. 2014; Su, Xu & Ren 2014), development of models and design provisions for predicting the punching load capacity of slabs (Neto, Barros & Melo 2013, 2014), bond characteristics of SFRC (García-Taengua, Martí-Vargas & Serna 2014; Schumacher et al. 2004) and development and application of reliable constitutive laws for modelling the behaviour of FRC (Blanco et al. 2014; Luccioni et al. 2012; Sanjayan, Nazari & Pouraliakbar 2015; Xu, Hao & Li 2012).

In fact, the use of discontinuous reinforcement (fibres) in concrete increases the post-cracking residual tensile strength and improves the behaviour of the material with the fibres bridging crack openings. Accordingly, the improvements achieved by adding fibres are commonly considered to be significant within the range of service loads where the reduction in the deflections and crack width are significant (Abas et al. 2013). It has been demonstrated that the inclusion of steel fibres in concrete can improve flexural-shear/shear, bending moment capacity and punching shear capacity of beams and slabs, respectively. The enhancing effect of steel fibres on the shear/punching shear capacity of beams/slabs has been extensively investigated (Kwak et al. 2002; Maya et al. 2012; Meda et al. 2005), however, less attention has paid to flexural strength enhancement provided by steel fibres in suspended concrete slabs or slabs on-girders with and without conventional reinforcing bars (Michels et al. 2012). Application of steel fibres as the secondary reinforcement in the slabs can improve strength and ductility and where it can be demonstrated that steel fibres can be used as main reinforcement in bridge decks (provided ductility comparable to conventionally reinforced slab deck is achieved with commercially viable fibres dosages) there is significant potential for reducing the cost of materials and labour and increasing the speed of construction. In recent researches the mechanical properties of concrete reinforced with recycled tyre steel fibres have been investigated to evaluate if the concrete with recycled steel fibres could meet the standard requirements for future industrial use in large scale (Al-Kamyani et al. 2018; Hu et al. 2018).

Therefore, in this chapter, behaviour of the transversely restrained precast SFRC slabs in a demountable composite bridge deck will be investigated experimentally to provide the benchmark data on structural behaviour of such slab deck system. For this purpose, fourteen one-half scale single-span precast concrete slabs compositely connected to steel girders using post-installed bolted shear connectors (PBSCs) are tested under a displacement-controlled point load applied at the mid-span. The dosage of steel fibres, proportion of conventional reinforcing steel bars, concrete compressive strength and the type, location and stiffness of restraining system (i.e. cross-bracings and straps) in the transverse direction are the main variables in the experimental programme. The global (applied load and vertical displacement at mid-span, rotation and transverse extension and failure mode) as well as the local response (strain in the steel bars, cross-bracings/straps and concrete) of the SFRC slabs were measured to determine how steel fibres contribute to ultimate flexural capacity of the concrete deck slabs with and without conventional steel bars. The experimental data are also used to evaluate the ductility of transversely restrained precast SFRC decks that can develop arch action. It should be mentioned fabrication and preparation of slabs and steel girders has been explained in previous chapter and thus, in this chapter only a summary of geometry test set up and instrumentation will be described. However, in material section the properties of steel fibres and SFRC specimens will be discussed.

4.2. Experimental program

4.2.1. Geometry and test setup

Fourteen one-half scale precast SFRC/RC slab decks were constructed with different reinforcing bar proportions/configuration, steel fibre dosage, concrete compressive strength and four different types of transverse restraining systems. As described in Chapter 3, the real (prototype) precast slab is part of a 12 m long simply supported steel-concrete composite bridge deck in NSW, Australia. The bridge deck is 7.0 m wide with no cantilever and it is supported by four steel girders 2.2 m c/c apart (see Figure 4.1). The bridge can accommodate two standard lanes, each lane being 3.2 m wide according to Australian standard AS5100.2 (2004) specifications.

The concrete deck slab in the transverse direction was designed as simply supported (i.e. spanning between two adjacent girders, see Figure 4.1) and the slabs complied with the minimum design requirements of AS5100.5 (2004). This study focuses on the behaviour of a one-half scale precast slab from the middle module of the real bridge deck (see Figure 4.1). The one-half scale precast slabs were 100 mm thick, 600 mm wide and 1100 mm long and they had haunch at each end, i.e. where the slabs were connected to the top flange of a 310UB32 supporting steel girder-Grade 300PLUs (Figure 4.2). The outline of geometry and test set up, dimensions of the precast slabs, size of sections and configuration of restraining system in the transverse direction are shown in Figure 4.2.

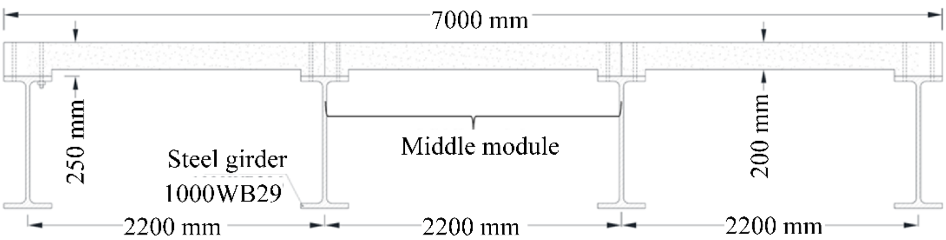

Figure 4.1 Outline of the geometry cross-section of real composite bridge deck.

It is noteworthy that the behaviour of one-span slab tested in this study is slightly different than the real bridge deck in which the slab deck continuity is preserved across multiple girders. In terms of stiffness, shear-bending moment interactions and bending moment regimes the continuous bridge deck exhibit smaller deflections than the protypes tested in this study and the real bridge decks are simultaneously subjected to both sagging and hogging bending moments whereas the single span deck slabs are only subjected to sagging bending moments.

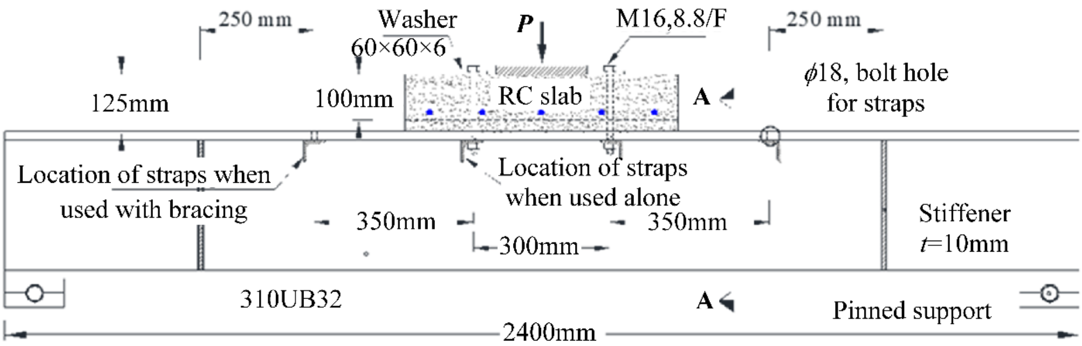

(a)

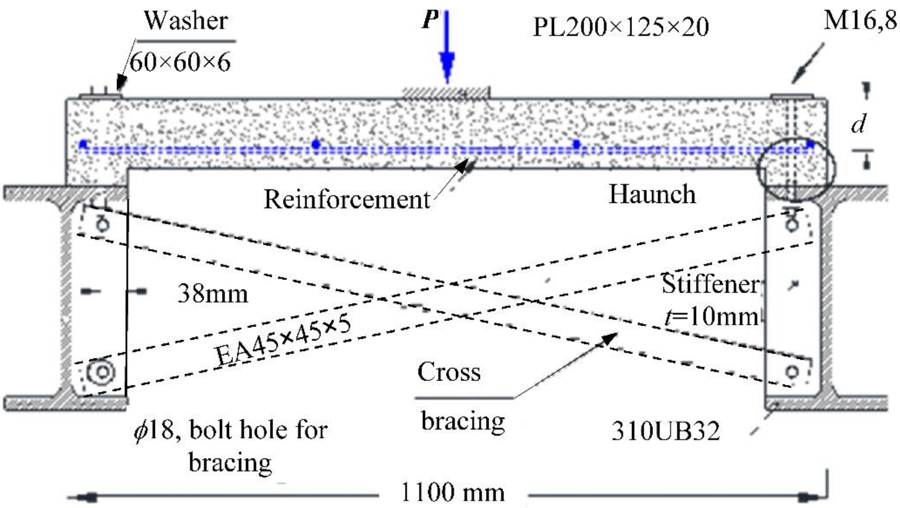

(b)

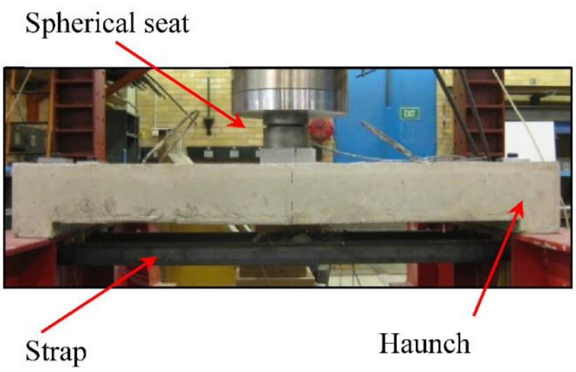

(c)

Figure 4.2 Outline of the geometry, cross-section and configuration of restraining system in the transverse direction and test set up for the one-half scale precast RC/SFRC slabs compositely connected to 310UB32 steel girders using PBSCs.

Details of the reinforcing bars including proportion, location and effective depth of the precast slabs (i.e. distance between the centroid of the flexural reinforcement and the top surface of the slab, d in Figure 4.2(b), are given in Table 4.1. The slabs were tested under a monotonically increasing displacement-controlled point load applied at the mid-span. The load was applied to the mid-span of slabs via a 300 KN hydraulic actuator operated in displacement control at a rate of 0.1 mm/s (Figure 4.2). As discussed in Chapter 3, in this study the composite action between precast SFRC/RC slabs and supporting girders is provided by post-installed bolted shear connectors PBSCs to facilitate dismantling and reusing of the structural components. At each end, the precast slabs were compositely connected to the top flange of a 310UB32 using two M16, 8.8/FT (friction) bolts. The M16, 8.8/F shear connectors were tightened by a torque wrench to provide a post-tensioning force of $0.4f_{uf} = 330MPa\ \gamma$ (f_{uf} being the tensile strength of class 8.8 bolts) in the connectors.

Table 4.1 Designation of specimens.

Specimen No.	Designation of specimens#	Numbers & location of reinforcing bars	f_{cm} (MPa)	Effective depth d (mm)	ρ_F Fibre dosage (%)	$\rho = A_{st}/bd$ (%)	$\rho_{Vol.} = A_{st}/bh$ (%)	$\rho_{Total} = \rho_F + \rho_{Vol.}$	Restraining system in the transverse direction ## (see Figure 4.2)	
1	SF00- S	----	60	----	0.00	----	----	0.00	Strap	under the slab
2	SF50- S	----		----	0.50	----	----	0.50	Strap	
3	SF50	----		----	0.50	----	----	0.50	--------------	
4	SF25- S	----		----	0.25	----	----	0.25	Strap	
5	SF25- S-M2	2N10 (middle)		56	0.25	0.48	0.26	0.51	Strap	
6	SF00 -M3	3N10 (middle)		56	0.00	0.72	0.40	0.40	--------------	Away from the slab
7	SF00-B -M3	3N10 (middle)	70	56	0.00	0.72	0.40	0.40	Bracing	
8	SF00-BS-M3	3N10 (middle)		56	0.00	0.72	0.40	0.40	Bracing + strap	
9	SF25-B	----		----	0.25	----	----	0.25	Bracing	
10	SF25-BS	----		----	0.25	----	----	0.25	Bracing + strap	
11	SF50-B	----		----	0.50	----	----	0.50	Bracing	
12	SF50-BS	----		----	0.50	----	----	0.50	Bracing + strap	
13	SF25-B -M2	2N10 (middle)		56	0.25	0.48	0.26	0.51	Bracing	
14	SF25-BS-M2	2N10 (middle)		56	0.25	0.48	0.26	0.51	Bracing + strap	

SFxx: 0.xx% steel fibre dosage, -B: bracing, -S: straps and -BS: bracing + strap.

The cross-bracings and straps were made of Equal Leg Angle, L45×45×5EA and L45×45×3EA-Grade 300PLUS, respectively.

The total volumetric ratio of reinforcement including steel bars and fibres.

The transverse restraining systems were cross-bracings only, strap only and combination of straps and cross bracings. The cross-bracings and straps were made of equal leg angle section, L45×45×5EA and L45×45×3EA of Grade 300PLUS steel, respectively. The cross-bracings were bolted to the stiffeners, whereas the transverse straps were bolted to the top flange of the steel girders using 16 mm diameter high-strength 8.8 bolts (see Figure 4.2). Two different arrangements were considered for the straps, i.e. straps under the slab and straps away from the slabs. The latter arrangement was when straps were used in conjunction with cross bracings (see Figure 4.2). Furthermore, the connection of cross-bracings and straps to the web-stiffeners and top flange of the 310UB32 steel girders were provided by the M16, 8.8/TF bolts tightened to a shank tension of $0.6f_{uf} = 495MPa$ (see Figure 4.2).

4.2.2. Material

Reinforcing bars

The reinforcing steel bars in the slabs were 10 mm diameter ribbed bars. The characteristic yield strength of steel bars was 500 MPa and the mean yield strength of the steel bars was $f_y = 575MPa$ (obtained from direct tension test on three specimens). The ultimate strength of steel bars was $f_u = 680MPa$ and average uniform elongation of bars at f_u was $\varepsilon_u = 8\%$. The strain- stress diagram for average of these three tensile tests is shown in Figure 4.3. The standard deviation of the tested reinforcing bars was 9 MPa.

Steel fibre reinforced concrete

The steel fibre reinforced concrete slabs were cast with 50 and 60 MPa concrete having maximum aggregate size of 10 mm. The steel fibres were 60 mm long by 0.9 mm diameter Dramix 5D-65/60-BG (see Figure 4.4a) with nominal strength of 2000 MPa at an average uniform elongation more than 5% (see Figure 4.4b). The 5D steel fibres can provide perfect anchor Figure 4.4a) and accordingly can be used for the most demanding structural applications.

In addition to the slabs, twenty four 300 mm high by 150 mm diameter cylinders and twelve 150 mm by 150 mm by 500 mm prisms according to ASTM (2005) were cast and tested to characterise the mechanical properties of SFRC including average compressive strength of concrete f_{cm}, splitting tensile strength of concrete $f_{ct,sp}$ (split cylinder), modulus of rupture $f_{ct,fl}$ and modulus of elasticity E_0 of concrete at 28 days and on the testing day. The testing specimens cast in two batches with the same concrete mix and chemical composition. The mean compressive strength of concrete f_{cm} was obtained from the average of three 300 mm high by 150 mm diameter cylinders tested after 28 days, in accordance with the Australian Standard AS1012.9 (1999). The stress-strain curve of the plain concrete and the SFRC (Figure 4.5) at the time testing obtained from a uniaxial compression test on 300 mm by 150 mm diameter cylinders. The average compressive strength of concrete is given in Table 4.1 and the splitting tensile strength $f_{ct,sp}$,modulus of rupture $f_{ct,fl}$ and elastic modulus E_0 of SFRC at 28 days are given in Table 4.2.

The SFRC modulus of rupture was obtained from the four-point bending test on prisms according to ASTM Standard (2005) testing procedure (see Figure 4.6) and the modulus of elasticity of SFRC was determined in accordance with AS1012.17 (1997). The average load versus mid-span deflection obtained from prism tests for the SFRC with 0.25% and 0.5% fibres and average compressive strength of 60 MPa and 70 MPa are shown in Figure 4.7 and Figure 4.8, respectively. The standard deviation for 60 MPa and 70 MPa SFRC was 3.5 MPa and 3.0 MPa, respectively.

It is noteworthy that a wide range of fibres are available in the market that can enhance mechanical properties of the concrete under service loading conditions. The mechanical of the concrete with such fibres under service loading condition have been subject of many experimental studies and it is well established that the performance of the fibre reinforced concrete depends on size and configuration of fibres. However, the 5D Dramix double hook long fibres used in this study are among few metallic fibres that can improve the structural performance of the concrete under ultimate limit state conditions which was the focus of present study. Therefore, in this study instead of using different steel fibres with different size and properties, one type steel fibre was used, and only effect of fibre dosage was considered as the main variable.

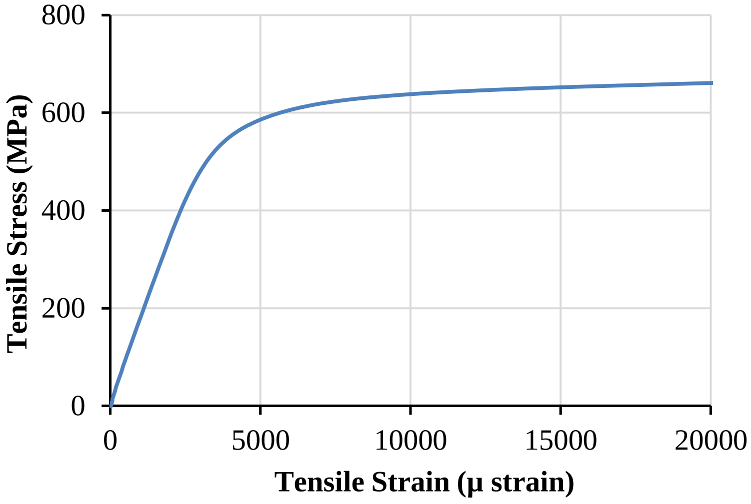

Figure 4.3 Uniaxial stress-strain diagram of reinforcing steel bars.

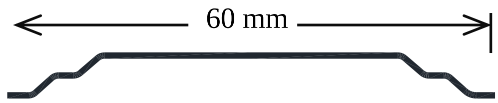

(a)

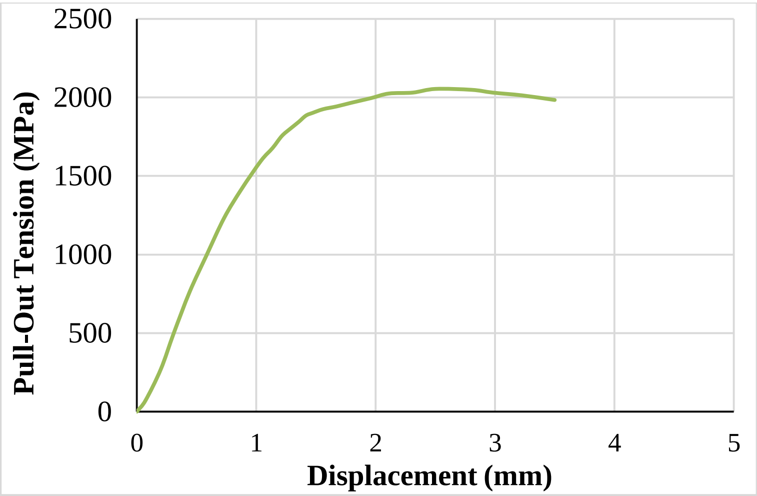

(b)

Figure 4.4 (a) Geometry of the Dramix 5D-65/60-BG steel fibre and (b) uniaxial stress-elongation diagram of 5D fibres(Bekaert 2012).

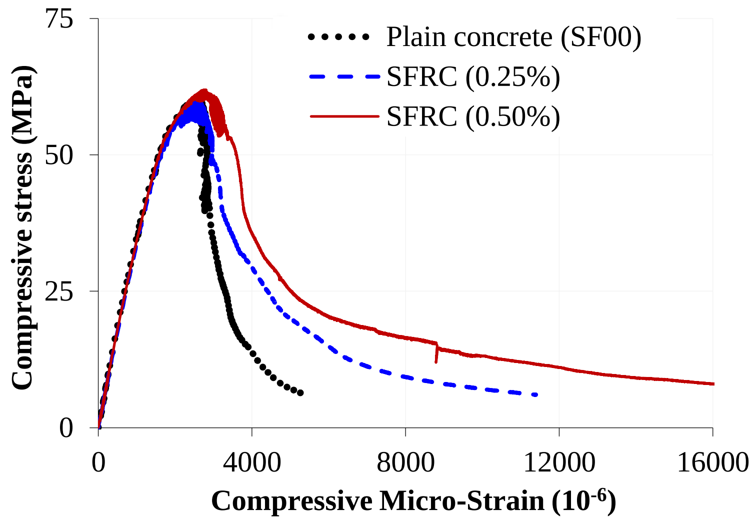

Figure 4.5 Uniaxial stress-strain diagram of plain and SFRC with 0.25% & 0.5% fibres.

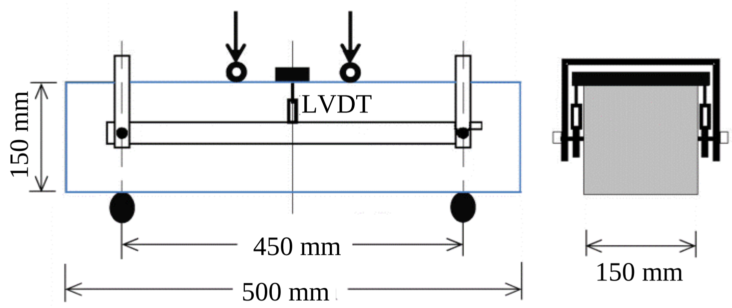

Figure 4.6 dimensions and set up of the prism test.

Table 4.2 Mechanical properties of SFRC (average of three specimens).

Compressive strength f_{cm} (MPa)	Fibre dosage (%)	splitting tensile strength $f_{ct,sp}$ (MPa)	Modulus of rupture $f_{ct,fl}$ (MPa)	Modulus of elasticity E_0 (MPa)	Tensile strength f_{ct} (MPa)#
60	0.25	7.2	5.90	32.7	3.9
	0.50	7.3	6.00	33.1	
70	0.25	7.7	6.20	36.5	4.2
	0.50	7.9	6.20	35.7	

The mean tensile strength of concrete was obtained from $f_{ct} = 0.5\sqrt{f_{cm}}$ (Amin, Foster & Muttoni 2014)

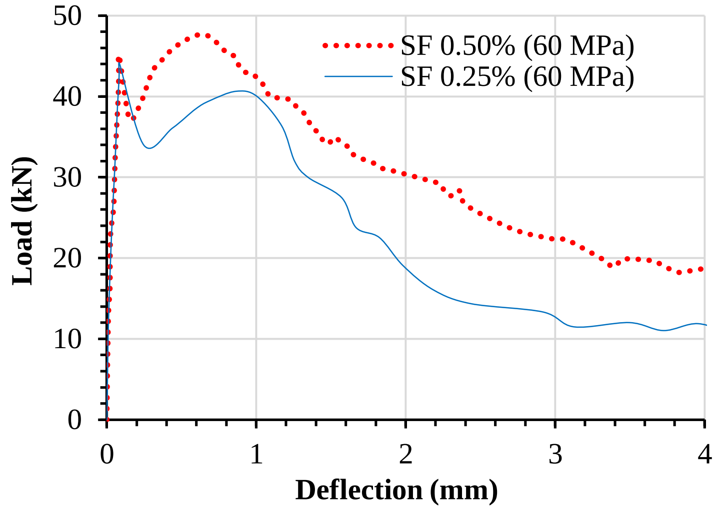

Figure 4.7 Average load versus mid-span deflection obtained from prism tests on SFRC with average compressive strength of 60 MPa.

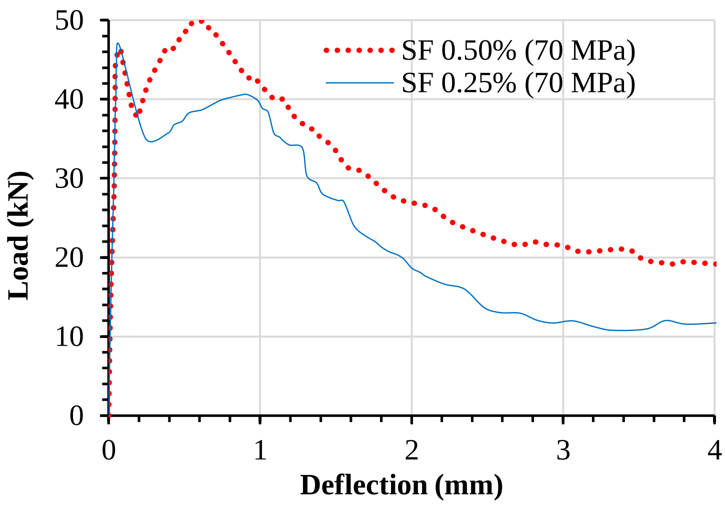

Figure 4.8 Average load versus mid-span deflection obtained from prism tests on SFRC with average compressive strength of 70 MPa .

The failure of SFRC prisms was mainly associated with formation and development of one major crack at the middle shear span. Accordingly, the model developed by Amin, Foster & Muttoni (2014) is used to determine the tensile stress-crack opening displacement or $(\sigma - w)$ characteristic of the SFRC with respect to the load-mid span deflection of the prisms. The $\sigma - w$ of the SFRC and the linearised form of the $\sigma - w$ obtained from Amin, Foster & Muttoni (2014) model are shown in Figure 4.9 and Figure 4.10. The linearised form of the $\sigma - w$ plots can be easily incorporated into the existing constitutive law of SFRC available in the finite element codes and used for predicting the behaviour SFRC slabs with 0.25% and 0.5% Dramix 5D-65/60-BG steel fibres.

4.2.3. Instrumentation

The load applied at mid-span was measured by a 500 kN flat load cell mounted on the loading ram and the mid-span deflection was measured using a 100 mm stroke LVDT. Moreover, the horizontal displacement and rotation at each end of the slab were measured using two LVDTs and inclinometers, respectively (Figure 4.11a). The strains in concrete slabs and reinforcing steel bars were measured at their mid- and end-spans (adjacent to the haunch, see Figure 4.11b). In total, two 6 mm long steel strain gauges and two 60 mm long concrete strain gauges were mounted on each precast slab (Figure 4.11b). In addition, four strain gauges (i.e. St-B-SG1 to 4) were attached to the cross-bracing and two strain gauges (i.e. St-S-SG1 and 2) were attached to the straps.

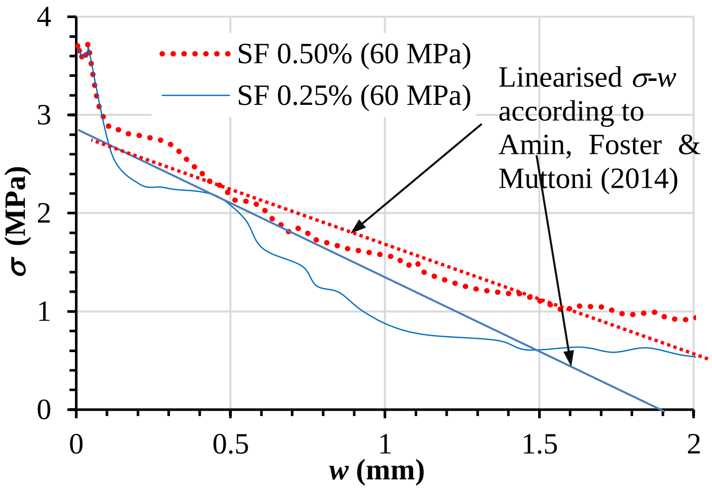

Figure 4.9 Tensile stress versus crack opening displacement for 60 MPa, derived from the prism. test results using Amin et al. model.

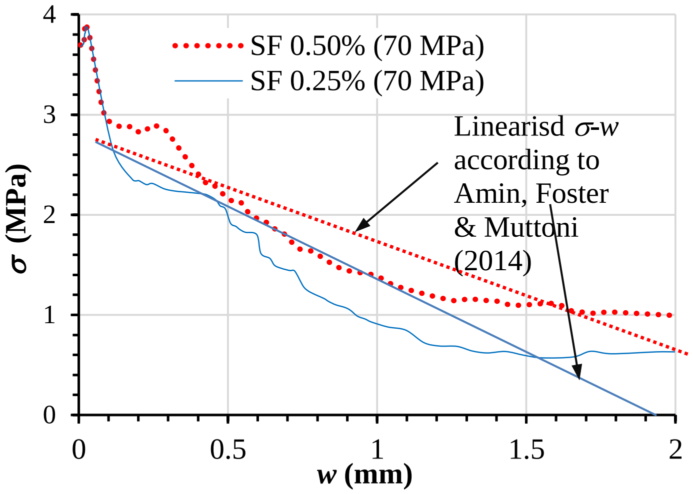

Figure 4.10 Tensile stress versus crack opening displacement for 70 MPa concrete, derived from the prism test results using Amin et al. model.

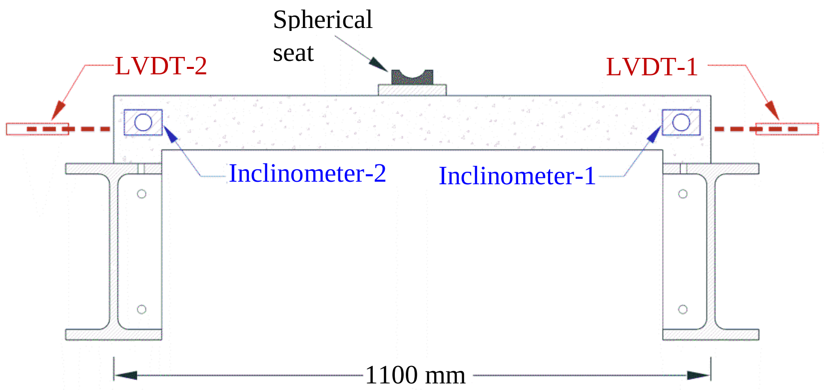

(a)

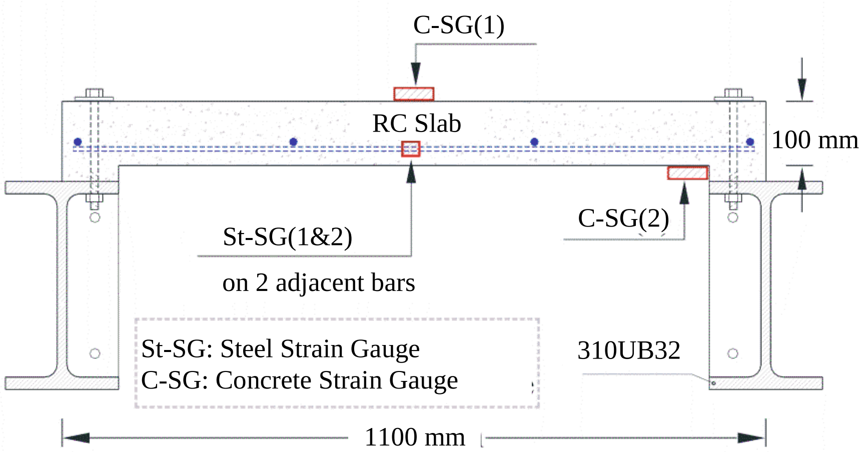

(b)

Figure 4.11 Locations of (a) LVDTs and inclinometers and (b) steel and concrete strain gauges on the precast slab.

4.3. Test Results & Discussions

4.3.1. Modes of failure

The extent of damage/cracking in each slab at the ultimate stages of loading is shown in Figure 4.12 to Figure 4.23, and a short description of failure modes are given in Table 4.3. Except for specimen SF50, cracks were observed at sections adjacent to the supported edge of the slabs, with these cracks indicative of bending moment and plastic hinge development in the hogging zone of the transversely restrained slabs.

With regard to Figure 4.12 to Figure 4.23 and Table 4.3, three distinctive failure modes can be identified. The first mode of failure (Mode I) was associated with development of large cracks in the soffit of the slab and yielding of the reinforcing steel bars at mid-span, followed by partial crushing of the concrete on the top surface of slabs at the mid-span. This mode of failure was ductile and it was observed in the precast slabs with conventional reinforcing steel bars (Specimens no. 5-8, 13 and 14).

The second mode of failure (Mode II) was associated with development of cracks in the soffit of the slab at mid-span, followed by cracking at sections adjacent to the supported edge of the slabs (between the bolt connectors). The failure Mode II was observed in the transversely restrained slabs without any conventional reinforcing bars (Specimens no. 1, 2, 4 and 9-12) and was less ductile than that of the first mode.

The third mode of failure (Mode III) was only observed in specimen no. 3 (SF50 with no reinforcing steel bars and no transverse restraining system). The third failure mode was brittle and it was triggered by development of cracks in the slab soffit at the mid-span. Accordingly, it was concluded that application of external transverse restraint can alter the mode of failure and deformability of the precast SFRC slabs.

At the end of the tests, the bolted shear connectors were easily untightened, removed and visually inspected. Despite extensive cracking and severe damage in the SFRC/RC slabs, no sign of damage or excessive deformation was observed in the bolted shear connectors and this was conducive to dismantling of the composite decks with precast slabs.

One of the failure modes in the transversely restrained deck slabs is associated with development of horizontal cracks along the haunches and on the faces of (Edalatmanesh & Newhook 2012; Klowak, Memon & Mufti 2006). In this failure mode, development of longitudinal horizontal cracks in the haunches leads to loss of transverse confinement and sudden drop in the load carrying capacity of the slabs (Mufti, Bakht & Newhook 2004). In the proposed deconstructable bridge deck with bolted shear connectors, no sign of damage or cracking was seen even at the ultimate stages of loading when slabs had undergone deflections as large as span/40.

Figure 4.12 Pattern and extent of cracking/damage and failure mode in specimen SF00-S.

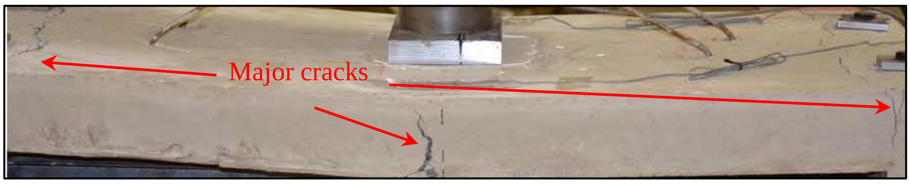

Figure 4.13 Pattern and extent of cracking/damage and failure mode in specimen SF50-S.

Figure 4.14 Pattern and extent of cracking/damage and failure mode in specimen SF50.

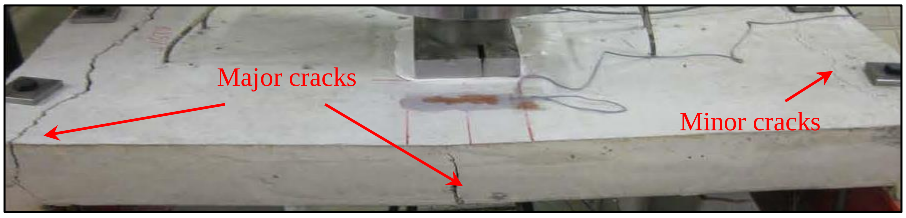

Figure 4.15 Pattern and extent of cracking/damage and failure mode in specimen SF25-S.

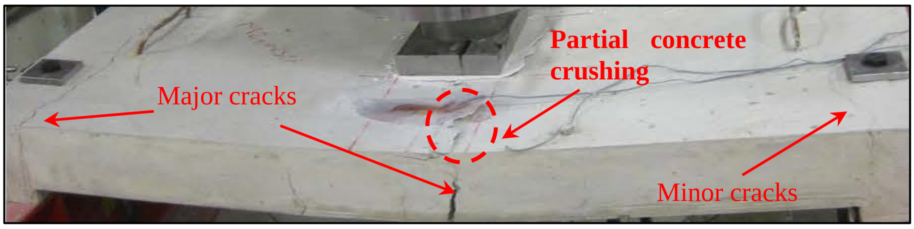

Figure 4.16 Pattern and extent of cracking/damage and failure mode in specimen SF25-S-M2.

Figure 4.17 Pattern and extent of cracking/damage and failure mode in specimen SF00-B-M3.

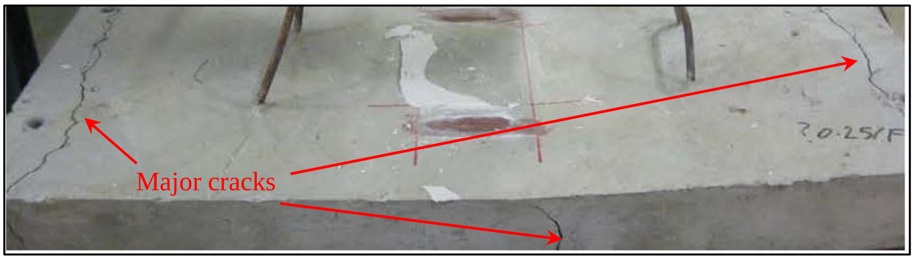

Figure 4.18 Pattern and extent of cracking/damage and failure mode in specimen SF25-B.

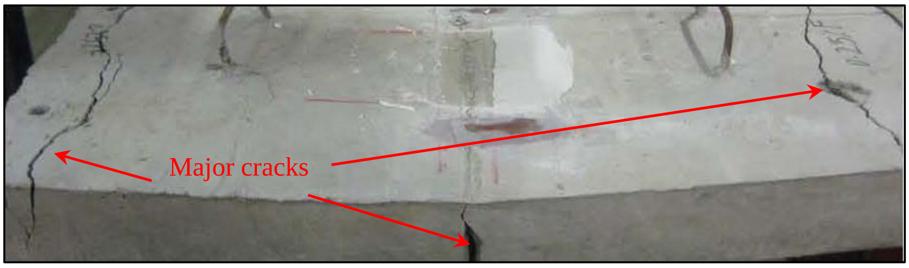

Figure 4.19 Pattern and extent of cracking/damage and failure mode in specimen SF25-BS.

Figure 4.20 Pattern and extent of cracking/damage and failure mode in specimen SF50-B.

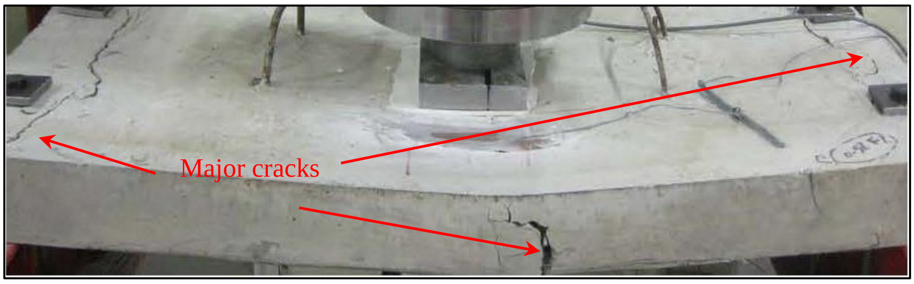

Figure 4.21 Pattern and extent of cracking/damage and failure mode in specimen SF50-BS.

Figure 4.22 Pattern and extent of cracking/damage and failure mode in specimen SF25-B-M2.

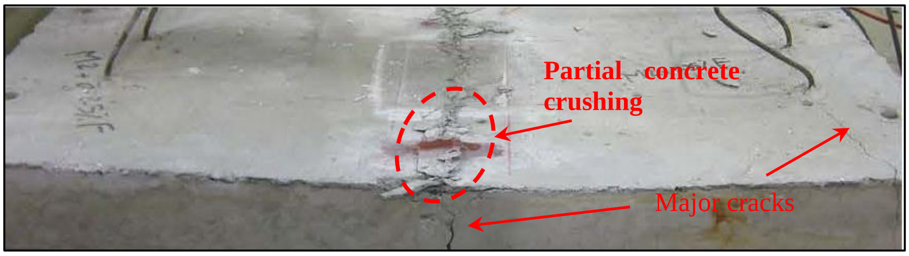

Figure 4.23 Pattern and extent of cracking/damage and failure mode in specimen SF25-BS-M2.

Table 4.3 Test results and observations.

Specimen No.	Designation of specimens	Experiment						Ductility index μE	Mode of failure
		Ultimate		Yield		Cracking			
		P_u kN	δ_u mm	P_y kN	δ_y mm	P_{cr} kN	δ_{cr} mm		
1	SF00-S	43.71	13.71	----	----	31.5	1.9	20.1	Development of cracks at mid-span (slab soffit) & end span (between the PBSCs)
2	SF50-S	62.70	12.78	----	----	31.4	2.2	28.2	
3	SF50	30.63	3.17	----	----	28.0	2.0	14.2	Development of cracks only at mid-span
4	SF25-S	65.90	13.43	----	----	33.3	2.0	29.6	Development of cracks at mid- & end-span
5	SF25-S-M2	81.63	24.80	63.7	10.1	25.2	2.6	6.5	Development of cracks at mid-span (slab soffit) & end span, yielding of steel bars at mid-span followed by partial crushing of concrete at mid-span
6	SF00-M3	47.0	25.72	34.6	8.9	17.5	1.6	8.3	
7	SF00-B -M3	73.58	33.24	63.1	19.3	19.4	2.1	3.9	
8	SF00-BS-M3	81.88	38.84	55.1	14.2	19.0	2.0	6.8	
9	SF25-B	49.34	14.74	----	----	25.1	2.6	19.7	Development of cracks at mid-span (slab soffit) and end span (between the PBSCs)
10	SF25-BS	52.19	13.89	----	----	28.0	1.7	46.7	
11	SF50-B	54.98	16.11	----	----	25.5	2.7	31.9	
12	SF50-BS	56.92	10.91	----	----	24.8	2.3	51.2	
13	SF25-B -M2	71.16	36.07	63.9	19.1	28.7	3.1	5.2	Development of cracks at mid- & end-span, yielding of steel bars at mid-span followed by partial crushing of concrete at mid-span
14	SF25-BS-M2	81.65	37.67	63.3	13.3	22.8	2.3	9.4	

The ductility index was obtained from the energy-based ductility formula,

$$\mu_E = \frac{W_{0.75u}}{W_c \text{ or } W_y}.$$

4.3.2. Global response

The loads versus mid-span deflections of the SFRC/RC slabs are shown in Figure 4.24 to Figure 4.26. the small dip following the peak load in the load-deflection diagrams is due to development of cracks at the supported edge of the slabs and between the bolted shear connectors. The peak load capacity and the mid-span deflection corresponding to the peak load capacity of the slabs are given in Table 4.3. It is seen that the external restraint (i.e. straps and bracings) has significantly increased the peak load capacity of precast slabs with conventional reinforcement as well as with steel fibres. Furthermore, it is seen that the mid-span deflection corresponding with the peak load capacity for the transversely confined SFRC slabs is around 12-16 mm (see Figure 4.24 to Figure 4.26) and just slightly smaller than that of the transversely restrained RC slabs.

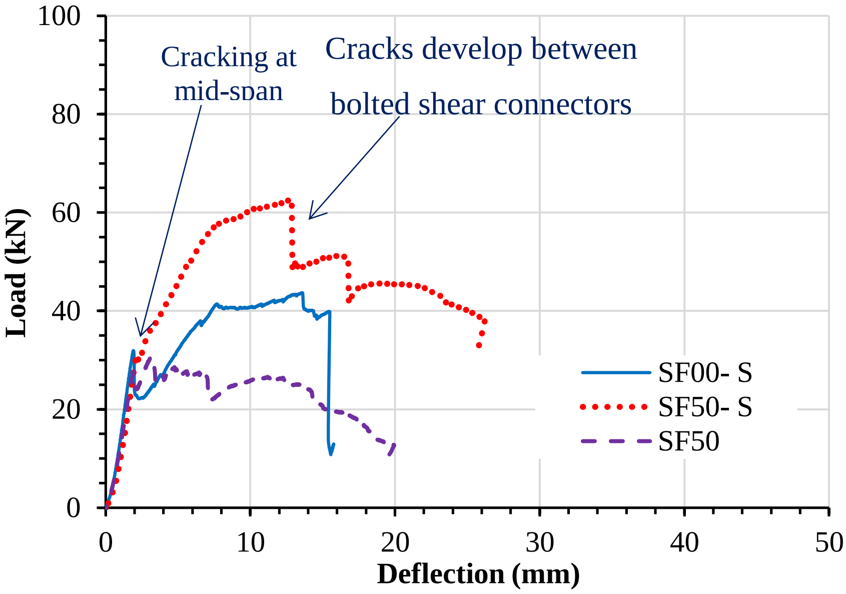

(a)

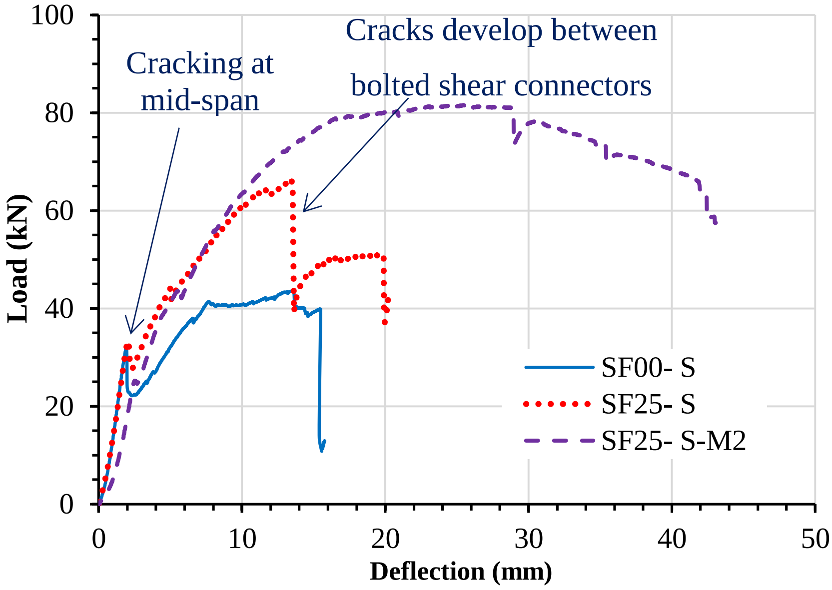

(b)

Figure 4.24 Load versus vertical displacement at mid-span of the slabs no. (a) 1-3 and (b) 1, 4 and 5.

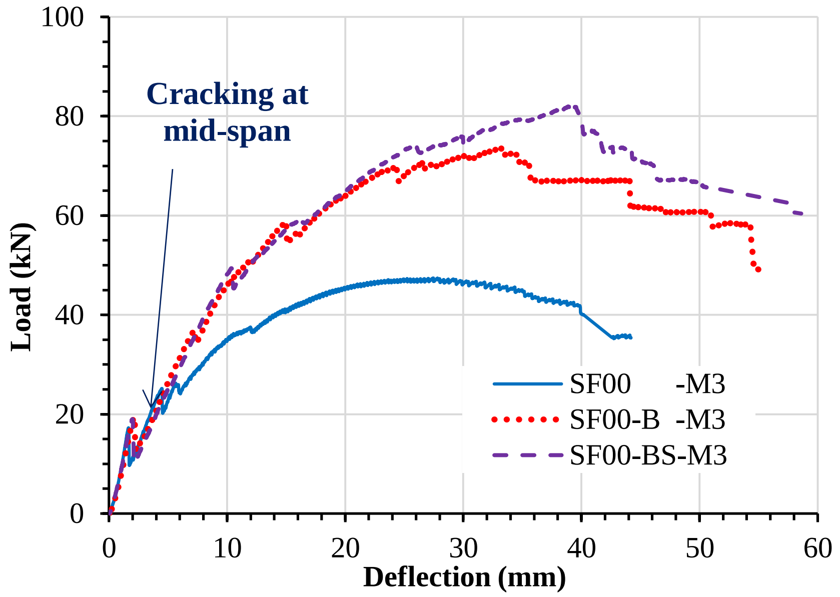

(a)

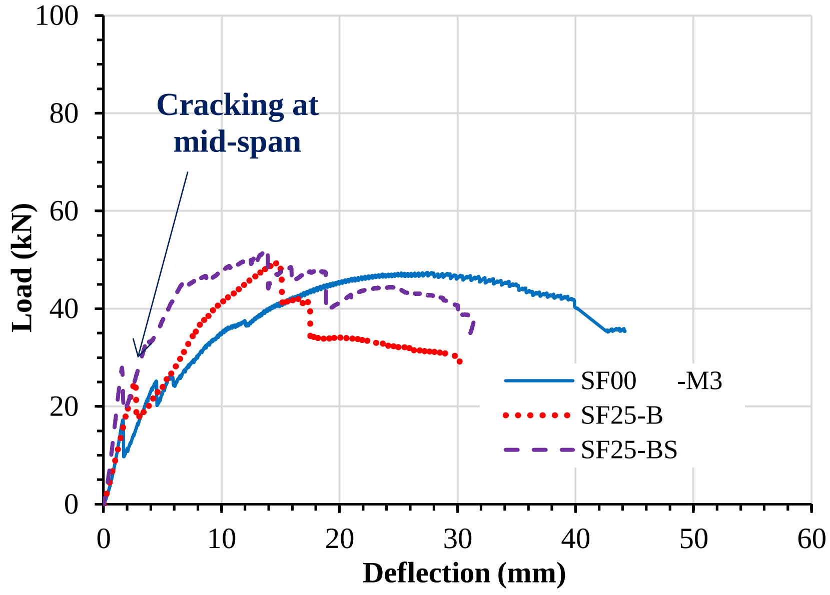

(b)

Figure 4.25 Load versus vertical displacement at mid-span of the slabs no. (a) 6-8 and (b) 6, 9 and 10.

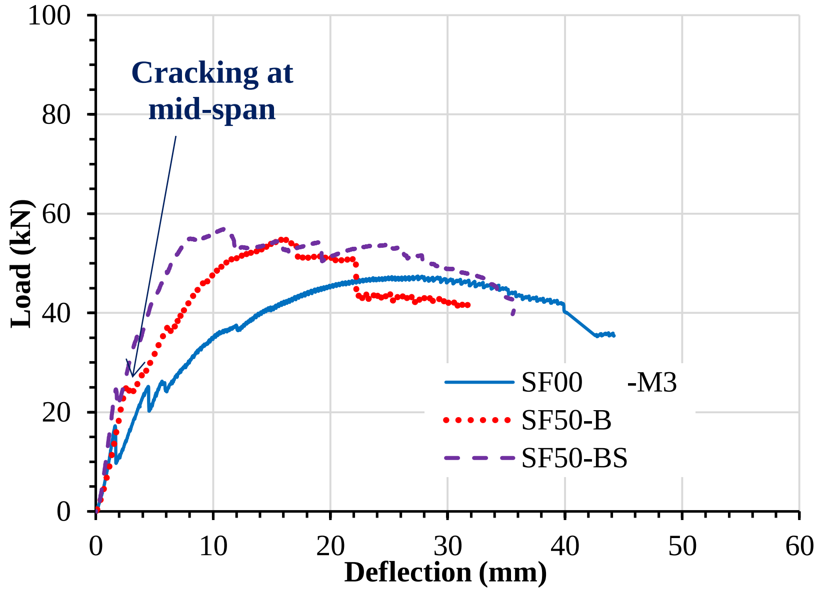

(a)

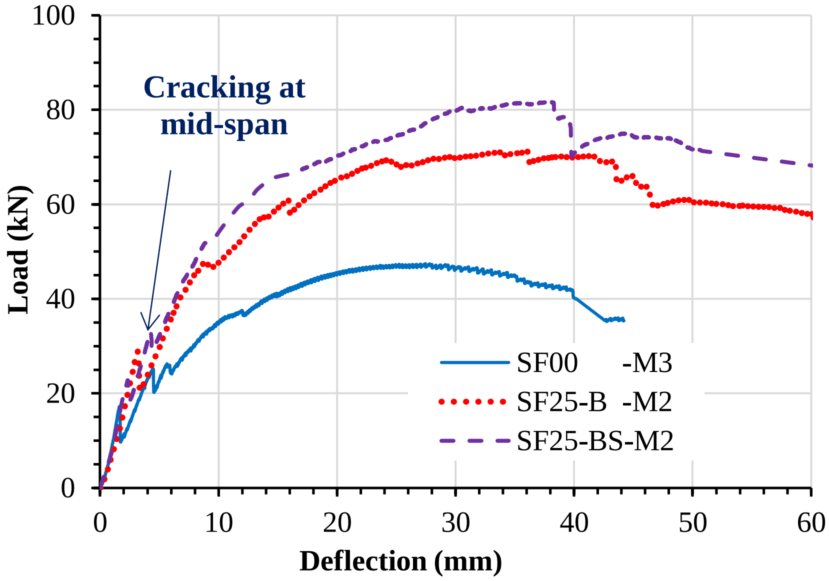

(b)

Figure 4.26 Load versus vertical displacement at mid-span of the slabs no. (a) 6, 11 and 12 (b) 6, 13 and 14.

The cracking load and the mid-span deflection corresponding to the cracking load of the specimens are given in Table 4.3. With regard to the values reported in Table 4.3, it is concluded that the cracking load of the precast slabs with conventional steel bars and no steel fibres (i.e. specimens no. 6, 7 and 8) is around 20-30% less than the cracking load of the slabs with steel fibres. This could be partly attributed to shrinkage induced cracks in the non-symmetrically reinforced sections, however, the relatively uniform distribution of steel fibres in the SFRC section can alleviate the shrinkage induced curvature.

The initiation and development of first cracks at mid-span took place at a mid-span deflection around 1.6 - 2.6 mm (see Table 4.3) and development of cracks at mid-span was associated with a small strength loss (the small dip in Figure 4.24 to Figure 4.26). This loss of strength following onset of cracks is characteristic of reinforced concrete, pre-stressed concrete and fibre reinforced concrete members tested under displacement control force (including the specimens tested in this study). Furthermore, the loss of strength following onset of cracks observed in the tests would not affect the structural performance of the transversely confined RC/SFRC slabs (SF50 specimen has no transverse confining system), because the load starts to pick up immediately after the cracking/strength loss (see Figure 4.24 to Figure 4.26) and in the transversely restrained SFRC slabs the second (ultimate) peak load carrying capacity Pu is at least 39% bigger than the cracking load, Pcr (see Table 4.3). Accordingly, under force (load) control the cracking load would be a limit point in which a snap through occurs (a small jump in displacement at a constant load).

The load versus average end support rotation of the slabs is shown in Figure 4.27 to Figure 4.29. With the exception of specimen SF50 (without reinforcing bars and without transverse restraint), a nonlinear relationship between load and average rotation at the supporting points was observed.

It is concluded that the external restraining system in the transverse direction (i.e. cross-bracings/straps) can provide some level of rotational fixity for single-span precast slabs that, in turn, leads to the development of a hogging bending moment and cracks in the sections parallel to the supporting girders (see Figure 4.12 to Figure 4.23).

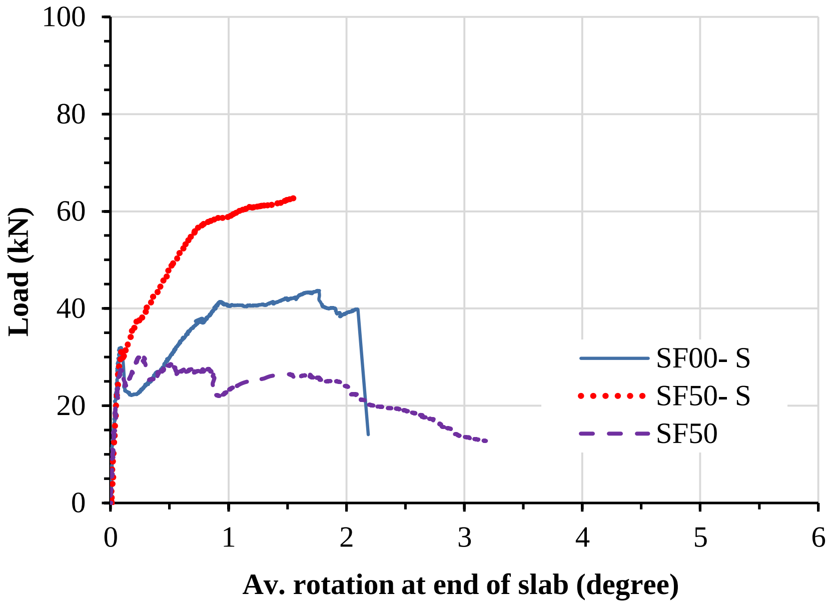

(a)

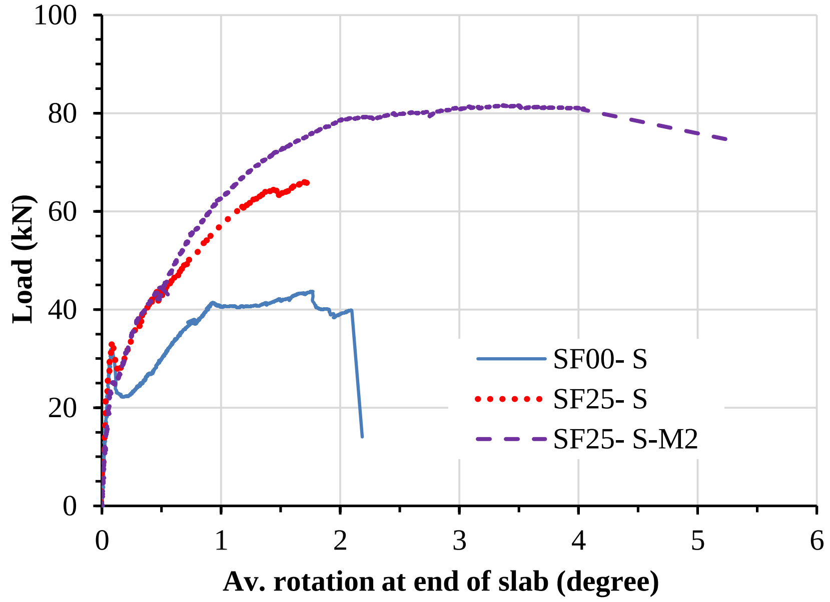

(b)

Figure 4.27 Load versus average rotation at the end of precast slabs no. (a) 1-3 and (b) 1, 4 and 5.

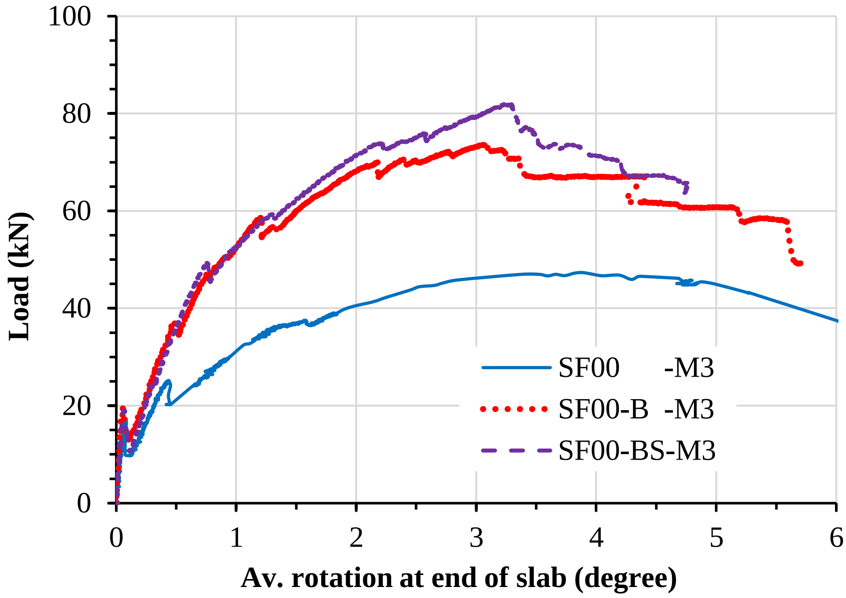

(a)

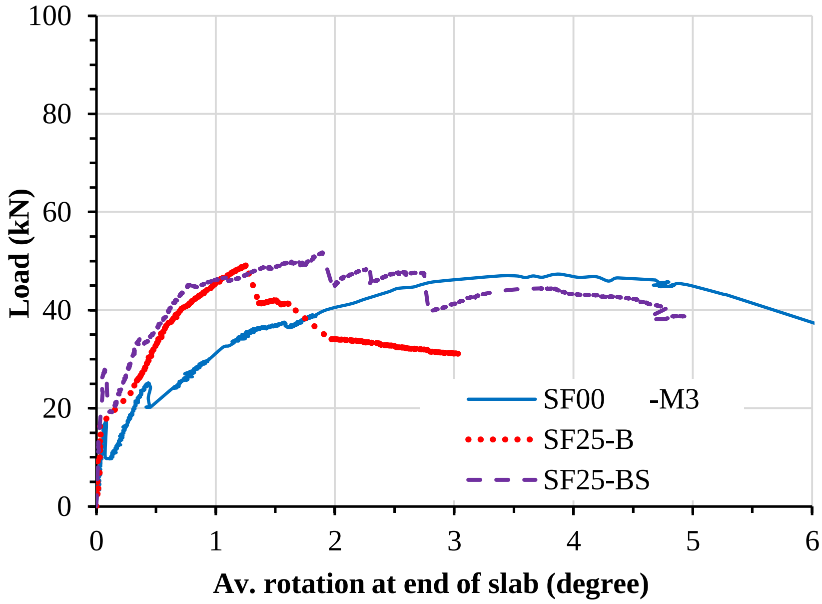

(b)

Figure 4.28 Load versus average rotation at the end of precast slabs no. (a) 6-8 and (b) 6, 9 and 10.

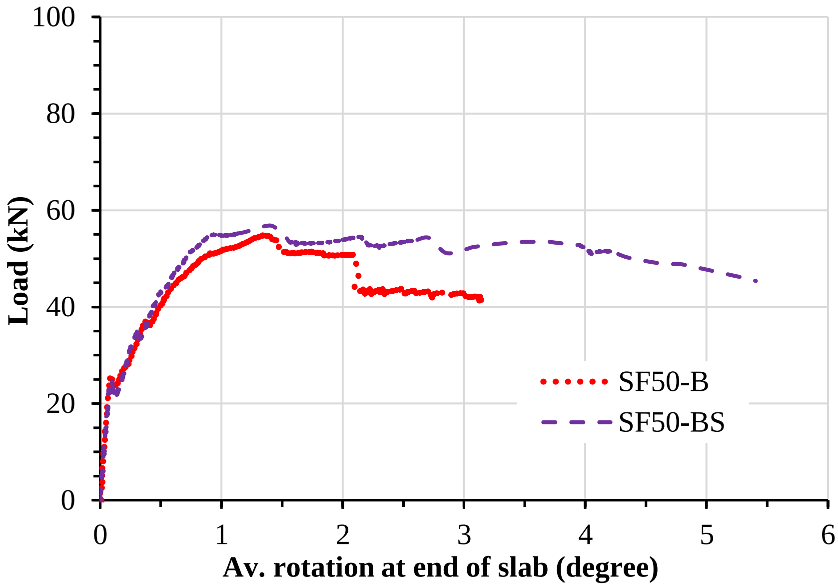

(a)

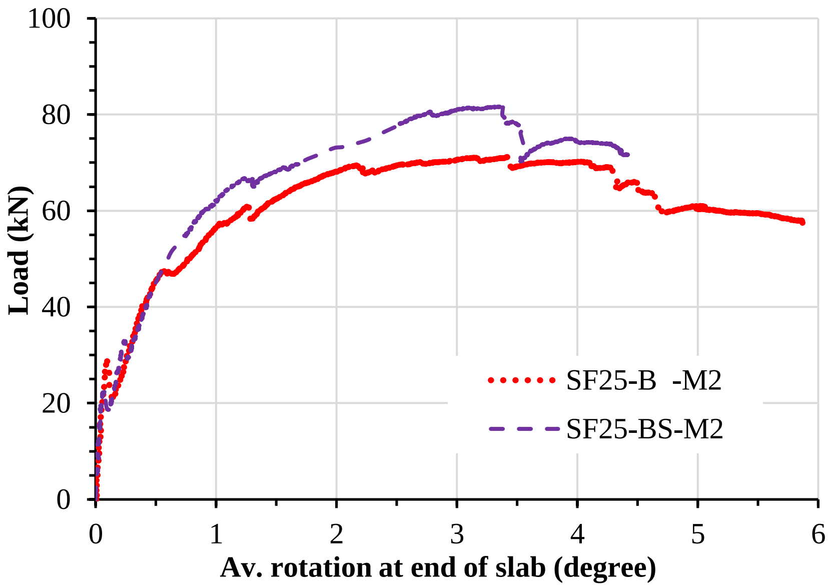

(b)

Figure 4.29 Load versus average rotation at the end of precast slabs no. (a) 11 and 12 (b) 13 and 14.

The load versus total elongation of the slabs is shown in Figure 4.30 to Figure 4.32. It is seen that the maximum elongation of the slabs is inversely proportional to the stiffness of restraining system. The total elongation of the slabs in the transverse direction was obtained from the algebraic sum of the horizontal movements measured by LVDT-1 and LVDT-2 mounted on the edges of the slabs. The locations of LVDT-1 and LVDT-2 are shown in Figure 4.11a.

4.3.1. Local response

The load versus the maximum tensile strain in the reinforcing steel bars (results of strain gauge St-SG(1) at mid-span) are shown in Figure 4.33; it is seen that yielding of reinforcing steel bars has taken place well before the peak load of the slabs is reached. Accordingly, it is concluded that the failure mode of transversely restrained precast RC slabs in the proposed demountable composite system is not brittle and some level of ductility is available in the transversely restrained RC slabs. The maximum tensile strain achieved in the reinforcing bars at mid-span were similar for all specimens. It is seen that the maximum tensile strain at mid-span in reinforcing bars has reached over 0.008 which is well above yield strain of the steel bars.

The load versus maximum concrete compressive strain (results of strain gauge C-SG(1) mounted on top of the slab at mid-span) are shown in Figure 4.34 to Figure 4.36. It is observed that the maximum strain in the farthest compressive fibre of the RC slab section at mid-span has reached values greater than the ultimate strain of concrete (i.e. $\varepsilon_{cu} = 0.003$) adopted in design codes.

The load versus average strain in the cross-bracings and straps (average results of strain gauges St-B-SG 1 to 4 installed on bracings and St-S-SG1 and 2 installed on straps) are shown in Figure 4.37 to Figure 4.39. It is seen that at all stages of loading, the tensile strain in the cross-bracings and straps remains well-below the yield strain of the 300PLUS grade steel (i.e. $\varepsilon_y = 0.0016$). Furthermore, it is seen that strain in the straps and cross-bracings continuously increase/decrease as the applied load increase/decrease and, as result, it is concluded that the friction grip bolts (including the bolted shear connectors) have effectively prevented the relative slip between different structural components (i.e. precast slab, straps, cross-bracings and steel girders). Comparing the strain in the bracings with strain in the straps reveals that the maximum tensile strain developed in the straps is 3-4 times bigger than that of the bracings (see Figures 4.37 to 4.39). This demonstrates better efficiency of the straps compared to bracings for developing/mobilising arching action.

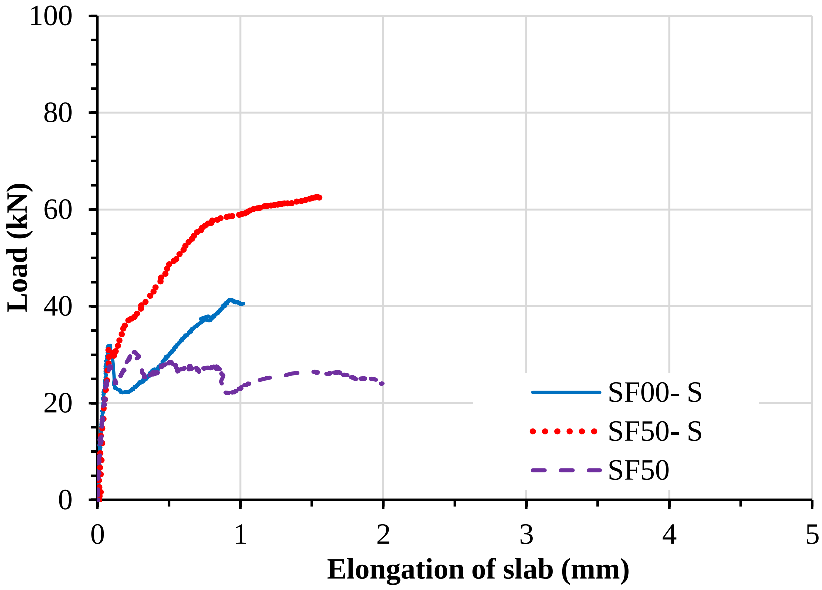

(a)

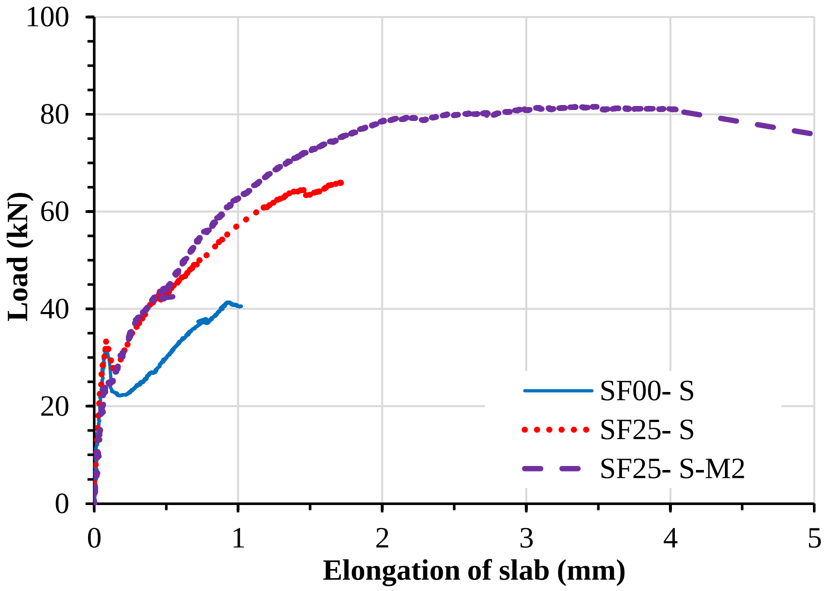

(b)

Figure 4.30 Load versus total elongation of the precast slab measured by horizontal LVDTs at the end of precast slabs no. (a) 1-3 and (b) 1, 4 and 5.

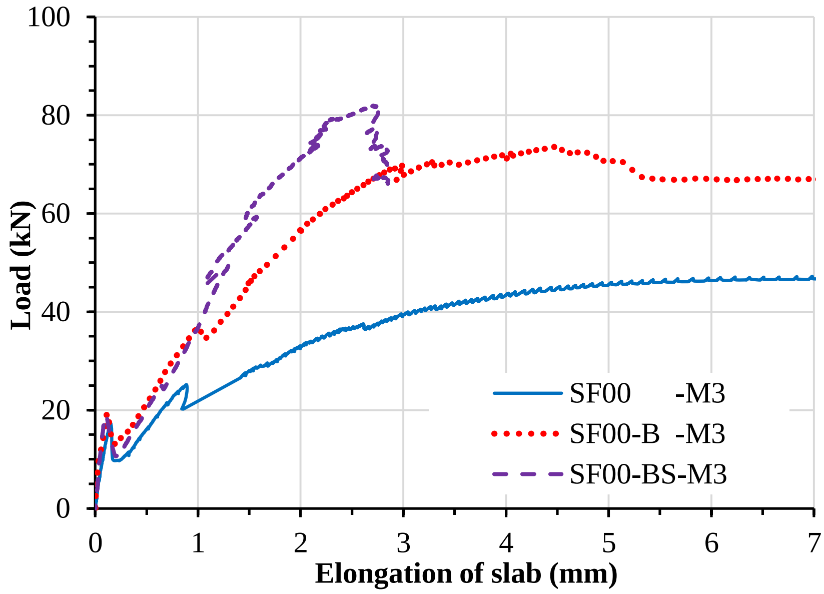

(a)

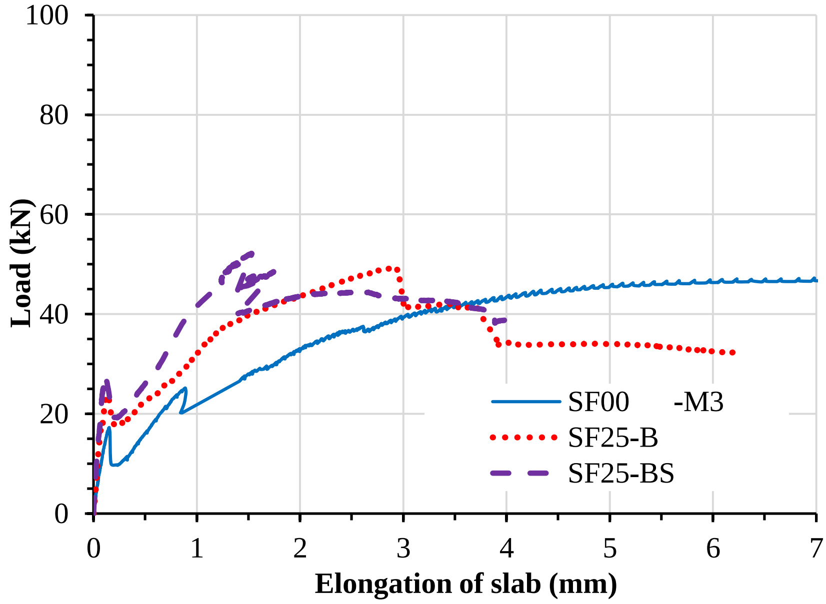

(b)

Figure 4.31 Load versus total elongation of the precast slab measured by horizontal LVDTs at the end of precast slabs no. (a) 6-8 and (b) 6, 9 and 10.

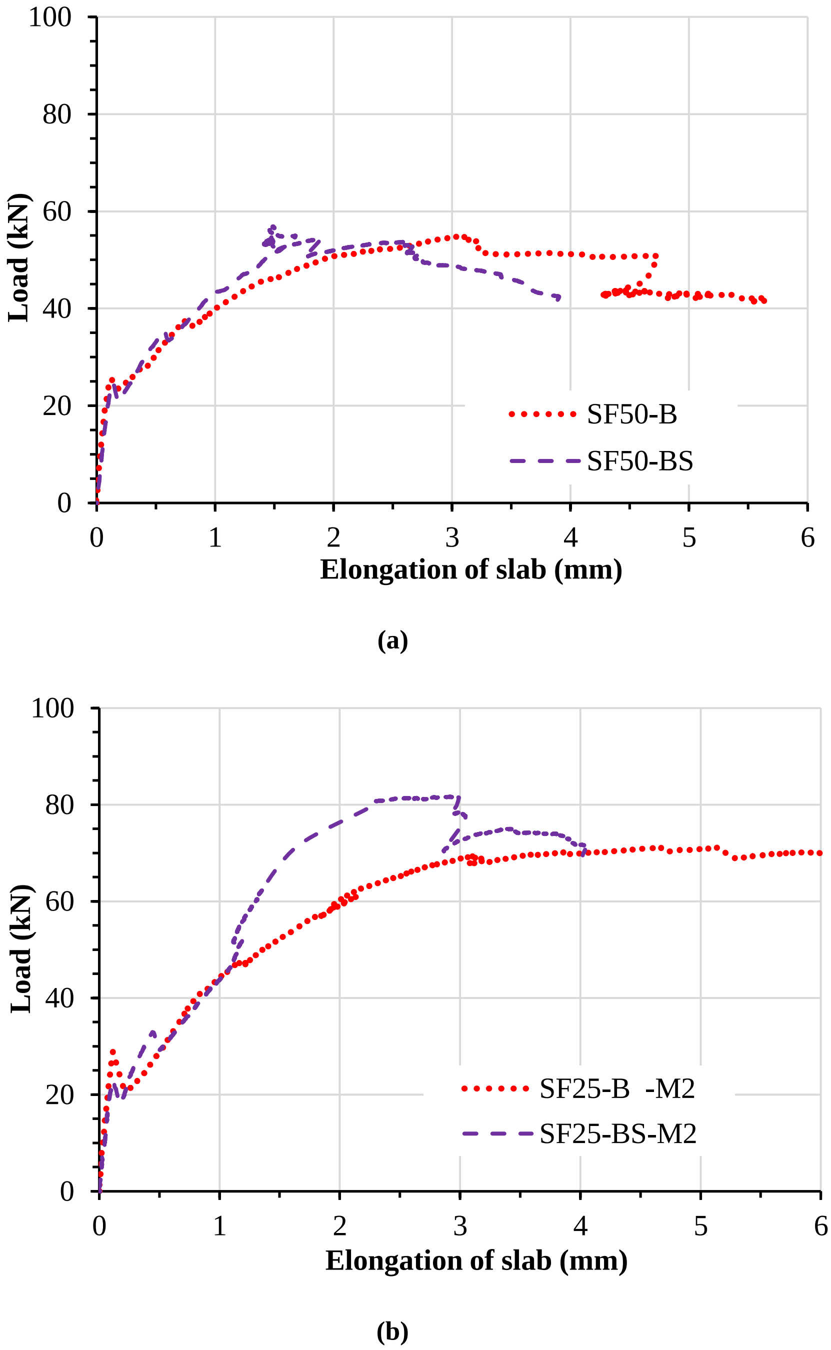

Figure 4.32 Load versus total elongation of the precast slab measured by horizontal LVDTs at the end of precast slabs (a) 11 and 12 (b) 13 and 14.

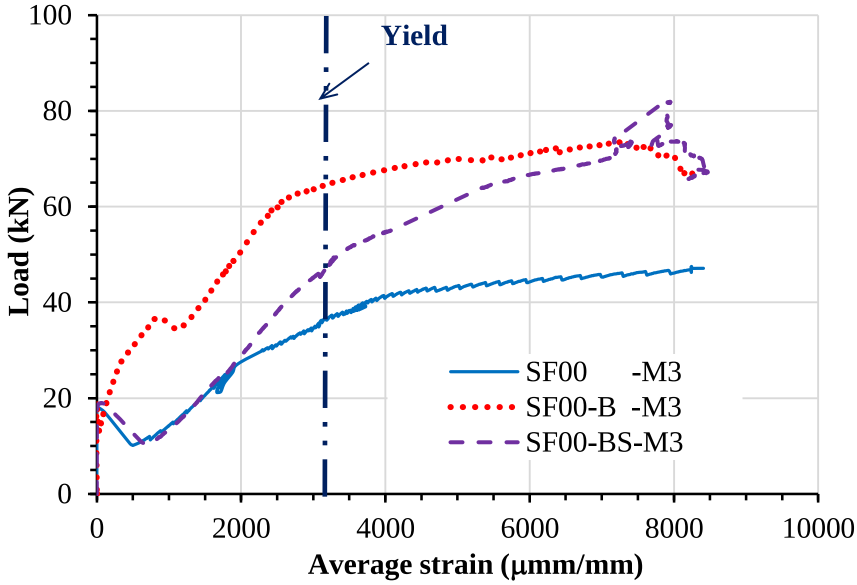

(a)

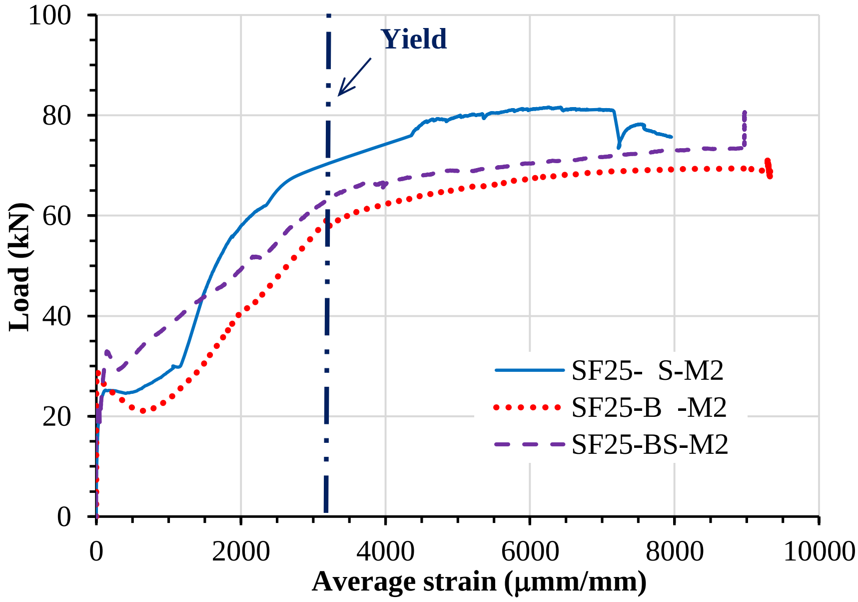

(b)

Figure 4.33 Load versus tensile strain at mid-span in reinforcing steel bars (St-SG1) for precast slabs no. (a) 6-8 and (b) 5, 13 and 14.

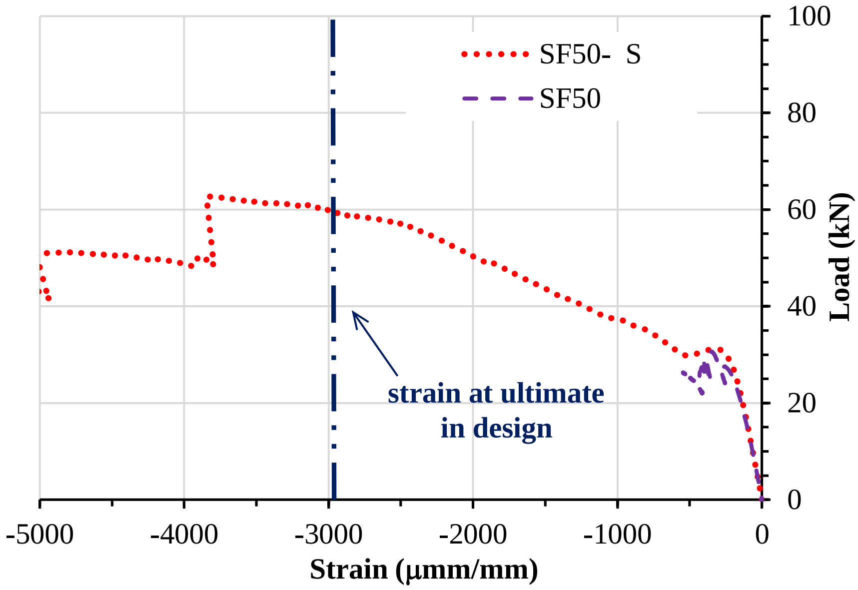

(a)

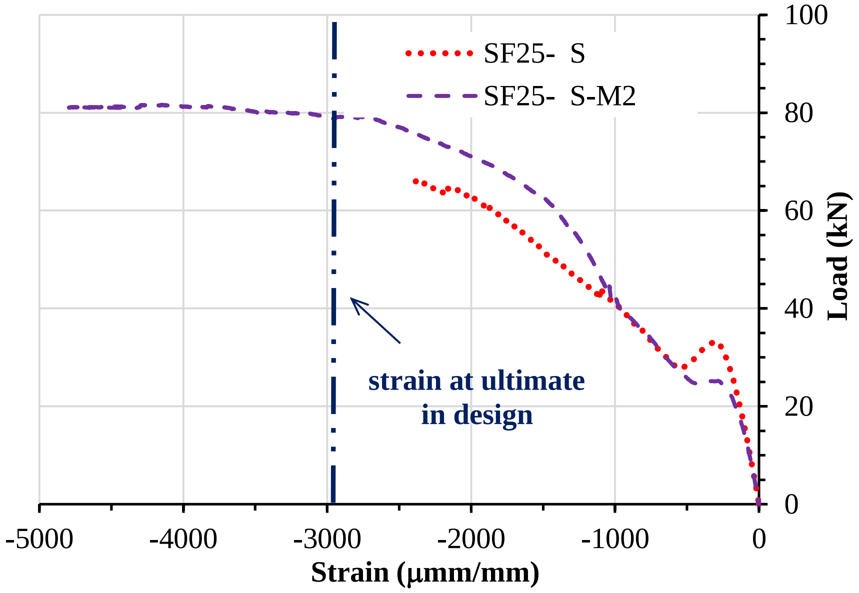

(b)

Figure 4.34 Load versus concrete compressive strain at mid-span on the top surface of the precast slabs no. (a) 2 and 3 (b) 4 and 5.

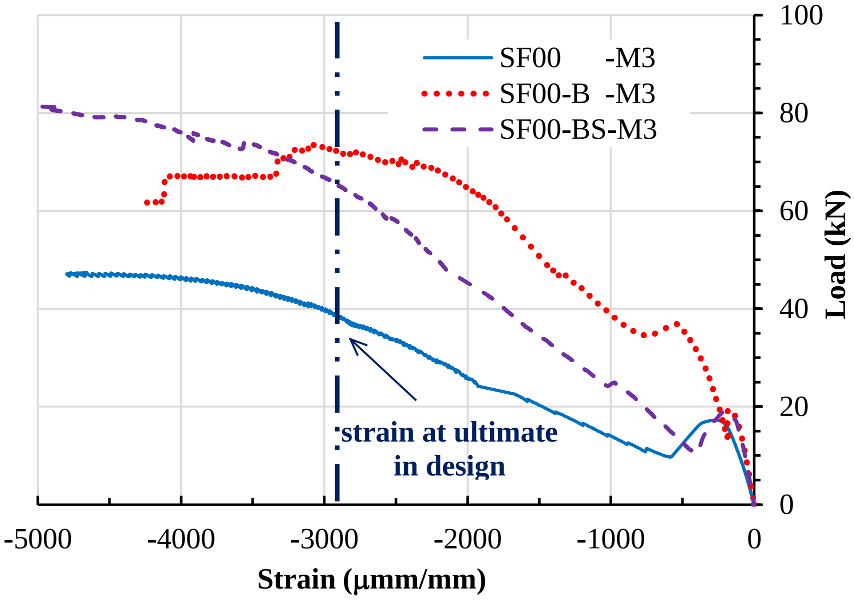

(a)

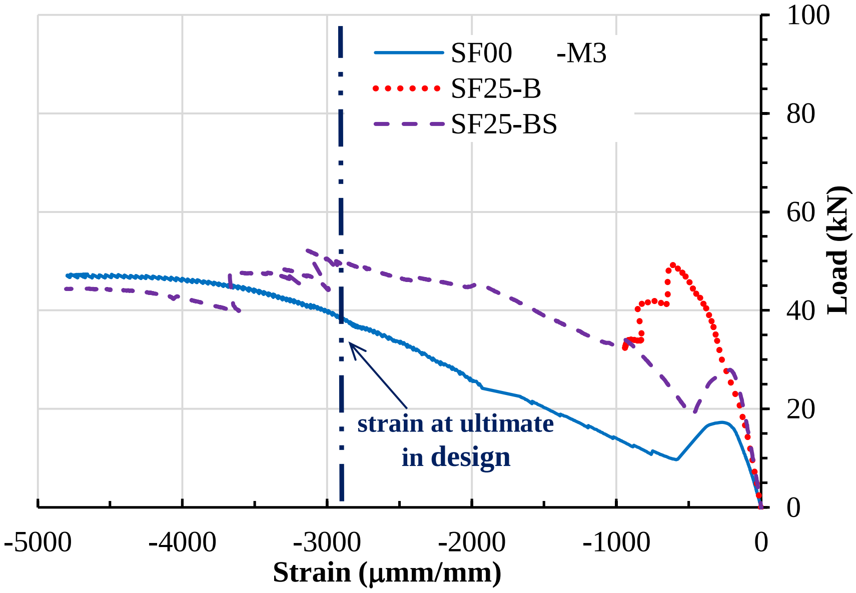

(b)

Figure 4.35 Load versus concrete compressive strain at mid-span on the top surface of the precast slabs no. no. (a) 6-8 and (b) 6, 9 and 10.

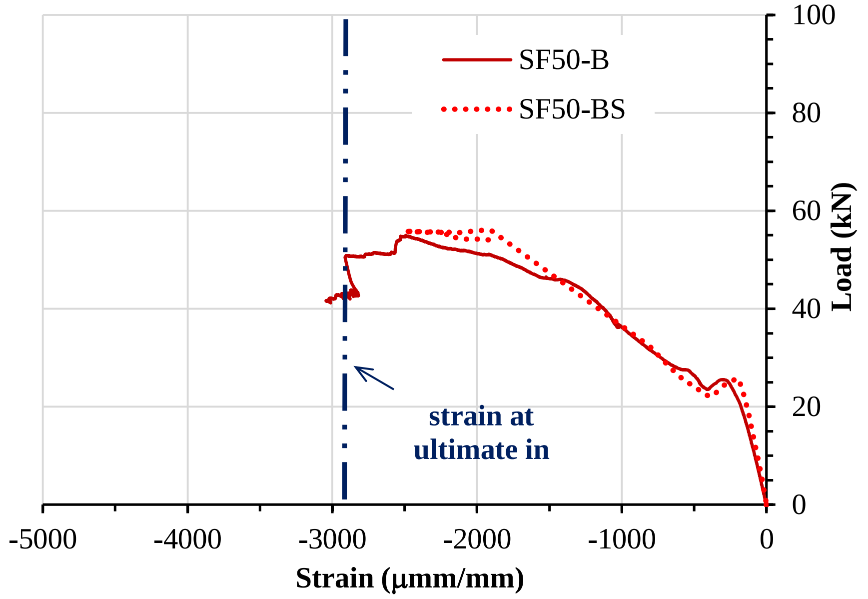

(a)

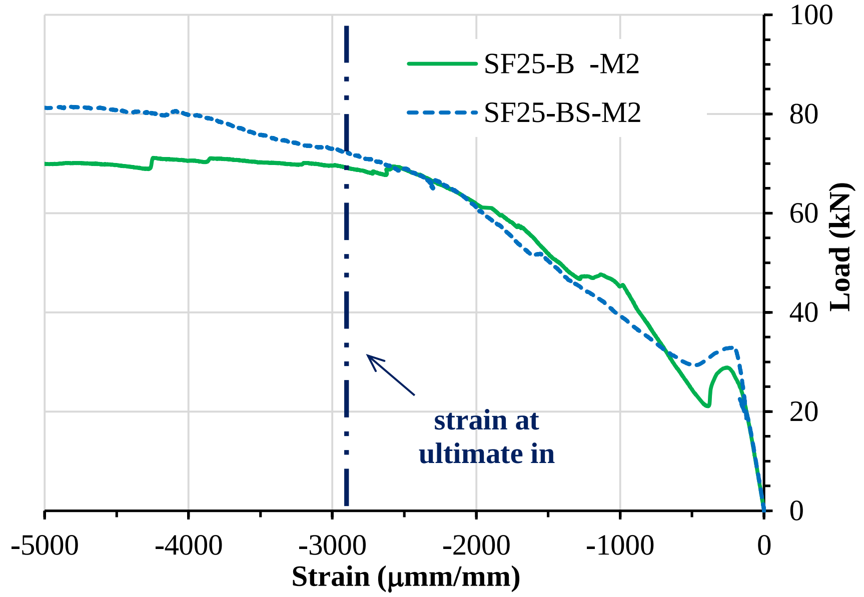

(b)

Figure 4.36 Load versus concrete compressive strain at mid-span on the top surface of the precast slabs no. (a) 11 and 12 (b) 13 and 14.

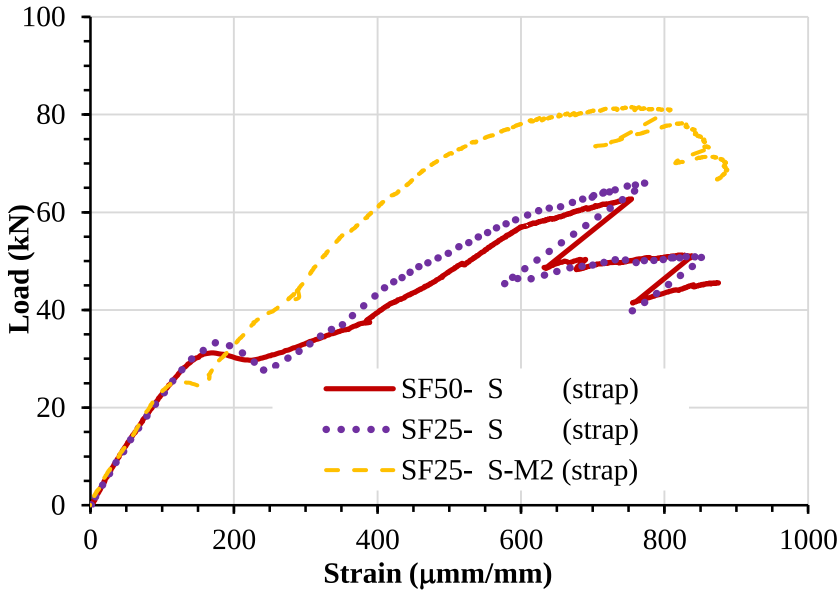

Figure 4.37 Load versus tensile strain in straps for the slabs transversely restrained only with straps

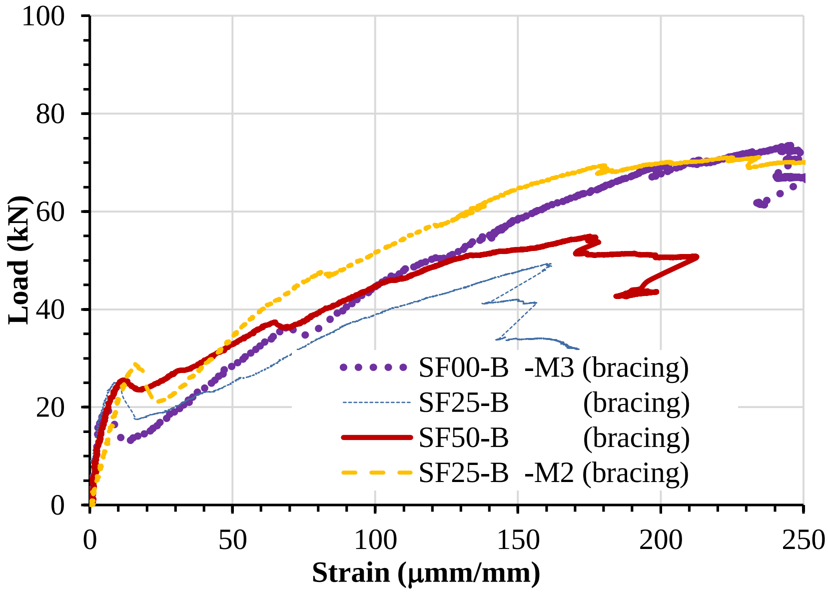

Figure 4.38 Load versus tensile strain in the cross bracings for the slabs transversely restrained only with cross bracings.

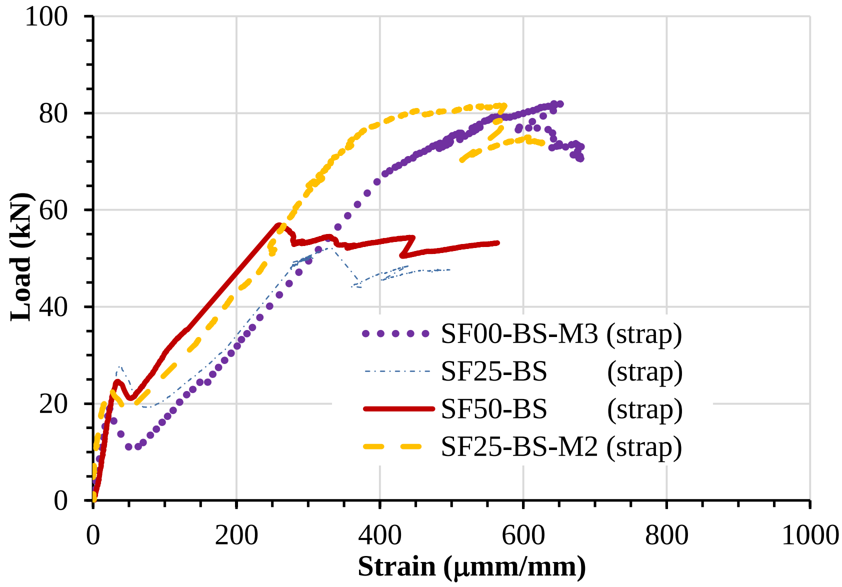

(a)

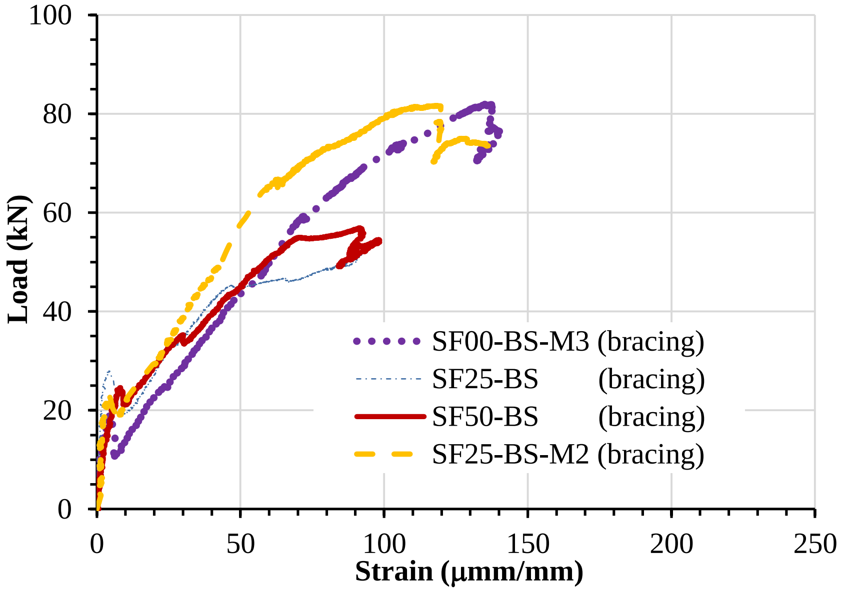

(b)

Figure 4.39 Load versus tensile strain in the cross bracings/straps for the slabs transversely restrained with straps + cross bracing (a) straps and (b) cross bracings.

4.3.2. Ductility of specimens

Over the past two decades, different indices have been introduced by researchers to evaluate the structural ductility or deformability of concrete beams and slabs reinforced with steel and polymeric reinforcing bars and/or fibres (Wang & Belarbi 2011). In this chapter, an energy-based ductility index is used to assess and compare the ductility of different SFRC/RC slabs. The energy-based ductility index μ_E is defined as,

$$\mu_E = \frac{W_{0.75u}}{W_y}$$ **Equation 4.1**

where W_y is area under the load-deflection response from the first loading to the deflection corresponding to the onset of yielding in steel bars and $W_{0.75u}$ is the area under the load-deflection curve from first loading to the deflection at which the load has reduced to 75% of the peak load. Similar energy-based measures have been used by other researchers to evaluate the structural ductility of concrete members strengthened with FRP sheets (Spadea, Swamy & Bencardino 2001). For the SFRC slabs without conventional reinforcing bar, W_y is the area under the load-deflection response from first loading to the deflection corresponding to the cracking load. Using **Equation 4.1**, the μ_E index for the tested precast slabs was calculated and the results are given in Table 4.3. It is seen that providing transverse confinement for the deck slabs (by using external ties/straps or bracings) can increase the energy-based ductility index of SFRC slabs with no conventional reinforcing bars, whereas, the transverse confining system reduce the ductility index μ_E of deck slabs with conventional steel bars. It should be noted that the energy-based ductility indices bigger than one are not necessarily indicator of better (higher) ductility of the specimens in terms of failure mode. For instance, specimen SF-50 (with no conventional reinforcing bars) had a brittle behaviour, however, the energy-based ductility index of SF-50 was μ_E= 14 and it was higher than the ductility index of the specimen SF25+M2 which failed in a ductile manner.

The ductility index μ_E of SFRC slabs with respect to the stiffness of the restraining system relative to the axial stiffness of slab (K Restraining system / KSlab) is shown in Figure 4.40. It is seen that for the SF50 series of tests (containing a 0.5% volume of fibre), the ductility index μ_E increases as the stiffness of the restraining system increase. This increase in the energy-based ductility of transversely-restrained SFRC slabs with 0.5% fibre dosage is in contrast to the reduction of ductility in externally restrained slabs with FRP or conventional steel bars (Taylor & Mullin 2006).

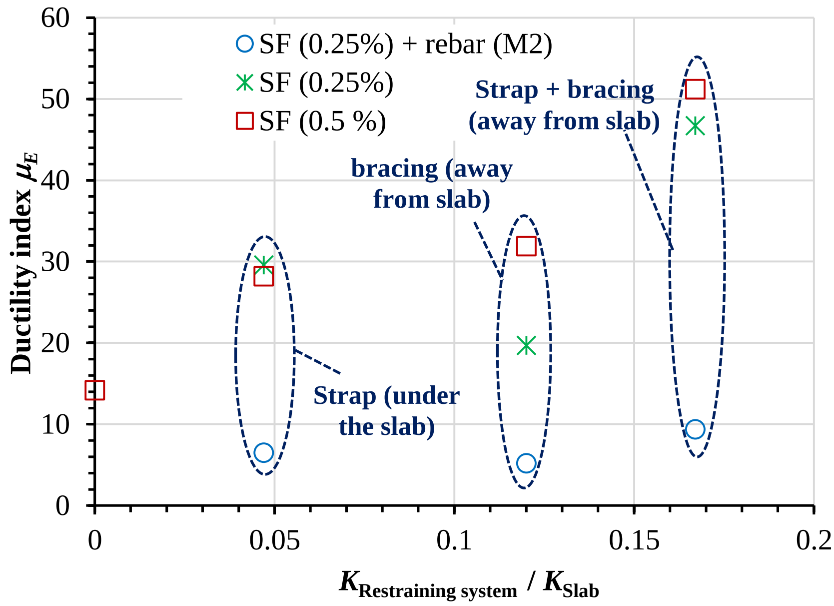

Figure 4.40 Variation of ductility index μE of the precast steel fibre reinforced concrete slab with respect to fibre dosage/reinforcing proportion and relative stiffness of transverse confining system.

The ductility indices μ_E of the transversely-restrained SFRC slabs with 0.25% and 0.50% 5D fibres were within the same range ($20 \leq \mu_E$) indicating that a 0.25% fibre dosage can provide sufficient ductility under static loads. The energy-based ductility index μ_E given in Table 4.3 and Figure 4.40 exhibit a large scatter that can be attributed to significant contribution of several factors such as reinforcing ratio, transverse confining system stiffness and steel fibre dosage in the ductility/deformability of the RC/SFRC slabs.

4.3.3. Peak load capacity and strength enhancement due to arching action

The peak load capacity of the RC and SFRC slabs obtained from the experiments are given in Table 4.3 and the experimental peak load capacity of the slabs with respect to fibre dosage and the stiffness of restraining system (in the transverse direction) over axial stiffness of slab (K Restraining system / K Slab) is shown in Figure 4.41. It is seen that the pattern of strength enhancement provided by the development of arching action in the transversely restrained precast slabs is similar for the SF25, SF50 and SF25+M2 series of tests. Furthermore, it is observed that the peak load capacity of the restrained SFRC slabs with 0.25% and 0.50% 5D fibres are nearly identical. The peak load capacities of the transversely restrained slabs normalised with respect to ultimate capacity of the SF50 slab (with no restraint) are shown in Figure 4.42. The figure shows the significant enhancement in the peak load capacity due to development of arching action.

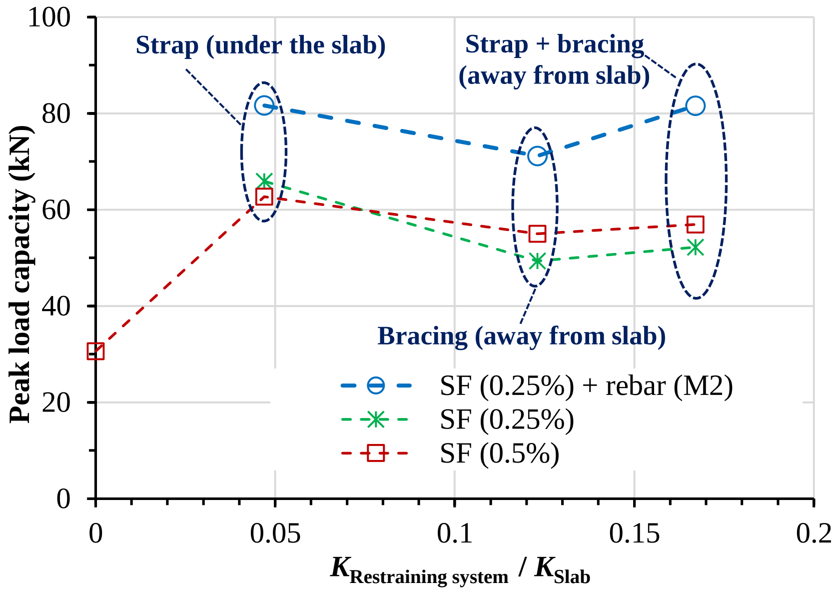

Figure 4.41 Variation of peak load capacity of the precast SFRC slabs, with respect to fibre dosage/reinforcing proportion and relative stiffness of transverse confining system.

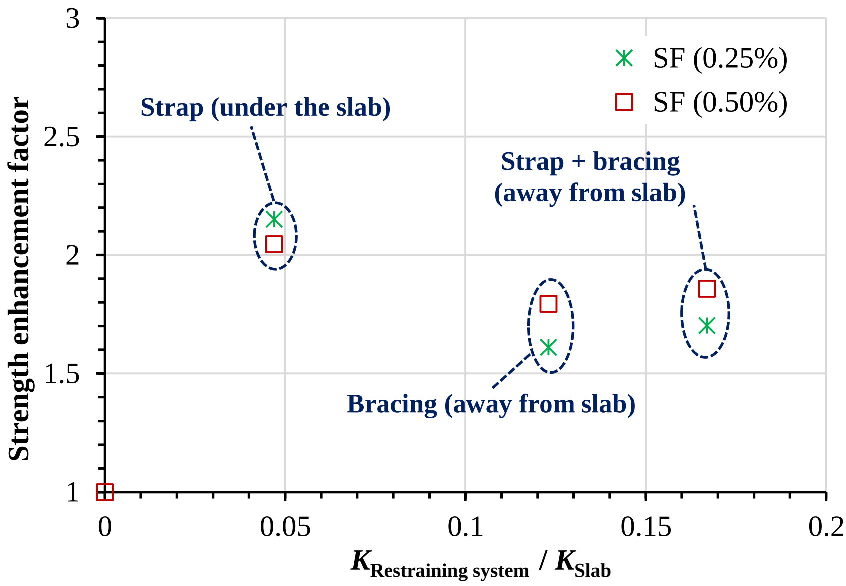

Figure 4.42 Normalised experimental peak load capacity of the transversely restrained SFRC slabs with respect to SF50 slabs (with no transverse restraint).

The total volumetric ratio of reinforcement (ρ_{Total}) including conventional steel bars and 5D steel fibres were calculated and given in Table 4.1. The ductility index μ_E and the peak load capacity of the precast slabs with only reinforcing bars and with combination of conventional reinforcement and steel fibres are shown in Figure 4.43.

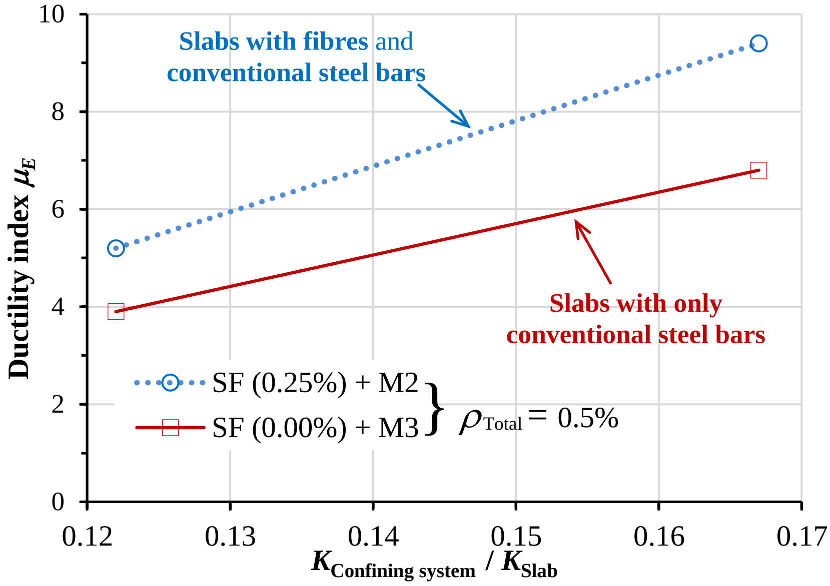

(a)

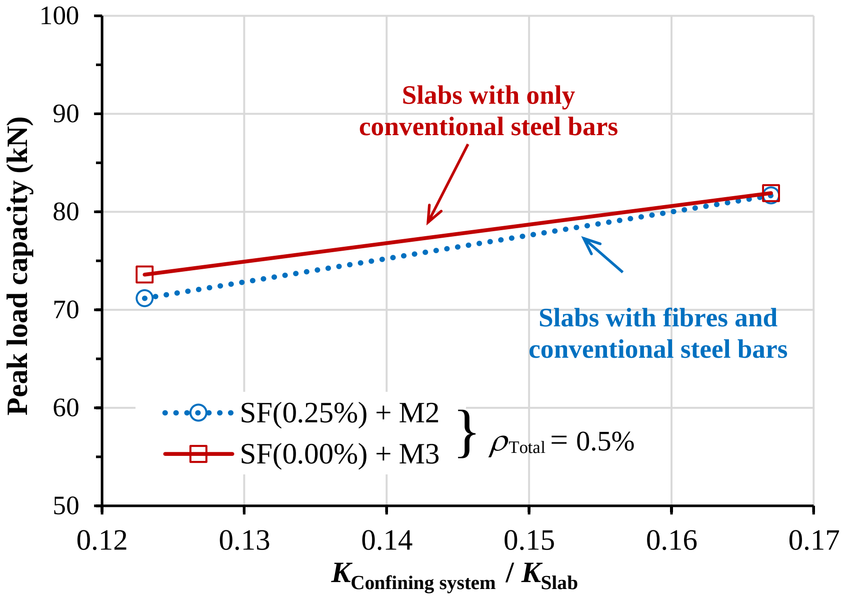

(b)

Figure 4.43 Comparison between the (a) Energy based ductility index μ_E and (b) peak load capacity of precast SFRC/RC slabs with the same volumetric reinforcing steel bar/fibre proportion.

It is seen that replacing part of conventional reinforcing steel bars with 5D steel fibres (i.e. using 0.25% fibres+M2 instead of M3 steel bar configuration that lead to similar ρ_{Total} = 0.5% for the precast slabs with the same transverse restraining system has negligible influence on the peak load carrying capacity. In addition, it is observed that replacing part of the steel bars with steel fibres (depending on the proportion of steel bars replaced with fibres), does not significantly affect the ductility index μ_E of the transversely restrained precast slab decks. In fact, replacing conventional reinforcing bars with 5D fibres led to a small increase in the energy-based ductility index μ_E of the specimens tested in this study (see Figure 4.43a). This is demonstrative of the potential application of 5D structural steel fibres as a replacement for conventional steel bars.

4.4. Conclusions and summary of results

A set of fourteen one-half scale transversely restrained precast RC/SFRC deck slabs were tested under a monotonically increasing point load applied at the mid-span. The precast slabs were compositely connected to steel girders using post-installed friction grip bolts for shear connection (PBSC). The application of three types of transverse restraining systems (i.e. straps under the slab strip, cross-bracings and combination of straps and cross-bracings away from the slab strip), in conjunction with high strength friction grip bolted connections for mobilising of arching action were studied experimentally. Also studied was the use of SFRC and the influence of steel fibre dosage (0.25% and 0.50%) on strength and ductility of transversely restrained precast deck slabs.

The results of this experimental study provided the benchmark data for evaluating the structural performance, mode of failure, load-deflection response and ductility of the transversely restrained SFRC slabs with and without conventional reinforcing bars. Moreover, the following conclusions are drawn from the experimental data;

– The PBSCs were found to be effective in preventing relative slip between the precast slab and steel girders in the transverse direction. This full composite action is essential for mobilising arching action in the proposed deconstructable composite deck slabs with transverse restraining systems.

- The slabs underwent extensive damage and large deflections following each test; however, no sign of damage or excessive deformation was observed in the bolted shear connectors and the severely damaged slabs were easily dismantled after testing. This can facilitate repairing and dismantling of the proposed composite deck system.

- During the tests, no horizontal cracks were sighted on the faces of the slabs along the haunches. Accordingly, it is hypothesised that the clamping force provided by PBSCs and steel fibres can hinder development of longitudinal cracks in the haunched edge and improve load capacity of transversely confined concrete slabs.

- Comparing the cracking load of the transversely restrained precast slabs with and without steel fibres showed that replacing the conventional reinforcing bars (unsymmetrical configuration in the section) with steel fibres can increase the cracking load of the precast slabs (around 20-30% increase was observed in this study). The shrinkage induced curvature in unsymmetrically reinforced slabs can lower the cracking load. However, the more uniformly distributed nature of fibres compared to unsymmetric reinforcing bars can alleviate the shrinkage induced warping in the concrete sections.

- The failure of transversely restrained SFRC slabs was associated with development of cracks in the soffit at mid-span and the onset of cracks at top of the slab at end span (adjacent to the haunches and between PBSCs). This failure mode is consistent with development of plastic hinges at the mid-span and at the clamped ends.

- The energy-based ductility of SFRC slabs with 0.5% 5D steel fibres increased with increasing stiffness of the restraining system. This observation is in marked contrast to that of transversely restrained RC slabs in which the ductility decreases as the stiffness of the transverse restraining system increases.
- Assuming that the cracking load in SFRC slabs is equivalent to the yield load in RC slabs, the energy-based ductility of SFRC slabs tested was greater than the

energy-based ductility of RC slabs with conventional steel bars. In addition, comparing the SF25-M2 and SF00-M3 series (with bracing or bracing and straps) shows that the partial replacement of conventional steel bars with steel fibres can slightly increase the energy-based ductility but the ultimate strength of the slabs remains unchanged.

- The development of arching action in the transversely restrained SFRC slabs significantly enhances the peak load capacity. For example, in the SF50 series (0.50% 5D fibres) with straps, development of arching action has led to 105% enhancement in the capacity.

- The capacity of the restrained SFRC slabs with 0.25% and 0.50% 5D fibres were identical and increasing fibre dosage from 0.25% to 0.50% neither improved the ductility nor enhanced the peak load capacity of the SFRC slabs under static loading condition.

CHAPTER 5

FATIGUE BEHAVIOUR OF TRANSVERSELY RESTRAINED PRECAST (SF) RC SLABS IN A DECONSTRUCTABLE COMPOSITE DECK

5. Fatigue Behaviour of Transversely Restrained Precast (SF) RC Slabs in A Deconstructable Composite Deck

5.1. Introduction

In previous chapters the efficiency of new deconstructable steel-concrete composite bridge deck system that takes advantage of bolted shear connectors has been evaluated under monotonically increasing static load. However, bridge decks can experience more than 100 million cycles of moving loads during their service life and such a severe loading scenario can significantly influence the structural performance of the deck slabs owing to stiffness degradation and damage accumulation (i.e. cracks propagation and crack widening) (Schlafli & Bruhwiler 1998). Consequently, study of fatigue behaviour and the possibility for replacing conventional reinforcing steel bars with steel fibres and application of transverse restraining system for enhancing the fatigue life of the novel deconstructable precast deck slabs system is inevitable. Therefore, in this chapter, fatigue performance and failure of transversely restrained precast reinforced concrete (RC) deck slabs with and without steel fibres (SF) is studied. Eight one-half scale precast (SF)RC slab strips are fabricated with the slabs being attached to the girders using PFBSCs and high cycle low magnitude tests are carried out to evaluate fatigue performance of the proposed deconstructable deck slab with external transverse restraining system. The cyclically tested specimens are identical to seven of those specimens previously tested under monotonically increasing static load. The type of transverse restraining system (i.e. cross-bracings or straps), configuration of reinforcing steel bars and dosage of steel fibre (i.e. 0.25% and 0.5%) are the main variables in the experimental program. During the cyclic/fatigue tests, the mid-span deflection, failure mode, level of strains and stress range in the reinforcing bars and transverse ties/bracings and crack width and patterns are measured and recorded to evaluate the fatigue performance of the proposed deconstructable system.

The fabrication of slabs and steel girders and test set up have been described in Chapter 3 and therefore, in this chapter only a summary of geometry, test set up and instrumentation of the specimens are provided. Furthermore, the mechanical properties of steel fibre reinforced concrete (SFRC) with 0.25% and 0.5% fibre dosage have been discussed in Chapter 4 and in this chapter only key material properties are presented.

5.2. Experimental program

5.2.1. Geometry of specimens and test prototypes

The adopted prototype deck slab was designed to meet the requirements of a 12 m long composite bridge deck in NSW, Australia. The deck is 7.0 m wide with no cantilever and it is supported by four 1000WB296 steel girders, 2.2 m centre-to-centre. The concrete deck slab in the transverse direction was designed as simply supported strips and the slab strips complied with minimum design requirements of Australian standard AS5100.5 (2004). Eight one-half scale (SF)RC slab strips with 100 mm depth, 600 mm width and 1100 mm length and 25 mm thick haunches at each end are fabricated. The single-span precast (SF) RC slabs at each end are attached to the top flange of a 310UB32 supporting steel girder using two M16, 8.8/F (friction-grip) bolted shear connectors (Figure 5.1).

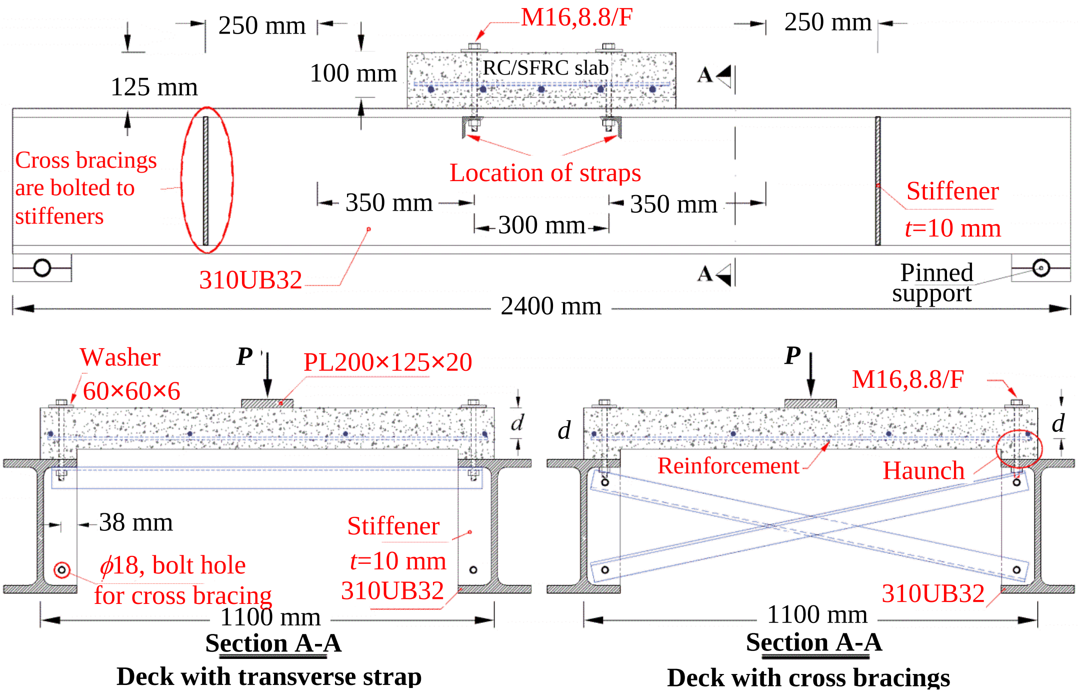

Figure 5.1 Outline of the geometry, cross-section, and type of transverse restraining system and test set up for the (SF)RC slabs compositely connected to 310UB32 girders using PFBSCs.

Before casting the slabs, a 20 mm diameter PVC sleeve was placed in the formwork to allow for easy installation of the PFBSCs. The bolted shear connectors were tightened by a torque wrench to provide a post-tensioning force of $0.4 f_{uf} = 330$ MPa in the connectors (f_{uf} being the tensile strength of class 8.8 bolts). Two different types of transverse restraining systems were used; X cross-bracings and ties made of equal leg angle section, L45×45×5EA and L45×45×3EA, respectively. The cross-bracings at each end were attached to the web stiffeners, using M16, 8.8/F bolts tightened to a shank tension of $0.6 f_{uf} = 495$ MPa , whereas the transverse ties at each end were bolted to the top flange of the steel girders under the precast slab through the M16, 8.8/F (friction-grip) bolted shear connectors (Figure 5.1). The bolt holes were pre-drilled in the top flange and the web stiffener and the bolt holes were 18 mm in diameter.

The outline of geometry and test set up, dimensions of the precast slabs, size of sections and configuration of restraining system in the transverse direction are shown in Figure 5.1 and the designation of specimens and proportion and location (effective depth of the slabs, *d* in Figure 5.1) of the reinforcement are given in Table 5.1. In Table 5.1 the designation Ln-R for specimens was made with respect to L the location (M: middle and BT: bottom and top layer), n number of reinforcing bars and -R the type of transverse restraining/confining system (-B: cross-bracing and -S: strap).

In addition to conventional reinforcing bars, 0.25% and 0.50% steel fibres (SF) were added to some of the precast slabs (see Table 5.1) with the view that the presence of steel fibres can potentially enhance the loading capacity as well as fatigue strength of the transversely restrained deck slabs in the deconstructable system. In the designation of specimens (see Table 5.1), –F25 and –F50 denote the specimens with 0.25% and 0.50% steel fibres, respectively. It is noteworthy that the full details of static tests conducted on specimens No. 1 to 7 have been discussed in previous chapters, however, for ease of comparison and referencing, the results of static tests conducted on specimens No. 1 to 7 are again provided in Table 5.1.

Table 5.1 Designation of specimens.

Specimen No.	Designation of specimens #	Test type	confining system	Number & location of reinforcing bars	d (mm)	Fibre dosage (%)
1	M3	Static	none	3N10 (middle)	55	0.00
2	M3-B	Static	Bracing	3N10 (middle)	55	0.00
3	M3-B- F25	Static	Bracing	3N10 (middle)	55	0.25
4	M3-B- F50	Static	Bracing	3N10 (middle)	55	0.50
5	M3-S	Static	Straps	3N10 (middle)	55	0.00
6	BT3	Static	none	3N10 (top & bottom)	75	0.00
7	BT3-S	Static	Straps	3N10 (top & bottom)	75	0.00
8	M3	Cyclic	none	3N10 (middle)	55	0.00
9	M3-B	Cyclic	Bracing	3N10 (middle)	55	0.00
10	M3-B- F25	Cyclic	Bracing	3N10 (middle)	55	0.25
11	M3-B- F50	Cyclic	Bracing	3N10 (middle)	55	0.50
12	M3-S	Cyclic	Straps	3N10 (middle)	55	0.00
13	BT3-S	Cyclic	Straps	3N10 (top & bottom)	75	0.00
14	BT3-S- F25	Cyclic	Straps	3N10 (top & bottom)	75	0.25
15	BT3	Cyclic	none	3N10 (top & bottom)	75	0.00

B: bracing, **-S**: straps, **Fxx**: 0.xx% fibre dosage.

5.2.2. Material

Reinforcing bars, steel girders and steel transvers restraining members

The reinforcing steel mesh in the precast slabs comprised of 10 mm diameter ribbed bars with mean yield strength of $f_y = 575$ MPa (taken as the average of direct tension tests on three specimens). The ultimate strength of steel bars was $f_u = 680$ MPa and average uniform elongation of bars at f_u was around $\varepsilon_u = 7\%$. The stress-strain curve for the reinforcing steel bars is illustrated in Figure 4.3.

The supporting steel girders and transverse restraining system (i.e. cross-bracings and straps) were made of Grade 350 steel with characteristic yield strength of 360 MPa, a tensile strength of 480 MPa and an elastic modulus of E_s = 185 GPa.

Steel fibre reinforced concrete

The (steel fibre reinforced) concrete used for casting slabs had a 28-day mean compressive strength of 60 MPa with maximum aggregate size of 10 mm. The mean compressive strength of concrete f_{cm} after 28 days and at the testing day was obtained from the average of three 300 mmx150 mm cylinders tested in accordance with AS1012.9 (1999). The uniaxial stress-strain curves of plain and SFRC concrete obtained from compression tests on 300 mmx150 mm cylinders are shown in Figure 4.5. The steel fibres used in SFRC were Dramix 5D-65/60-BG with a length of 60 mm and diameter of 0.9 mm and a nominal strength of 2000 MPa.

In addition to compressive strength, the modulus of rupture $f_{\mathrm{ct,fl}}$ for the SFRC was determined by conducting four-point bending tests on twelve 150 mmx150 mmx500 mm (testing span of 450 mm) prisms in accordance with ASTM (2005). The average load versus mid-span deflection obtained from four-point bending tests on the SFRC prisms with 0.25% and 0.5% steel fibres is shown in Figure 4.7.

The results of four-point bending tests were used only when the failure of prisms was associated with development of one major crack in the pure bending moment region of the specimen. The splitting tensile strength $f_{\mathrm{ct,\,sp}}$ of SFRC was obtained by conducting split cylinder tests on 300 mmx150 mm SFRC cylinders and the modulus of elasticity E_0 of concrete was determined in accordance with AS1012.17 (1997). The results of the material tests are given in Table 5.2, where $f_{\mathrm{ct,\,sp}}$ is the splitting tensile strength, $f_{\mathrm{ct,\,fl}}$ is the modulus of rupture and E_0 is the 28-day modulus of elasticity of SFRC.

Table 5.2 Mechanical properties of SFRC (average of three specimens).

Compressive strength f_{cm} (MPa)	Fibre dosage (%)	splitting tensile strength $f_{\mathrm{ct,sp}}$ (MPa)	Modulus of rupture $f_{\mathrm{ct,fl}}$ (MPa)	Elastic modulus E_0 (MPa)
60	0.25	7.2	5.90	32.7
	0.50	7.3	6.00	33.1

5.2.3. Test procedure and instrumentation

All precast slabs were tested under a concentrated static/cyclic load applied at mid-span by a 1000 kN capacity hydraulic actuator. Before undertaking the cyclic/fatigue test, seven specimens were tested statically to determine the static load carrying capacity of the specimens. The fatigue tests were carried out in two phases. First, the samples were monotonically loaded with a rate of 0.1 mm/s up to 60% of their static load carrying capacity, P_u and then the specimens were unloaded to zero. The loading protocol for fatigue tests was adopted from Perdikaris and Beim (1988) studies. The maximum load range (i.e. $0.6P_u$) in the static test was used to induce and determine the location of initial cracks prior to cyclic fatigue tests. The load ranges of specimens in the fatigue tests was 10-60% of their ultimate load capacity, P_u obtained from the static tests. Accordingly, in the second phase, all slabs except BT3-S-F25 and M3-S were loaded monotonically under deflection control at a rate of 0.1 mm/s up to $0.35P_u$. Next, the cyclic load was exerted under the load control using a sinusoidal wave with a frequency of 1 Hz. Specimen BT3S-F25 was tested with the same load range as specimen BT3-S to determine the influence of low dosage fibres on the fatigue performance of transversely restrained slabs. Specimen M3-S was tested in two cyclic phases with different load ranges. In the first phase, slab M3-S was loaded in the same load range as specimen M3 (i.e. 10-60% of the peak load capacity of specimen M3) and in second phase, it was loaded at the load range of 10-60% of its (M3-S) ultimate load capacity. The designations M3-S (1) and M3-S refers to the first and second phase of fatigue test, respectively.

In addition to mid-span applied load and deflection measured by load cell and LVDTs, strains in steel and concrete were measured by use of strain gauges. Two, 60 mm long strain gauges were attached to top and bottom surface of concrete slab and two, 5 mm long strain gauges were mounted on reinforcing steel bars at mid-spans. The locations of steel and concrete strain gauges are shown in Figure 5.2. The steel strain gauge ST-SG(1) was mounted on the middle bar and St-SG(2) was mounted on the side bar (see Figure 5.2) Moreover, four steel strain gauges were mounted on the cross-bracing members and two steel strain gauges were attached to the straps at their mid-length to evaluate the effectiveness of restraining systems. All data including the magnitude of cyclic load, deflection at mid-span, strain in steel bars and concrete slab and strain in restraining members (i.e. bracings or straps) were recorded continuously during the test. During the fatigue tests, in specific cycles, at median load the actuator was paused to monitor and measure the crack patterns and crack widths. The crack pattern and crack width monitoring was carried out at 10, 10^2, 10^3, 10^4, 2×10^4, 5×10^4 and 10^5 cycles and then after every 10^5 cycles until failure.

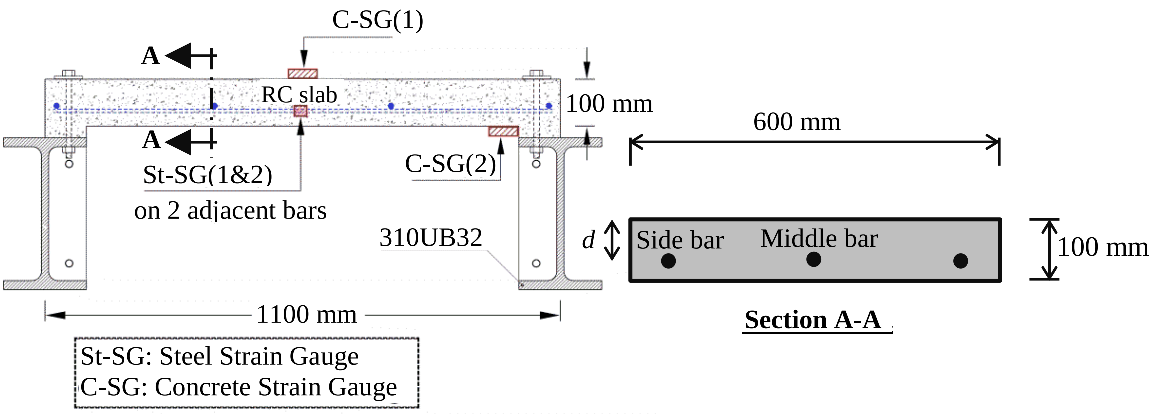

(a)

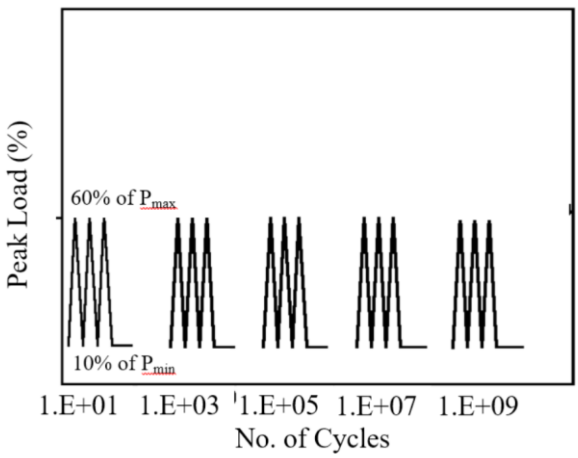

(b)

Figure 5.2 (a) Location of steel and concrete strain gauges and (b) adopted loading pattern for fatigue tests.

5.3. Discussion of test results

5.3.1. Fatigue life and modes of failure

Eight precast slabs were tested under cyclic load to evaluate the fatigue performance of the transversely restrained prefabricated deconstructable RC deck slabs with and without steel fibres. The main test variables were the transverse restraining system (i.e. bracings or straps), reinforcement arrangement and dosage of steel fibres. Additionally, the results of seven specimens tested previously under static loads (with geometry and fibre dosage identical to the specimens in the fatigue tests) are used as benchmark to determine the peak load capacity of the cyclic tests. The load versus mid-span deflection of the slabs obtained from the static tests is shown in Figure 5.3; the capacity and failure mode for both the static and fatigue tests are given in

Table 5.3.

The transversely restrained RC/SFRC precast slabs exhibited two distinctive, brittle, modes of failure under cyclic (fatigue) loading. The first mode of failure was associated with fracture of reinforcing bars and all specimens except M3-S failed in this mode (Figure 5.4 to Figure 5.10).The second mode of failure was only observed in specimen M3-S and it was triggered by rupture in the transverse ties/straps and followed by sudden yielding of reinforcing bars and excessive deflection in the slabs (Figure 5.11). However, the failure mode of slabs under static loads was rather ductile and associated with yielding of steel bars combined with compressive crushing of concrete at mid-span as shown in Figure 5.4 to Figure 5.10.

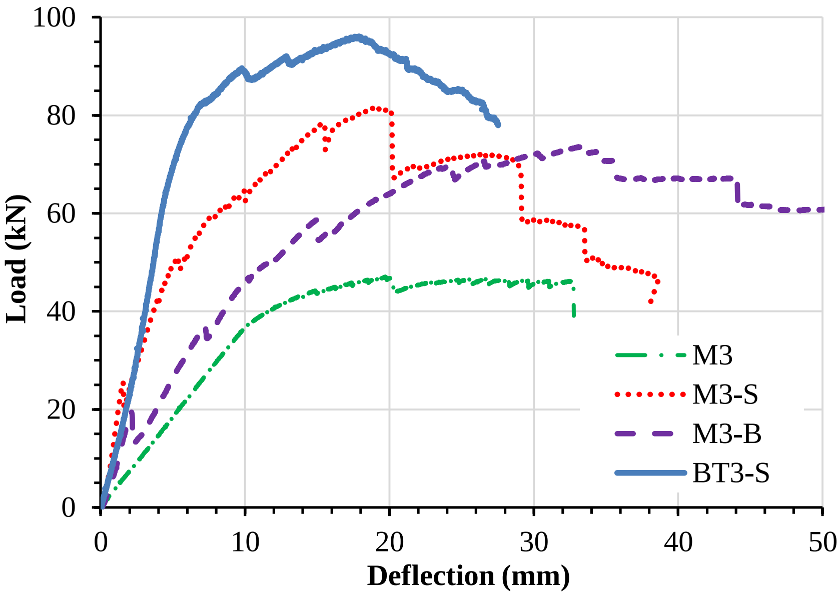

Figure 5.3 Load versus vertical displacement at mid-span of the slabs.

Table 5.3 Test results including static peak load capacity, fatigue life and mode of failure.

Specimen No.	Designation of specimens	Test type	Static load capacity P_u (kN)	Min-Max Load range (%) P_u	Number of cycles to failure	Mode of failure
1	M3	Static	47.0	–	–	Yielding of reinforcing steel bars and crushing of concrete in compressive zone at mid-span
2	M3-B	Static	72.3	–	–	
3	M3-B- F25	Static	87.0	–		
4	M3-B- F50	Static	88.0	–		
5	M3-S	Static	81.5	–	–	
6	BT3	Static	56.0	–	–	
7	BT3-S	Static	96.1	–	–	
8	M3	Cyclic	47.0	10-60	51,760	bar fracture
9	M3-B	Cyclic	72.3	10-60	78,472	bar fracture
10	M3-B- F25	Cyclic	87.0	10-60	52,455	bar fracture
11	M3-B- F50	Cyclic	88.0	10-60	120,447	bar fracture
12#	M3-S(1)	Cyclic	81.5	The same as M3	1,000,000	–
	M3-S			10-60	1,082,856	tie fracture
13	BT3	Cyclic	56.0	10-60	248,568	bar fracture
14	BT3-S- F25	Cyclic	> 96.1	The same as BT3-S	1,500,000	–
15	BT3-S	Cyclic	96.1	10-60	1,500,000	–

Specimen M3-S were tested under cyclic loads in two phases.

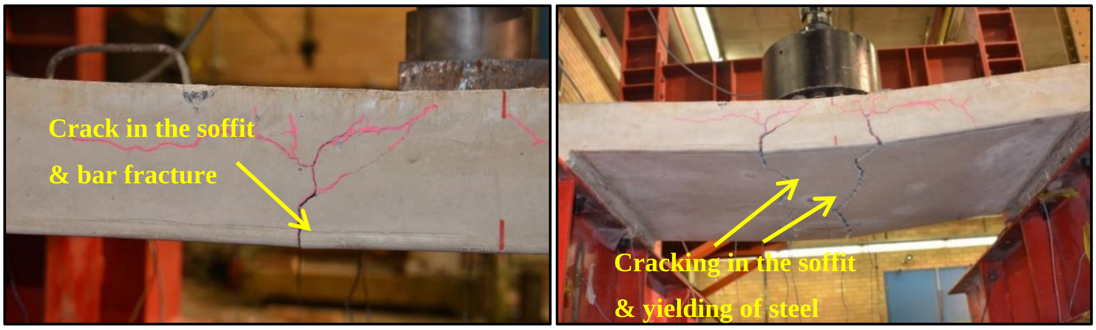

(a) (b)

Figure 5.4 Failure mode under (a) cyclic/fatigue and (b) static loading in specimen M3.

(a) (b)

Figure 5.5 Failure mode under (a) cyclic/fatigue and (b) static loading in specimen M3-B.

(a) (b)

Figure 5.6 Failure mode under (a) cyclic/fatigue and (b) static loading in specimen M3-B-F-25.

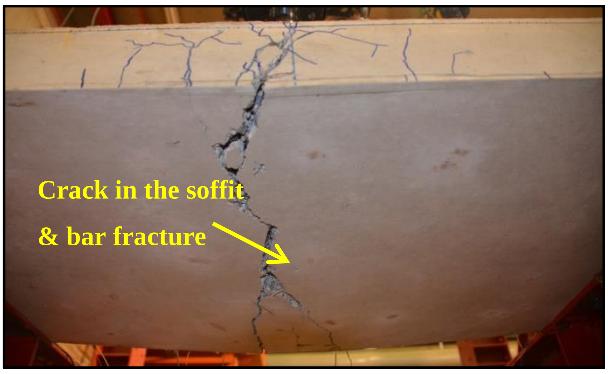

Figure 5.7 Failure mode under (a) cyclic/fatigue in specimen M3-B-F50.

(a) (b)

Figure 5.8 Failure mode under (a) cyclic/fatigue and (b) static loading in specimen BT3.

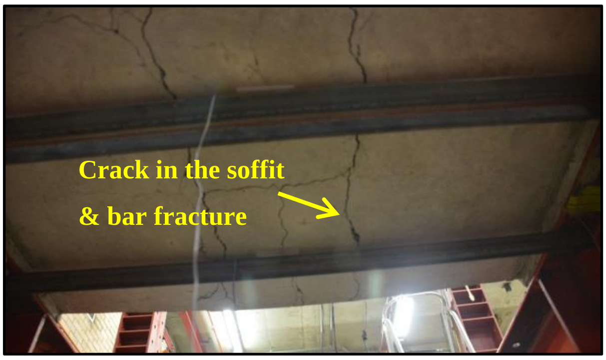

Figure 5.9 Failure mode under cyclic/fatigue in specimen BT3-S-F25.

(a) (b)

Figure 5.10 Failure mode under (a) cyclic/fatigue and (b) static loading in specimen BT3-S.

(a) (b)

Figure 5.11 Mode of failure under (a) cyclic/fatigue and (b) static loading in specimen M3-S.

5.3.2. Strain in steel reinforcement and transverse restraining members

The local strains in the reinforcing bars, bracings and transverse straps/ties were measured during the fatigue testing. The maximum tensile strains in the reinforcing bars versus number of cycles at maximum load (i.e. bracings and straps/ties) are shown in Figure 5.12 to Figure 5.15 . It is noteworthy that the maximum tensile strain occurred in the middle reinforcing steel bars (see Figure 5.2) was around 10-15% less than the strain in the middle steel bars.

There was an initial rapid increase in the reinforcing steel bar strains in the first few hundred (100-1,0000) cycles of the fatigue tests and then after the strain in reinforcing bars became steady or exhibited a very mild gradual increase until the sudden jump in the strain prior to fatigue failure. Comparing the results of M3 with M3-S and BT3 with BT3-S shows that the transverse straps/ties have significantly reduced the level of strains in the steel bars (see Figure 5.15). It is noted that the level of strain in M3 specimen was slightly (around 12%) less than level of strain in M3-B (see Figure 5.12), owing to significantly lower maximum load applied on specimen M3 during fatigue tests. The maximum load applied on specimen M3 was 0.6x47.0 kN= 28.2 kN, which is 54% less than the maximum load of 0.6x72.3 kN= 43.4 kN applied on specimen M3-B during the cyclic/fatigue experiments. Assuming that the level of strain in steel bars is proportional to the level of load, it is concluded transverse bracings away from the slab also are effective in reducing the level of strains in the steel bars, but they are not as effective as straps. Moreover, the steel fibres were found to be effective in lowering the maximum strain in the reinforcing bars (Figure 5.13 and Figure 5.14), provided that a sufficient amount of fibres (0.5% according to fatigue test results) is used. The comparison between static peak load capacity (see

Table 5.3) and fatigue life of specimens M3-B and M3-B-F25 (see Figure 5.14) shows that adding 0.25% fibres can enhance the static load carrying capacity by up to 20% in this case (see

Table 5.3), however, increasing the fatigue load with respect to the enhanced static load carrying capacity (due to 0.25% fibres) can reduce the fatigue life. This is similar to an observation by Parvez & Foster (2014), where low fibre dosage were shown to adversely affect resistance against fatigue in pre-stressed railway sleepers. However, a fibre dosage of 0.50% can improve both static loading capacity and fatigue life of the transversely restrained precast (SF) RC deck slabs. Moreover, it is observable that the 0.25% fibre dosage in specimens BT3-S-F25 and M3-B-F25 has minor influence on the level of maximum strain in the reinforcing steel bars under cyclic/fatigue loading condition (see Figure 5.13 and Figure 5.14). Adding fibres could increase fatigue life of the deck slabs, provided the fibres can effectively bridge across the cracks at later stages of crack propagation. However, in SFRC with 0.25% fibre dosage, the low amount and relatively uneven distribution of fibres was such that the bridging of cracks and prevention of the progressive damage could not be effectively achieved. Hence the slab with 0.25% fibre dosage exhibited deterioration of stiffness, increase of the deflection and the level of stress in reinforcement and finally reduction of fatigue life due to larger fatigue loads which had been applied.

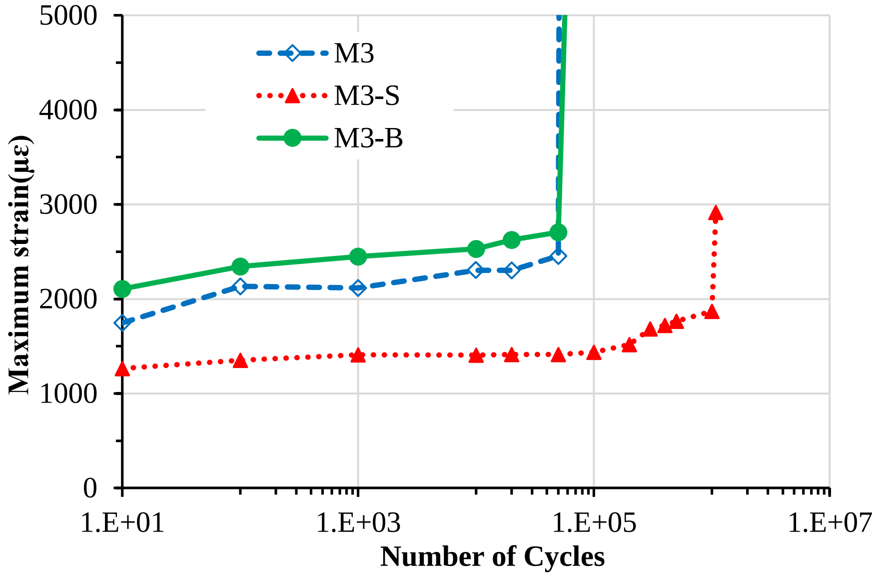

Figure 5.12 Maximum tensile strain in reinforcing steel bars versus number of cycles for M3 series with/without restraining systems.

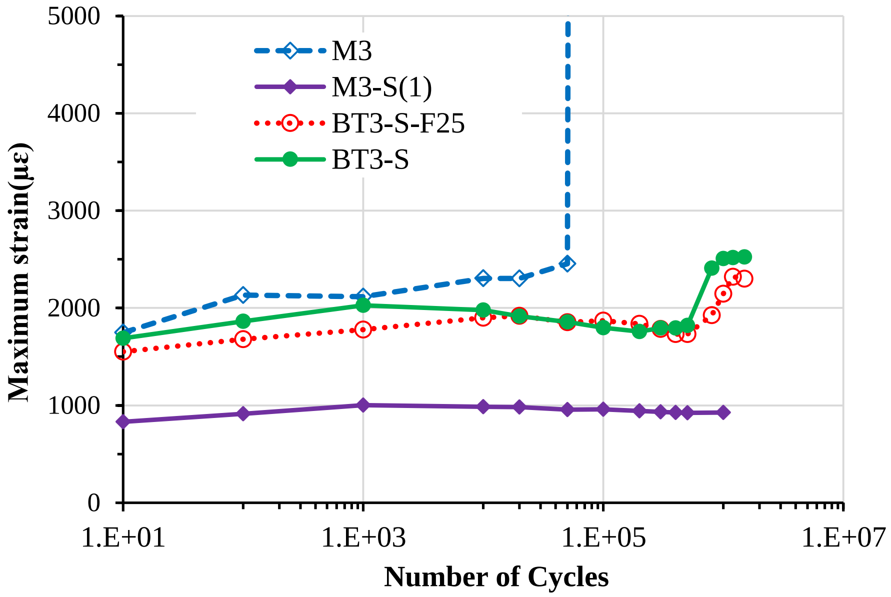

Figure 5.13 Maximum tensile strain in reinforcing steel bars versus number of cycles for BT3 (SF)RC and M3 with straps/ties.

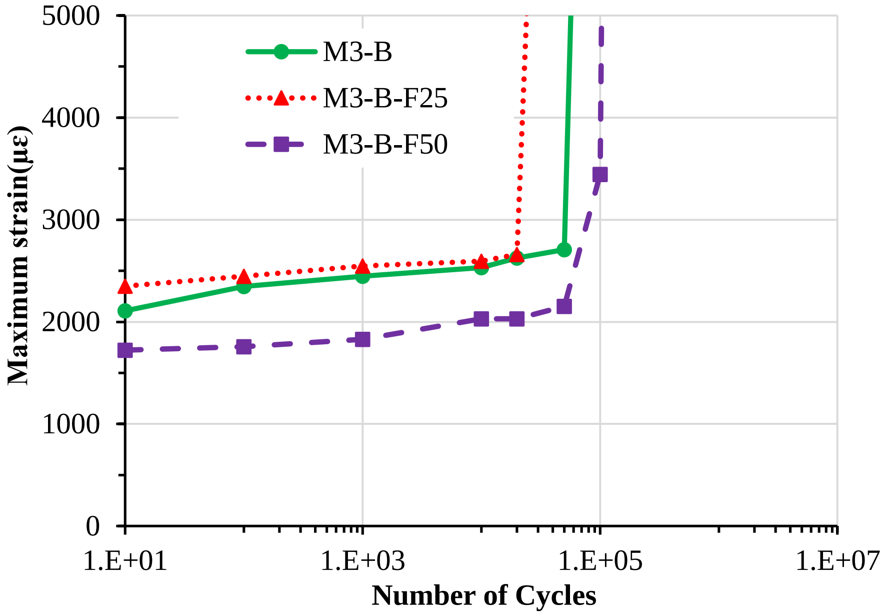

Figure 5.14 Maximum tensile strain in reinforcing steel bars versus number of cycles for M3-B series with/without steel fibres.

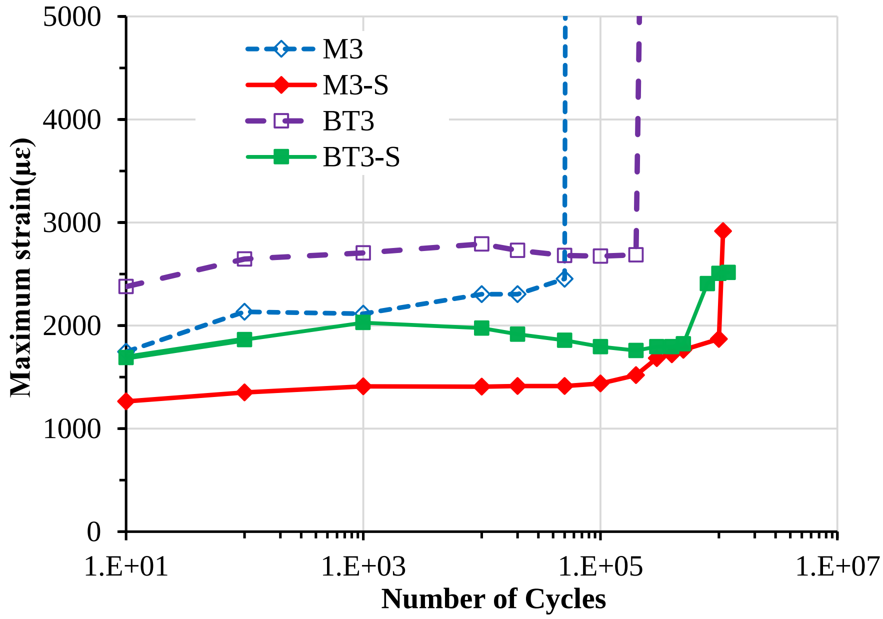

Figure 5.15 Maximum tensile strain in reinforcing steel bars versus number of cycles for BT3 and M3 with/without straps/ties.

The maximum strain measured in the transverse straps/ties and bracings versus number of cycles is shown in Figure 5.16 and it is demonstrated that the transverse restraining system (i.e. straps/ties and cross bracings) experiences progressively increasing tensile strains at the last stages of the fatigue tests. Furthermore, it is observed that the level of tensile strain in straps/ties is higher than cross bracings that, in turn, is demonstrative of higher efficiency of ties compared to bracings for providing restraint and preventing elongation of the slabs.

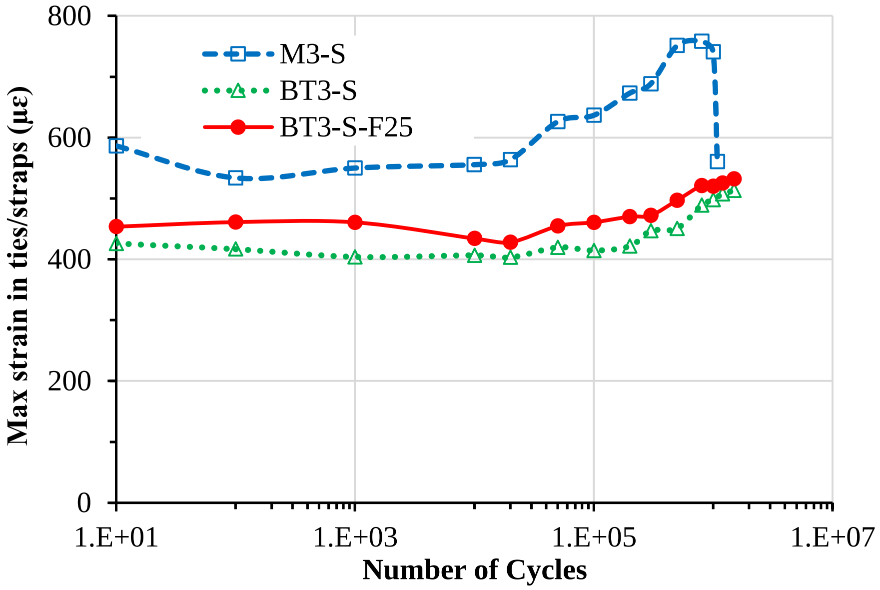

(a)

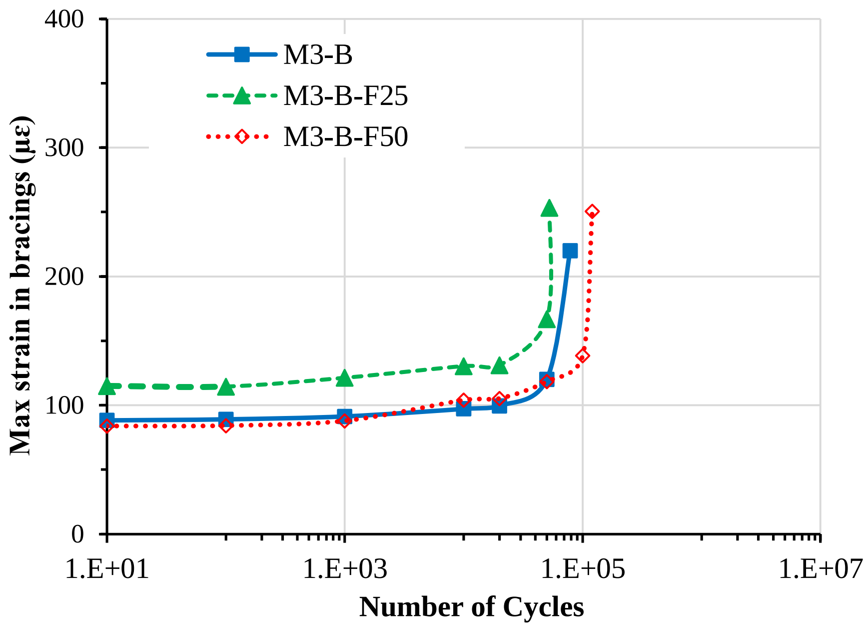

(b)

Figure 5.16 Maximum strain in transverse restraining system (a) straps and (b) bracings versus number of cycles.

5.3.3. Crack patterns and crack width

The crack patterns and crack width at level of the bottom reinforcement were monitored and measured at certain cycles (intervals) during the fatigue tests. The crack width measurements were conducted at the median of the cyclic load range. The maximum crack width versus number of cycles for all specimens is shown in Figure 5.17 to Figure 5.20 and the patterns of crack for all specimens are shown in Figure 5.21 to Figure 5.28.

The fatigue load applied on each specimen was determined with respect to the static load carrying capacity of the (SF)RC specimens (see

Table 5.3). Since the magnitude of fatigue load as well as level of stress in reinforcing bars (directly affecting the crack width) varied from one specimen to another, the maximum crack width in the (SF)RC specimens could not be used for comparing the performance and influence of different transverse restraining systems on the fatigue life of the (SF)RC slabs. Instead, the rate of crack growth (in mm/cycle) which is slope of the crack width versus number of cycles plots in Figure 5.17 to Figure 5.20 is used to compare the fatigue performance of (SF)RC slabs and discuss influence of the transverse restraining systems.

It is observable (see Figure 5.17 to Figure 5.20) that the specimens with transverse straps/ties (i.e. M3-S, BT3-S and BT3-S-F25) exhibit a low rate of crack growth throughout the cyclic/fatigue loading experiments. Furthermore, the rate of crack growth in specimens M3-S is smaller than M3 and M3-B and the rate of crack growth in M3-B is smaller than M3, particularly after $1x10^3$ cycles (see Figure 5.17). Similarly, specimens M3-B, M3-B-F25 and M3-B-F50 (with cross bracings) exhibited a higher crack growth rate after $1x10^3$ cycles (see Figure 5.19). Accordingly, it is concluded that use of transverse straps/ties can effectively control the propagation and widening of the cracks during the cyclic (fatigue) loading condition. However, the cross bracings were not as effective as the straps/ties in controlling the crack width.

In addition to magnitude of the load (or stress level in the steel bars), the crack width also depends on the concrete cover (Frosch 1999; Makhlouf & Malhas 1996). An increase in the concrete cover results in larger crack width based on the available models (e.g. tension chord model (Marti et al. 1998)) for crack width calculation (Frosch 1999; Makhlouf & Malhas 1996). Accordingly, the smaller crack width in BT3 specimens compared to M3 group (see Figure 5.18 and Figure 5.20) can be attributed to smaller concrete cover (i.e. 25 mm) in BT3 specimens compared to 45 mm concrete cover in M3 series. Adding 0.5% by volume of steel fibres (in M3-B-F50) was found to be effective in arresting the cracks and significantly reducing the crack width. A minimum 35% reduction in the crack width was observed in the transversely restrained SFRC slab with 0.5% steel fibre dosage (see Figure 5.19).

The number of cracks in the specimens with transverse straps/ties or 0.5% steel fibres was significantly higher than other specimens as shown in Figure 5.24 and Figure 5.25, for M3 series specimens. However, during the fatigue test the precast deck slabs with cross bracings or low fibre dosage (i.e. 0.25% fibre) had fewer cracks and the cracks in these specimens propagated swiftly towards the most extreme compressive fibre of the cross section (see Figure 5.22 and Figure 5.23). The lower rate of crack growth (in mm/cycle) in specimens with steel fibres is evident from Figure 5.19, in which M3-B-F50 has the lowest rate of crack growth and M3-B has the highest rate of crack growth (particularly after $1x10^3$ cycles) among M3-B, M3-B-F25 and M3-B-F50 specimens.

In contrast with M3 series slabs, the number of cracks in BT3 specimens are similar (see Figure 5.26 to Figure 5.28). It seems that the concrete cover (effective depth of reinforcement in cross section) has more dominant effect on number of cracks compare to presence/dosage of steel fibre or transvers straps. However, use of transvers straps/ties in BT3 slabs significantly controlled progress of crack development towards the compressive fibre of the cross section (see Figure 5.26 to Figure 5.28). The lower width and higher number of cracks in specimens with transverse straps should be attributed to the effect of force loop. In specimens restrained with transvers straps, the concrete cross section in conjunction with the transverse straps form a closed loop such that the compressive force in the concrete is in balance with the tensile forces in reinforcing bars and the tensile forces in the straps. During the fatigue tests, the force loop generated by the transverse ties/straps effectively mobilise arching action that in turn prevents growing and widening of the crack. Accordingly, the crack width in specimens with straps tends to be smaller than other specimens. According to tension chord model, the smaller width of cracks is also associated with larger number of cracks. Similarly, the smaller crack width and larger number of cracks in SFRC specimens with sufficient fibre dosage can be explained. The steel fibres bridging the cracks can effectively prevent swift growth of the cracks and accordingly reduce the crack width.

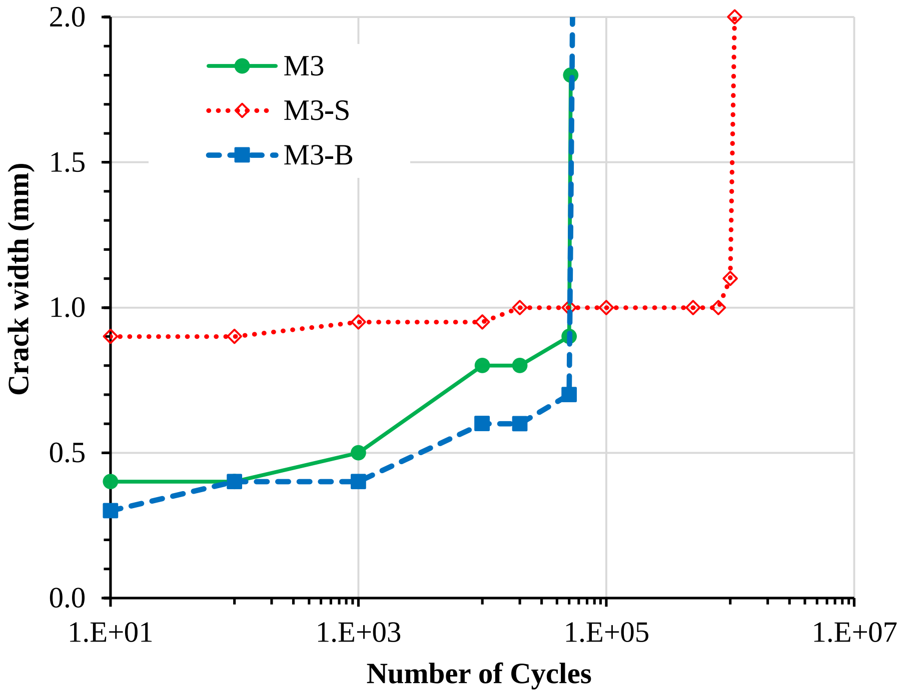

Figure 5.17 Maximum crack width versus number of cycles for M3 series with/without restraining systems.

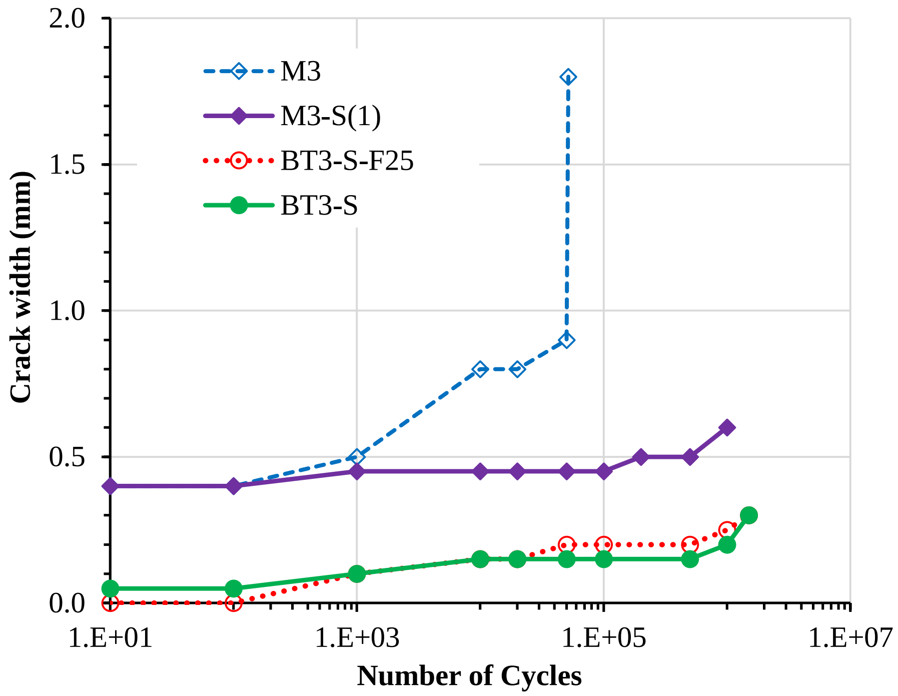

Figure 5.18 Maximum crack width versus number of cycles for BT3 (SF)RC and M3 with straps/ties.

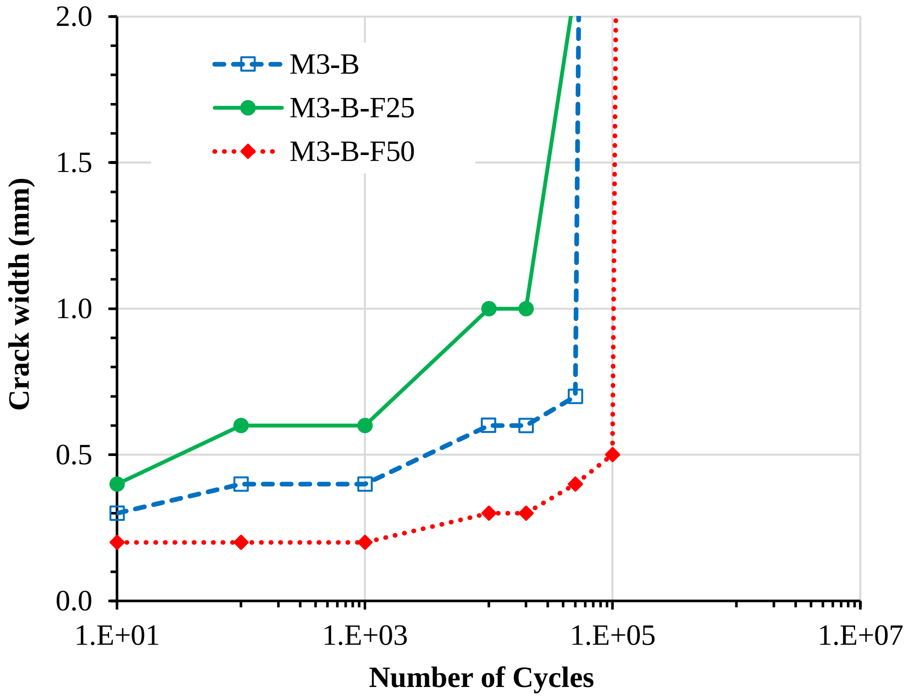

Figure 5.19 Maximum crack width versus number of cycles for M3-B series with/without steel fibres.

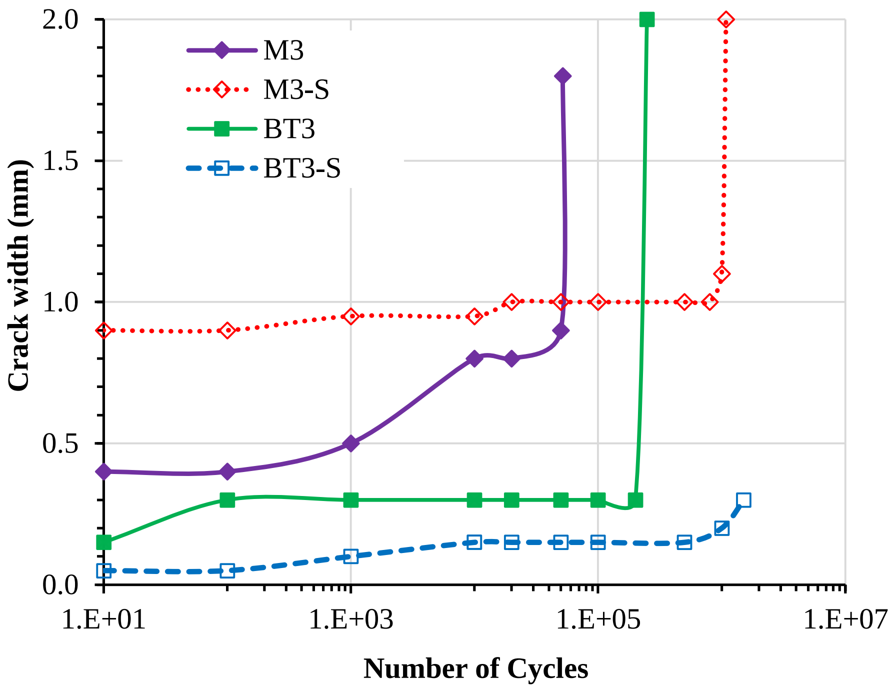

Figure 5.20 Maximum crack width versus number of cycles for BT3 and M3 with/without straps/ties.

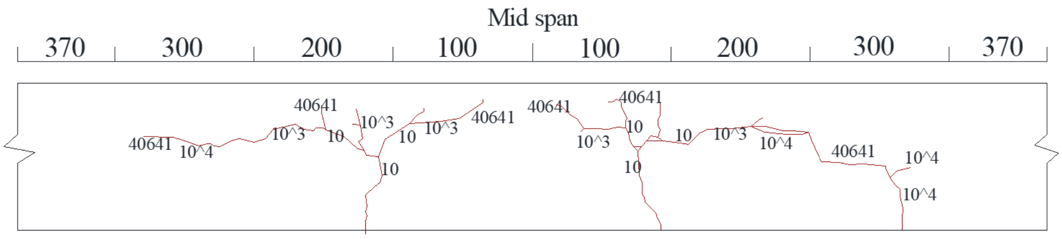

Figure 5.21 Pattern of cracks obtained at different cycles for specimen M3.

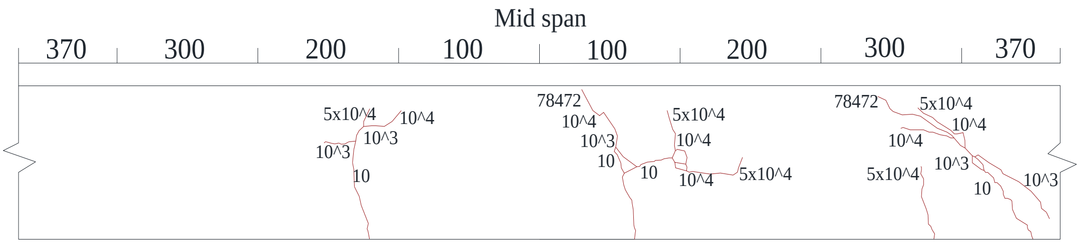

Figure 5.22 Pattern of cracks obtained at different cycles for specimen M3-B.

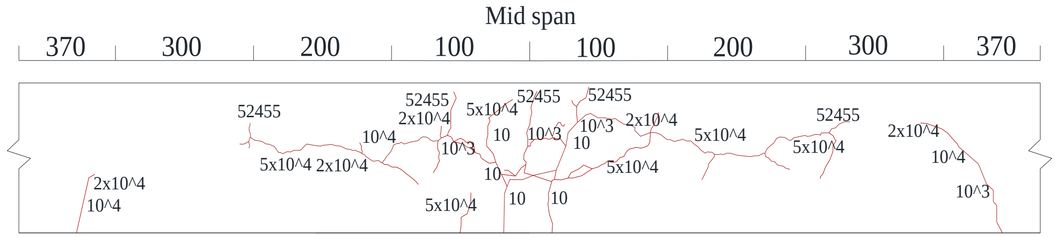

Figure 5.23 Pattern of cracks obtained at different cycles for specimen M3-B-F25.

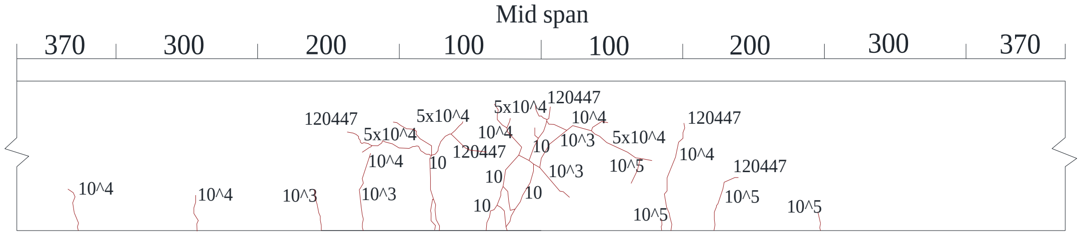

Figure 5.24 Pattern of cracks obtained at different cycles for specimen M3-B-F50.

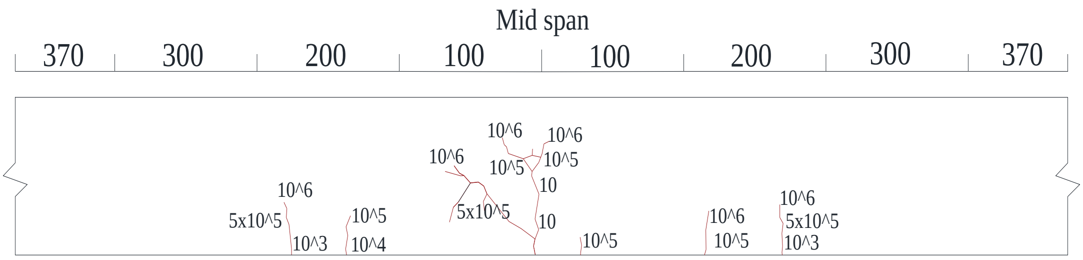

(a)

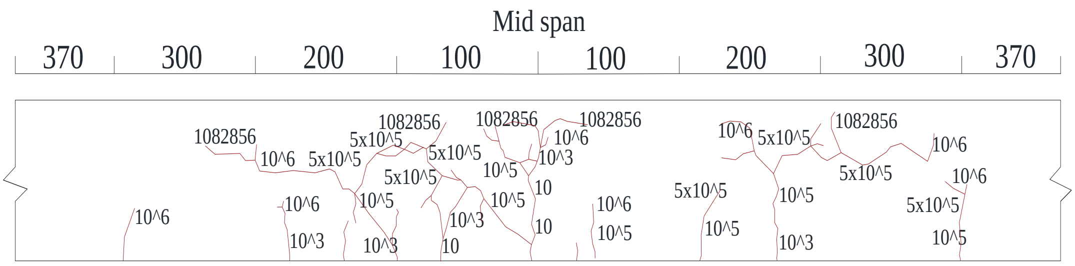

(b)

Figure 5.25 Pattern of cracks obtained at different cycles for specimen (a) M3-S1 and (b) M3-S.

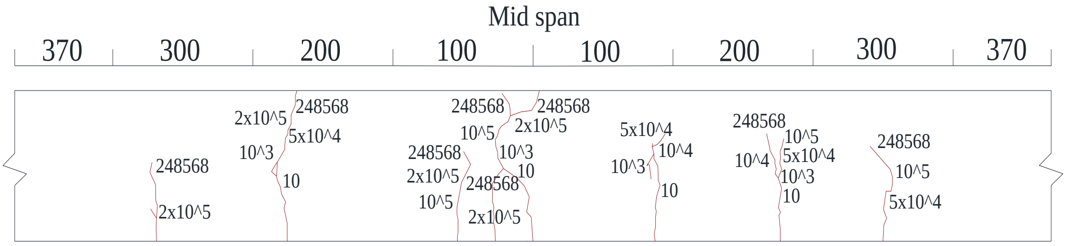

Figure 5.26 Pattern of cracks obtained at different cycles for specimen BT3.

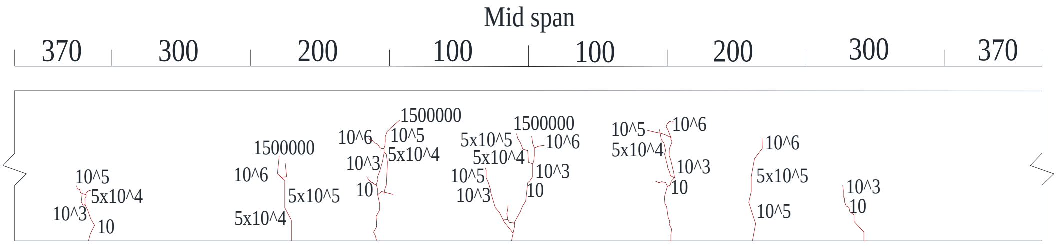

Figure 5.27 Pattern of cracks obtained at different cycles for specimen BT3-S-F25.

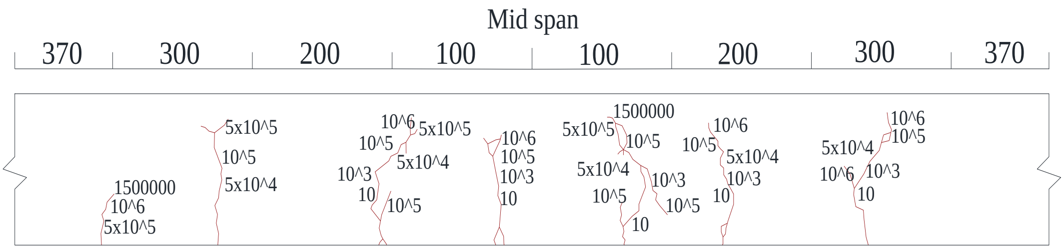

Figure 5.28 Pattern of cracks obtained at different cycles for specimen BT3-S.

5.3.4. Deflections

The maximum mid-span deflection versus number of cycles for all specimens is plotted in Figure 5.29 to Figure 5.32. The progressively increasing mid-span deflection observed in the fatigue tests is attributed to stiffness degradation associated with formation and development of cracks. It is observed that the mid-span deflection of specimen M3-B is smaller than M3 and M3-S (see Figure 5.29). The smaller mid-span deflection of M3-B can be attributed to the end rotational stiffness/restraints provided by the cross bracings for the precast (SF)RC slabs. Comparing the mid-span deflection of specimen M3 with M3-S(1) (see Figure 5.30) shows that transverse ties can significantly improve the stiffness of precast slabs (a minimum 90% enhancement in the stiffness of slab was observed in this case). The fibre dosage of 0.25% and 0.5% had identical effect on the static load carrying capacity of the slabs (see

Table 5.3); however, the specimen with 0.25% fibre dosage had significantly larger mid-span deflection compared to the specimen with 0.5% fibre dosage (Figure 5.31). The BT-3 series have smaller mid-span deflection compared to M3 series (Figure 5.32), owing to larger effective depth of the BT-3 specimens that results in larger post-cracking stiffness for BT-3 compared to M3 specimens.

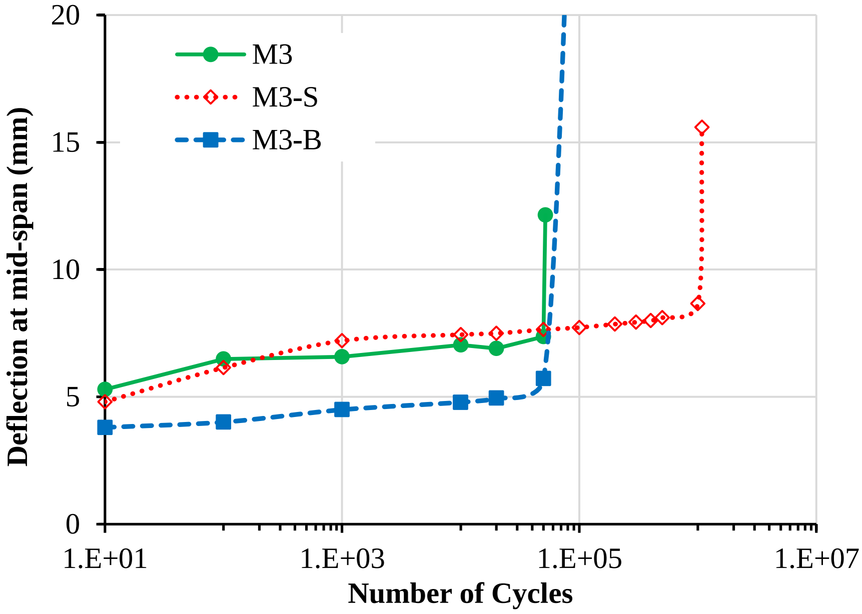

Figure 5.29 Deflection at mid span versus number of cycles for M3 series with/without restraining systems.

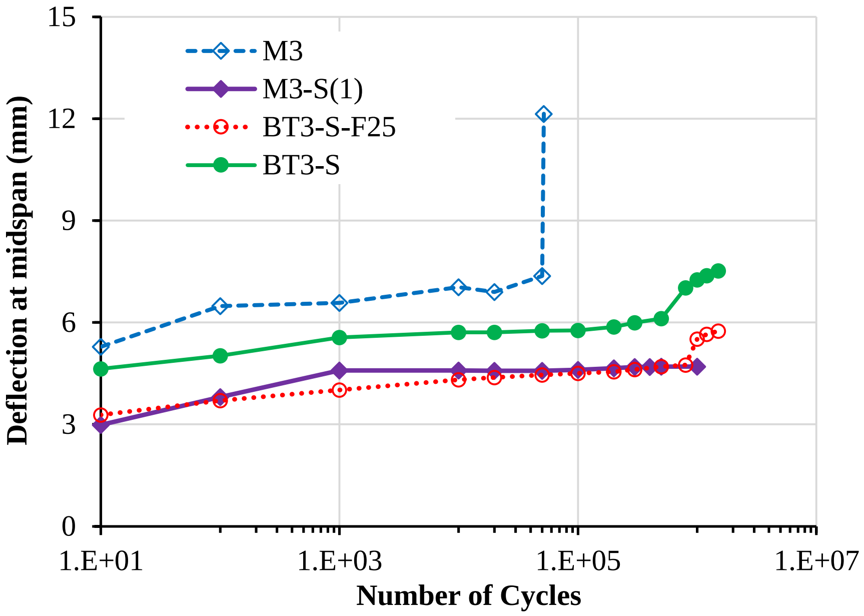

Figure 5.30 Deflection at mid span versus number of cycles for BT3 (SF)RC and M3 with straps/ties.

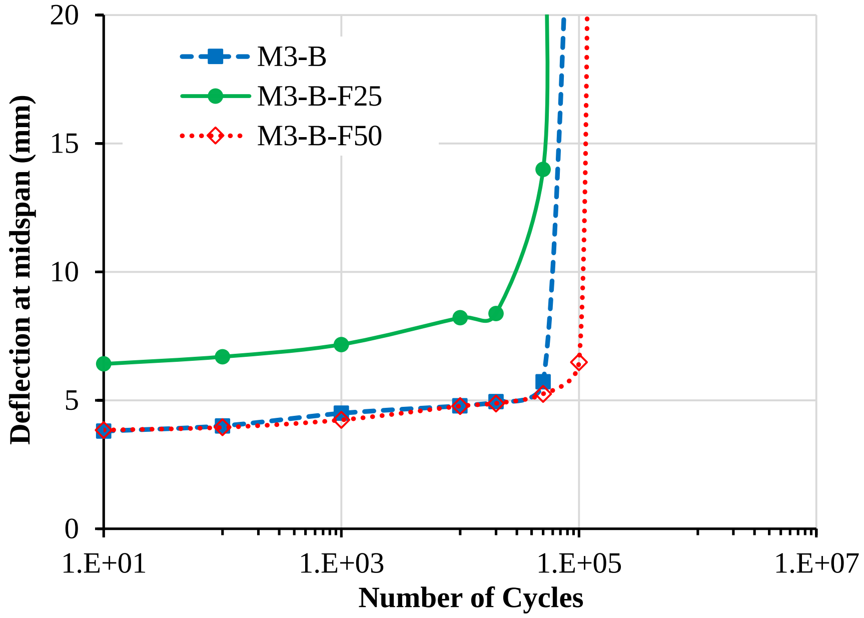

Figure 5.31 Deflection at mid span versus number of cycles for M3-B series with/without steel fibres.

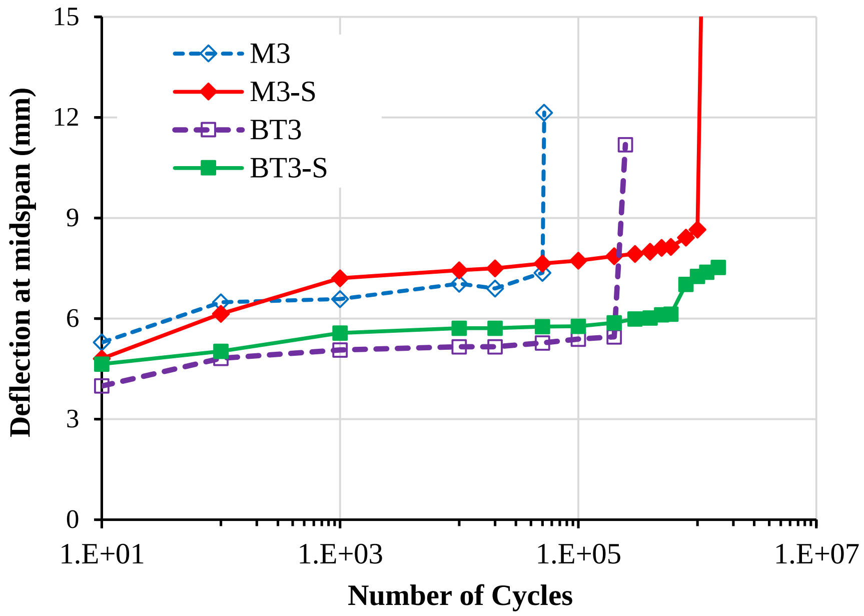

Figure 5.32 Deflection at mid span versus number of cycles for BT3 and M3 with/without straps/ties.

5.3.5. Stress range in the reinforcing bars and fatigue life predicted by S-N curve

There are three different approaches for fatigue life prediction: S–N curve, fracture mechanics and damage accumulation models that can be used for fatigue assessment of steel elements. However, the concept of S-N curves has gained popularity and, owing to its simplicity is widely adopted by design codes. S-N curve have also been successfully used for fatigue assessment of steel bars in bridge deck slabs (Schlafli & Bruhwiler 1998). The fatigue life of slabs tested in this study was mainly governed by fatigue fracture of the reinforcing steel bars. Accordingly, the S–N curve of CEB-FIP (1993) (developed for steel bar under constant amplitude stress range) were utilised to assess the fatigue life of the slabs.

The maximum stress range in the reinforcing bars versus number of cycles for different specimens are compared in Figure 5.33 to Figure 5.36. It is seen that the maximum stress range in the reinforcing steel bars becomes steady after a few hundred (between

100 and 1,000) cycles and a sudden increase in the stress range occurs in the last few hundred cycles of fatigue tests. Comparing the stress range in specimens with and without transverse straps (see Figure 5.33, Figure 5.34 and Figure 5.36) clearly demonstrates the efficiency of straps/ties for reducing the stress range in the steel bars and, accordingly, increasing the fatigue strength of the deck slabs. Furthermore, comparing the maximum stress range in M3-B specimens with and without steel fibres (see Figure 5.35) shows that using 0.5% steel fibres can effectively reduce the stress range in the conventional steel bars and, consequently, increase the fatigue life of transverse restrained (SF) RC slabs.

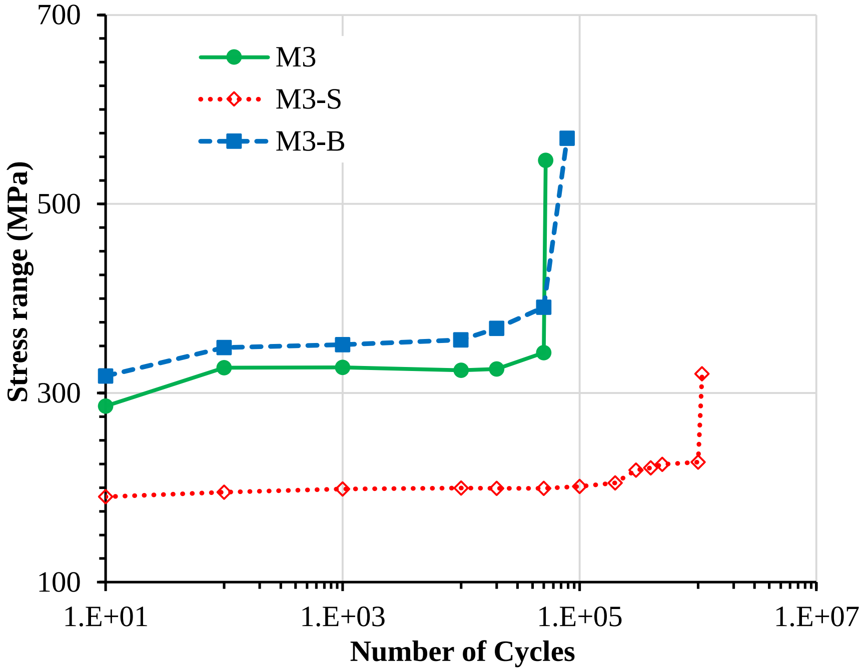

Figure 5.33 Maximum stress range in reinforcing bars during fatigue tests versus number of cycles M3 series with/without restraining systems.

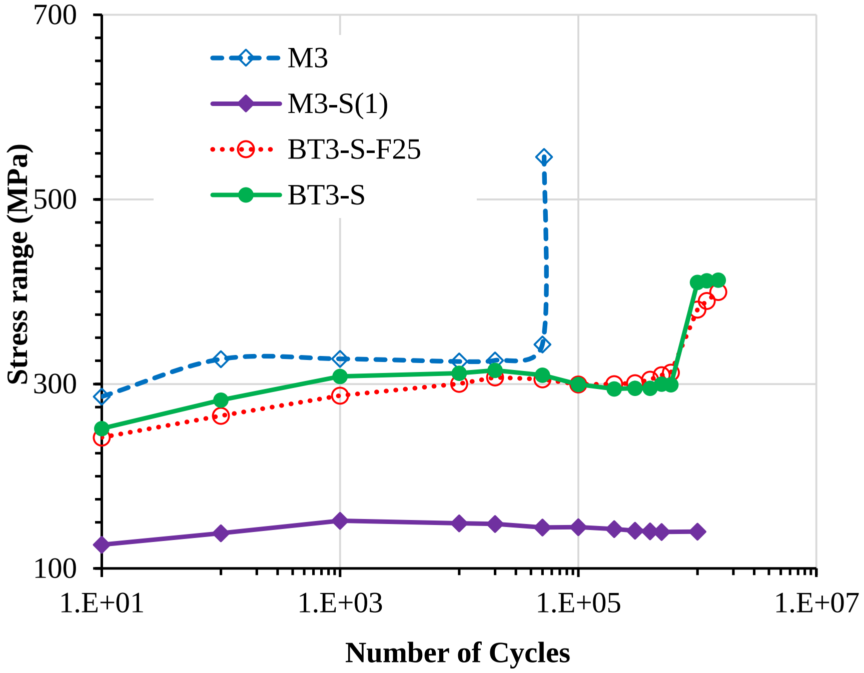

Figure 5.34 Maximum stress range in reinforcing bars during fatigue tests versus number of cycles BT3 (SF) RC and M3 with straps/ties.

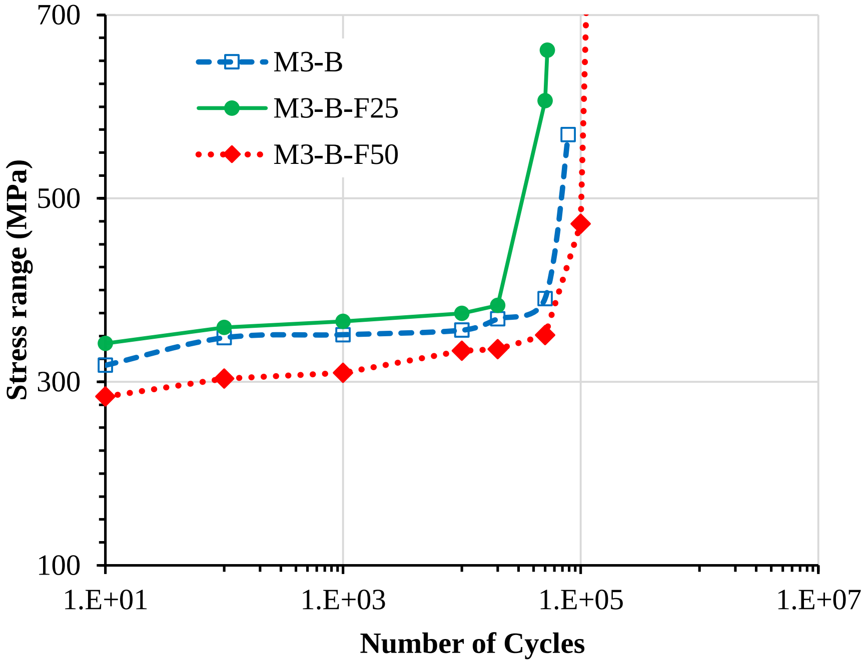

Figure 5.35 Maximum stress range in reinforcing bars during fatigue tests versus number of cycles M3-B series with/without steel fibres.

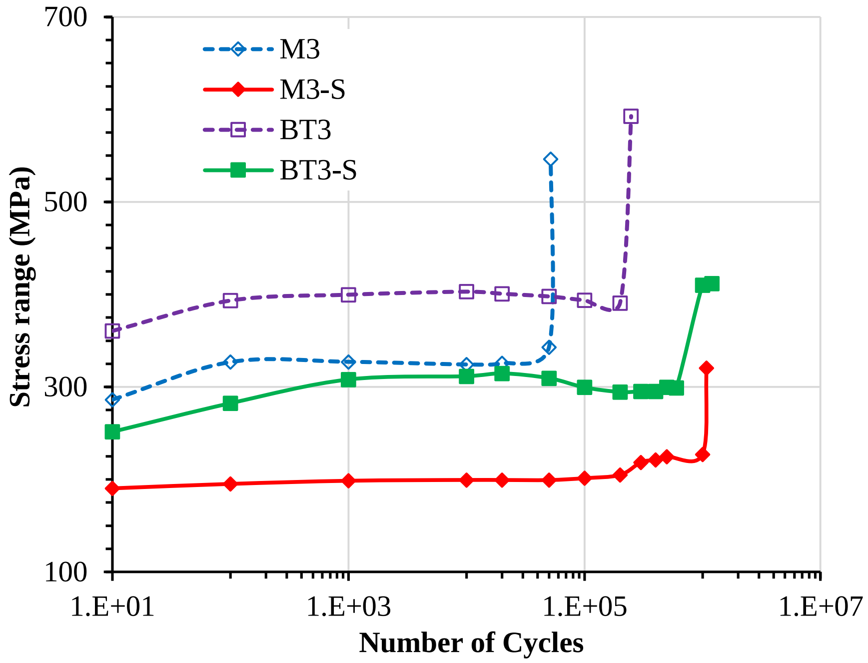

Figure 5.36 Maximum stress range in reinforcing bars during fatigue tests versus number of cycles for BT3 and M3 series with/without ties.

In Figure 5.37, the fatigue life versus maximum stress range in the reinforcing bars of the slabs are compared with S–N curve of CEB-FIP (1993). It is seen that the CEB-FIP Model Code S-N curves provide a rather conservative prediction of the fatigue life of BT3 series (with 25 mm concrete cover) and this conservatism is typical of the S-N curves adopted in different design codes. However, the fatigue life of M3 series (with 45 mm concrete cover) predicted by S–N curve of CEB-FIP Model Code is not conservative. The seemingly less conservative fatigue life predicted for M3 series by S-N curves is attributed to significantly high level of strain localisation (at the location of cracks) in M3 specimens that has not been considered in S-N curves (derived with respect to average strain/ stress in the bars). This higher level of strain localisation in M3 series compared to BT3 series is evident from the larger crack width in M3 series compared to BT3 specimens (see Figure 5.20).

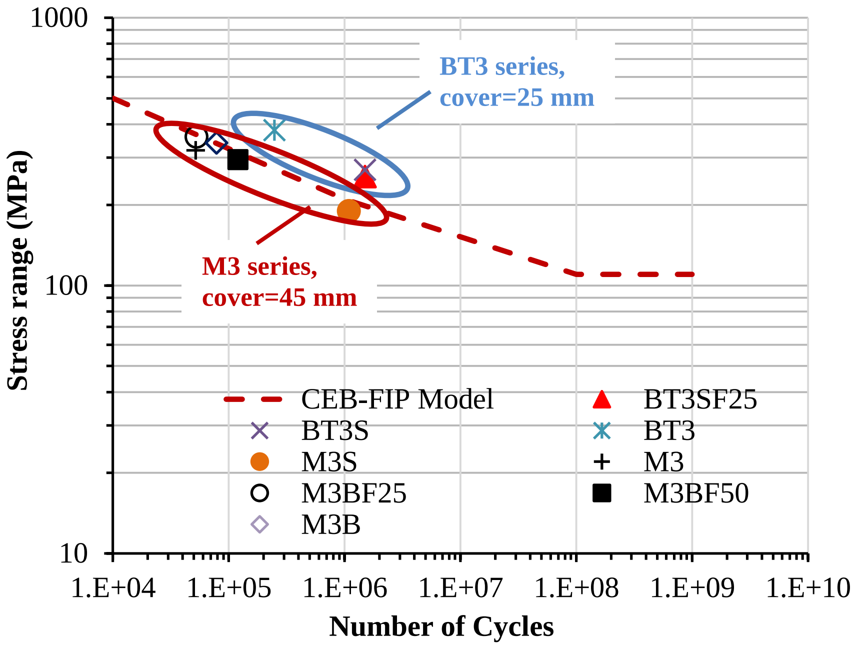

Figure 5.37 Comparison between fatigue life of M3 and BT3 series and S-N curve of CEB-FIP.

5.4. Conclusions

A set of fifteen, one-half scale, transversely restrained deconstructable precast RC/SFRC deck slabs were tested under static and cyclic fatigue load applied at the mid-span. The precast slabs were connected to the supporting steel girders by means of post-installed friction grip bolted shear connectors (PFBSC) and two types of transverse restraining systems (i.e. ties/straps under the slab strip and cross-bracings away from the slab strip) for mobilizing arching action in precast (SF)RC deck slabs were utilised. Also, the influence of conventional reinforcing bar proportion and location and influence of steel fibres dosage (0.25% and 0.50%) on the load carrying capacity and fatigue performance of the transversely restrained (SF) RC slabs was examined. The results of this experimental study provide benchmark data required for evaluating the fatigue behaviour, mode of failure and fatigue life of the transversely restrained precast (SF) RC deck slabs. The following conclusions were drawn with respect to the results of laboratory tests;

– The post-installed bolted shear connectors employed for connecting the precast

(SF) RC slabs to steel girders did not show any sign of deformation or damage, despite significant damage and cracking that slabs had undergone under cyclic loading conditions. This feature can facilitate dismantling and replacing of the precast (SF) RC deck slabs.

- The provision of transverse bracings and straps (ties) can improve the fatigue life of precast deconstructable (SF) RC deck slabs. In particular, the strength enhancement provided by the transverse restraining systems can be taken into account under cyclic service loading conditions without negatively affecting the fatigue life of the deck slabs. However, transverse ties/straps under the deck slabs have superior performance compared to bracings in terms of improving the load carrying capacity as well as fatigue life of the deconstructable (SF)RC deck slabs. In addition to mobilising the arch action, the transverse ties/straps under the slabs form a force loop in conjunction with the (SF)RC slab and carry large tensile stresses (forces) and accordingly reduce the tensile stresses/forces in the reinforcing bars and crack width in the concrete slab.
- Mobilising the arch action by using transverse ties or cross bracings can be used as an effective strengthening method for RC deck slabs.
- The precast deconstructable (SF)RC deck slabs tested with transverse ties/straps exhibited two distinctive modes of failure under cyclic (fatigue) loads. The first failure mode was triggered by fracture of reinforcing bars; the second mode of failure was triggered by rupture in the transverse ties/straps at the location of shear connectors bolt hole.
- Under static loading conditions the transversely restrained (SF)RC slabs exhibited a rather ductile mode of failure associated with yielding of steel bars and compressive crushing of concrete at mid-span.
- Under a seemingly constant average strain/stress range, the location of reinforcing steel bars can significantly affect the fatigue life of (SF) RC deck slabs. Increasing the concrete cover on steel bars (or reducing the effective depth *d* of the deck slabs) can lead to higher level of strain localisation (at the location of cracks) in steel bars that, in turn, can significantly reduce the fatigue life of RC deck slabs.
- Adding 0.5% steel fibres to transversely restrained (SF) RC deck slabs

significantly improved the static load carrying capacity as well as fatigue life of the tested specimens.

- Adding 0.25% fibre dosage can enhance the static load carrying capacity by up to 20%, however, increasing the fatigue load with respect to the enhanced static load carrying capacity (due to 0.25% fibre dosage) can reduce the fatigue life.

CHAPTER 6

3D FINITE ELEMENT MODELLING OF DEMOUNTABLE PRECAST REINFORCED CONCRETE DECK SLABS WITH EXTERNAL CONFINING SYSTEM

6. 3D Finite Element Modelling of Demountable Precast Reinforced Concrete Deck Slabs with External Confining System

6.1. Introduction

The nonlinear finite element analysis has gained popularity among researchers and engineers to simulate and study behaviour of complex structures instead of time consuming and costly laboratory experimentation. Accordingly, different types of finite element models (i.e. 1D beam, 2D plane stress and 3D continuum-based) have been developed for analysis of RC members capable of considering geometrical nonlinearities and material nonlinearities such as concrete cracking, concrete crushing, yielding and rupture of reinforcements.

In previous chapters, structural behaviour of new proposed deck slab system has been evaluated experimentally with only a few variables considered in the laboratory tested bridge deck slabs. In this chapter, structural performance of the deconstructable bridge deck with precast concrete slabs and PFGB shear connectors and a transverse confining system is evaluated numerically to expand the library of data on structural performance of the new proposed deck slabs. Detailed non-linear 3D continuum-based finite element (FE) models of the deconstructable precast deck slabs with transverse ties and/or cross-bracings are developed using ABAQUS (ABAQUS User´s Manual 2009) software and the FE models are analysed. The developed FE models are validated against experimental results from Chapter Two. For this purpose, the global and local response (i.e. load-deflection, peak load carrying capacity, failure mode and load-strain) of the transversely confined deck slabs obtained from FE analysis are compared with the test data. Afterwards, the validated FE model is used to conduct a parametric study in which the influence of different parameters including yield strength of reinforcing bars, concrete compressive strength, reinforcement ratio, clearance between concrete slab and PFGB shear connectors and pretension stress in the PFGB shear connectors and thickness of the precast concrete slab on the structural behaviour of the precast deck slabs with external confining system in the transverse direction are investigated.

6.2. Finite element (FE) modelling

Structural behaviour of the precast RC deck slabs with transverse confining system in a deconstructable composite deck is numerically studied using nonlinear 3D FE models. In the first step, the 3D finite element models of a one-span precast concrete deck slab with transverse ties and/or cross-bracings (Figure 6.1 and Figure 6.2) is developed and validated against experimental results. Commercial software ABAQUS (ABAQUS User´s Manual 2009) is used to develop and analyse the FE models. The non-linearity associated with contacts/interfaces, geometrical and material non-linearities including concrete cracking and crushing, yielding of reinforcing steel bars, bolted shear connectors, steel profiles and transverse ties/straps and cross-bracings are considered in the FE models. In the following sections, details of the modelling, constraints, material constitutive laws, meshing, contacts, boundary conditions and loading procedure are provided and briefly discussed.

6.2.1. Boundary conditions and constraints

The Cartesian coordinate system adopted for creating the FE models is illustrated in Figure 6.1 and Figure 6.2. The Y and Z axes define the plane of the cross-section of the precast RC deck slab with external confining tie (and/or cross bracings) in the X (transverse) direction. The displacements in Z and Y direction over a small region on the bottom flange at the end of the steel beams are restrained to model a pinned support at each end of the supporting steel beams (Figure 6.1 and Figure 6.2).

6.2.2. Modelling interaction between contacting components

The composite precast deck slab with external confining strap and deconstructable PFGB shear connectors comprises several components including the steel beam, bolt shear connectors and square washers, precast concrete slab and the external confining system that interact with each other through direct contacts (see Figure 6.3). The interaction between these components is modelled by the surface-to-surface contact feature available in the ABAQUS software. In total, seven contact pairs including the steel beam-precast concrete slab, bolt-precast concrete slab, bolt-steel girder, bolt-steel washer, washer-precast concrete slab, bolt-tie (or bolt cross bracing), steel girder-tie (or cross bracing-stiffener) are considered in the FE model. The HARD contact and PENALTY options are employed in the directions normal and parallel to the contact interface planes, respectively. A friction coefficient of 0.45 is adopted for the contact interface between the steel beam and the precast concrete slab (Figure 6.3c), and a friction coefficient of 0.25 was adopted for other interface contacts (Liu et al. 2016; Liu, Bradford & Lee 2015). The diameter of clearance holes in the steel beams, steel washers, ties and cross bracings was 1 mm and in the precast concrete slab was 2 mm bigger than the size of PFGB shear connectors (or bolted connections). A perfect bond between reinforcing steel bars and concrete is assumed and accordingly the EMBEDDED option in ABAQUS software is used to model the interaction (perfect bond) between the reinforcing bars and precast concrete slab. The weld between the steel beam and the stiffeners is modelled by the TIE option that provides full compatibility of displacements.

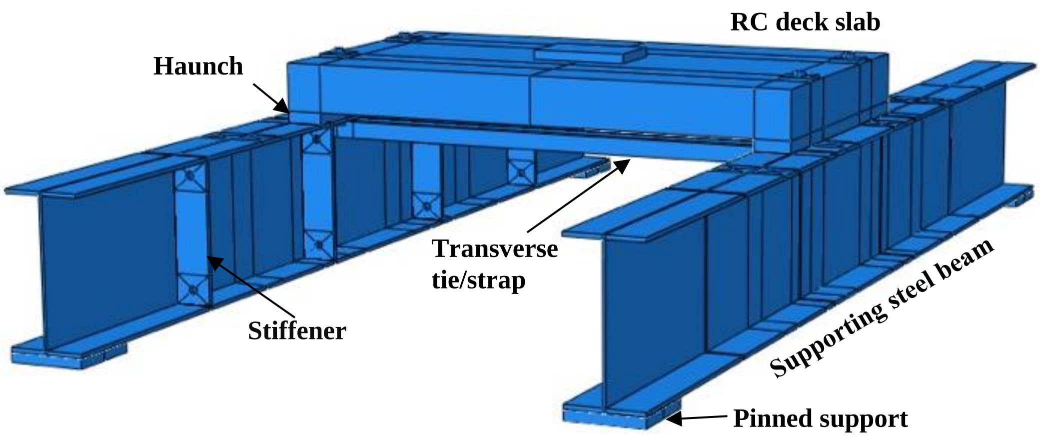

Figure 6.1 Outline of the deconstructable composite precast deck RC slab with external ties/straps in the transverse direction.

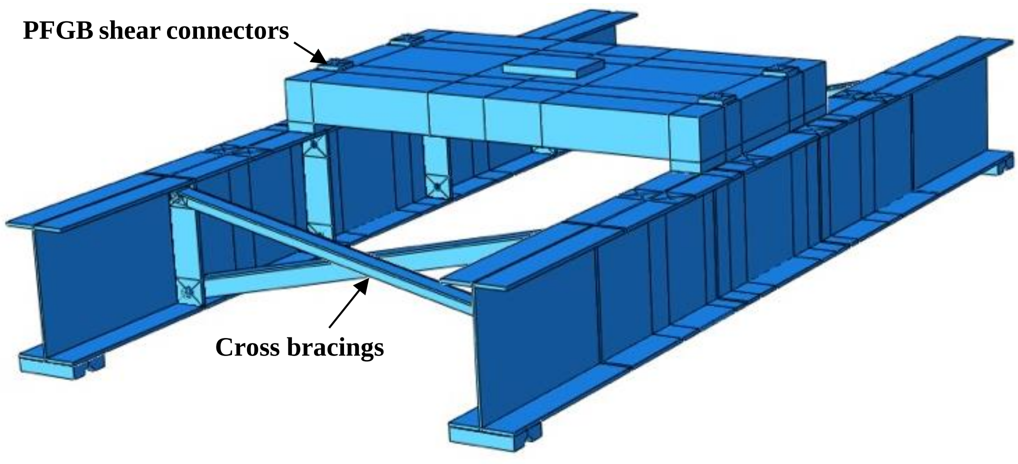

Figure 6.2 Outline of the deconstructable composite precast deck RC slab with external cross bracings in the transverse direction.

6.2.3. Loading procedure and analysis technique

The FE models were loaded in two stages similar to that of followed in the experiments. In the first stage of loading, the high-strength bolts (PFGB) connecting the precast concrete slab to the steel girder and the straps are post-tensioned using the bolt load option provided in ABAQUS software. The contact interactions are established in the first stage of loading to reduce the possible numerical instability in the ensuing loading/analysis steps. In the second stage, a displacement-controlled load is applied at mid-span and the FE model is analysed using Riks method that can capture the highly nonlinear collapse response of the RC slab with transverse confinement.

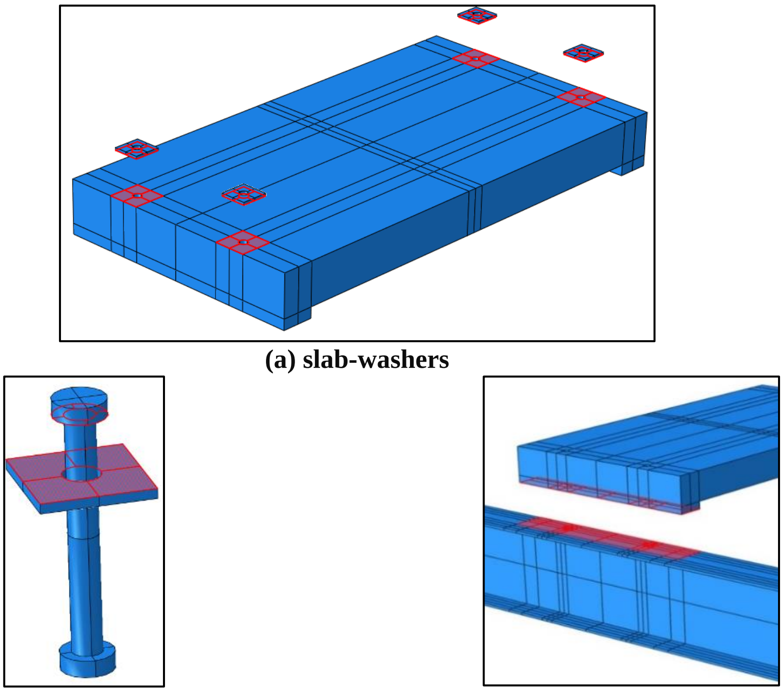

(a) slab-washers

(b) PFGB-washer **(c) Steel girders-precast slab**

Figure 6.3 Contacts defined at interfaces between different components in the 3D FE model.

6.2.4. Meshing

Except reinforcing steel bars, all components are modelled by 8-node linear hexahedral solid elements with reduced integration and hourglass control (C3D8R). The reinforcing steel bars are modelled by truss elements (T3D2) with a linear displacement shape function. It is noteworthy that element C3D8I with incompatible modes performs better than C3D8R, but element C3D8R is employed in this study to reduce the cost of computation (Tahmasebinia, Ranzi & Zona 2012; Tahmasebinia, Ranzi & Zona 2013). A sensitivity analysis was conducted to determine size of the mesh that provide a good compromise between accuracy and efficiency. The outline of the FE mesh for beams, precast slab, PFGB and washers are shown in Figure 6.4.The final mesh size that assigned for the structural components (except the reinforcing bars) varied between 5 mm to 25 mm depending on the location of elements, i.e. concrete deck slab, steel girders, steel washer plates and bolted shear connectors. For instance, for area of the deck slab near the bolted shear connectors, the size of FE mesh was limited to 5 mm but in outer face of the slabs and area away from the bolted shear connectors, a mesh size of 25 mm was used. For the reinforcing bar also 10 to 25 mm mesh size was assigned. In general, three average mesh size, i.e. 10 mm, 25 mm and 45 mm was chosen to study the mesh sensitivity of the FE model. The results of a sample mesh sensitivity analysis are shown in Figure 6.4d. It is seen that the load vs displacement response of the slab is slightly affected by the mesh size, however, the influence of mesh size on the predicted peak load carrying capacity is negligible.

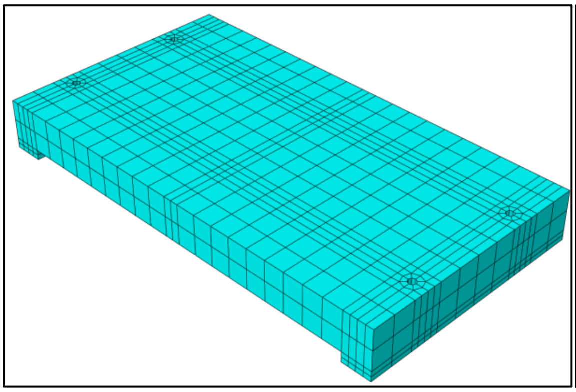

(a) Precast concrete slab

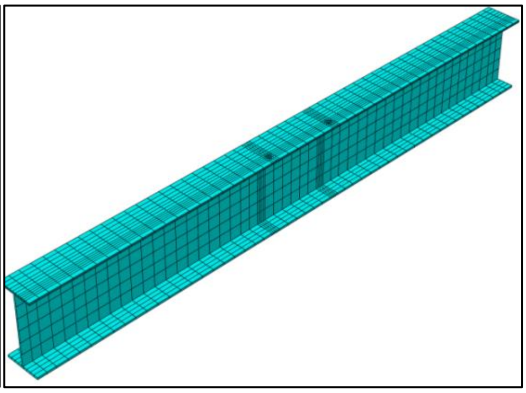

(b) Steel beam

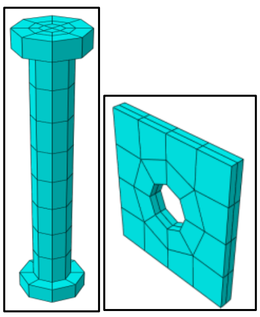

(c) Bolt & washer

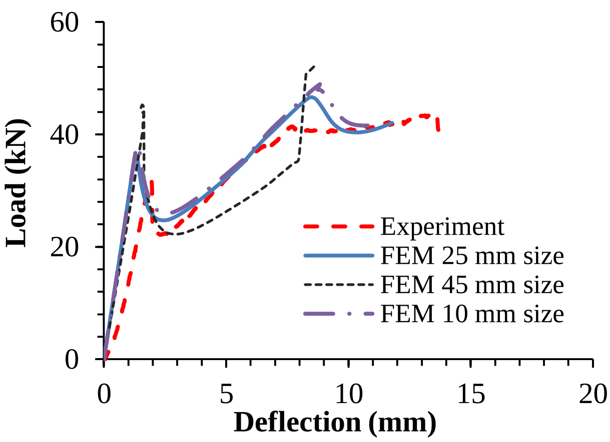

(d) results for different mesh size

Figure 6.4 (a, b & c) 3D FE mesh size and configuration adopted different components and (d) load vs displacement predicted by different FE mesh size.

Distribution of the von Mises' stresses in M16/8.8 PFGB shear connectors predicted by the 3D FE models after the first stage of loading (bolt pretension) is shown in Figure 6.5. It is seen that the maximum stress of 334.6 MPa (Figure 6.5) in the FE model (at the end of first stage of loading) is sufficiently close to the shank tension of $0.4 f_{uf} = 330\,\text{MPa}$ (f_{uf} being the tensile strength of class 8.8 bolts) in the laboratory experiment.

6.2.5. Material models

Structural steel, high strength bolt shear connectors and reinforcing steel bars

Multi-linear elastic-hardening plastic stress-strain models with different yield and ultimate strength are adopted for steel bolts, beams/straps and reinforcement both in tension and compression (see Figure 6.6). Furthermore, the von Mises yield criterion is used to capture onset of the steel yielding under multiaxial stress states. The key mechanical properties of steel including modulus of elasticity, yield strength, ultimate strength and ultimate strain used for developing the multi-linear stress-strain curves in Figure 6.6 are taken from the material tests conducted on the small specimens (Ataei, Bradford & Liu 2016; Bursi & Jaspart 1998).

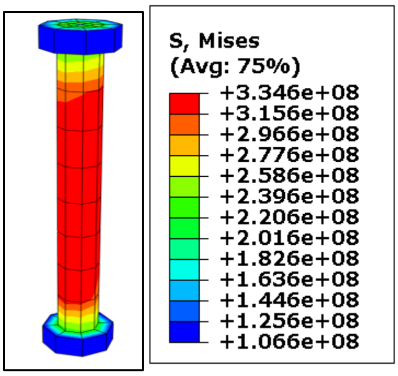

Figure 6.5 Stress distribution (in Pa) at the first step of loading (pre-stressing PFGB connector).

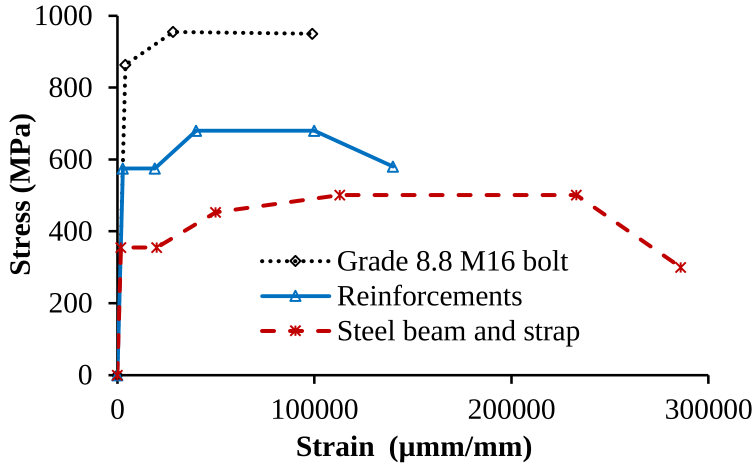

Figure 6.6 Stress-strain relationship adopted for reinforcing steel bars, steel beams/ties and high-strength PFGB shear connectors.

Concrete

In the FE models, plastic-damage constitutive law (Lee & Fenves 1998) is used for modelling nonlinear behaviour of concrete. The plastic-damage model can capture concrete cracking and crushing, stiffness degradation (damage) as well as development of plastic strains. For concrete in compression, Carreira & Chu (1985) model was used assuming that the stress increases linearly to 35% of the mean compressive strength f_c and then followed by,

$$\sigma_c = \frac{f_c \gamma(\varepsilon/\varepsilon_0)}{\gamma - 1 + (\varepsilon/\varepsilon_0)^{\gamma}} \qquad \textbf{Equation 6.1}$$

where ε_0= 0.002 and γ= $(f_c/32.4)^3$+1.55 is a parameter that controls the curvature of stress-strain diagram. The concrete ultimate strain (strain at failure in compression) is taken as ε_{cu}= 0.01.

For concrete in tension, a linear–elastic representation until the tensile strength f_t followed by a linear softening branch after concrete cracking is adopted. The failure strain of concrete in tension is taken as $\varepsilon_{tu} = 10 \times (f_t / E_c)$, where E_c is the elastic modulus of concrete.

6.3. Validation of the FE models

The accuracy of the FE models and assumptions adopted for predicting the structural behaviour of the composite precast deck slabs with transverse ties and/or cross-bracings and PFGB shear connectors is investigated by comparing the FE predictions with the experimental results. Eight transversely confined precast concrete deck slabs, with transverse ties and/or cross bracings and different reinforcing proportion and location from experiments were used in the validation study. The outline of geometry, dimensions and designation of the specimens used for validation of the FE results are shown in Figure 6.7 and Table 6.1, respectively.

In Table 6.1, the designation Ln-R for specimens was made with respect to L the location (T: top, M: middle and B: bottom layer), n number of N10 reinforcing bars and -R the type of transverse confining system (-C: cross-bracing and -S: strap). The precast RC slabs were 600 mm wide and 100 mm thick and supported on a pair of 310UB32 which were 1100 mm apart. Normal ductility N10 steel bars were used to provide reinforcement for the slabs. At each end, the slabs had a 25 mm thick haunch to increase the arching actions. The M16 Grade 8.8 bolted shear connectors were tightened to a shank tension of $0.4f_{uf} = 330MPa$. The transverse confining system were comprised of either a pair of ties (Equal leg angel EA45x45x3 of Grade 300PLUS) or two pairs of bracings (Equal leg angel EA45x45x5 of Grade 300PLUS). The transverse ties were attached to the bottom surface of the 310UB32 top flange by 16 mm bolted shear connectors and the cross bracings were attached to the stiffeners by M16 bolts (see Figure 6.7). For easy installation and removal of PFGB shear connectors, the oversized hole in the flange of the steel beam profile and precast concrete slab for all specimens was 18 mm and 20 mm in diameter respectively, meaning that the diameter of holes in the steel beam/stiffeners and precast concrete slab were 2 mm and 4 mm larger than the bolt size.

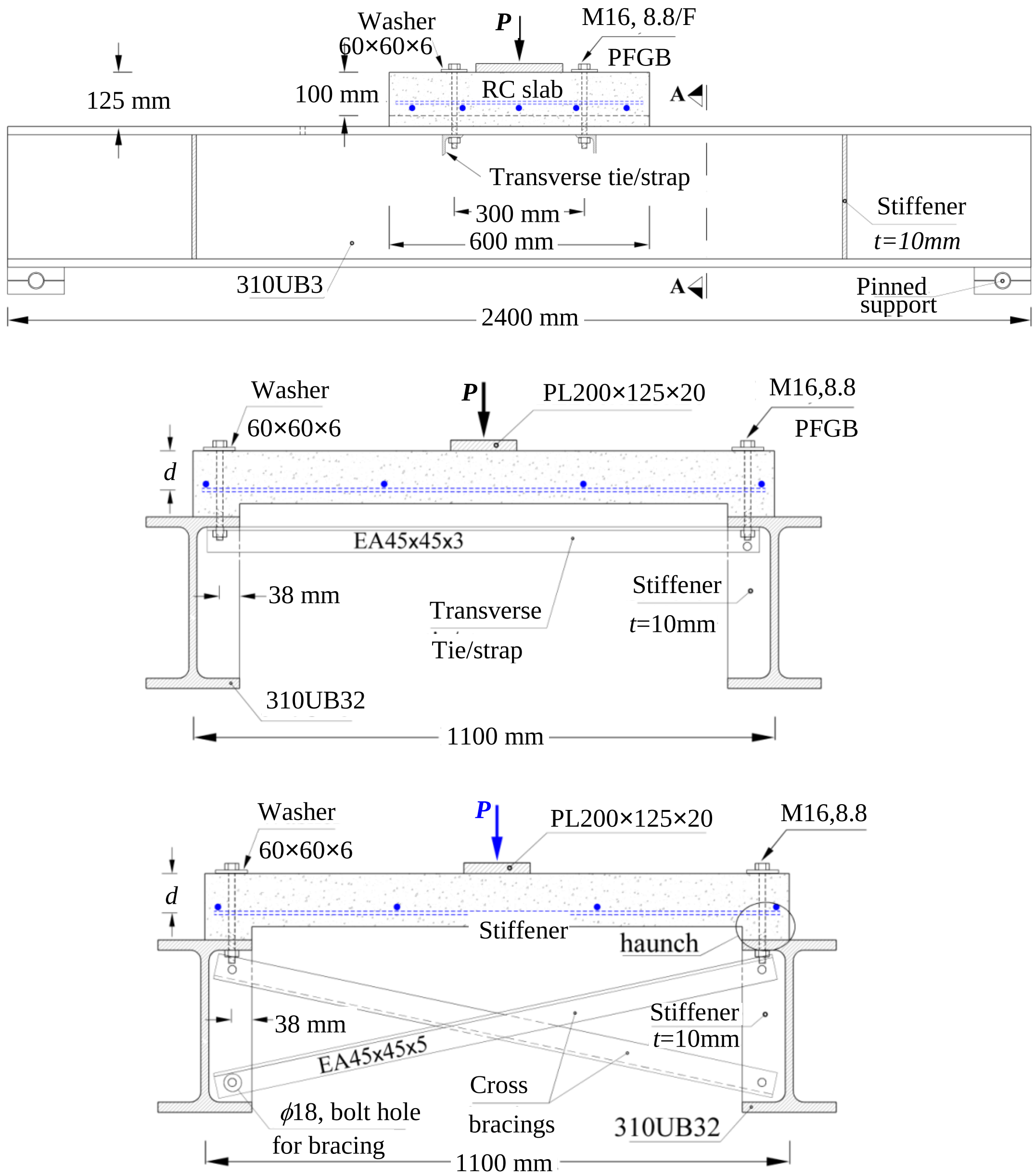

Figure 6.7 Outline of the geometry, dimensions and cross sections of the specimens tested.

The load versus mid-span deflection which are illustrated in Figure 6.8 to Figure 6.15, the load versus reinforcement strain which are depicted in Figure 6.16 to Figure 6.21, and the load versus strain in transverse ties/cross bracings predicted by the FE models which are shown in Figure 6.22 to Figure 6.27 are compared with the experimental results, demonstrating the reasonable accuracy of the proposed FE models for predicting the global and local response. The experimental peak loads are compared with the peak load captured by the FE models in Table 6.1 and a good correlation with less than 7.2% difference between the experimental and FE peak loads is observable, (see Table 6.1). The failure modes of the specimens M4 and B4-S associated with cracking of concrete at mid-span and/or cracking at end-span (adjacent to PFGB shear connectors) are shown in Figure 6.28 and Figure 6.29 and a good correlation between the experimental results and failure mode captured by the FE model is observable. The contours of von Mises stresses and deformation of PFGB shear connectors in specimen M4-S at a load of P= 70 kN is shown in Figure 6.30 that is demonstrative of very small deformations and stress levels (below yield strength) in the PFGB shear connectors. With regard to the results provided in Figure 6.8 to Figure 6.30 and Table 6.1, it is concluded that the proposed FE models adequately simulate the global and local levels structural response of the deconstructable precast RC slabs with transverse confinement. The FE models could nearly capture the load-deflection behaviour of the specimens; however, the peak loads and the failure modes of the tested specimens has been predicted with good accuracy, The maximum difference between the peak loads of FE models and experiments was less than 8% (see Table 6.1). The discrepancy between the FE load-displacement and experimental load-displacements should be attributed to inaccuracy of the FE models for capturing complex nature of the friction between different components (i.e. strap-steel girder interface, bracing-stiffener interface, deck soffit-steel girder interface) that could not be measured accurately during the experiments and used for calibration of the FE models.

Table 6.1 Details of the precast concrete slabs transversely confined by ties and/or bracings.

Trans. restraint & designation		Steel bars	Reinforcing ratio	d ## (mm)	f_{cm} ## (MPa)	Peak load (kN)		$\frac{(P_{Exp.}-P_{FE})}{P_{Exp.}}$
						$P_{Exp.}$	P_{FE}	
Ties/ Straps	M4	4N10	0.97	55	60	55.8	54.8	1.8 %
	M4-S	4N10	0.97	55	60	84.5	84.5	0.0 %
	M0-S	N/A	0.00	N/A	60	43.7	46.6	6.6 %
	B4-S	4N10	0.97	75	60	111.8	111.8	0.0 %
Cross-bracing	M3-B	3N10	0.73	55	70	73.6	78.9	7.2%
	B3-B	3N10	0.53	75	70	91.3	91.7	0.5%
	BT3-B##	3N10	0.53	75	70	92.7	93.6	1.0%
	M6-B	6N10	1.47	55	70	102.9	101.2	1.6%

All specimens except BT3-B only have one layer of reinforcement. Specimen BT3-B has two layers of reinforcements at 25 and 75 mm from the furthest top fibre of the slab cross section.

d = effective depth of longitudinal reinforcing bars; f_{cm}= mean compressive strength of concrete.

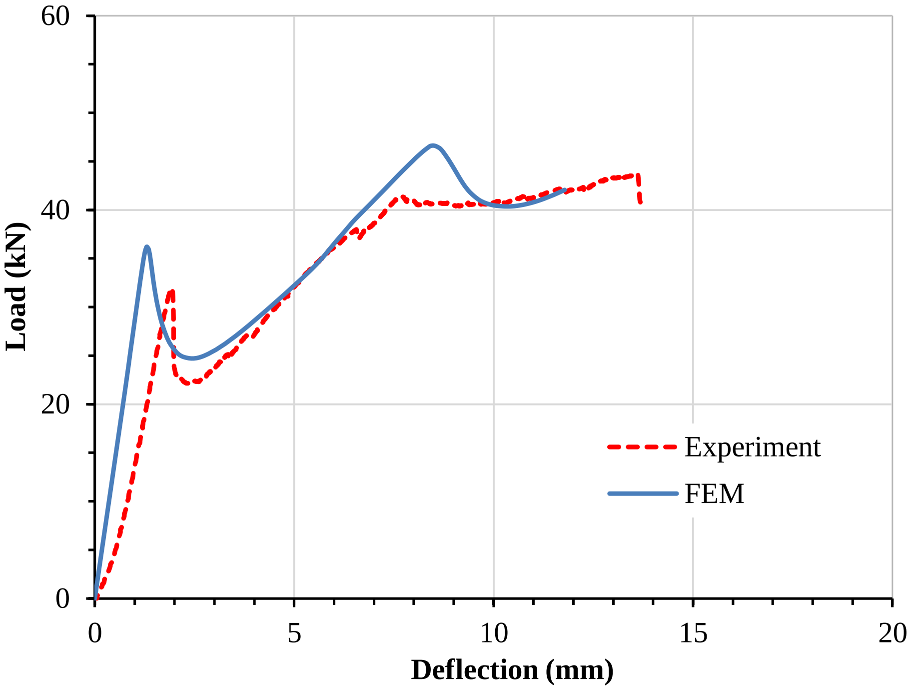

Figure 6.8 Comparison of the experimental load versus mid-span deflection with FE predictions for specimen M0-S.

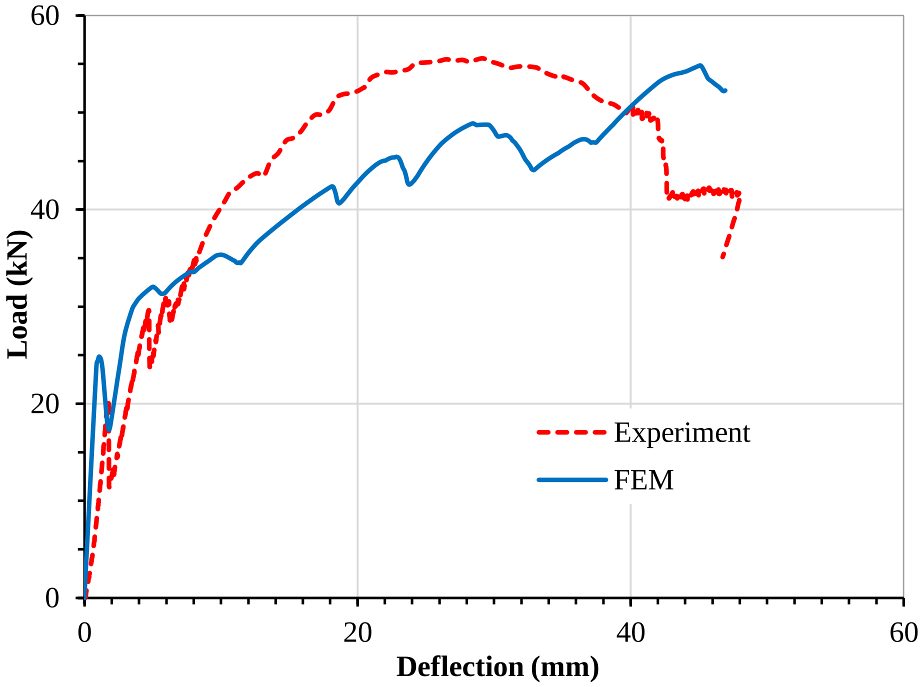

Figure 6.9 Comparison of the experimental load versus mid-span deflection with FE predictions for specimen M4.

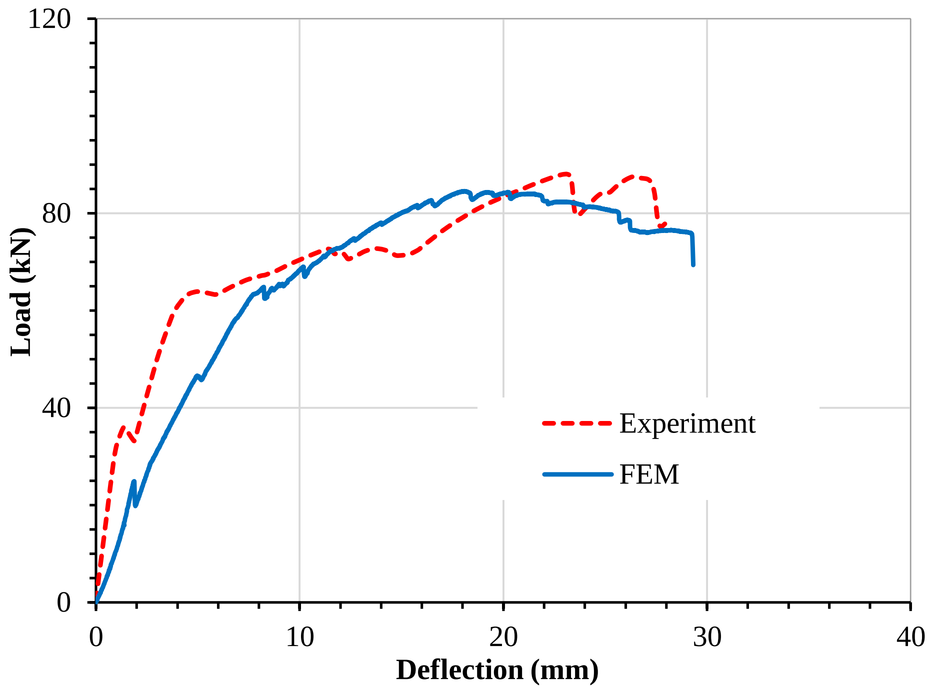

Figure 6.10 Comparison of the experimental load versus mid-span deflection with FE predictions for specimen M4-S.

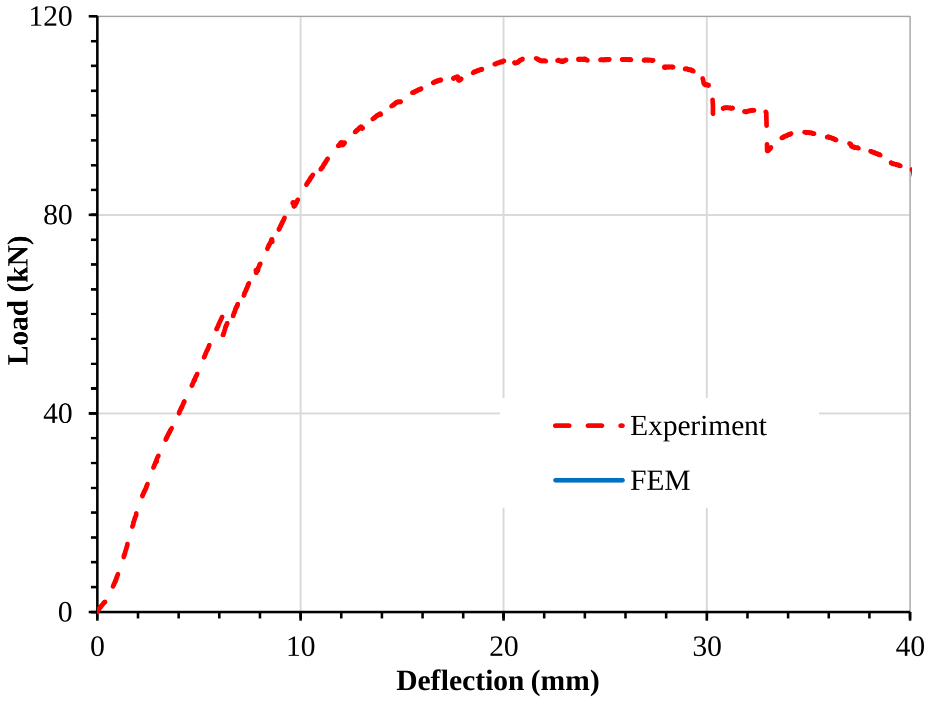

Figure 6.11 Comparison of the experimental load versus mid-span deflection with FE predictions for specimen B4-S.

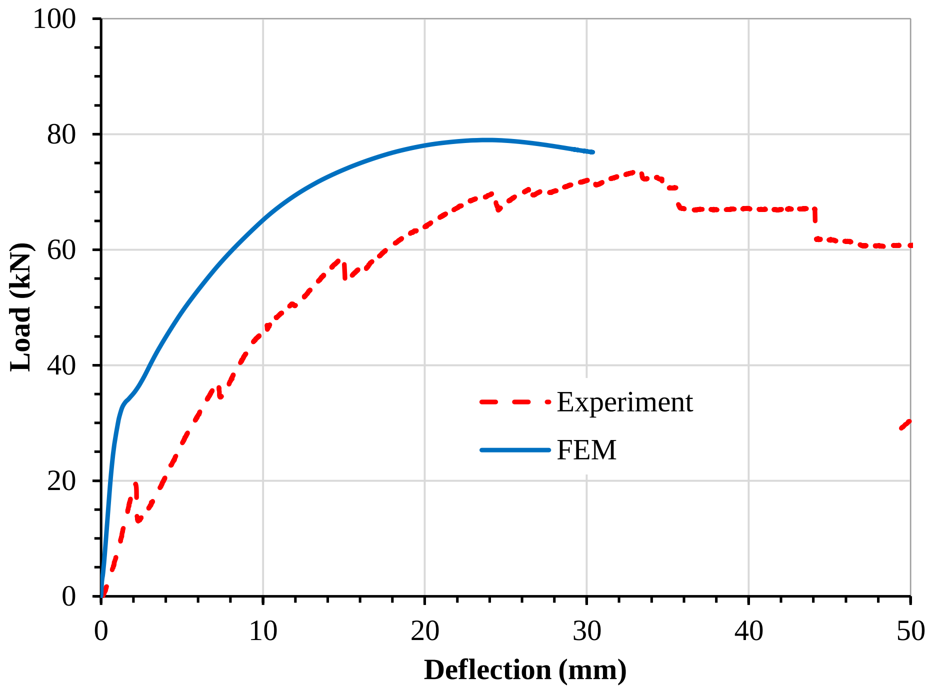

Figure 6.12 Comparison of the experimental load versus mid-span deflection with FE predictions for specimen M3-B.

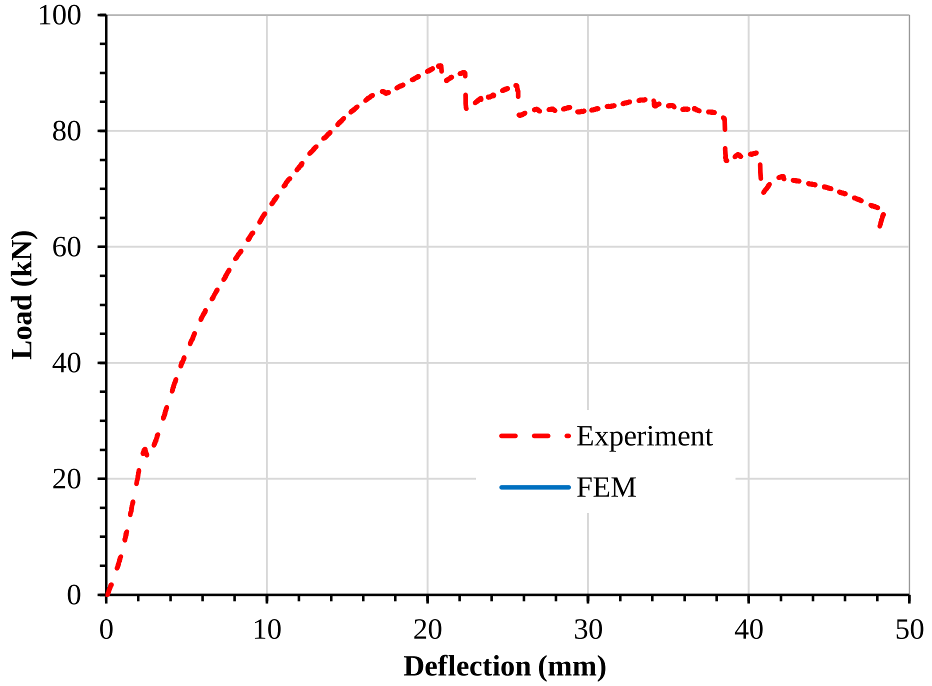

Figure 6.13 Comparison of the experimental load versus mid-span deflection with FE predictions for specimen B3-B.

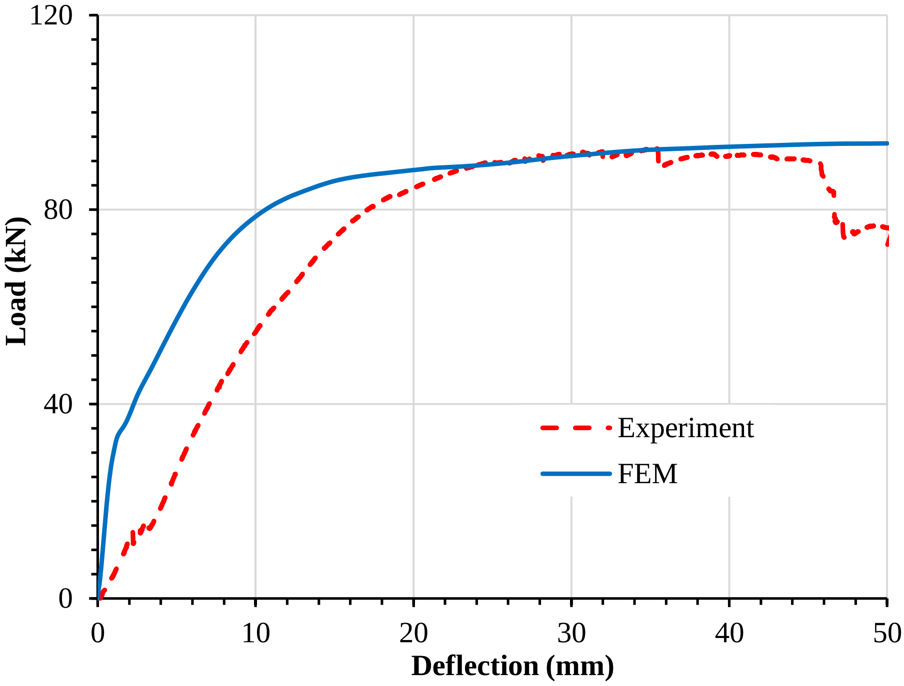

Figure 6.14 Comparison of the experimental load versus mid-span deflection with FE predictions for specimen BT3-B.

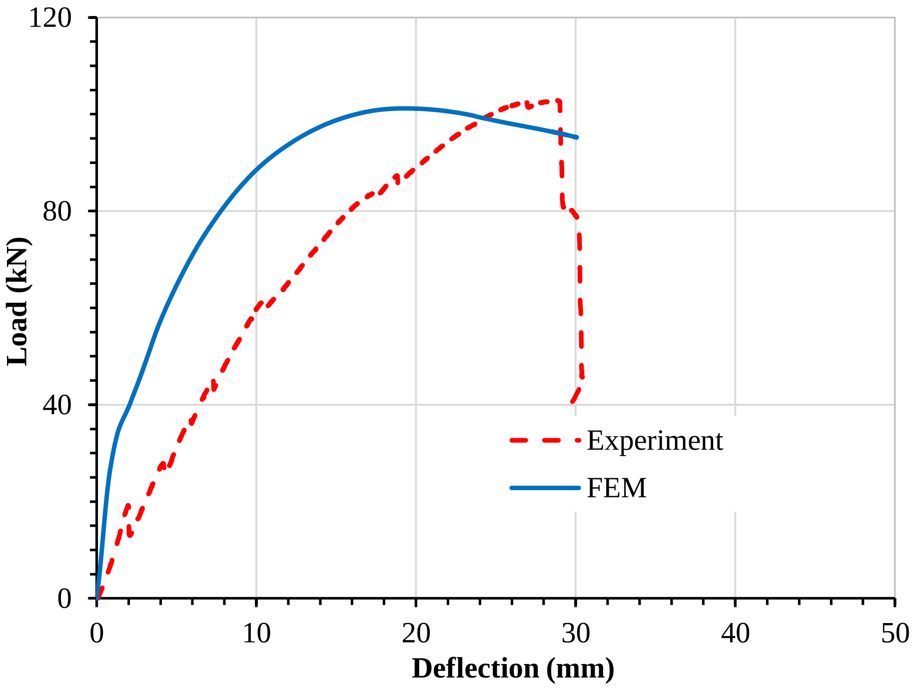

Figure 6.15 Comparison of the experimental load versus mid-span deflection with FE predictions for specimen M6-B.

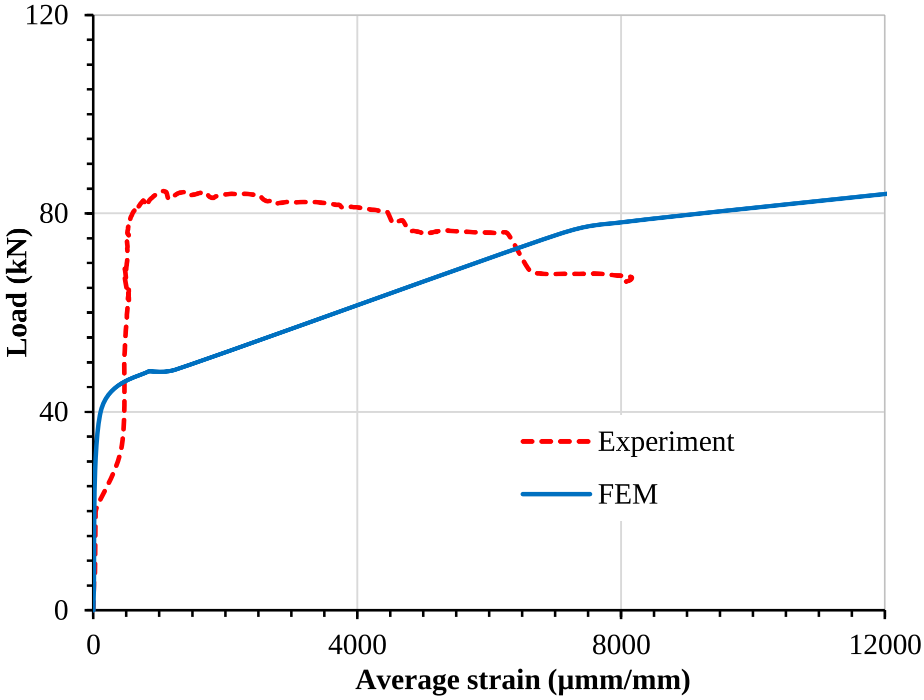

Figure 6.16 Comparison of the experimental load versus reinforcement strain with FE predictions for specimen M4-S.

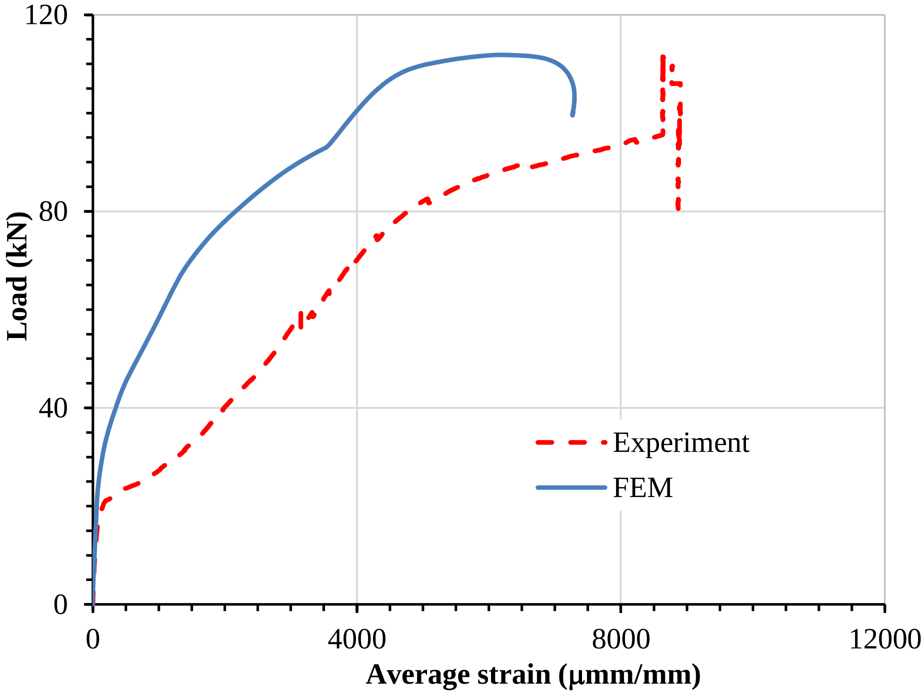

Figure 6.17 Comparison of the experimental load versus reinforcement strain with FE predictions for specimen B4-S.

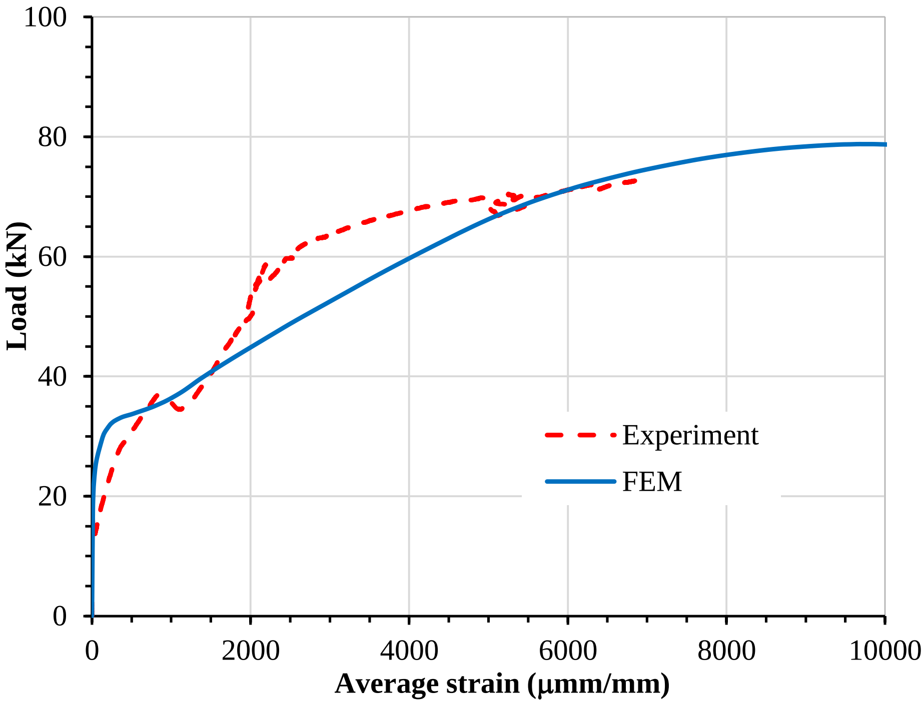

Figure 6.18 Comparison of the experimental load versus reinforcement strain with FE predictions for specimen M3-B.

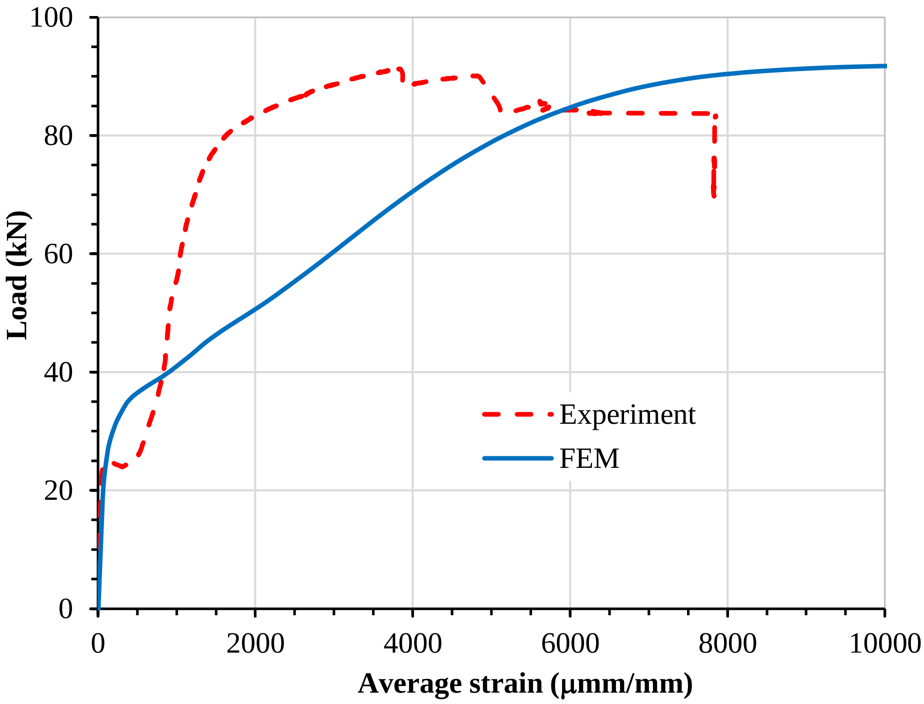

Figure 6.19 Comparison of the experimental load versus reinforcement strain with FE predictions for specimen B3-B.

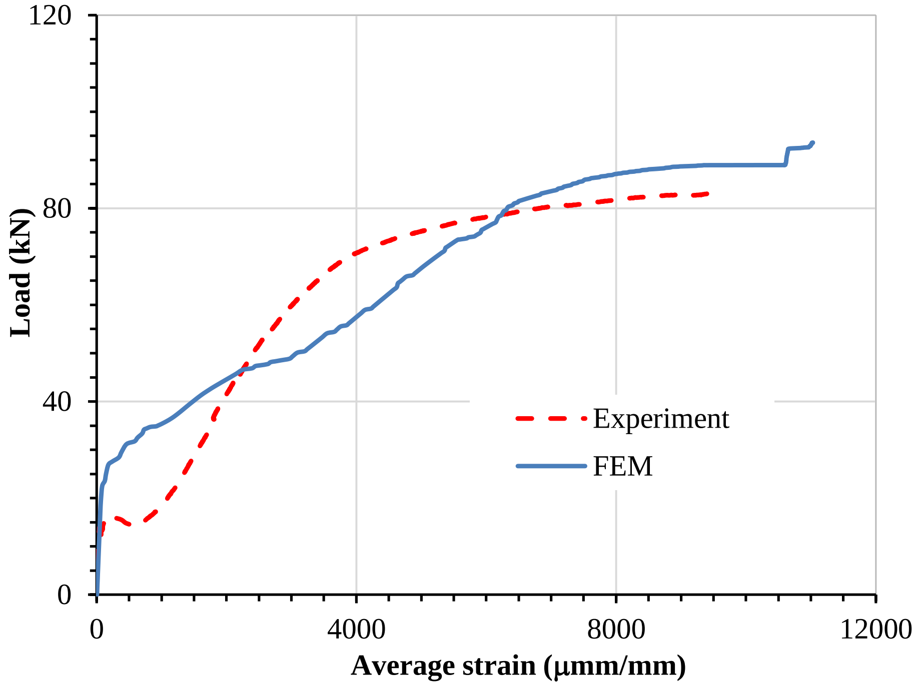

Figure 6.20 Comparison of the experimental load versus reinforcement strain with FE predictions for specimen BT3-B.

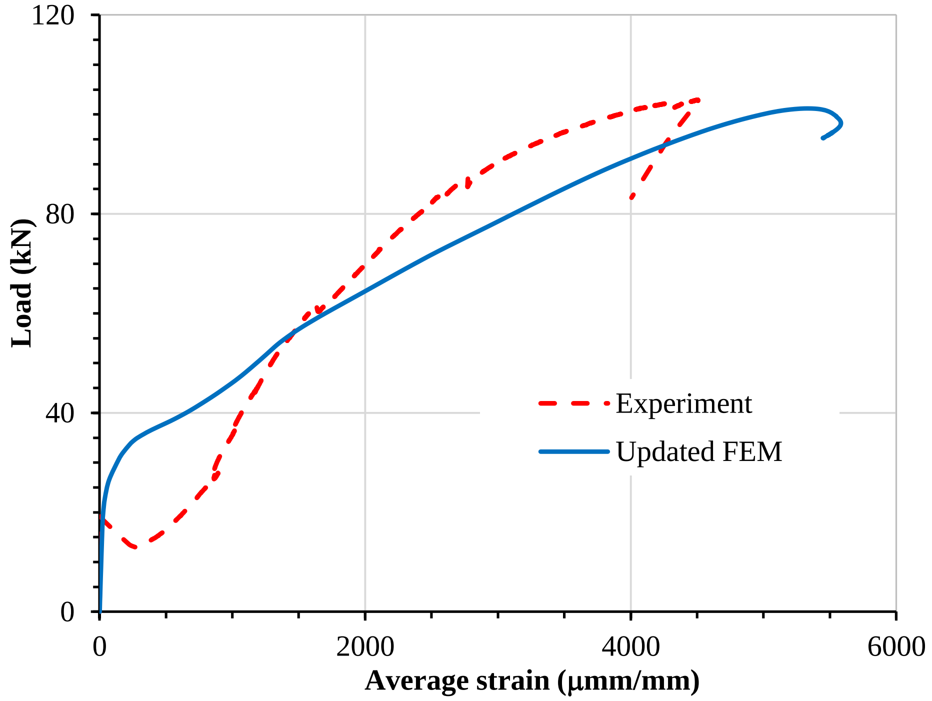

Figure 6.21 Comparison of the experimental load versus reinforcement strain with FE predictions for specimen M6-B.

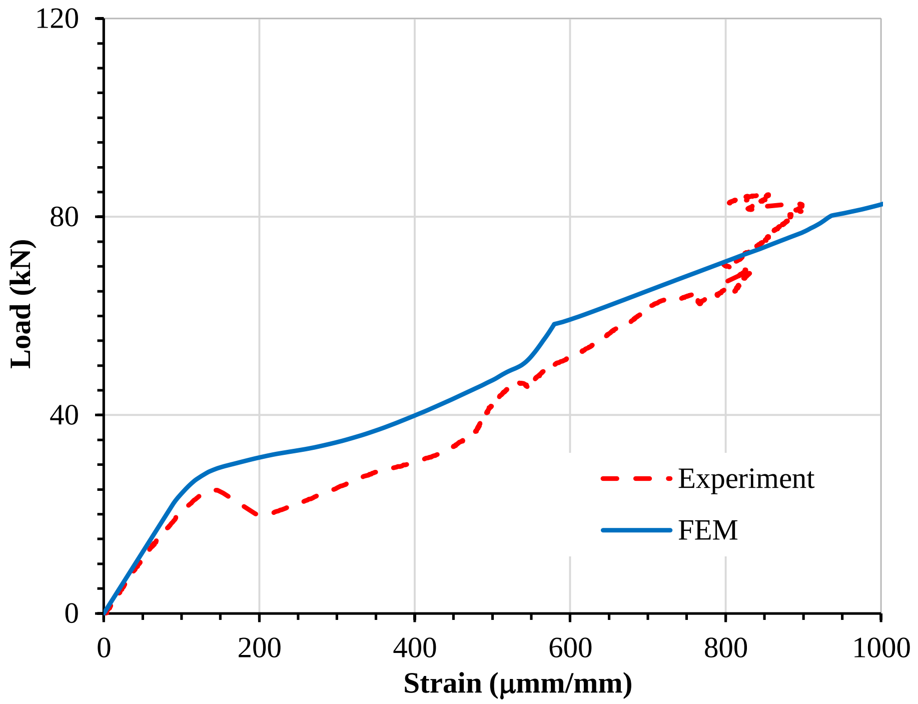

Figure 6.22 Comparison of the experimental load versus strain in transverse ties with FE predictions for specimen M4-S.

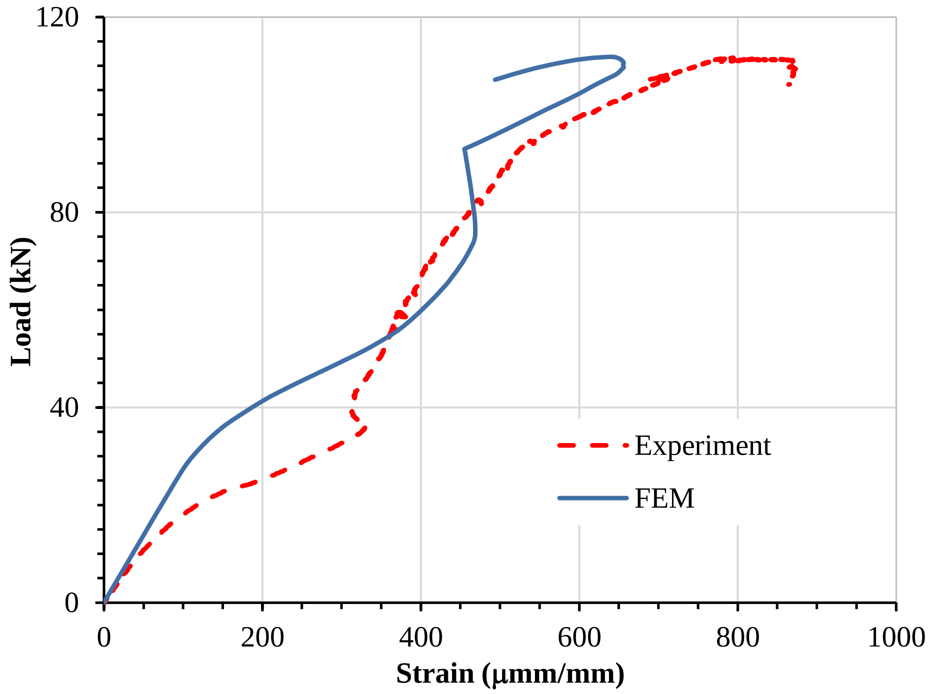

Figure 6.23 Comparison of the experimental load versus strain in transverse ties with FE predictions for specimen B4-S.

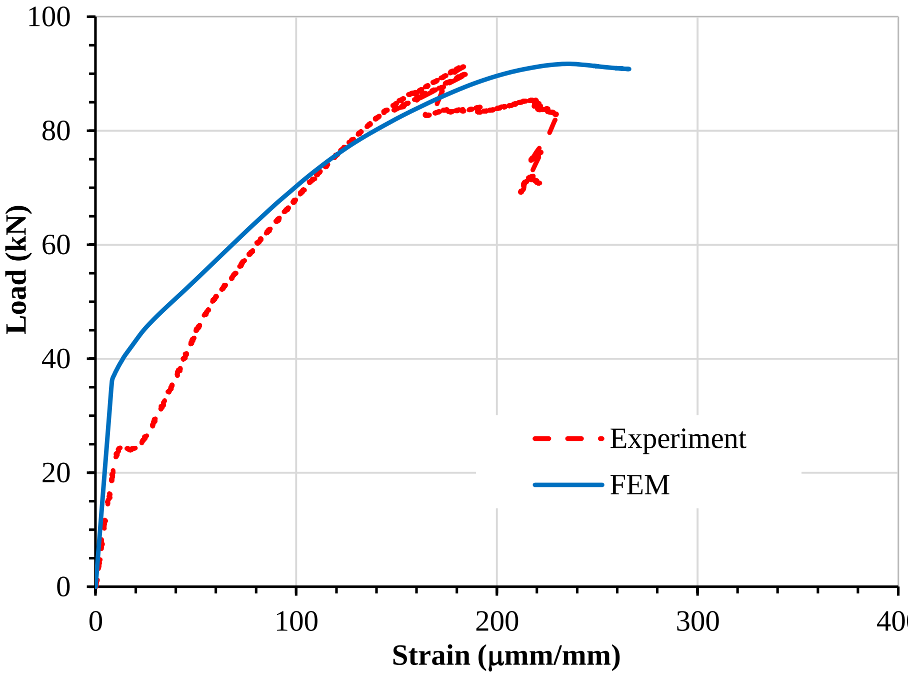

Figure 6.24 Comparison of the experimental load versus strain in transverse cross bracings with FE predictions for specimen M3-B.

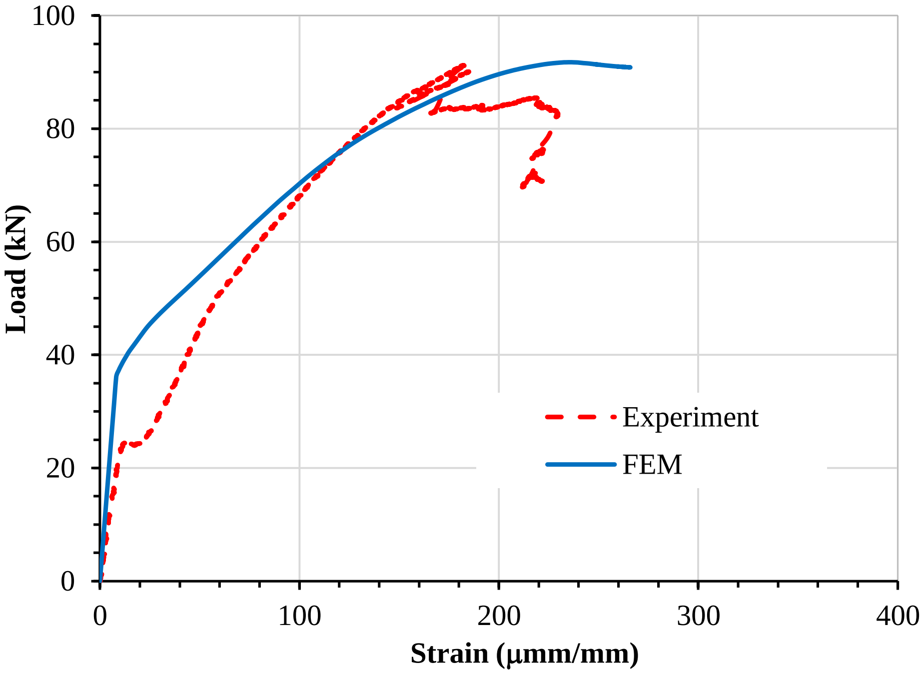

Figure 6.25 Comparison of the experimental load versus strain in transverse cross bracings with FE predictions for specimen B3-B.

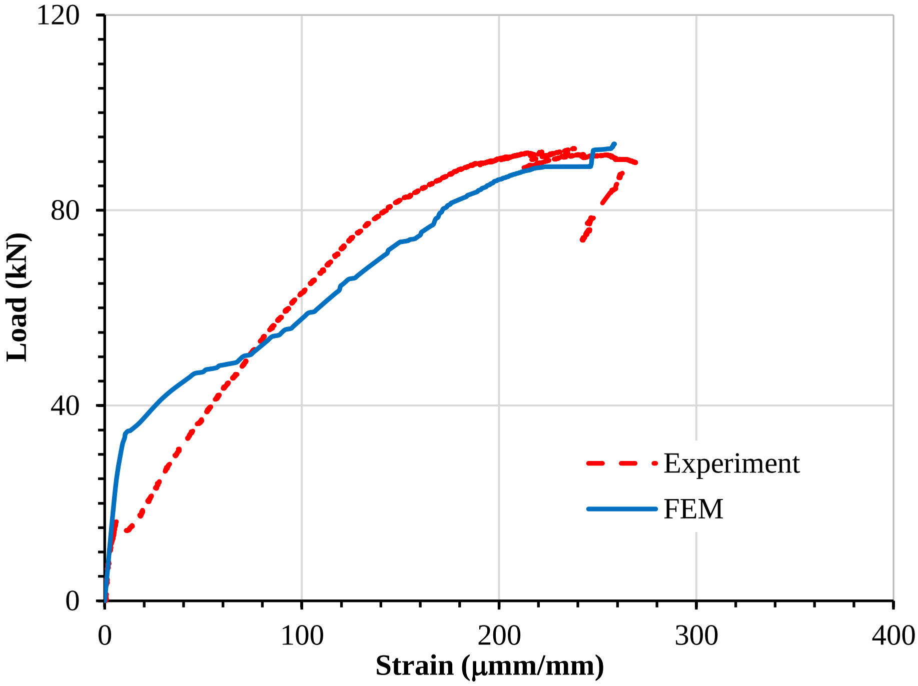

Figure 6.26 Comparison of the experimental load versus strain in transverse cross bracings with FE predictions for specimen BT3-B.

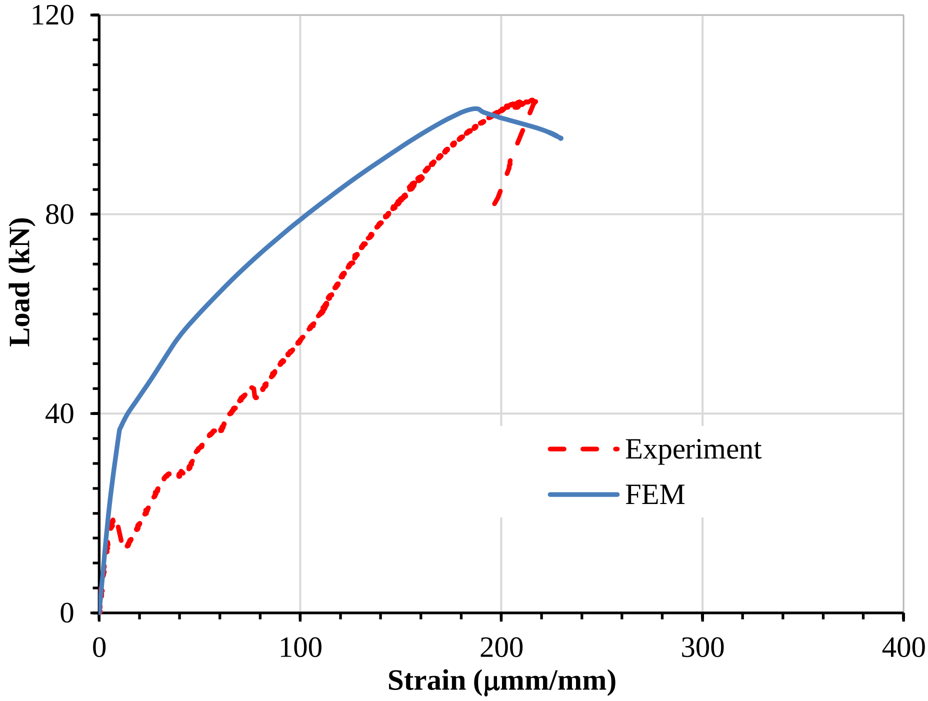

Figure 6.27 Comparison of the experimental load versus strain in transverse cross bracings with FE predictions for specimen M6-B.

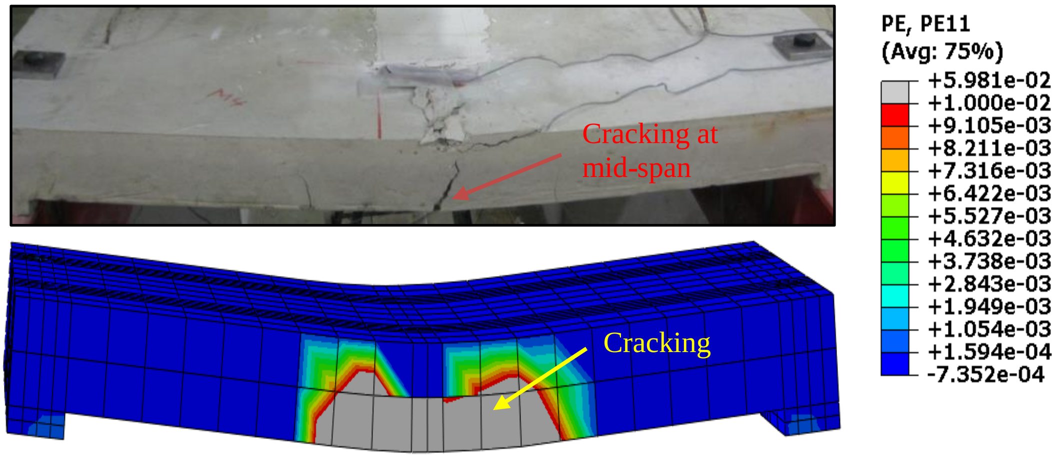

Figure 6.28 Failure mode and contours of average strain in the transverse direction for specimens M4 at peak load.

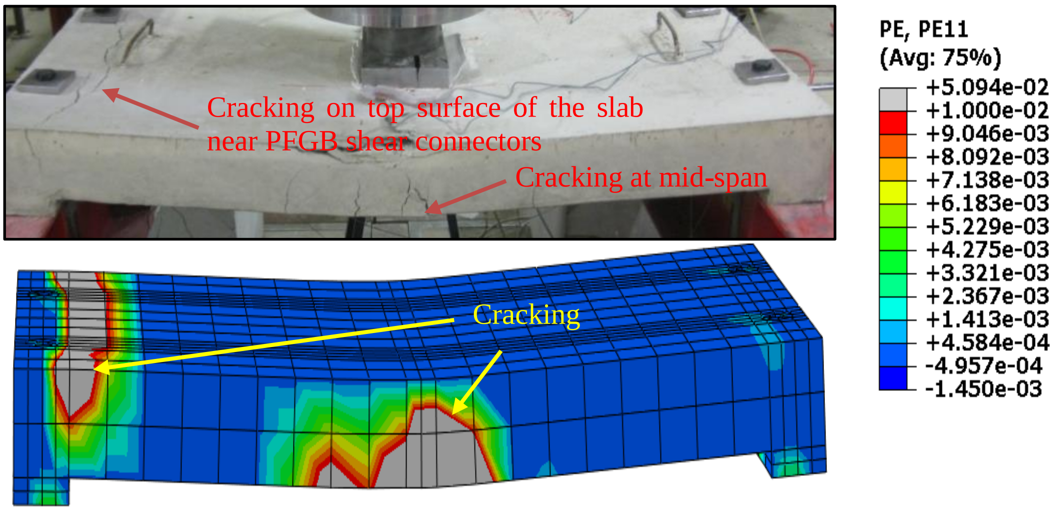

Figure 6.29 Failure mode and contours of average strain in the transverse direction for specimens B4-S at peak load.

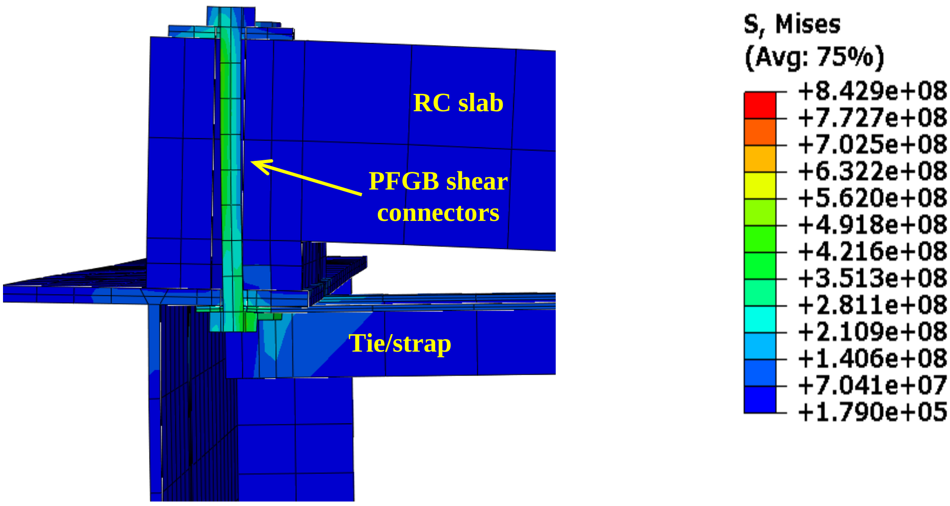

Figure 6.30 Contour of von Mises stresses & PFGB deformation in specimen M4-S at *P*= 70 kN.

6.4. Comparison of 3D and 2D FE models

In addition to validation of 3D continuum-based FE results of ABAQUS against experimental results, ATENA 2D (Cervenka, Cervenka & Pukl 2002) software was used to conduct FE modelling of the deck slabs with transverse straps/ties. Since failure of the slabs was not associated with punching shear, the 2D (plane stress) FE modelling of the precast slabs and supporting girders were deemed to be adequate. In the 2D FE models, quadrilateral elements with maximum size of 10 mm and an updated Lagrangian formulation are employed for capturing geometrical nonlinearities (Cervenka, Cervenka & Pukl 2002).

In the ATENA FE models, concrete slab was modelled using SBETA constitutive law. The SBETA model is a hypoelastic constitutive law recast in the framework of a total secant damage formulation and equivalent uniaxial strain concept. In the SBETA model, concrete failure under bi-axial stress sate is captured by a piecewise continuous failure envelop. The adopted failure envelop under compression-compression and tension-tension stress states follows Kupfer, Hilsdorf & Rusch (1969) and Rankine (1857) failure criterion, respectively. The SBETA can effectively capture the crushing (compressive softening) and cracking (tensile softening) of the concrete under biaxial stress states. In particular, the cracking and post-cracking behaviour of concrete is captured by the smeared rotated crack model described in Rots & Blaauwendraad (1989). For crack opening, Hordijk (1991) exponential law with a constant specific fracture energy $G_f = 20$ N/m in conjunction with the crack band approach is employed to restore the objectivity (Bazant & Oh 1983). A crush band of 0.1 mm is also used for concrete under compression.

The N10 steel bars were modelled as truss elements with the multi-linear stress-strain relationship shown in Figure 6.6. The high-strength 8.8 friction grip bolted connectors did not show any sing of deformation and also no slip was observed in the bolted shear connectors during and after the test. Accordingly, the bolted connectors were modelled by 1D truss element with an initial post-tensioning stress of 330 MPa. For modelling of the supporting steel girders, web stiffeners, transverse ties and washers, a plane stress linear elastic material model was used with elastic modulus of 200 GPa.

In the FE models, the interfaces between the slab and the steel components (i.e. washers, loading foot print and girders) are modelled by the contact elements and a friction coefficient of $\mu = 0.45$, normal stiffness of $K_{nn} = 2\times10^{3}\,\mathrm{MN/m^2}$ and tangential stiffness of $K_{tt} = 2\times10^{3}\,\mathrm{MN/m^2}$ are adopted for the steel-concrete and steel-steel interfaces. The outline of the FE model (mesh) developed for analysis of the precast concrete slabs with transverse ties/straps is shown in Figure 6.31. The load vs mid-span vertical displacement of three slabs with transverse ties/straps (i.e. M4, M4-S and B4-S) predicted by the ATENA models is compared with the experimental and ABAQUS model predictions in Figure 6.32 to Figure 6.34. Furthermore, load vs tensile strains in the steel bars obtained from the ATENA models compared with the experimental and ABAQUS predictions in Figure 6.35 and Figure 6.36. It is seen that the developed 2D FE models adequately predict the global and local response of the precast slabs with transverse ties/straps. The peak load carrying capacity of the slabs predicted by the ABAQUS and ATENA FE models correlate very well with the experimental results. It is seen that load-deflection response of the slabs computed by both FE packages (i.e. ATENA and ABAQUS) correlate reasonably well with test results. However, both FE models predicted stiffer response than that obtained from the tests. A similar overly stiff response has also been encountered in NLFEA conducted by Zheng et al. (2008), Hon, Taplin & Al-Mahaidi (2001) and Einsfeld, Martha & Bitttenourt (2000). In addition to global response (i.e. load-deflection), local response i.e. load versus strain in reinforcement bar diagram obtained from both FE models also showed good agreement with each other and with the experimental results (see Figure 6.35 and Figure 6.36).

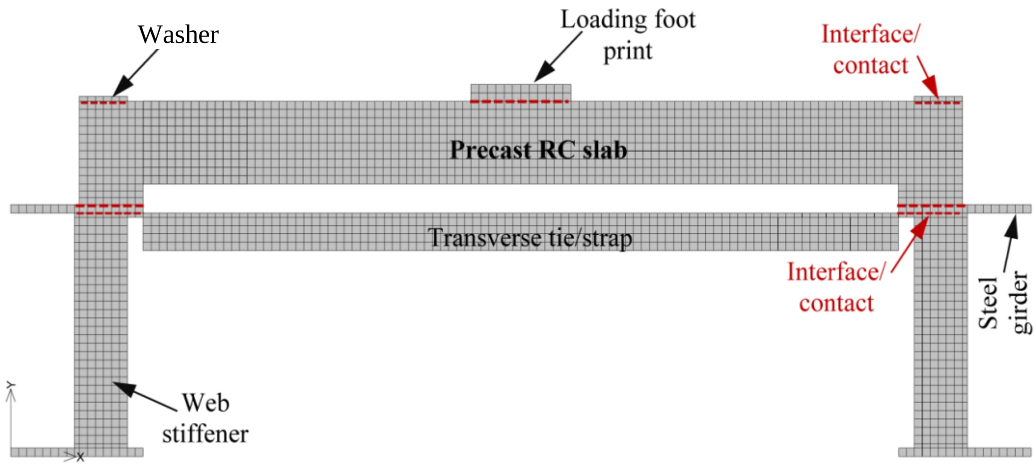

Figure 6.31 Outline of the 2FE mesh and interface elements of the transverse confining system.

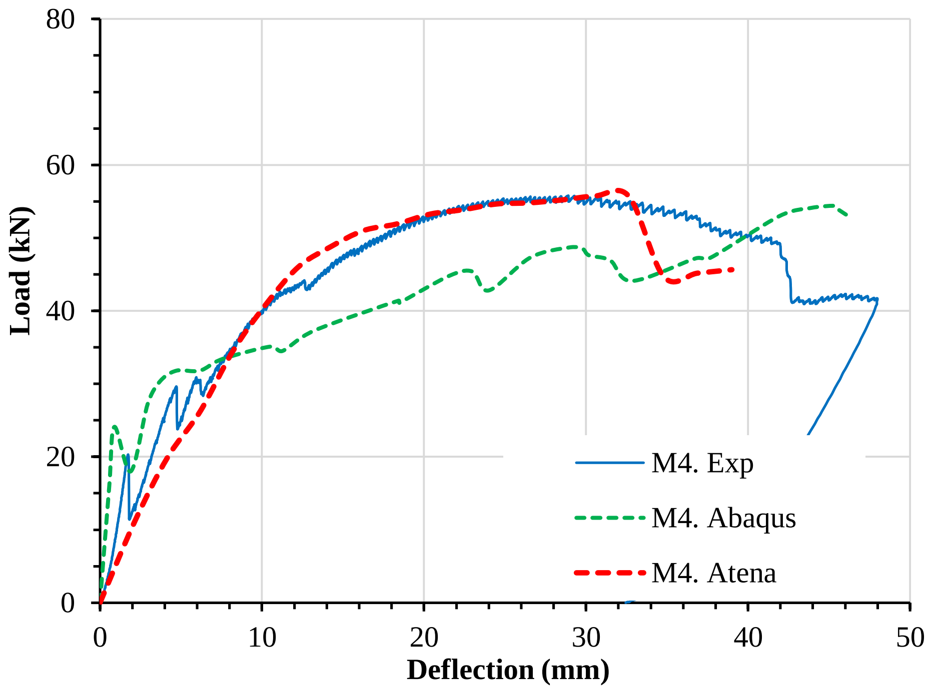

Figure 6.32 Comparison of load-deflection response predicted by ABAQUS-3D and ATENA-2D FE model for specimen M4.

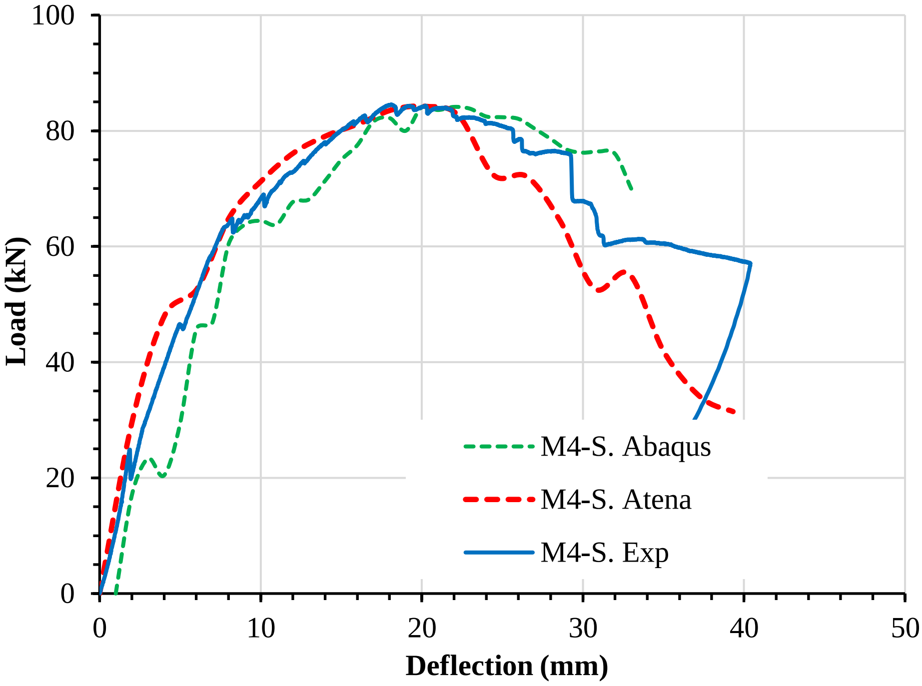

Figure 6.33 Comparison of load-deflection response predicted by ABAQUS-3D and ATENA-2D FE model for specimen M4-S.

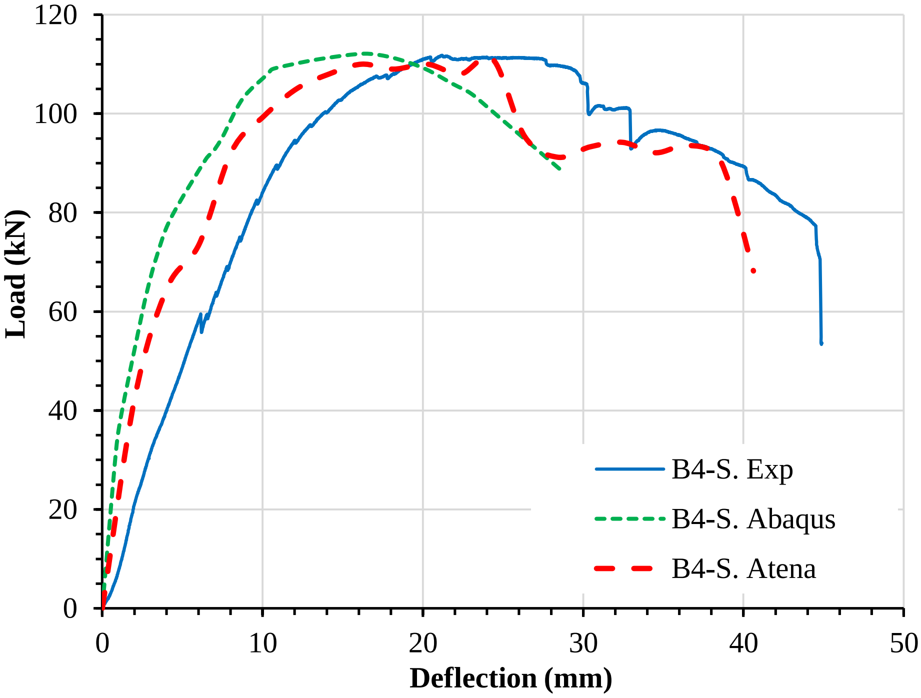

Figure 6.34 Comparison of load-deflection response predicted by ABAQUS-3D and ATENA-2D FE model for specimen B4-S.

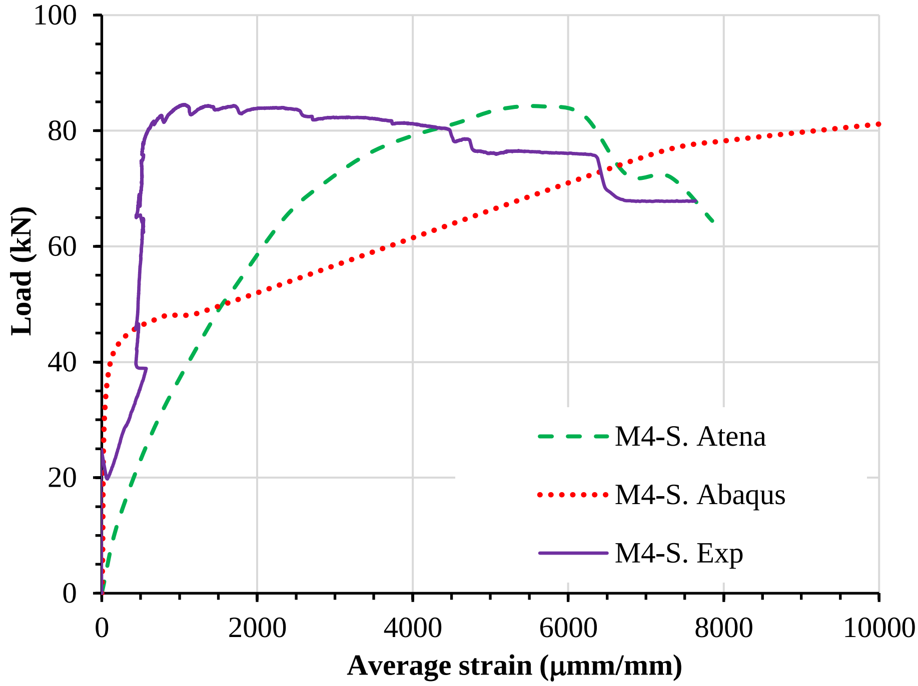

Figure 6.35 Comparison of load-strain in reinforcing bar response predicted by ABAQUS-3D and ATENA-2D FE model for specimen M4-S.

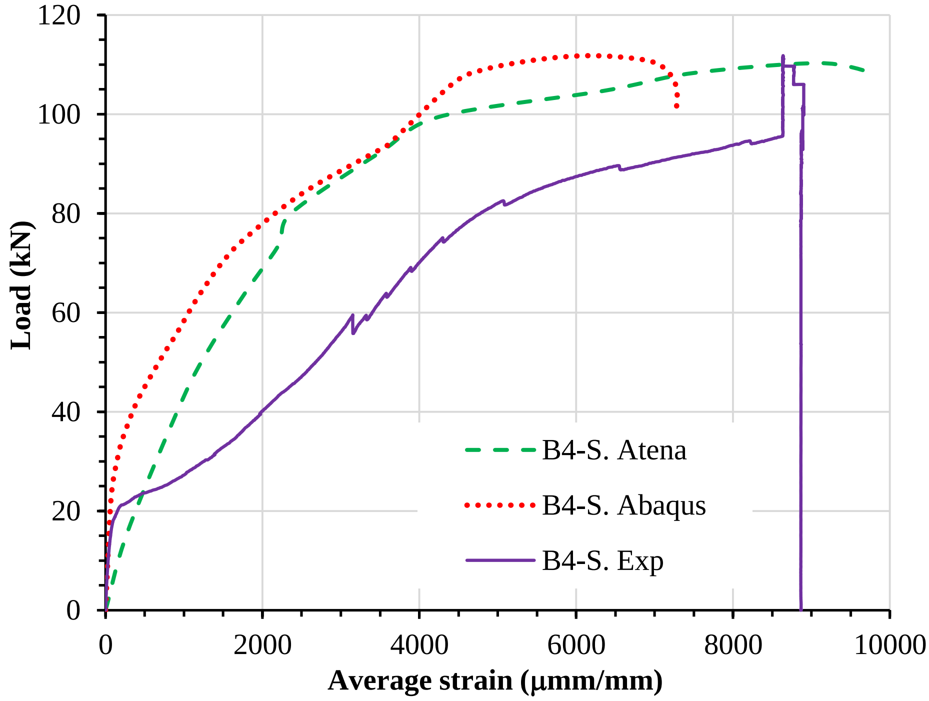

Figure 6.36 Comparison of load-strain in reinforcing bar response predicted by ABAQUS-3D and ATENA-2D FE model for specimen B4-S.

6.5. Parametric study

The validated 3D FE model in ABAQUS is used to conduct a parametric study and elucidate various aspects of the structural behaviour of the precast RC deck slabs with external confining ties/straps and deconstructable PFGB shear connectors. A precast RC slab with dimensions, boundary conditions and transverse ties shown in Figure 6.1 and Figure 6.7 is used as the benchmark in the parametric study. The benchmark model has a reinforcing ratio of 0.52% (3N10), slab thickness of 100 mm, haunch thickness of 25 mm and effective depth of d = 75 mm for the main reinforcing steel bars. Furthermore, the post-tensioning stress in the PFGB shear connectors of the benchmark model is $0.4f_{ub}$ (f_{ub} being ultimate strength of Grade 8.8 bolts).

In the parametric study, effect of size of clearance between the PFGB shear connectors and holes, magnitude of p1ost-tensioning force in the PFGB shear connectors, reinforcing bar yield strength, concrete compressive strength, thickness of slab/haunch, effective depth d of the reinforcing bars on the structural behaviour (i.e. ultimate strength and ductility/deformability measured by Δ_u/Δ_y index) of the precast RC slabs with external transverse ties in a deconstructable composite deck are evaluated. The loads versus mid-span deflection responses are appraised and the key performance attributes of the precast deck slab with transverse confining system are also evaluated with respect to the results of parametric study.

6.5.1. Effect of clearance between PFGB shear connectors and holes in the RC slabs

To gain further insight into the effect of clearance between the precast RC slab and bolted shear connectors on the composite precast deck slab with external confining straps, nine different clearances, i.e. 0.5 mm to 5 mm with 0.5 mm increments are considered and the load versus mid-span deflection results for different clearances are plotted in Figure 6.37. It is seen that the mid-span deflection and ductility (i.e. deflection at ultimate Δ_u over deflection at yield Δ_y) of the specimen increase significantly as the clearance increases. However, the increase in the clearance appears to have minor influence on the peak load capacity and strength enhancement provided by arching action. Furthermore, the clearance has minor influence on the initial

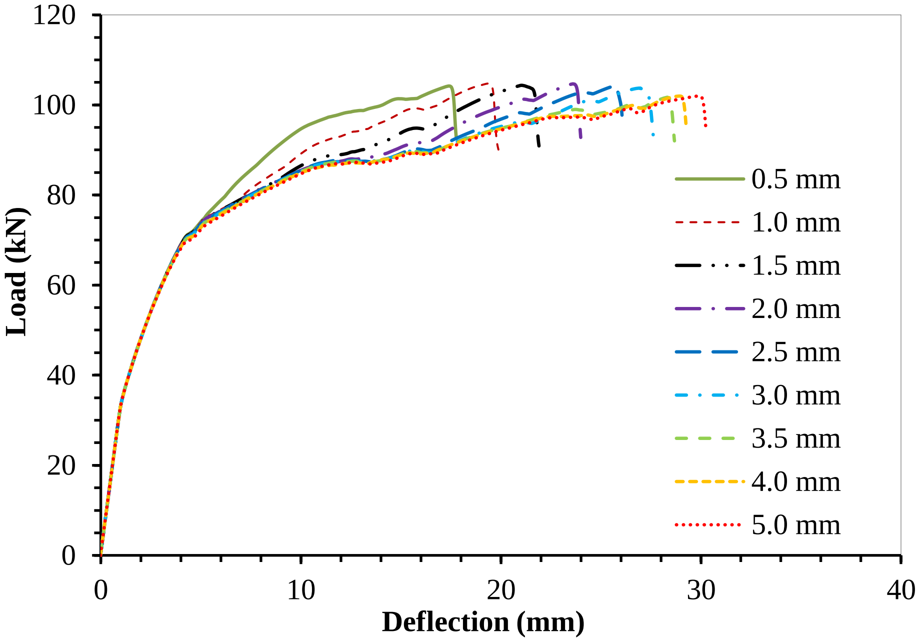

Figure 6.37 Effect of clearance between the RC slab and PFGB connectors.

stiffness of the deconstructable RC deck slabs with transverse ties.

6.5.2. Effect of post-tensioning stress in PFGB shear connectors

Seven different magnitudes for post-tensioning stress, corresponding to 10% to 70% of the tensile strength of class 8.8 bolts (with 10% increments) are considered in the parametric study and the load versus mid-span deflection are plotted in Figure 6.38 showing that the post-tension stress/force has negligible influence on the initial stiffness of the deconstructable precast RC deck slab. But, the increase in the post-tension stress of PFGB connectors can significantly increase the secondary stiffness and reduce the ductility/deformability of the precast deck slab (see Figure 6.38). The minor influence of post-tensioning stress of PFGB shear connectors on the peak load capacity is also evident from the plots in Figure 6.38.

6.5.3. Effect of reinforcement ratio

The size of benchmark precast RC slab and effective depth *d* of steel bars are kept constant and the slab is analysed assuming seven different values, i.e. 0.19%, 0.33%, 0.52%, 0.75%, 1.03% and 1.34% for the reinforcing proportion. The reinforcing proportion is calculated by dividing the total area of tensile reinforcement over the gross cross-sectional area of the RC slab. The load versus mid-span deflection of the slabs with different reinforcing rations is illustrated in Figure 6.39. It is seen that increasing the reinforcing ratio not only increase the peak load capacity but also increase the ductility= Δ_u/Δ_y of the specimen. It should be noted that providing a very low reinforcing ratio causes limited strength, as can be seen for model having a reinforcing ratio of 0.19%.

6.5.4. Effect of precast concrete slab depth or span length over thickness ratio

Four different precast concrete slab thicknesses, i.e. 100, 120, 140 and 160 mm were considered to investigate the effect of span length over slab thickness ration (*l*/*h* ranging from *l*/*h*= 6.1 to 9.8 on the arching behaviour of precast RC deck slab with external confining ties. The load versus mid-span deflection of the slabs with *l*/*h*= 6.1, 7.0, 8.2 to 9.8 is illustrated in Figure 6.40 which is demonstrative of the significant influence of the *l*/*h* parameter on the peak load carrying capacity of the transversely confined precast RC deck slabs.

Assuming that the behaviour of analysed RC slab was only dominated by pure flexural (bending) action, increasing slab thickness from 100 mm (effective depth *d*= 75 mm) to 160 mm (*d*= 135 mm) should have increased the peak load capacity by around ((135-75)/75) x100% = 80%. But, it is observed that by increasing the thickness of the concrete slab from 100 mm to 160 mm, the peak load capacity has increased around 110%. This significantly higher enhancement in the peak load capacity can be attributed to development of arch action, particularly for transversely confined RC slabs with smaller *l*/*h* ratios. Moreover, Figure 6.40 shows that increasing the slabs thickness from 120 mm to 160 mm has reduced Δ_u as well as the ductility index Δ_u/Δ_y by approximately 25%, owing to development of arch action that can shift the failure mode of restrained RC members from ductile associated with yielding of steel bars to brittle mode which is predominantly associated with concrete crushing.

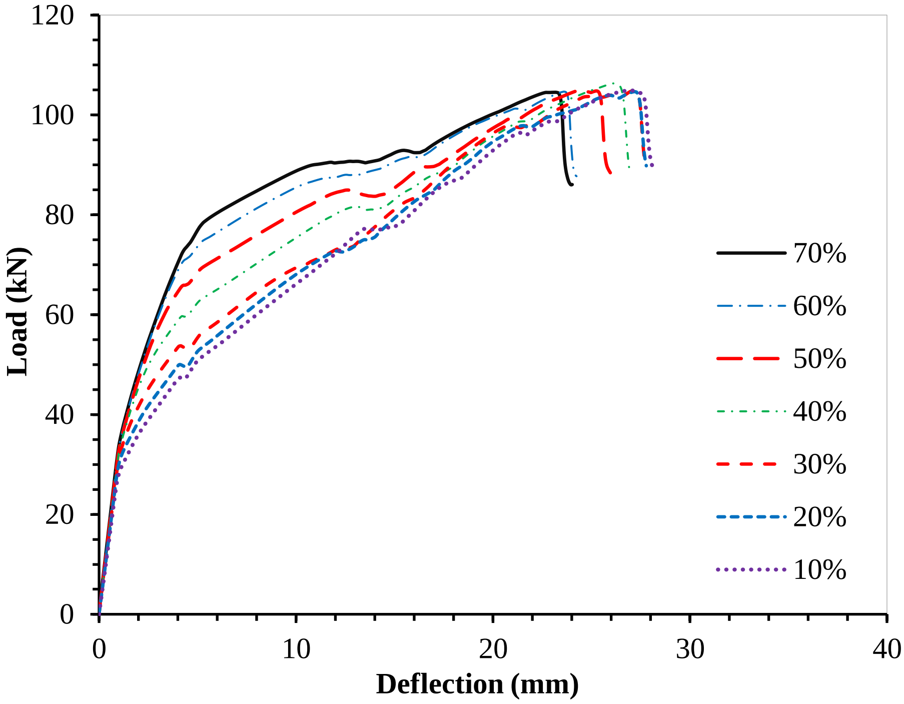

Figure 6.38 Effect of post-tensioning force in the PFGB on the load-deflection diagram.

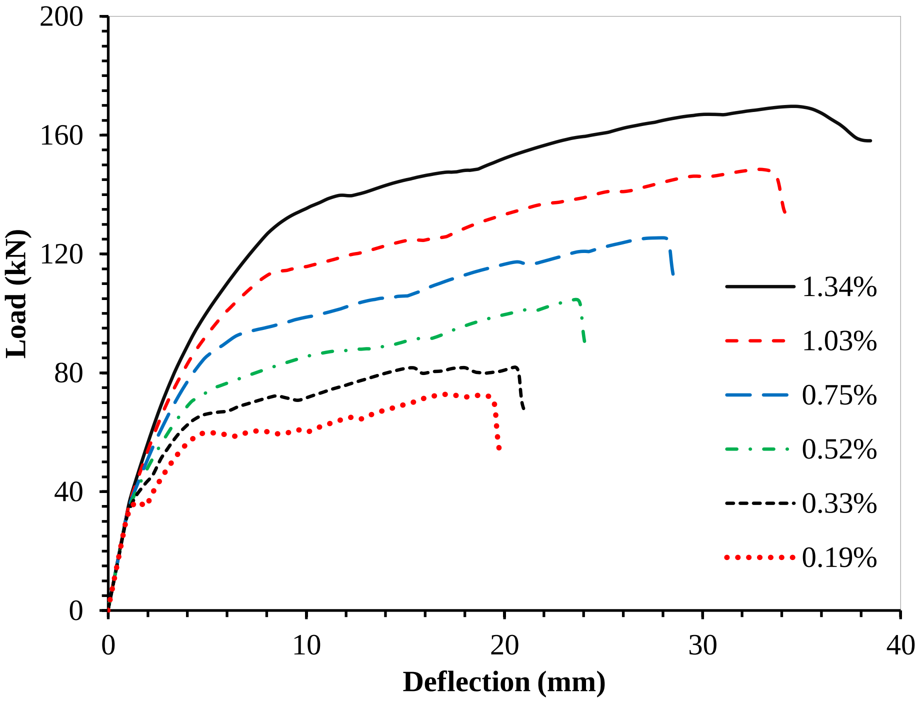

Figure 6.39 Effect of reinforcing proportion on the load-deflection diagram.

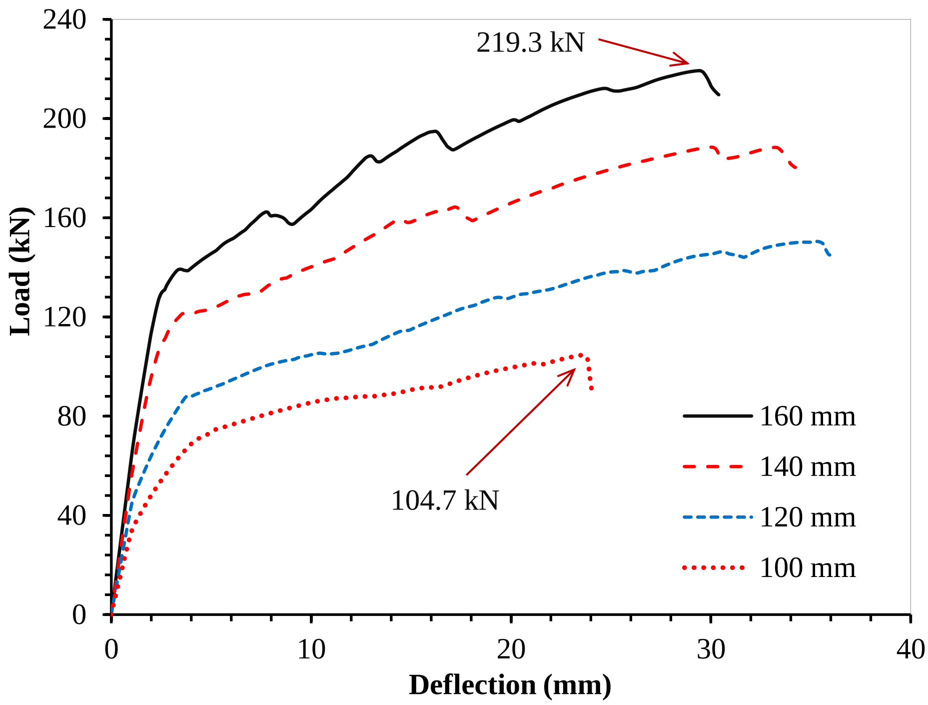

Figure 6.40 Effect of precast RC slab thickness on the load-deflection diagram.

6.5.5. Effect of concrete compressive strength

Specimens B3-B with cross bracings and specimen B4-S with transverse ties are analysed assuming four different concrete compressive strength, f_c= 25, 40, 50 and 80 MPa and the load-mid span deflections are plotted in Figure 6.41 and Figure 6.42. Also, the peak load carrying capacity of the specimens B3-B and B4-S with respect to concrete compressive strength are shown in Figure 6.43. The significant effect of compressive strength on the stiffness and peak capacity of precast slabs with transverse confining system is evident from Figure 6.41 to Figure 6.43. However, concrete compressive strength has minor influence on the ductility of the slabs. Concrete compressive strength has minor influence on the ultimate peak load carrying capacity of the purely flexural RC members (without end restraints), but Figure 6.43 shows concrete compressive strength has major influence on the peak load carrying capacity of the tested slabs which is indicative of arch action development. Considering the bigger cross section of the bracings compared to ties, the slightly higher slope of the plot for specimen B4-S than specimen B3-B (Figure 6.43) can be attributed to better efficiency of the transverse ties compared to cross bracing for mobilising arch action.

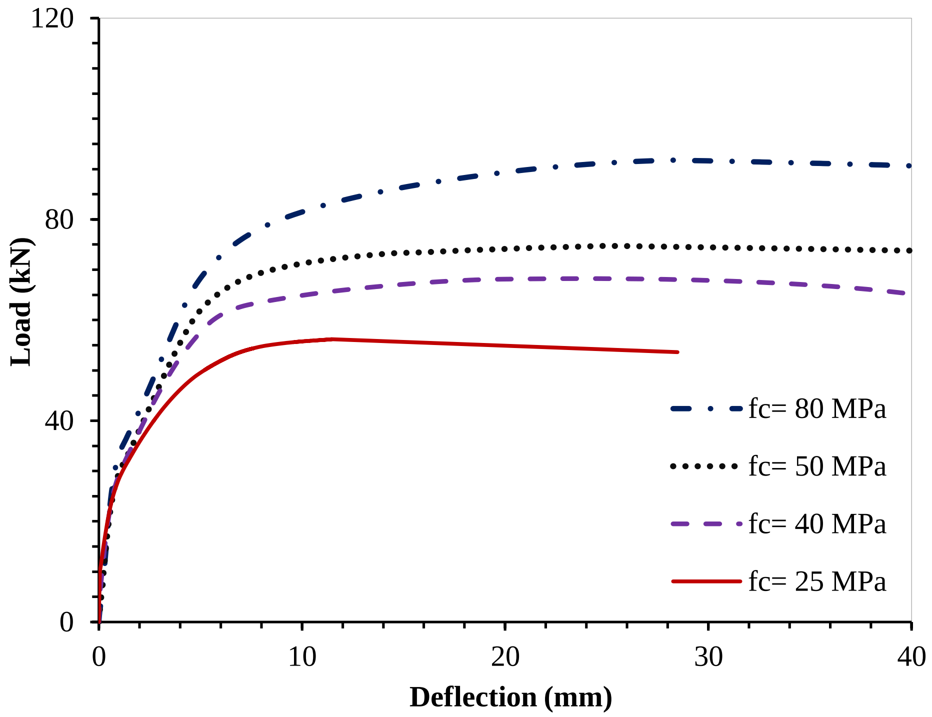

Figure 6.41 Effect of concrete compressive strength on the load-deflection diagram of specimen B3-B.

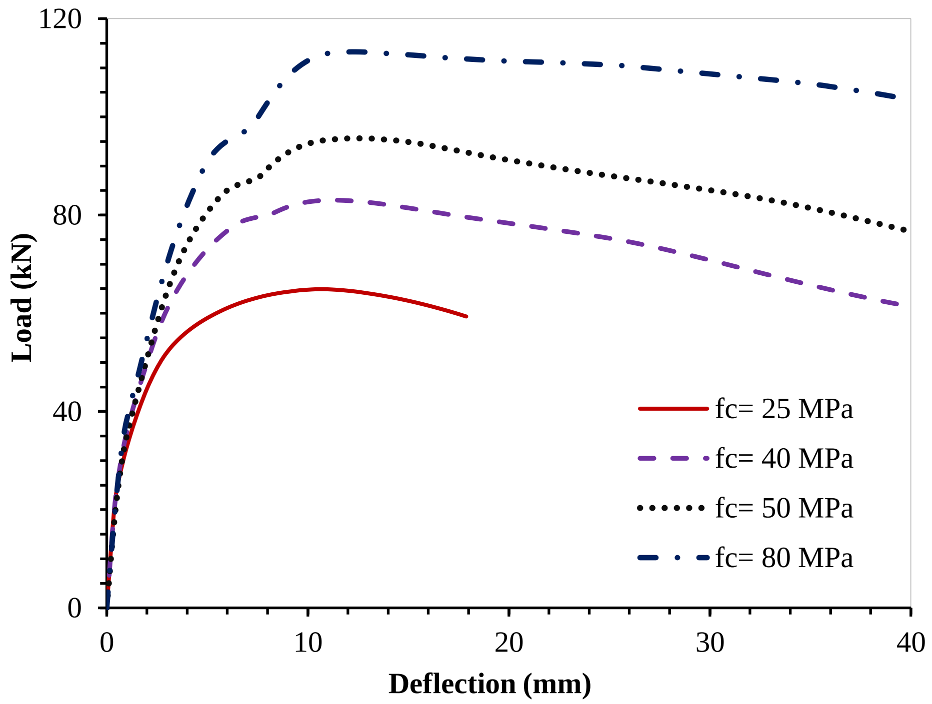

Figure 6.42 Effect of concrete compressive strength on the load versus deflection diagram of specimen B4-S.

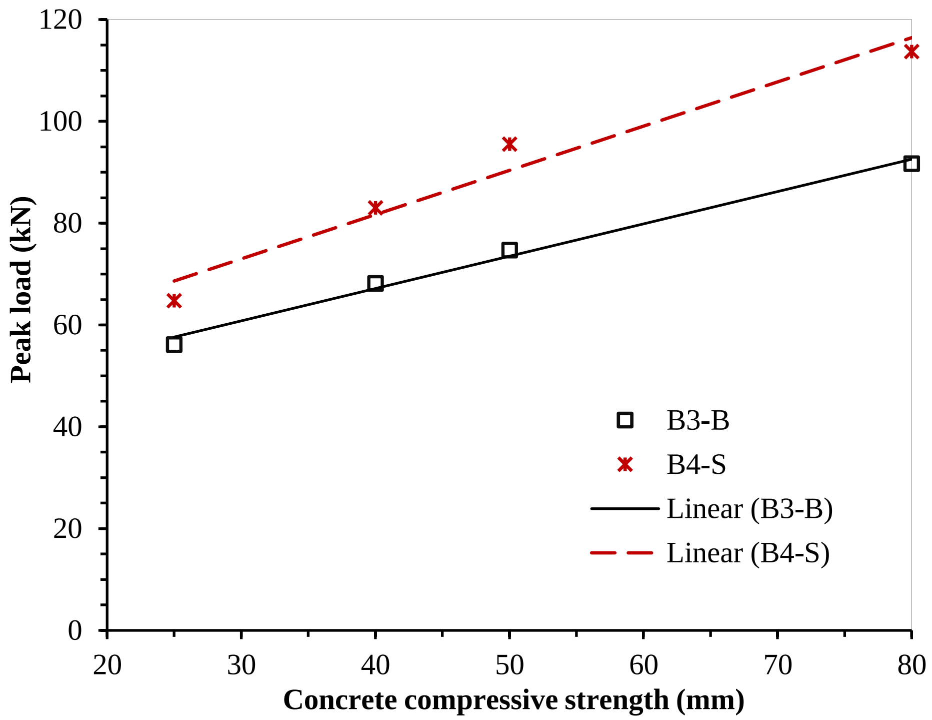

Figure 6.43 Effect of concrete compressive strength on the ultimate load carrying capacity of specimens B3-B and B4-S.

6.5.6. Effect of yield strength of reinforcing steel bars

Specimens B3-B with cross bracings and specimen B4-S with transverse ties are analysed assuming steel bars have yield strength of f_y= 400, 500 and 600 MPa. The minor influence of the yield strength on the load-deflection behaviour and peak load carrying capacity of the transversely confined precast RC deck slabs is evident from Figure 6.44 and Figure 6.45.

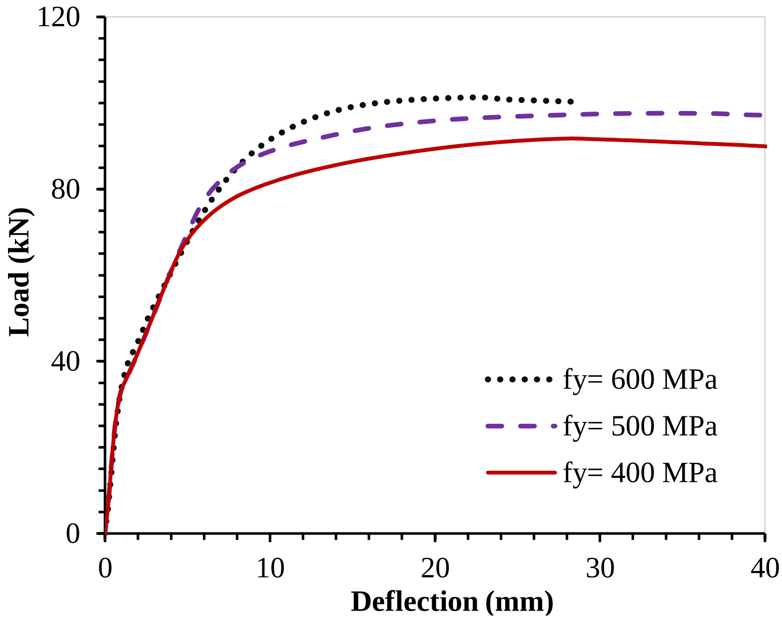

Figure 6.44 Effect steel bars yield strength on the load-deflection diagram of specimen B3-B.

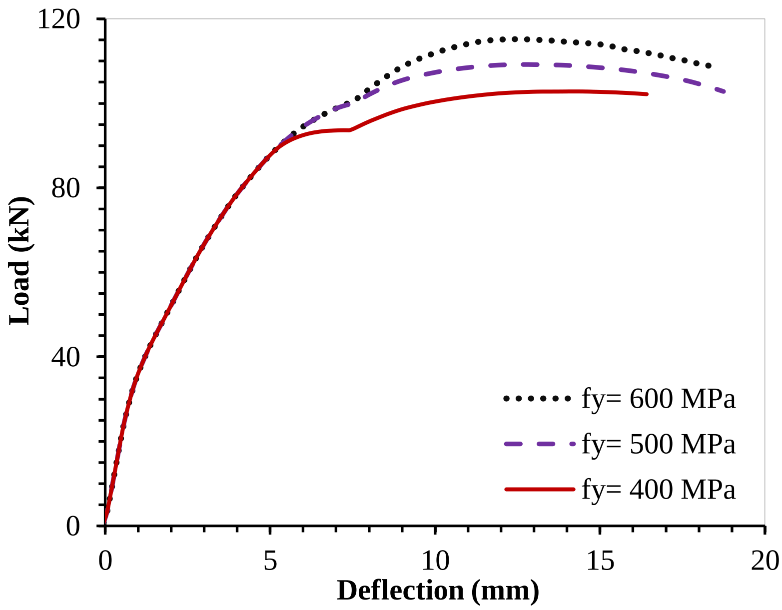

Figure 6.45 Effect steel bar yield strength on the load-deflection diagram of specimen B4-S.

6.6. Conclusions

Non-linear 3D and 2D continuum-based FE models are presented to simulate the structural behaviour of reinforced concrete (RC) deck slabs with transverse confining systems in a deconstructable composite deck with post-installed friction grip bolted

(PFGB) shear connectors. In the FE models developed, all non-linearity of the interfaces, geometrical and material non-linearities are considered. Accuracy of the developed FE models are assessed and verified against experimental results obtained from laboratory tests. The results of validation study showed that both 3D and 2D (plane stress) continuum-based FE models can predict the peak load carrying capacity of the transversely confined precast RC deck slabs with good accuracy, however, both of the FE models (i.e. 2D and 3D) tend to overestimate the stiffness and underestimate the deflection corresponding to ultimate load carrying capacity of the RC deck slabs.

A parametric study is conducted in which the influence of clearance between concrete slab and bolts, post-tensioning stress in the PFGB shear connectors, reinforcement ratio, thickness of the precast concrete slab, concrete compressive strength and yield strength of reinforcing steel bars on the structural behaviour of precast RC deck slabs with external confining systems are studied. The following conclusions are drawn from the results of parametric study;

- The clearance between the precast concrete slab and post-installed friction grip bolted (PFGB) shear connectors and the magnitude of post-tensioning stress in the PFGB shear connectors appear to have minor influence on the initial stiffness and ultimate strength of the deck slabs. However, reducing the clearance and/or increasing the level of post-tensioning in the PFGB shear connectors can improve the post-cracking stiffness of the slabs.

- Due to development of arch action, the yield strength of reinforcing bars has minor influence on the peak load carrying capacity of the precast RC deck slabs. However, increasing the concrete compressive strength can significantly increase the peak load carrying capacity of the slabs.

- Due to arch action contribution, increasing slab thickness or reducing the span length over slab thickness ratio can increase the peak load carrying capacity of the RC slabs beyond what is observed in purely flexural members.

CHAPTER 7

RESERVE OF STRENGTH IN INVERTED U-SHAPE RC CULVERTS: EFFECT OF BACKFILL ON ULTIMATE LOAD CAPACITY AND FATIGUE LIFE

7. Reserve of Strength in Inverted U-Shape RC Culverts: Effect of Backfill On Ultimate Load Capacity and Fatigue Life

7.1. Introduction

Due to extensive application and critical role of reinforced concrete (RC) culverts in ground transport systems, the structural performance of culverts is required to be assessed on a regular basis. Recent assessment of existing RC culverts and review of literature have shown that in spite of increasing number of vehicles and their axle load, the majority of existing RC culverts have some reserve of strength available that allows them to cope well with these additional loads (Cook & Bloomquist 2002; Maximos, Erdogmus & Tadros 2010). However, using the available design provisions, which typically ignore the effect of soil-culvert interaction, does not demonstrate such a reserve of strength in culverts (Abdel-Haq 1987). This issue underlines the need for developing more realistic design guidelines and load rating provisions that can be used to better estimate the load carrying capacity and evaluate the structural performance of RC culverts (Lawson et al. 2010).

Realistic analysis and assessment of RC culverts requires that nonlinear behaviour of concrete as well as the effect of surrounding soil (top and backfill) and soil-structure interaction are adequately taken into account. Over the past decades, there has been considerable research on the soil-culvert interaction mechanism and these studies have covered various aspects of soil behaviour such as proposing formulas for prediction of soil pressure on RC culverts (Tadros, Benak & Gilliland 1989), calculating the bending moment, shear force and deflection of culverts under soil pressure and comparing the results with experimental data (Dasgupta & Sengupta 1991) and measuring and estimating vertical pressure of soil on top of RC box culverts with respect to geometry of culvert and height of embankment (Bennett et al. 2005; Kim & Yoo 2005; Yang 2000). Furthermore, the effect of culvert type and size, in conjunction with embankment type and height, on vertical earth pressure was studied by (Vaslestad, Johansen & Holm 1993). The influence of various types of backfill and installation techniques on earth pressure was investigated by(Chen, Zheng & Han 2010; Vaslestad, Johansen & Holm 1993) and (Chelliat 1992) studied the influence of soil-structure interaction on the failure mode of the culverts. In a recent study by Pimentel et al. (2009), effect of nonlinear behaviour of RC box culverts on soil pressure was investigated experimentally and numerically (McGrath & Mastroianni 2002). Also, new procedures for load rating and performance evaluation of culverts have been proposed (Acharya 2012; Yeau & Sezen 2012). Less attention, however, has been paid to quantifying the influence of backfill on the load capacity and fatigue life of RC culverts, which is the focus of this chapter.

In addition to the effect of culverts on top and backfill soil pressure, the structural behaviour of RC culverts by themselves has been subject of a few studies. Due to inadequacy of standards for shear design of RC culverts in conjunction with provisions for distributing live loads (Abdel-Karim, Tadros & Benak 1990; Orton et al. 2013), experimental and numerical studies have been carried out to investigate the shear behaviour of RC culverts (Smeltzer & Bentz 2005), and also formulas for distributing imposed action (live load) and estimating effective width of RC box culverts have been proposed (McGrath et al. 2004). Furthermore, comprehensive experimental and numerical studies have been undertaken to investigate the shear behaviour of standard sizes of box culverts as per ASTM C1433 (2004) and influence of different variables including size of culverts and location of load on the shear critical section and capacity of culverts have been investigated (Abolmaali & Garg 2008; Garg & Abolmaali 2009; Garg 2007; Garg, Abolmaali & Fernandez 2007). Yee, Bentz & Collins (2004) performed load tests on the shear capacity of precast RC box culverts and concluded that design procedures outlined in both the Canadian Highway and Bridge Design Code (CHBDC) and American Association of State Highway and Transportation Officials (AASHTO) code were conservative to a degree.

In a study by Maximos, Erdogmus & Tadros (2010), the structural performance and fatigue behaviour of box culverts under cyclic loads were experimentally investigated. The study showed minimal fatigue effect on the flexural capacity of the RC box culverts and some amendments to fatigue provisions of the AASHTO standard were recommended. Research has also been focused on the effect of surrounding soil properties and climate conditions on design of single, double and multi cell RC Box culverts (Ahmed & Alarabi 2011) and in the application of Glass Fibre Reinforced

Polymer (GFRP) bars in RC culverts to address issues associated with corrosion of steel reinforcing bars and durability (Alkhrdaji & Nanni 2001).

It is hypothesized that the lateral stiffness of backfill can potentially increase the ultimate load capacity and fatigue life of RC culverts due to development of arching action. Accordingly, in this chapter nonlinear continuum-based models of culverts in conjunction with surrounding soils are developed and analysed to investigate enhancing effects due to arching action on the peak load capacity and fatigue life of top slabs in RC culverts with no or little skew. Using the FE models developed, a parametric study is undertaken to quantify the influence of culvert geometry (span length over rise ratio), compressive strength of concrete, reinforcing proportion and stiffness (modulus of subgrade reaction) of backfill on the peak load capacity and fatigue life (represented by magnitude and range of stress in steel bars) of inverted U-shape RC culverts.

7.2. Nonlinear finite element model

Properly validated nonlinear FE models are considered a good alternative to expensive and time-consuming experimental studies. Accordingly, in this study nonlinear FE models are employed to evaluate effect of different variables that can influence the peak load capacity of RC culverts and the magnitude and level of stress in tensile steel bars. A 2D continuum-based FE model is developed and validated against available experimental data. The developed FE models can capture nonlinearities of materials (i.e. concrete, reinforcing steel, soil and contact/interface between RC culvert and soil) as well as geometrical nonlinearities (large displacements but small strains).

The 2D continuum-based finite element models are developed using ATENA software (Cervenka, Cervenka & Pukl 2002). In ATENA, reinforced concrete (RC) culvert and backfill soils are modelled under a 2D stress state and the effect of soil cover under burial conditions is neglected. In the 2D continuum-based FE models, concrete is modelled using StahlBETon Analyse (SBETA) constitutive law which is a hypoelastic material model recast in the framework of total secant damage and equivalent uniaxial constitutive law (Cervenka, Cervenka & Pukl 2002). The steel reinforcing bars are modelled as elastic-perfectly plastic uniaxial (truss) elements. The SBETA material model is used to capture nonlinearity of concrete under compression as well as concrete cracking (tensile softening) and crushing (compressive softening). The SBETA equivalent uniaxial stress-strain diagram adopted for concrete is shown in Figure 7.1a and the equivalent uni-axial tensile and compressive strength of concrete are obtained from the bi-axial failure envelop shown in Figure 7.1b. The behaviour of concrete after cracking is modelled by the rotated crack concept (Rots & Blaauwendraad 1989) and objectivity of results is restored by the crack/crush band approach.

The size of the elements in the 2D FE mesh is limited to 15 mm and geometrical nonlinearities are taken into account using updated Lagrangian formulation. In the 2D FE models, backfill soil is assumed to be a linear elastic-brittle failure material that follows a Rankin failure criterion. The backfill soil is characterised by its modulus of subgrade reaction, K_{soil} and its load bearing capacity (0.12 MPa as the minimum load bearing capacity of the backfill soil). Furthermore, the interaction between RC wall of culverts and backfill soil is modelled by interface (contact) elements. The interface element used in this study is characterised by cohesion *c*, coefficient of friction μ, normal stiffness K_{nn} and tangential stiffness of interface K_{tt} of interface that assumed to be linear elastic.

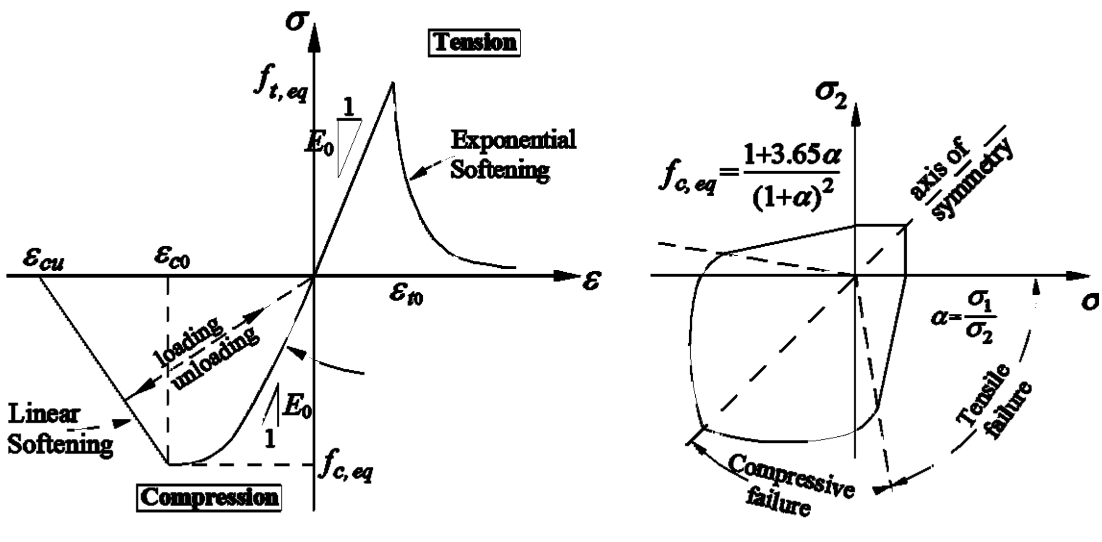

Figure 7.1 Outline of the adopted (a) equivalent uni-axial stress-strain relationship and (b) failure envelop for concrete.

In this study a very small coefficient of friction $\mu = 0.01$ with no cohesion (c=0) is assigned to the RC wall-soil interface to minimise any possible enhancing effect of backfill strength on the capacity of the culvert. In addition, the culvert-to-foundation connection point (concrete-concrete interface) is modelled by a friction contact element with the coefficient of friction taken as $\mu = 0.4$ (deemed to be a lower bound value). The accuracy of the adopted assumptions and FE model for capturing ultimate load capacity of RC culverts is verified in the following section.

7.3. Verification of the nonlinear finite element models

A GFRP reinforced concrete (RC) box culvert tested by Alkhrdaji & Nanni (2001) is analysed in the first part of this example. The geometry and reinforcing details of the specimen are shown in Figure 7.2a and material properties are taken as, $f_c = 42.7$ MPa (concrete compressive strength), $f_t = 0.36\sqrt{f_c} = 2.3$ MPa (concrete tensile strength), $E_f = 40.7$ GPa (GFRP elastic modulus) and $f_u = 758$ MPa (ultimate strength of GFRP bars). The box culvert is analysed under a point (wheel) load applied at the mid-span of the top slab (Figure 7.2a). The element size in the 2D continuum-based FE model is limited to 15 mm. The ultimate load capacity predicted by the 2D continuum-based FE model is 162.6 kN, which correlates well with the peak load capacity of P_u=155.7 kN obtained from the experiment.

In the second part of the verification study, five reinforced concrete box culverts designed and constructed according to ASTM C1577 (2005) and ASTM C1433 (2004) specifications and, respectively, tested by Maximos, Erdogmus & Tadros (2010) and Garg, Abolmaali & Fernandez (2007) are analysed. The geometry, reinforcing configuration and location of loads for the tested culverts are shown in Figure 7.2b and Table 7.1.The steel reinforcement used in the culverts was deformed welded wire with a minimum yield strength of $f_y = 470$ MPa and an average concrete compressive strength of $f_c = 52$ MPa and $42 MPa$ for the culverts tested by Maximos, Erdogmus & Tadros (2010) and Garg, Abolmaali & Fernandez (2007), respectively. The tensile strength of concrete is taken as $f_t = 0.36\sqrt{f_c}$. It is noteworthy that the support for the WB culvert is modelled as a linearly elastic material with an elastic modulus of 20

MPa (i.e. medium to dense gravel bedding). In the NB series, the reaction floor is modelled using a linearly elastic material with an elastic modulus of 25 GPA (i.e. concrete). The culverts are modelled using Table 7.1 and are seen to correlate well with the peak loads obtained from the tests. The load versus deflection response of the culverts tested by Garg et al. (2007) and predicted by the FE model are shown in Figure 7.3. The results demonstrate a reasonable correlation. Also, the modes of failure and the cracking patterns predicted by the FE model correlate reasonably well with the experimental observations (see Figure 7.4).

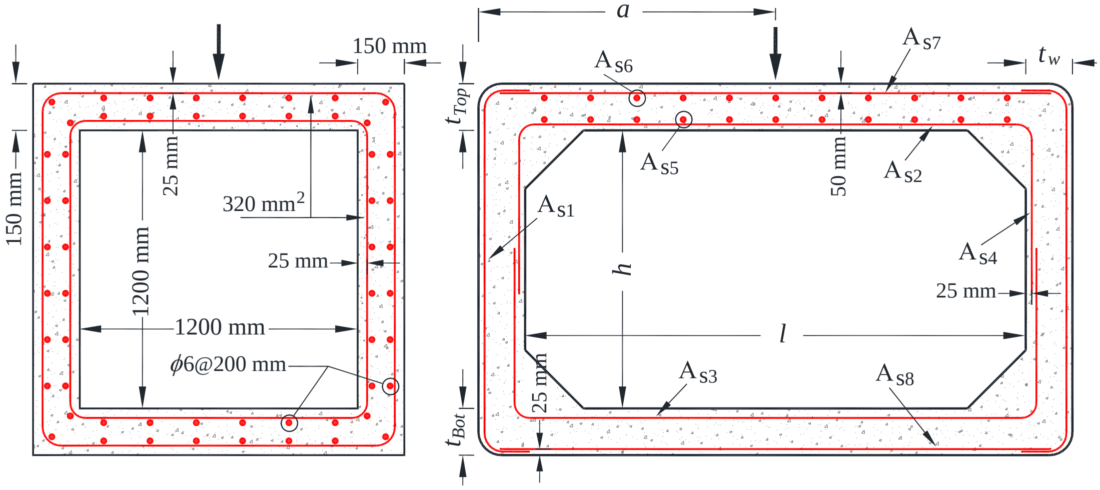

(a) (b)

Figure 7.2 Outline of geometry & reinforcement (a) GFRP reinforced culvert tested by Alkhrdaji & Nanni (2001) and (b) box culvert tested by Maximos, Erdogmus & Tadros (2010) & Garg, Abolmaali & Fernandez (2007).

Table 7.1 Dimension, location of load, reinforcing steel configuration (area) and peak load capacity of the culverts tested by Maximos, Erdogmus & Tadros (2010) and Garg, Abolmaali & Fernandez (2007).

<table>
<tr><th rowspan="2">Reference</th><th rowspan="2">Specimen</th><th rowspan="2">location a (mm)</th><th colspan="5">Dimensions (mm)</th><th colspan="8">Steel reinforcement (mm²/m)</th><th colspan="2">Peak load (kN)</th></tr>
<tr><th>l</th><th>h</th><th>t_w</th><th>t_{Top}</th><th>t_{Bot}</th><th>A_{s1}</th><th>A_{s2}</th><th>A_{s3}</th><th>A_{s4}</th><th>A_{s5}</th><th>A_{s6}</th><th>A_{s7}</th><th>A_{s8}</th><th>Exp.</th><th>FE model</th></tr>
<tr><td>Maximos, Erdogmus & Tadros (2010)</td><td>B</td><td>1270</td><td>2120</td><td>1220</td><td>203</td><td>203</td><td>203</td><td>445</td><td>730</td><td>530</td><td>415</td><td>415</td><td>415</td><td>445</td><td>445</td><td>515</td><td>493</td></tr>
<tr><td rowspan="4">Garg, Abolmaali & Fernandez (2007) #</td><td>WB-5</td><td>381</td><td rowspan="4">1220</td><td rowspan="4">1220</td><td rowspan="4">127</td><td rowspan="4">191</td><td rowspan="4">152</td><td rowspan="4">380</td><td rowspan="4">990</td><td rowspan="4">530</td><td rowspan="4">255</td><td rowspan="4">485</td><td rowspan="4">---</td><td rowspan="4">380</td><td rowspan="4">300</td><td>632</td><td>648</td></tr>
<tr><td>NB-5</td><td>381</td><td>712</td><td>719</td></tr>
<tr><td>NB-6 ½</td><td>420</td><td>645</td><td>649</td></tr>
<tr><td>NB-11 ½</td><td>547</td><td>578</td><td>559</td></tr>
</table>

WB and NB refers to culverts tested with and without aggregate bedding, respectively.

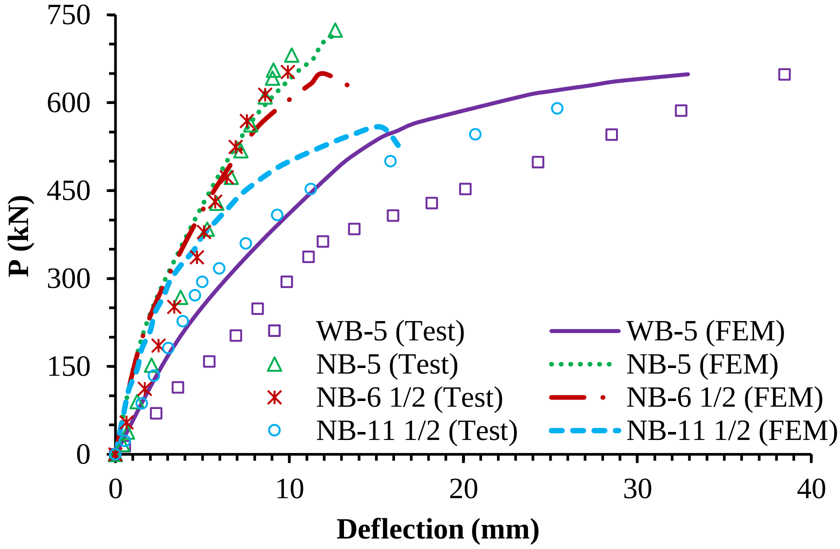

Figure 7.3 Load versus deflection response of the culverts tested by Garg, Abolmaali & Fernandez (2007).

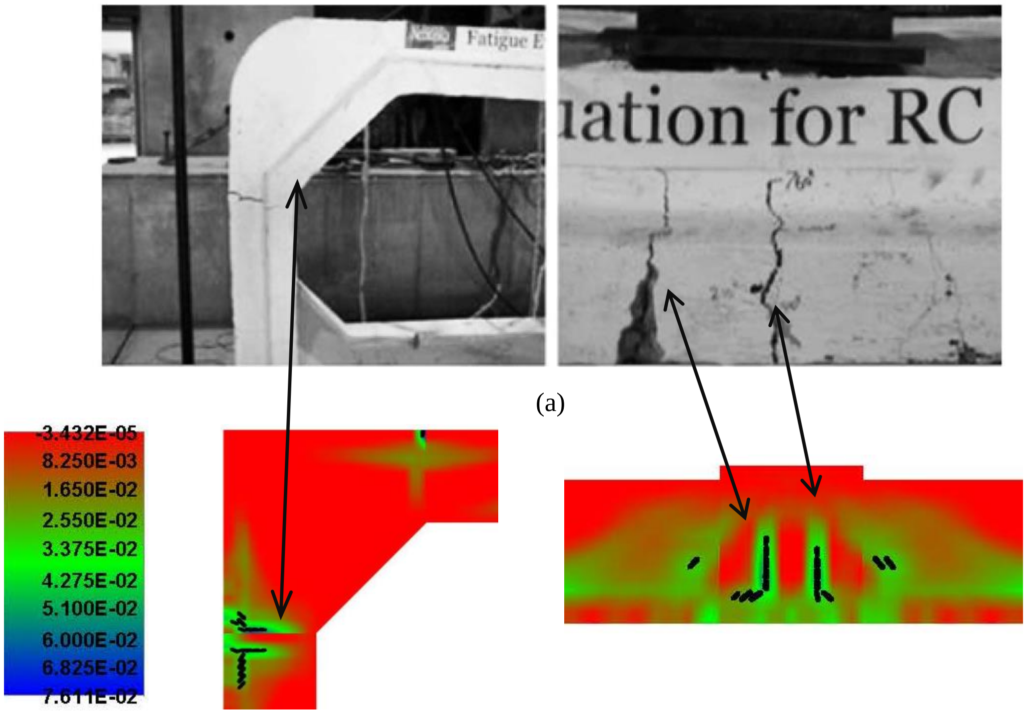

(b)

Figure 7.4 Patterns of cracks and principle strains at failure (a) observed in the test by Maximos, Erdogmus & Tadros (2010) and (b) predicted by the continuum-based FE model.

The results of finite element simulations show that the adopted material laws and 2D continuum-based FE models can adequately capture the structural response (i.e. load-deflection, peak load capacity and failure mode) of RC culverts.

7.4. Parametric study and discussion of results

It is hypothesised that the backfill soil can provide a longitudinal restraint for the top slab of the RC culverts and this restraint can mobilise the mechanism of arching action and enhance the capacity of the RC culvert. It is further hypothesised that the longitudinal restraint provided by the backfill soil reduces the level of stress (stress range) in the tensile steel reinforcement and, subsequently, increases the fatigue life of RC culverts. In this section, a parametric study is undertaken to determine the influence of backfill soil stiffness in conjunction with concrete compressive strength and steel reinforcing proportion on the peak load capacity of inverted U-shape RC culverts with no or little skew.

In the parametric study, four different types of inverted U-shape RC culvert with the schematic geometry outlined in Figure 7.5 are modelled and analysed under their self-weight and a monotonically increasing point (wheel) load applied at the mid-span of the top slab. The designation of culverts and their dimensions as per Australian Standards AS1597.1 (2010) and AS1597.2 (2013) are given in Table 7.2. Furthermore, the material properties including concrete compressive strength f_c, concrete tensile strength f_t, concrete modulus of elasticity E_c, yield strength of steel f_y and steel reinforcing proportion ρ and backfill modulus of subgrade reaction K_{soil} adopted for the parametric study are given in Table 7.3. The culvert backfills typically comply with some compaction requirements that lead to a minimum compressive strength and stiffness for backfills. However, a significant variability in the mechanical characteristic of backfill soil has been observed during field and lab tests (Jayawickrama, Lawson & Wood 2011). Accordingly, three different horizontal modulus of subgrade reactions (5, 15 and 30 MN/m^3) are adopted to represent the wide range of modulus of subgrade reaction obtained from field testing and back calculated from field test data (Jayawickrama, Lawson & Wood 2011).

In the 2D continuum-based FE models, the maximum element size is limited to 15 mm and the influence of far-field boundary conditions (fixed support in Figure 7.5) on the response of the culvert is minimised by modelling the backfill soil over a width of 2*l*

(l being the culvert span) on each side of the culvert wall (Figure 7.5).

Table 7.2 Dimensions of the culverts adopted in the parametric studies (also see Figure 7.5).

Class size	Culvert designation	Span (mm)	Height (mm)	Slab cross section (mm×mm)
Medium	2412	2400	1200	1000×200
	2418	2400	1800	1000×200
Large	4230	4200	3000	1000×300
	4242	4200	4200	1000×300

Table 7.3 Summery of variables and material properties adopted in the parametric study.

f_c # (MPa)	E_c (GPa)	f_y (MPa)	f_u (MPa)	E_s (GPa)	ρ ## (%)	Modulus of subgrade reaction (MN/m^3)	Relative density of subgrade
20	19.0	500	505	200	0.4 0.8	5.0	Loose
32	26.0	500	505	200		15.0	Medium
60	36.0	500	505	200		30.0	Dense

Tensile strength of concrete is obtained from $f_t = 0.36\sqrt{f_c}$.

The reinforcing proportion is calculated from $\rho = \dfrac{A_s}{1000\,t}$, where A_s is area of reinforcing steel bars and t is thickness of slab/wall (see Figure 7.5).

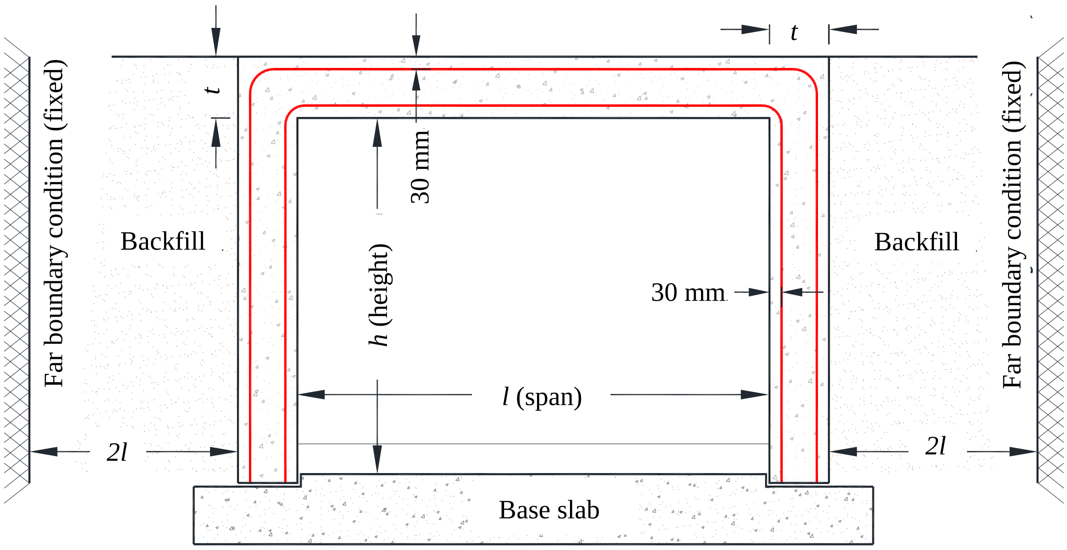

Figure 7.5 Outline of the inverted U-shape culvert with backfill adopted in the parametric studies.

7.4.1. Peak load capacity

Using the 2D continuum-based FE models, the load-deflection response of the culverts under a point wheel load applied over a contact area of 400 mm x 250 mm applied at the mid-span are attained, as per Australian Standard AS5100.2 (2004)). To ensure that possible damage and stiffness degradation of the backfill soil is taken into account, the culverts with backfill are initially loaded up to the peak load capacity of the culverts without backfill and then fully unloaded. In the second cycle, the load is monotonically increased until failure.

The normalised peak load capacity (ratio of the peak load capacity with backfill soil included to the peak load capacity without the backfill soil) of the culverts versus soil stiffness (modulus of subgrade reaction) are shown in Figure 7.6 to Figure 7.9. The normalised peak load capacity of the medium size culverts versus compressive strength of concrete is shown in Figure 7.10 and Figure 7.11. The normalised peak load capacities (Figure 7.6 to Figure 7.11) represent the ratio of strength enhancement provided by development of arch action in the top slab due to backfill soil stiffness. In addition, the peak load capacity of the culverts obtained from the continuum-based FE model and the plastic hinge analysis method (symmetric mechanism with 3 hinges) using Australian Standard AS3600 (2009) requirements are given in Table 7.4. It was observed that the stiffness of backfill soil can provide lateral restraints for the culverts and, thus, enhance the peak load capacity of the culverts by mobilising the mechanism of arching (compressive membrane) action in the top slab. It is also concluded that the load capacity of the culverts is not overly sensitive (less than 6%) to the soil stiffness (modulus of subgrade reaction) in the considered range (5-30 MN/m^3).

For the cases analysed in this study, incorporating the stiffness of backfill soil into the FE models led to a minimum 20% enhancement in the peak load carrying capacity of the culverts (for the culvert with ρ= 0.008 and f_c= 20 MPa).

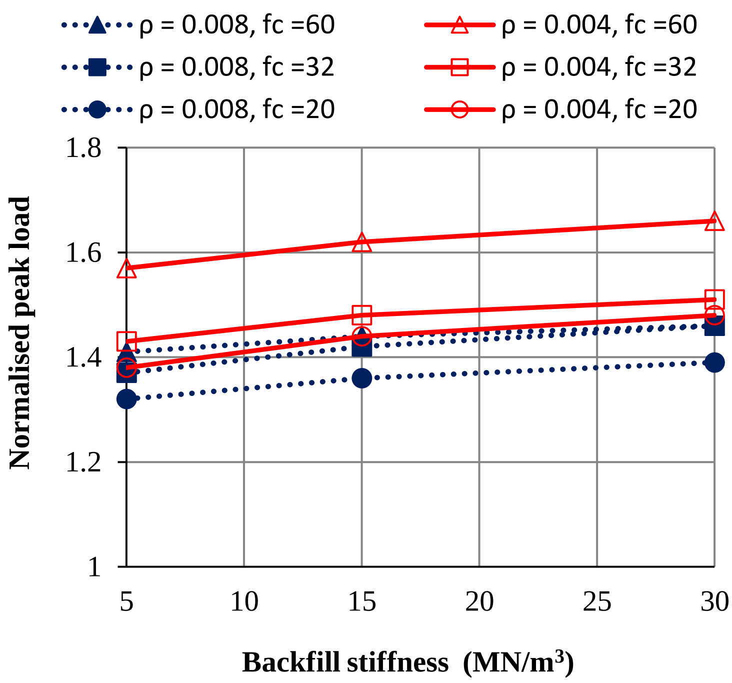

Figure 7.6 Normalised peak load of the culverts versus backfill soil stiffness (characterise by modulus of subgrade reaction) for culvert 2412.

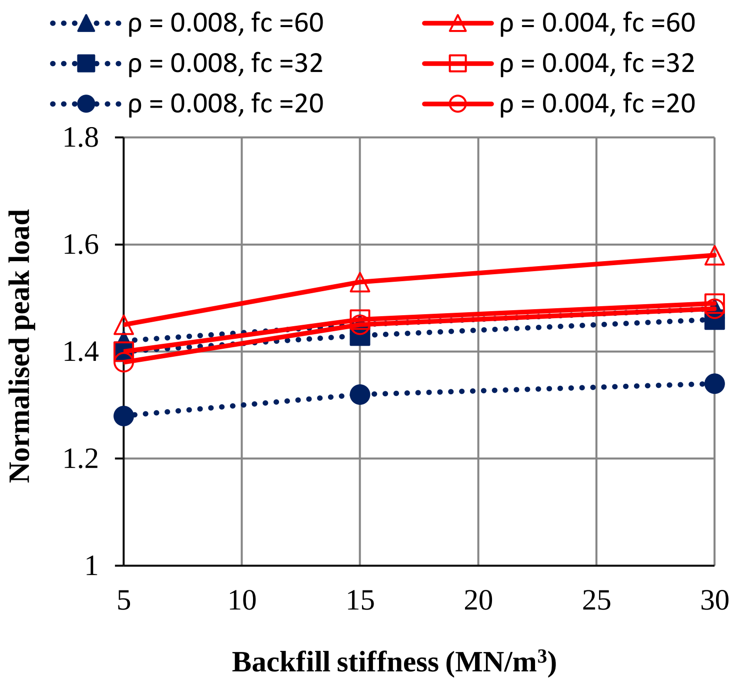

Figure 7.7 Normalised peak load of the culverts versus backfill soil stiffness (characterise by modulus of subgrade reaction) for culvert 2418.

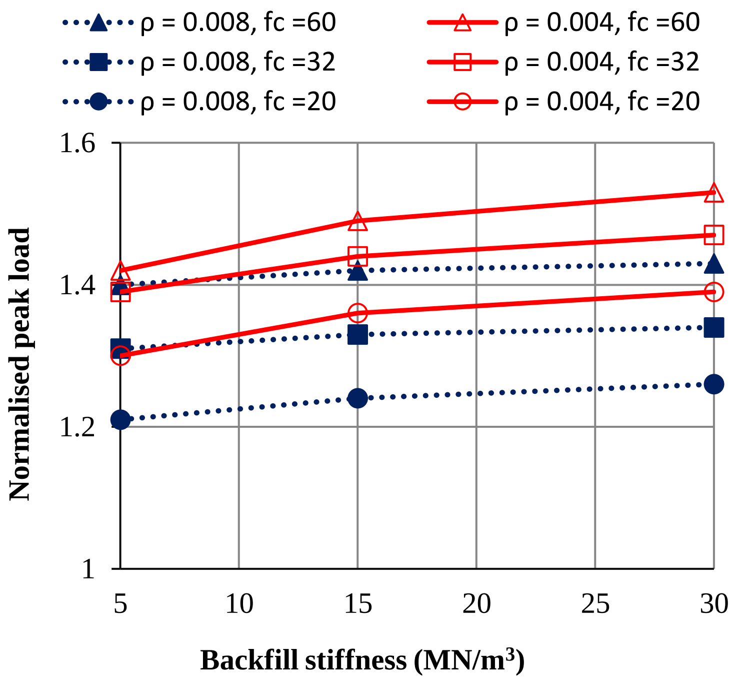

Figure 7.8 Normalised peak load of the culverts versus backfill soil stiffness (characterise by modulus of subgrade reaction) for culvert 4230.

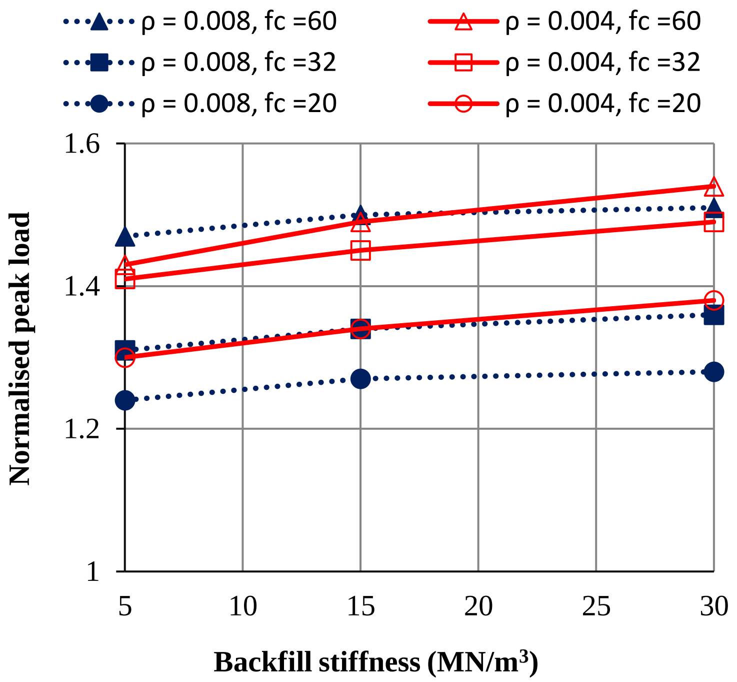

Figure 7.9 Normalised peak load of the culverts versus backfill soil stiffness (characterise by modulus of subgrade reaction) for culvert 4242.

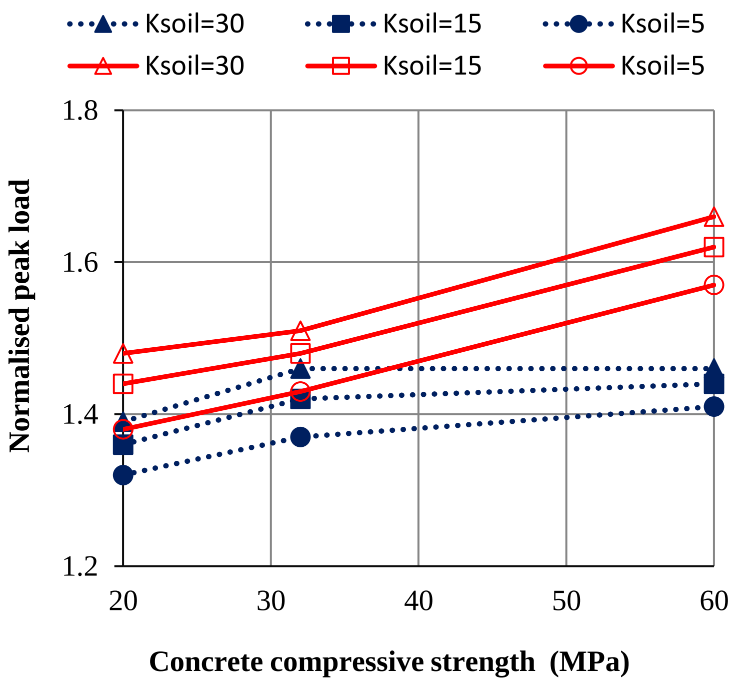

Figure 7.10 Normalised peak load capacity of the culverts versus compressive strength of concrete for culverts with different backfill soil stiffness (K_{soil} denotes the modulus of subgrade reaction for backfill soil) for culvert 2412.

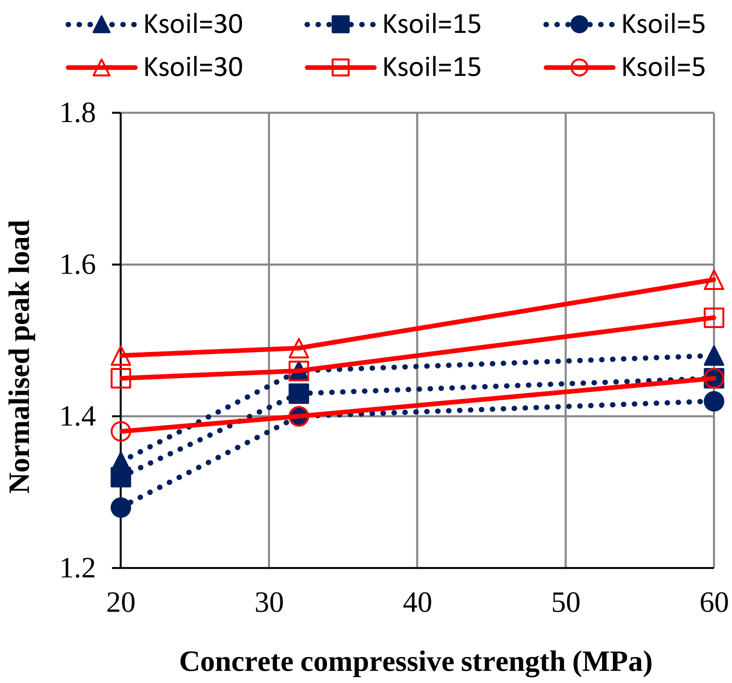

Figure 7.11 Normalised peak load capacity of the culverts versus compressive strength of concrete for culverts with different backfill soil stiffness (K_{soil} denotes the modulus of subgrade reaction for backfill soil) for culvert 2418.

Table 7.4 Peak load capacity of the culverts predicted by plastic hinge analysis and 2D continuum-based FE models.

ρ (%)	f_c (MPa)	Peak load capacity (kN)									
		2D FE model								Plastic hinge AS3600 (2009)#	
		without backfill soil				with backfill soil (5 MN/m^3)					
		2412	2418	4230	4242	2412	2418	4230	4242	2412/2418	4230/ 4242
0.4	20	188	188	232	230	259	259	302	299	207	288
	32	202	200	251	243	289	280	349	343	210	290
	60	215	213	262	256	338	309	372	366	212	294
0.8	20	318	316	362	362	420	406	438	449	389	535
	32	349	352	415	403	478	493	544	528	403	554
	60	391	382	482	459	551	542	675	675	412	568

Symmetric mechanism with three plastic hinges, i.e. one plastic hinge at each end of the slab and one hinge at the mid-span.

With regard to Figure 7.10 and Figure 7.11, it is concluded the peak load capacity enhancement (i.e. $[P_{peak\ (with\ soil)} - P_{peak\ (without\ soil)}]/P_{peak\ (without\ soil)}$) provided by the stiffness of backfill depends on the compressive strength of concrete, which is characteristic of strength enhancement due to development of arching action in restrained RC members (Farhangvesali et al. 2013). It is also concluded that the load capacity enhancement due to the lateral restraint provided by the backfill soil is proportional to the compressive strength of the concrete (f_c) and inversely proportional to the reinforcing steel ratio (ρ).

The results in Table 7.4 show that the plastic hinge analysis overestimates the capacity of the culverts; this is because the adopted mechanism (with 3 hinges and fixed supports) does not properly represent the failure mechanism with the realistic boundary conditions provided by the soil backfill. Similarly, the simplistic assumption of pinned supports for the top RC slab of a monolithic inverted U-shape culvert would lead to an underestimation of capacity. It is noteworthy that the capacity of inverted U-shape culverts (captured by the 2D FE model and without backfill) is associated with formation of two plastic hinges and an unsymmetrical mode of failure, as shown in Figure 7.12a. The average axial compressive force at mid-span of top slab obtained from FE models, with and without backfill soil included, for medium size culvert 2412 and large size culvert 4230 with concrete compressive strength of $f_c = 20$ MPa and reinforcing proportion of $\rho = 0.004$ are shown in Figure 7.12b. The compressive force in the top slab of culverts with backfill is much bigger than the case where backfill is not considered ($K_{soil} = 0$) and this is demonstrative of arching action mobilised by stiffness of backfill soil. Obviously, this axial compressive force can significantly increase the load capacity of the RC culverts. The results of 2D FE analysis show that no damage/plastic deformation occurs in the backfill and the maximum stress induced in the backfill always remains well below the load bearing capacity of 0.12 MPa, adopted for the backfill soil (see Figure 7.13).

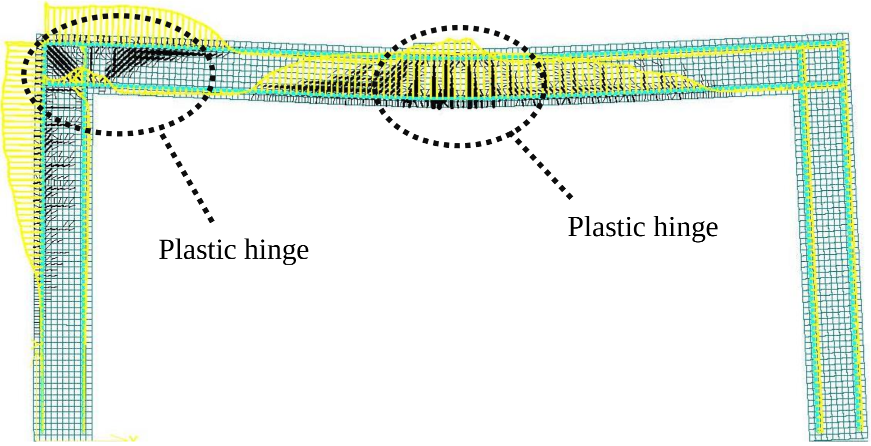

(a)

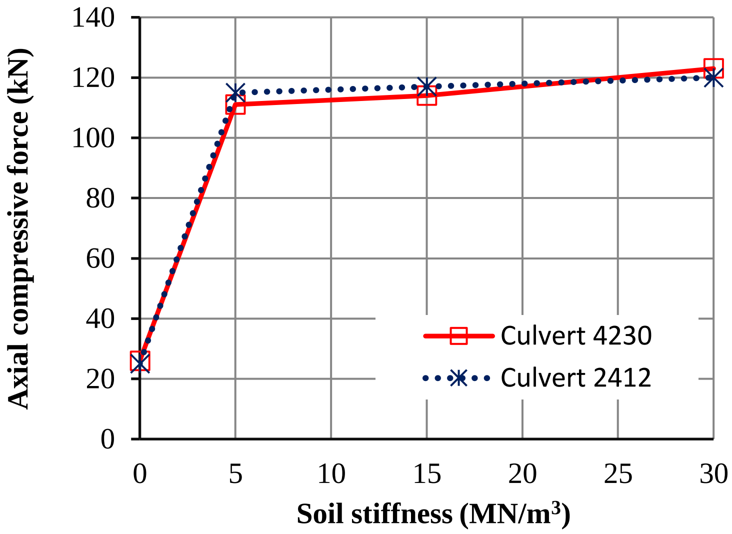

(b)

Figure 7.12 (a) Pattern of cracks/damages in concrete and stress in longitudinal steel bars at the failure load for the culvert 2412 without backfill and (b) axial compressive force in the top slab of medium size culvert 2412 and large size culvert 4230 with ρ = 0.004 and f_c=20 MPa.

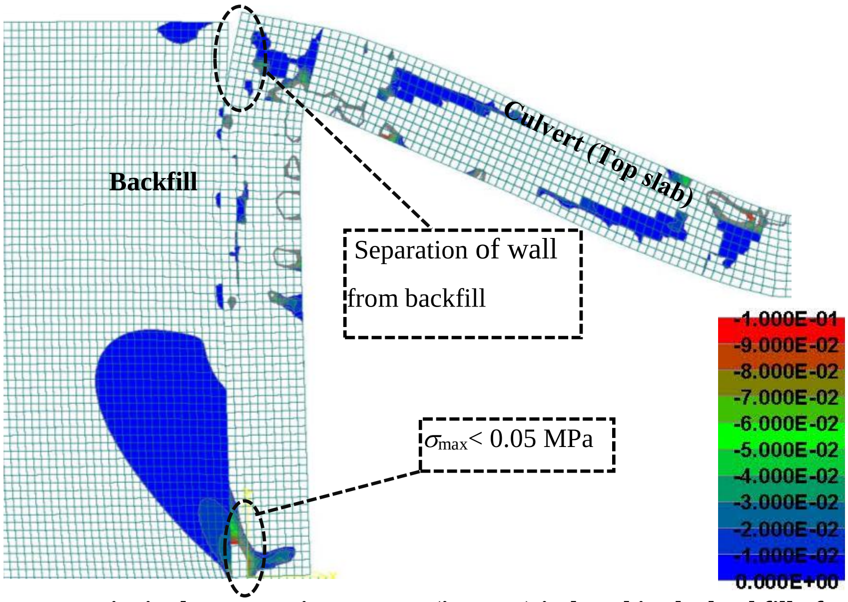

Figure 7.13 The max. principal compressive stresses (in MPa) induced in the backfill of culvert 2412 (ρ=0.004 and f_c= 60 MPa) at the peak load capacity.

7.4.2. Fatigue life

According to Australian Standard AS1597.2 (2013), on principal interstate freeways and highways and on urban freeways or other routes with significant volumes of heavy vehicles, fatigue design loads for roadway culverts under less than 1 m of fill should be considered in accordance with requirements of AS5100.2 (2004).

Fatigue in RC depends on the amplitude of stress in steel and concrete, number of cycles and stress level in concrete. Accordingly, in this part, the max. amplitude of stress in tensile steel bars is used to compare the fatigue life of RC culverts before and after considering the influence of backfill soil. The culverts are analysed under their self-weight and a fatigue load of 78 kN applied over 250 mm at mid-span. The applied load was calculated as, 0.7 x (1+α) x 80=0.7 x (1+0.4) x 80= 78 kN. To calculate the fatigue load, a dynamic load allowance of α= 0.4 and a reduction factor of 0.7 was applied on the standard wheel load of 80 kN, as per AS5100.2 (2004) requirements. The maximum stress in the bottom steel bars at mid-span obtained from FE models, with and without backfill soil included, for medium and large size culverts are shown in Figure 7.14 to Figure 7.17. The stress in the steel bars is obtained after two full loading-unloading cycles to ensure that the concrete is fully cracked.

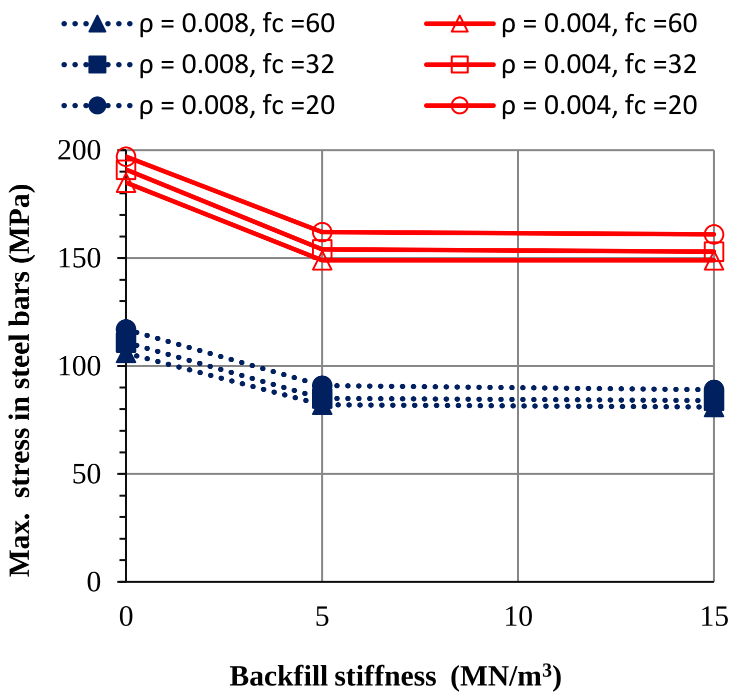

Figure 7.14 Maximum tensile stress in bottom steel bars at mid-span versus backfill soil stiffness for culvert 2412.

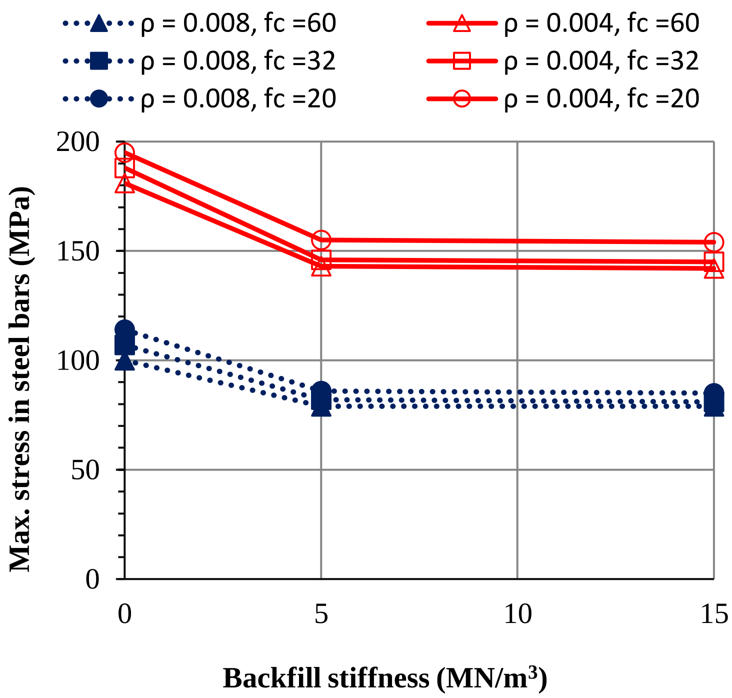

Figure 7.15 Maximum tensile stress in bottom steel bars at mid-span versus backfill soil stiffness for culvert 2418.

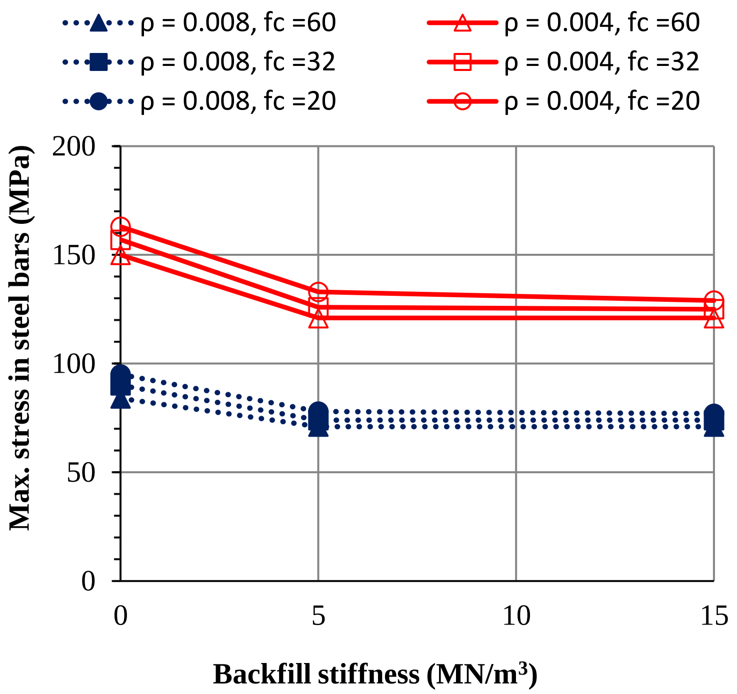

Figure 7.16 Maximum tensile stress in bottom steel bars at mid-span versus backfill soil stiffness for culvert 4230.

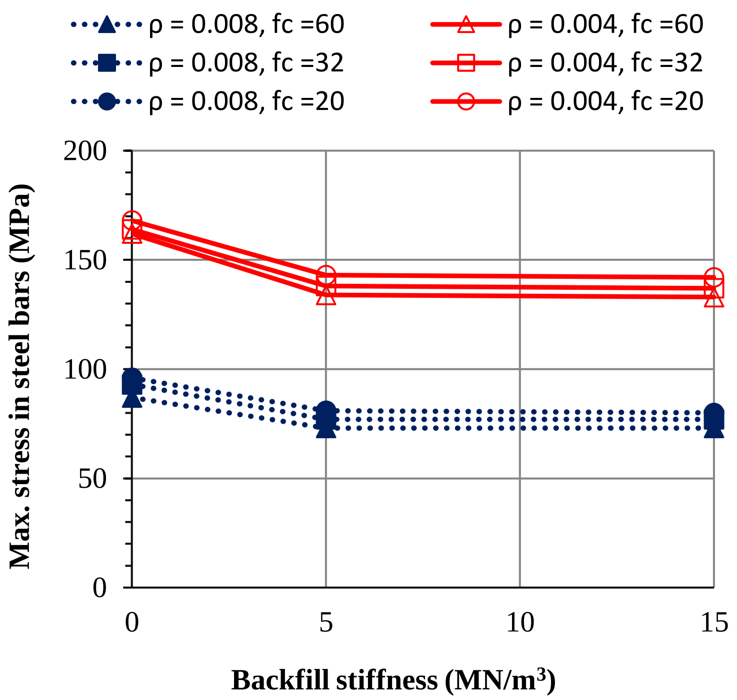

Figure 7.17 Maximum tensile stress in bottom steel bars at mid-span versus backfill soil stiffness for culvert 4242.

It is seen that the transverse restraint provided by the backfill can reduce the maximum tensile stress in the bottom steel bars by around 15% (see Figure 7.14 to Figure 7.17) and, accordingly, the backfill influence can potentially increase the fatigue life of inverted U-shape culverts through mobilising the arching action mechanism in the top slab.

7.5. Conclusions

This chapter investigates the available reserve of strength in inverted U-shape reinforced concrete (RC) culverts due to development of arching action in the top slab. Nonlinear 2D continuum-based finite element (FE) models of culverts with backfill on each side were developed and analysed to investigate the effects of arching action (mobilised by the lateral stiffness of backfill) on the peak load capacity and fatigue life of inverted U-shape RC culverts.

It is demonstrated that the FE models developed can capture both the material and geometrical nonlinearities. The nonlinearity of backfill soil, concrete cracking and crushing and yielding of reinforcing steel are considered by using appropriate material laws. The accuracy of the FE models, together with the adopted material models and assumptions for capturing the response of RC culverts without backfill are verified by comparing the FE predictions with the experimental results taken from the literature. It is shown that the proposed continuum-based FE models can adequately capture the peak load capacity and load-deflection response of the RC culverts. The developed FE models are used to undertake a parametric study and quantify the influence of culvert geometry (span length over wall height ratio), compressive strength of concrete, reinforcing proportion and stiffness (modulus of subgrade reaction) of backfill on the peak load capacity and fatigue life (represented by magnitude and range of stress in steel bars) of inverted U-shape RC culverts.

From the results of parametric studies, the following conclusions are drawn;

- Backfill provides sufficient lateral stiffness/restraint to mobilise arching action in the top slab of RC culverts and, accordingly, the load capacity and fatigue life of buried culverts are higher than that of the culvert without the influence of backfill accounted for.

- For the cases analysed in this study, due to development of arching action in top slab, a minimum 20% enhancement in the peak load capacity of the inverted U-shape RC culverts (with ρ= 0.008 and f_c= 20 MPa) was observed. However, the variation of load capacity with respect to magnitude of soil stiffness (modulus of subgrade reaction within the range considered, 5-30 MN/m^3) was found not to be significant (less than 6% for the considered cases).

- The mechanism of arching action can reduce the maximum tensile stress in steel bars (around 15% reduction was observed for the inverted U-shape culverts analysed in this study) that, in turn, provides an increase in fatigue life.

- The load capacity enhancement provided by the mechanism of arching action depends on the compressive strength of concrete; specifically, it is concluded that the load capacity enhancement due to the lateral restraint provided by the backfill is approximately proportional to the compressive strength of concrete (f_c) and inversely proportional to the reinforcing steel ratio (ρ).

- The geometry (i.e. span over rise ratio) of the culverts within the same class, that is small, medium and large as per Australian Standards AS1597.1 (2010) and AS1597.2 (2013), was found to have only a minor influence on the strength enhancement factor (ratio of the peak load capacity of the culvert without backfill soil to the peak load capacity of the culvert with backfill soil) provided by development of arching action in the top slab due to backfill soil stiffness (see Figure 7.6 to Figure 7.9).

CHAPTER 8

Conclusion

8. Conclusion

8.1. Introduction

The enhanced strength of transversely restrained concrete deck slabs has been demonstrated through different studies, however, the existing transverse confining systems used in conjunction with cast in situ concrete deck slabs are not conducive to deconstruction. To benefit from enhancing effect of arching action and use of prefabricated RC slab concurrently, a practical and efficient construction method was proposed for steel-concrete composite bridge deck slabs. The structural behaviour of transversely restrained precast RC deck slabs with and without steel fibres in this novel deconstructable steel-concrete composite deck that takes advantage of bolted shear connectors have been studied. In addition, developing the arching action resulted from lateral stiffness of backfill in buried prefabricated RC culverts has been investigated numerically using finite element (FE) simulations.

In this chapter, the conclusions drawn from the experimental program and FE modelling of the precast deck slab with transverse confining system in composite deck as well as FE simulation of buried RC culverts are summarised and some suggestions for the future research on development of arching action in steel-concrete composite deck slabs and reinforced concrete (RC) culverts are made.

8.2. Experimental Study

In the experimental program of this research project, thirty-four one-half scaled transversely restrained reinforced concrete (RC) and steel fiber reinforced concrete (SFRC) deck slab composites with steel girders by use of post-installed friction grip bolts (PFGB) as shear connectors were constructed and tested under static and cyclic tests to determine the effect of type of transverse restraining system (i.e. cross-bracings or straps), reinforcement arrangement, reinforcement ratio, dosage of steel fibre (i.e. 0.25% and 0.5%) and concrete compressive strength on the peak load carrying capacity, stiffness, ductility and fatigue life of the precast deck slabs. The results of laboratory experiments have been studied and discussed to evaluate structural performance of the new proposed deconstructable deck slab system and to provide benchmark data for validation of numerical models.

The conclusions drawn from the static and cyclic fatigue experiments on the deconstructable steel-precast concrete deck slabs with bolted shear connectors are summarised below;

- The strain in confining members i.e. ties/straps and cross-bracings continuously increased as the load increased. This proved the efficiency of the bolted shear connectors in preventing relative slip between the precast slab and the transverse confining system.

- In addition to strength enhancement of (SF) RC slabs in static tests, fatigue life of transversely restrained precast (SF) RC deck slabs improve remarkably due to development of arch action. Therefore, the strength enhancement provided by the transverse restraining systems can be taken into account under cyclic service loading conditions without negatively affecting the fatigue life of the deck slabs.

- The transverse ties/straps under the deck slabs have superior performance compared to bracings in terms of improving the load carrying capacity as well as fatigue life of the precast (SF) RC deck slabs.

- In addition to mobilising the arch action, the transverse ties/straps in conjunction with the (SF) RC slab form a force loop and carry large tensile forces. Consequently, it reduces the tensile stresses/forces in the reinforcing bars and increases the load carrying capacity of the (SF) RC slabs.

- The slabs experienced large deflections and extensive damage under static as well cyclic loading conditions in each test; however, no sign of damage or excessive deformation was observed in the post-installed bolted shear connectors and the severely damaged slabs were easily dismantled after testing. This can facilitate repairing and disassembling of the proposed composite deck system.

- In contrast to previous tests conducted on laterally restrained composite decks with cast in situ slabs, no horizontal cracks were observed on the faces of the slabs along the haunches during the tests. It is hypothesised that the clamping force provided by friction grip bolted shear connectors and steel fibres can hinder development of longitudinal cracks in the haunched edge and improve load carrying capacity of transversely confined concrete slabs.

- The strength enhancement (due to development of arch action) observed in the transversely confined decks would have significant implications for strength assessment of existing RC deck slabs, where transverse bracings are typically provided for the steel–concrete composite decks to prevent overturning and lateral torsional buckling of steel girders during the construction. However, the effect of these transverse bracings on the ultimate load-carrying capacity of the concrete decks is not considered in the current strength assessment practices. In this study, the experimental peak load capacity of the concrete deck slabs with transverse cross-bracings was around 60–70% more than the peak load predicted by the plastic hinge analysis, which is demonstrative of the level of conservatism in the current strength assessment practices for concrete deck slabs. Therefore, not only ignoring the strength enhancement provided by arching action in the transversely confined deck slabs can lead to overly conservative design but also mobilising the arch action by using transverse ties or cross bracings can be used as an effective strengthening method for RC deck slabs.

- The development of arching action in the transversely restrained SFRC slabs also significantly increases the peak load capacity of SFRC slab however, the capacity of the restrained SFRC slabs with 0.25% and 0.50% 5D fibres were identical and increasing fibre dosage from 0.25% to 0.50% did not enhance the peak load capacity of the SFRC slabs under static loading condition.

- Adding 0.5% steel fibres to transversely restrained (SF) RC deck slabs improved fatigue life of the tested specimens whereas, adding 0.25% fibre dosage reduced the fatigue life of slabs where slab tested under fatigue load regime with respect to the enhanced static load carrying capacity.

- Except overly-reinforced precast slab, in all the other transversely confined slabs with moderate or low amount of reinforcement ratio, the failure was associated with development of cracks and yielding of steel bars in the soffit of the slab at mid-span, followed by crushing of concrete on the top surface of slabs at the mid-span and onset of cracks at the supported edges of the slab. Furthermore, the failure of transversely restrained SFRC slabs was associated with development of cracks in the soffit at mid-span and the onset of cracks at top of the slab at end span (adjacent to the haunches and between PFBSCs). This failure mode is consistent with development of plastic hinges at the mid-span and at the clamped ends.

– Two distinctive failure modes were observed under fatigue load conditions for transversely restrained precast deconstructable (SF)RC deck slabs. The first failure mode was triggered by fracture of reinforcing bars and the second mode of failure was triggered by rupture in the transverse ties/straps at the location of shear connectors bolt hole.

– Comparing the cracking load of the transversely restrained precast slabs with and without steel fibres showed that replacing the conventional reinforcing bars (unsymmetrical configuration in the section) with steel fibres can increase the cracking load of the precast slabs. The shrinkage induced curvature in unsymmetrically reinforced slabs can lower the cracking load. However, the more uniformly distributed nature of fibres compared to unsymmetric reinforcing bars can diminish the shrinkage induced warping in the concrete sections.

– Under a seemingly constant average strain/stress range, the location of reinforcing steel bars can significantly affect the fatigue life of (SF) RC deck slabs. Increasing the concrete cover on steel bars (or reducing the effective depth *d* of the deck slabs) can lead to higher level of strain localisation (at the location of cracks) in steel bars that can significantly reduce the fatigue life of RC deck slabs.

– The curvature-based ductility/deformability index μ_ψ and the robustness index *R* for all transversely confined precast RC slabs were calculated. Except for overly-reinforced specimens and no reinforcement specimen, in all other specimens, the μ_ψ index was greater than 6.0 and *R* index was greater than 4.0. It can be concluded that moderated or low reinforced precast slabs comply with minimum ductility/deformability requirement of *J*= 4.0 specified in CHBDC (2006).

– For SFRC slabs energy-based ductility indices were estimated and it was observed that the energy-based ductility of SFRC slabs with 0.5% 5D steel fibres increased with increasing stiffness of the restraining system. This observation is in marked contrast to that of transversely restrained RC slabs in which the ductility decreases as the stiffness of the transverse restraining system increases.

8.3. Finite Element Simulation

The 3D non-linear continuum-based FE model of RC deck slabs with transverse confining systems in composite deck with bolt shear connectors, which is capable of considering all non-linearity of the interfaces, geometrical and material, showed that the FE models can estimate the peak load carrying capacity of the transversely confined precast RC deck slabs with good accuracy, however, it tends to overestimate the stiffness and underestimate the deflection corresponding to ultimate load carrying capacity of the RC deck slabs. From the parametric study in which the influence of clearance between concrete slab and bolts, post-tensioning stress in the PFGB shear connectors, reinforcement ratio, thickness of the precast concrete slab, concrete compressive strength and yield strength of reinforcing steel bars on the structural behaviour of precast RC deck slabs with external confining systems are studied, the following conclusions are inferred;

- The clearance between the precast concrete slab and bolt shear connectors and the magnitude of post-tensioning stress in the PFGB shear connectors appear to have minor influence on the initial stiffness and ultimate strength of the deck slabs. However, reducing the clearance and/or increasing the level of post-tensioning in the PFGB shear connectors can improve the post-cracking stiffness of the slabs.

- Due to development of arch action, the yield strength of reinforcing bars has minor influence on the peak load carrying capacity of the precast RC deck slabs. However, increasing the concrete compressive strength can significantly increase the peak load carrying capacity of the slabs.

- Due to arch action contribution, increasing slab thickness or reducing the span length over slab thickness ratio can increase the peak load carrying capacity of the RC slabs beyond what is observed in purely flexural members.

From the 2D nonlinear continuum-based finite element (FE) models of RC culverts with backfill on each side, which can capture both the material and geometrical nonlinearities of backfill soil, concrete cracking and crushing and yielding of reinforcing steel, it was indicated that the proposed continuum-based FE models can adequately capture the peak load capacity and load-deflection response of the RC culverts. The developed FE models were used to undertake a parametric study and quantify the influence of concrete compressive strength, culvert geometry, reinforcing proportion and stiffness of backfill on the peak load capacity and fatigue life of inverted U-shape RC culverts. From the results of this parametric studies, the following conclusions are drawn;

- Backfill provides sufficient lateral stiffness/restraint to mobilise arching action in the top slab of RC culverts and, accordingly, the load capacity and fatigue life of buried culverts are higher than that of the culvert without the influence of backfill accounted for. For the cases analysed in this study, due to development of arching action in top slab, a minimum 20% enhancement in the peak load capacity of the inverted U-shape RC culverts was observed. Furthermore, the mechanism of arching action can reduce the maximum tensile stress in steel bars that leads to enhancement of the fatigue life.

- The load capacity enhancement provided by the mechanism of arching action depends on the compressive strength of concrete; specifically, the load capacity enhancement due to the lateral restraint provided by the backfill is approximately proportional to the compressive strength of concrete and inversely proportional to the reinforcing steel ratio.

- The geometry (i.e. span over rise ratio) of the culverts within the same class, that is small, medium and large as per Australian Standards AS1597.1 (2010) and AS1597.2 (2013), was found to have only a minor influence on the strength enhancement factor provided by development of arching action in the top slab due to backfill soil stiffness.

8.4. Recommendations for Future Study

Regarding the results obtained from experimental and numerical studies in this research project and existing literature, the following topics has been identified for further future investigation on development of arching action and its implications in prefabricated slab deck;

- Extending the current experimental studies particularly in fatigue part to include other effective parameters contributing in the development of the arching action such as restraining systems and span to depth ratio of slab.

- The effect of continuity of slabs by carrying out the experimental program, where there are two or more spans, on structural performance of the precast deck slabs.

- Use of different dosage of steel fibre as well as effect of various types of fibres on flexural and fatigue behaviour of deconstructable precast deck slabs.

- Investigation of long-term behaviour of post-tensioned PFGB as shear connectors with respect to loss of post-tensioning force due to creep and shrinkage of concrete in the precast slabs.

- Use of FRP rods or straps instead of steel straps/ties and investigating the feasibility of the system.

- Use of geo-polymer concrete instead of conventional concrete in precast slabs to improve the sustainability.

- Development of more detailed 3D FE models that can accurately capture the effect of cross bracings in steel composite concrete slab decks.

- Development of more reliable 3D computer simulation, that can capture nonlinear behaviour, failure mode and fatigue life of fibre reinforced concrete deck slabs under complex static and cyclic stress states.

- Laboratory or field testing of the buried RC culverts and considering effect of different variables such as surrounding soil properties, concrete and reinforcement characteristics that effect behaviour of buried RC culverts due to development of arching action.

References

References

AASHTO 1983, *Standard Specification for highway bridges* American Association for of State Highway and Transport Officials, Washington ,DC.

AASHTO 1996, *Standard specification for highway bridges, third edition*

American Association of State Highway and Transport Officials, Washington, DC.

ABAQUS User´s Manual 2009, 'Version 6.9', in D. Systèmes (ed.).

Abas, F.M., Gilbert, R.I., Foster, S.J. & Bradford, M.A. 2013, 'Strength and serviceability of continuous composite slabs with deep trapezoidal steel decking and steel fibre reinforced concrete', *Engineering Structures*, vol. 49, no. 0, pp. 866-75.

Abdel-Haq, A.H. 1987, 'Analysis and design of box culverts', Ohio University, Ohio.

Abdel-Karim, A.M., Tadros, M.K. & Benak, J.V. 1990, 'Live load distribution on concrete box culverts', *Transportation Research Record: Journal of the Transportation Research Board*, vol. 1288, pp. 136-51.

Abdul-Qader, S.S. 2008, 'A generalized yield criterion for orthotropically RC rectangular slabs under combined bending and membrane action

', University of Technology.

Abolmaali, A. & Garg, A. 2008, 'Effect of wheel live load on shear behavior of precast reinforced concrete box culverts', *Journal of Bridge Engineering*, vol. 13, no. 1, pp. 93-9.

Abu, A., K., Burgess, I.W. & Plank, R.J. 2013, 'Tensile membrane action of thin slabs exposed to thermal gradients', *Journal of Engineering Mechanics*, vol. 139, no. 11, pp. 1497-507.

Acharya, R. 2012, 'Improved load distribution for load rating of low-fill box structures', University of Kansas, Lawrence, Kansas.

ACI 318 1989, *Building Code Requirements for Reinforced* American Concrete Institute, Detroit.

ACI ITG-3-04 2004, *Report on Bridge Decks Free of Steel Reinforcement*, ACI ITG-3-04, American Concrete Institute, Farmington Hills, Mich.

Ahmed, A.O.M. & Alarabi, E. 2011, 'Development formulation for structural design of concrete box culverts', *Practice Periodical on Structural Design and Construction*, vol. 16, no. 2, pp. 48-55.

Al-Hassani 1978, ' Behaviour of axially restrained concrete slabs.', University of London, London,England.

AL-Hassani , H.M., Husain, H.M. & AL-Badri, S.S.A.Q. 2009, 'Experimental tests on orthotropically RC rectangular slabs having various restrained edges and subjected to uniform load', *Eng. & Tech*, vol. 27, no. 5, pp. 913-29.

Al-Kamyani, Z., Figueiredo, F.P., Hu, H., Guadagnini, M. & Pilakoutas, K. 2018 'Shrinkage and flexural behaviour of free and restrained hybrid steel fibre reinforced concrete'. *Construction and Building Materials*, vol. 189, pp. 1007-1018.

Alberti, M.G., Enfedaque, A., Gálvez, J.C., Cánovas, M.F. & Osorio, I.R. 2014, 'Polyolefin fiber-reinforced concrete enhanced with steel-hooked fibers in low proportions', *Materials & Design*, vol. 60, pp. 57-65.

Alkhrdaji, T. & Nanni, A. 2001, 'Design, construction, and field-testing of an RC box culvert bridge reinforced with glass FRP bars', paper presented to the *Fibre Reinforced Plastic For Reinforced Cncrete Structure,* Cambridge, England, July 2001.

Amin, A., Foster, S.J. & Muttoni, A. 2014, 'Derivation of the σ-w relationship for SFRC from prism bending tests', *Structural Concrete*.

Amin, A., Foster, S.J. & Watts, M. 2015, 'Modelling the tension stiffening effect in SFR-RC', *Magazine of Concrete Research*.

AS1012.9 1999, 'Methods of testing concrete - Determination of the compressive strength of concrete specimens', in S. Australia (ed.).

AS1012.17 1997, *Methods of testing concrete: Determination of the static chord modulus of elasticity and Poisson's ratio*

AS1597.1 2010, 'Precast reinforced concrete box culverts - Small culverts (not exceeding 1200 mm span and 1200 mm height)', Australian standards, Sydney, Australia.

AS1597.2 2013, 'Precast reinforced concrete box culverts - Large culverts (exceeding 1200 mm span or 1200 mm height and up to and including 4200 mm span and 4200 mm height)', Australian standard, Sydney, Australia.

AS3600 2009, 'Concrete Structures', in Australian Standard (ed.).

AS5100 2004, *Australian Standard, Bridge Design*.

AS5100.2 2004, 'Bridge design - Part2: Design load', Austrarial standard, Sydney, Australia.

AS5100.5 2004, 'Bridge Design, Part 5: Concrete, Standards Australia', Australian Standard.

ASTM C1433 2004, 'Standard specification for precast reinforced concrete box sections for culverts, storm drains, and sewers', in A.S.f.T.a. Materials (ed.).

ASTM C1577 2005, 'Standard specification for precast reinforced concrete box sections for culverts, storm drains, and sewers designed according to AASHTO LRFD', in A.S.f.T.a. Materials (ed.).

ASTM, I. 2005, 'Standard test method for flexural performance of fiber-reinforced concrete (using beam with third-point loading)', ASTM International, West Conshohocken, PA, US.

ASTM Standard 2005, 'C1609/C1609M,(2005)', *Standard Test Method for Flexural Performance of Fiber-Reinforced Concrete (Using Beam With Third-Point Loading),” ASTM International, West Conshohocken, PA*.

Ataei, A., Bradford, M.A. & Liu, X. 2016, 'Experimental study of flush end plate beam-to-column composite joints with precast slabs and deconstructable bolted shear connectors', *Structures*, vol. 7, no. August, pp. 43-58.

Bae, H.U., Oliva, M.G. & Bank, L.C. 2011, 'Reinforcement-free decks using modified strut-and-tie model', *ACI Structural Journal* vol. 108, no. 5, pp. 562-71.

Bailey, C.G. 2001, 'Membrane action of unrestrained lightly reinforced concrete slabs at large displacements', *Engineering Structures* vol. 23, pp. 470-83.

Bailey, C.G., Toh, W.S. & Chan, B.M. 2008, 'Simplified and advanced analysis of membrane action of concrete slabs', *ACI Structural Journal*, vol. 105, pp. 30-40.

Bakht, B. & Agarwal, A.C. 1995, 'Deck slabs of skew girder bridges', *Canadian Journal of Civil Engineering*, vol. 22, no. 3, pp. 514-23.

Bakht, B., Al-Bazi, G., Banthia, N., Cheung, M., Erki, M.A., Faoro, M., Machida, A., Mufti, A.A., Neale, K.W. & Tadros, G. 2000, 'Canadian bridge design code provisions for fiber-reinforced structures', *JOURNAL OF COMPOSITES FOR CONSTRUCTION* vol. 4, no. 1, pp. 3-15.

Bakht, B. & Lam, C. 2000, 'Behavior of transverse confining systems for steel-free deck slabs', *ASCE, Journal of Bridge Engineering*, pp. 139-47.

Bakht, B. & Mufti, A.A. 1996, 'FRC deck slabs without tensile reinforcement', *Concrete International*, vol. 18, no. 2, pp. 50-5.

Bakht, B. & Mufti, A.A. 1998, ' Five steel-free bridge deck slabs in Canada', *Structural Engineering International, IABSE*, vol. 8, no. 3, pp. 196-200.

Bakht, B., Mufti, A.A. & Jaeger, L.G. 1998, ' Design provision for steel-free deck slabs.', paper presented to the *Proceeding, Fifth International Conference on Short and Medium Span Bridges*, , Calgary,

Canada, , October, 1998.

Bakht, B., Mufti, A.A. & Tadros, G. 2002, 'Transverse confinement of deck slabs by metallic stay-in-place forms', *4th Structural Specialty Conference of the Canadian Society for Civil Engineering*.

Batchelor, B.V., Hewitt, B.E., Csagoly, P. & Holowka, M. 1978, 'Investigation of the ultimate strength of deck slabs of composite steel concrete bridge ', *TRR664* pp. 162-70.

Batchelor, B.V. & Tissington, I.R. 1976, 'Shear strength of two-way bridge slabs', *ASCE Journal of Structural Engineering*.

Bazant, Z.P. & Oh, B.H. 1983, 'Crack band theory for fracture of concrete', *Materiaux et Constructions, Materials and Structures*, vol. 16, no. 93, pp. 155-77.

BD 81/02 2002, 'Use of compressive membrane action in bridge decks', in U.H. Agency (ed.), *Design Manual for Roads and Bridges, V. 3, Section 4, Part 20*, p. 20 pp.

Bednář, J., Wald, F., Vodička, J. & Kohoutková, A. 2013, 'Experiments on membrane action of composite floors with steel fibre reinforced concrete slab exposed to fire', *Fire Safety Journal*, vol. 59, pp. 111-21.

Beeby, A.W. & Fathibitaraf, F. 2001, 'Membrane effect in the reinforced concrete frames—a proposal for change in the design of frames structures', *Engineering Structures*, vol. 23, no. 1, pp. 82-93.

Bekaert 2012, 'Brochure of Dramix 5D 4D 3D', in T.B. Corporation (ed.).

Belletti, B., Vitulli, F. & Walraven, J.C. 2014, 'Compressive membrane action in confined RC and SFRC circular slabs', *Computational Modelling of Concrete Structures - Proceedings of EURO-C 2014*, vol. 2, pp. 807-18.

Bennett, R.M., Wood, S.M., Drumm, E.C. & Rainwater, N.R. 2005, 'Vertical loads on concrete box culverts under high embankments', *Journal of Bridge Engineering*, vol. 10, no. 6, pp. 643-9.

Birke, H. 1975, *Kupoleffekt vid Betongplattor.*, 108 (in Swedish). Institutionen for Byggnadsstatik, Royal Technical University, Stockholm, Sweden.

Blanco, A., Cavalaro, S., De la Fuente, A., Grünewald, S., Blom, C.B.M. & Walraven, J.C. 2014, 'Application of FRC constitutive models to modelling of slabs', *Materials and Structures*.

Braestrup, M.W. 1979, 'Punching Shear in Concrete Slabs', paper presented to the *IABSE Colloquium,Plasticity in Reinforced Concrete*, Copenhagen, 28, Oct. 1978.

Braestrup, M.W. 1980, 'Dome effect in RC slabs: rigid-plastic analysis,' *ASCE, Journal of structural engineering*, vol. 106, no. ST6, pp. 1237-53.

Braestrup, M.W. & Morley, C.T. 1980, 'Dome effect in RC slabs: elastic-plastic analysis', *ASCE, Journal of structural engineering*, vol. 106, pp. 1255-63.

Bridge design code Northern Ireland 1986, 'Design of M-Beam Bridge Decks', *Bridge Design Code"N.I, Roads Service Headquarters*, vol. Mendment No 3, Department of Regional Development for Northern Ireland, Northern Ireland, pp. 11.1-.5.

Brotchie, J.F. & Holley, M.J. 1971, 'Membrane action in slabs, cracking, deflection, and ultimate load of concrete slab systems', *ACI Special Publication SP-30,*.

BS 5400 1978, *Steel concrete and composite bridges,* , Standards Institution, London, British

BS 8110 1985, *Code of Practice for Design and Construction,*, British Standards Institution, London.

Bursi, O.S. & Jaspart, J.P. 1998, 'Benchmarks for finite element modeling of bolted steel connections', *Journal of Constructional Steel Research*, vol. 43, no. 1-3, pp. 17-42.

Carreira, D.J. & Chu, K.H. 1985, 'Stress-strain relationship for plain concrete in compression', *ACI Structural Journal*, vol. 82, no. 6, pp. 797-804.

CEB-FIP 1993, *Model code 1990: Design code,* Thomas Telford, London.

Cervenka, V., Cervenka, J. & Pukl, R. 2002, 'ATENA - A tool for engineering analysis of fracture in concrete', *Sadhana - Academy Proceedings in Engineering Sciences*, vol. 27, no. 4, pp. 485-92.

CHBDC 1996, *Canadian Highway Bridge Design Code.*

, Canadian Standard Association,, Raxdale, Ontario, Canada.

CHBDC 2000, *Canadian Highway Bridge Design Code,* Toronto, Ontario, Canada.

CHBDC 2006, 'Canadian Highway Bridge Design Code', Canadian Standard Association, Ontario, Canada.

CHBDC 2010, *Canadian highway bridge design code*, Canadian Standards Association, Toronto.Canada.

Chelliat, D. 1992, 'Experimental and numerical analysis of a pipe arch culvert subjected to exceptional live load', Ohio University, Athens, Ohio.

Chen, B., Zheng, J. & Han, J. 2010, 'Experimental study and numerical simulation on concrete box culverts in trenches', *Journal of Performance of Constructed Facilities*, vol. 24, no. 3, pp. 223-34.

Choi, H. & Kim, J. 2011, 'Progressive collapse-resisting capacity of RC beam–column sub-assemblage', *Magazine of Concrete Research*, vol. 63, no. 4, pp. 297-310.

Christiansen, K.P. 1963, ' The effect of membrane stresses on the ultimate strength of the interior panel in a reinforced concrete slab. ', *Structural Engineer*, vol. 41, no. 8, pp. 261-5.

Christiansen, K.P. & Fredriksen, V.T. 1983, 'Experimental investigation of rectangular concrete slabs with horizontal restraints', *Materials and Structures*, vol. 16, pp. 179-92.

Concrete Society 1999, *Design guidance for high strength concrete*

Report for the Concrete Society Working Party.

Cook, R.A. & Bloomquist, D. 2002, *Evaluation of precast box culvert systems*, 49104504857 12, University of Florida, Gainesville, Florida, USA.

Dasgupta, A. & Sengupta, B. 1991, 'Large-scale model test on square box culvert backfilled with sand', *ASCE, Journal of Geotechnical Engineering*, vol. 117, no. 1, pp. 156-61.

Datta, T.K. & Ramesh, C.K. 1975, 'Some experimental studies on a reinforced concrete slab-beam system', *Magazine of Concrete Research*, vol. 27, pp. 111-20.

Department of Regional Development for Northern Ireland 1986, 'Design of M-Beam Bridge Decks', *Bridge Design Code"N.I, Roads Service Headquarters*, vol. Mendment No 3, Northern Ireland, pp. 11.1-.5.

Desayi, P. & Kulkarni, A.B. 1977, ' Load-deflection behaviour of restrained reinforced concrete slabs ', *ASCE, Journal of structural engineering*, vol. 103, pp. 405-19.

Edalatmanesh, R. & Newhook, J.P. 2012, 'Behavior of externally restrained noncomposite concrete bridge deck panels', *ACI Structural Journal*, vol. 109, no. 2, pp. 161-70.

Edalatmanesh, R. & Newhook, J.P. 2013, 'Investigation of fatigue damage in steel-free bridge decks with application to structural monitoring', *ACI Structural Journal*, vol. 110, no. 4, pp. 557-64.

Einsfeld, R.A., Martha, L.F. & Bitttenourt , T.N. 2000, 'Combination of smeared and discrete approaches with the use of interface elements. ', *European Congress on Computational Methods in Applied Sciences and Engineering*

El-Gamal, S., El-Salakawy, E. & Benmokrane, B. 2005, 'Behavior of concrete bridge deck slabs reinforced with fiber-reinforced polymer bars under concentrated loads', *ACI Struct. J.*, vol. 102, p. 727.

El-Ragaby, A., El-Salakawy, E. & Benmokrane, B. 2007, 'Fatigue life evaluation of concrete bridge deck slabs reinforced with glass FRP composite bars', *J. Compos. Constr.*, p. 258.

Elgabbas, F., Ahmed, E.A. & Benmokrane, B. 2016, 'Experimental testing of concrete bridge-deck slabs reinforced with Basalt-FRP reinforcing bars under concentrated loads', *Journal of Bridge Engineering*, vol. 21, no. 7.

EN 1992-1-1 2004, 'Design of concrete structures - Part 1-1 : General rules and rules for buildings', in E.c.f. standardization (ed.).

European Committee for Standardization 2004, 'Eurocode 4: Design of composite steel and concrete structures -part 1-1: General rules and rules for buildings', in L.B.S. Institution (ed.)vol. EVN 1994-1-1.

Eyre and Kemp, K. 1984, ' A graphical solution predicting increase in strength of slabs. ', *Magazine of Concrete Research*, vol. 35, pp. 151-6.

Eyre, J., R 1990, 'FLOW RULE IN ELASTICALLY RESTRAINED ONE-WAY SPANNING RC SLABS. ', *Journal of Structural Division, ASCE,*, vol. 116, pp. 3251-67.

Eyre, J., R 2006, 'Membrane action in ground-bearing concrete slabs', *ACI Structure and Building*, vol. 159, no. SB3, pp. 153-63.

Eyre, J., R 2007, 'Surround stiffness to membrane action in concrete slabs', *Magazine of Concrete Research*, vol. 59, no. 2, pp. 107-19.

Eyre, J.R. 1997, 'Direct assessment of safe strengths of RC slabs under membrane action', *ASCE*, *Journal of structural engineering*, vol. 123, no. 10, pp. 1331-8.

Eyre, J.R. & Kemp, K.O. 1994, 'In-plane stiffness of reinforced concrete slabs under compressive membrane action. ', *Magazine of Concrete Research*, vol. 46, pp. 67-77.

Famiyesin , O.R.a.H.K.M.A. 1998, 'Optimised design charts for fully restrained slabs By FE predictions', *ASCE Journal of Structural Engineering* vol. 1.124, no. 5, pp. 560-9.

Fang , I.K., Lee, J.H. & Chen, C.R. 1994, 'Behaviour of partially restrained concrete slabs Under concentrated load ', *ACI Structural Journal*, vol. 91, no. 2, p. 133—9.

Fang, I.K., Worley ,J.and Burns 1990, 'Behaviour of isotropic RC bridge decks on steel Girders ', *ASCE Journal of Structural engineering*, vol. 116, no. 3, pp. 659-77.

Fang, J.A.W., N. H. Burns, and R. E. Klingner 1986, *BEHAVIOR OF ONTARIO-TYPE BRIDGE DECKS ON STEEL GIRDERS*, Center for Transportation Research The University of Texas at Austin Austin, Texas, Austin Austin, Texas.

Farhangvesali, N., Valipour, H., Samali, B. & Foster, S. 2013, 'Development of arching action in longitudinally-restrained reinforced concrete beams', *Construction and Building Materials*, vol. 47, no. October, pp. 7-19.

FIB-Model Code 2010, *fib-Model Code 2010 – final draft, fib Bulletin*

Foster, S.J. 2009, 'The application of steel-fibres as concrete reinforcement in Australia: From material to structure', *Materials and Structures/Materiaux et Constructions*, vol. 42, no. 9, pp. 1209-20.

Frosch, R.J. 1999, ' Another look at cracking and crack control in reinforced concrete', *ACI Structural Journal*, vol. 96, no. 3, pp. 437–42.

Fujiyama, C. & Maekawa, K. 2009, *A numerical analysis of damage mechanism of bridge deck slab under high cycle moving load*.

García-Taengua, E., Martí-Vargas, J.R. & Serna, P. 2014, 'Splitting of concrete cover in steel fiber reinforced concrete: Semi-empirical modeling and minimum confinement requirements', *Construction and Building Materials*, vol. 66, pp. 743-51.

Garg, A. & Abolmaali, A. 2009, 'Finite-Element modeling and analysis of reinforced concrete box culverts', *Journal of Transportation Engineering*, vol. 135, no. 3, pp. 121-8.

Garg, A.K. 2007, 'Experimental and finite element-based investigations of shear behavior in reinforced concrete box culverts', Ph.D.dissertation thesis, university of Texas at Arlington, Arlington,Texas.

Garg, A.K., Abolmaali, A. & Fernandez, R. 2007, 'Experimental investigation of shear capacity of precast reinforced concrete box culverts', *Journal of Bridge Engineering*, vol. 12, no. 4, pp. 511-7.

Ghani Razaqpur, A., Shedid, M. & Nofal, M. 2013, 'Experimental investigation of load distribution in a composite girder bridge at elastic versus inelastic states', *Engineering Structures* vol. 49, pp. 707-18.

Ghodoosi, F., Bagchiand, A. & Zayed, T. 2016, 'Reliability-based condition assessment of an externally restrained bridge deck system considering uncertainties in key design parameters', *ASCE Journal of Perform. Constr. Facil*, vol. 30, no. 1, pp. 1-10.

Graddy, J.C., Kim, J., Whitt, J.H., Burns, N.H. & Klingner, R.E. 2002, 'Punching-shear behavior of bridge decks under fatigue loading', *Structural Journal*, vol. 99, no. 3.

Guice, L.K. 1986, *Behavior of partially restrained reinforced concrete slabs*, SL-86-32, U.S. Army Engineer Waterways Experiment Station, Vicksburg, MS.

Guice, L.K. & Rhomberg, E.J. 1988, 'Membrane action in partially restrained slabs', *ACI Structural Journal*, vol. 85, no. 4, pp. 365-73.

Guice, L.K., Slawson, T.R. & Rhomberg, E.J. 1986, 'Membrane analysis of flat plate slabs', *ACI Structural Journal*, vol. 86, no. 10, pp. 83-92.

Guice, L.K., Slawson, T.R. & Rhomberg, E.J. 1989, 'Membrane analysis of flat plate slabs', *ACI Structural Journal*, vol. 86, no. 1, pp. 83-92.

Gvozdev, A.A. 1939, 'Comments on clause 33 of the Russian code for reinforced concrete', *Stroitelnaya Promyshlennest*, vol. 17, no. 3, pp. 51-8.

Haido, J.H., Bakar, B.A., Abdul-Razzak, A.A., Jayaprakash, J. & Choong, K.K. 2011, 'Simulation of dynamic response for steel fibrous concrete members using new material modeling', *Construction and Building Materials*, vol. 25, no. 3, pp. 1407-18.

Hao, Y. & Hao, H. 2013, 'Dynamic compressive behaviour of spiral steel fibre reinforced concrete in split Hopkinson pressure bar tests', *Construction and Building Materials*, vol. 48, no. 0, pp. 521-32.

Hashin, Z. 1980, 'Failure Criteria for Unidirectional Fiber Composites', *ASME Journal of Applied Mechanics*, vol. 47, no. 2, pp. 329-34.

Hassan, A., Kawakami, M., Niitani, K. & Yoshioka, T. 2002, 'An experimental investigation of steel-free deck slabs', *Can. J. Civ. Eng.*, vol. 29, pp. 831-41.

Hayes, B. 1968, 'Allowing for membrane action in the plastic analysis of rectangular reinfroced concrete slabs', *Magazine of Concrete Research*, vol. 20, no. 65, pp. 205-12.

Hewitt, B.E. & Batchelor, B.V. 1975, 'Punching shear strength of restrained slabs', *J. Struct. Div.*, vol. 101, p. 1837.

Highway bridge design code 1979, *Highway bridge design code,* , Ontario Ministry of Transportation and Communications, Toronto, Ontario.

Hon, A., Taplin, G. & Al-Mahaidi, R. 2001, 'Compressive membrane action in reinforced concrete one way slabs. ', *The Eighth East Asia-Pacific Conference on Structural Engineering and Construction*, vol. Paper No 1276, Nangyang Technological University, , Singapore.

Hon, A., Taplin, G. & Al-Mahaidi, R.S. 2005, 'Strength of reinforced concrete bridge decks under compressive membrane action', *ACI, Structural Journal*, vol. 102, no. 3, pp. 393-403.

Hordijk, D.A. 1991, 'Local approach to fatigue of concrete', Delft University of Technology, Delft, Netherlands.

Hossain, K.M.A. & Famiyesin, O.O.R. 1996a, *Design charts for fully clamped reinforced concrete slabs*, Department of Engineering, University of Aberdeen, Aberdeen, U.K., Res. Rep. No. EG-SE96-8.

Hossain, K.M.A. & Famiyesin, O.O.R. 1996b, *Finite element simulation of isotropically reinforced concrete slabs*, Department of Engineering, University of Aberdeen, Aberdeen,U.K., Rep. No. EG-SE96-I.

Hu, H., Papastergiou, P., Angelakopoulos, H., Guadagnini, M. & Pilakoutas, K. 2018 Mechanical properties of SFRC using blended Recycled Tyre Steel Cords (RTSC) and Recycled Tyre Steel Fibres (RTSF). *Construction and Building Materials*, vol. 187, pp. 553-564.

Huang, Z., Burgess, I.W. & Plank, R.J. 2003a, 'Modeling membrane action of concrete slabs in composite buildings in fire. I: Theoretical development', *J. Struct. Eng.*, vol. 129, p. 1093.

Huang, Z., Burgess, I.W. & Plank, R.J. 2003b, 'Modeling membrane action of concrete slabs in composite buildings in fire. II: Validations', *J. Struct. Eng.*, vol. 129, p. 1103.

I.K. Fang, J.A.W., N. H. Burns, and R. E. Klingner 1986, *BEHAVIOR OF ONTARIO-TYPE BRIDGE DECKS ON STEEL GIRDERS*, Center for Transportation Research The University of Texas at Austin Austin, Texas, Austin Austin, Texas.

Jacobson, A. 1967, 'Membrane flexural modes of restrained slabs ', *Structural Division, ASCE*, vol. 93, pp. 85-112.

Jayawickrama, P.W., Lawson, W.D. & Wood, T.A. 2011, *Evaluation of soil properties for culvert load rating applications*, ASCE, Dallas, Texas, United States, pp. 2659-68.

Johansen, K.W. 1943, 'Yield-line formulae for slabs', *London: Cement and Concrete Association*.

Kaïkea, A., Achoura, D., Duplan, F. & Rizzuti, L. 2014, 'Effect of mineral admixtures and steel fiber volume contents on the behavior of high performance fiber reinforced concrete', *Materials & Design*, vol. 63, pp. 493-9.

Karr, P.H., Hanson, N.W. & Capell, H.T. 1987, *Stress-strain characteristics of high-strength concrete.* , ACI, Portland Cement Association Report, Detroit, Mich. USA,.

Kemp, K.O. 1967, 'Yield of a square reinforced concrete slab on simple supports, allowing for membrane forces', *The Struct. Engr*, vol. 45, no. 7, pp. 235-40.

Kim, K. & Yoo, C. 2005, 'Design loading on deeply buried box culverts', *Journal of Geotechnical and Geoenvironmental Engineering*, vol. 131, no. 1, pp. 20-7.

Kinnunen, S. & Nylander, H. 1960, *Punching of concrete slabs without shear reinforcement*, vol. No. 158, Transactions of the Royal Institute of Technology, Stockholm, Sweden.

Kirkpatrick , J., Long ,A.E .and Thompson ,A 1982, 'Load distribution characteristics of M beam bridge decks', *Struct. Eng.*, vol. 60 b, no. 2, pp. 34-43.

Kirkpatrick, J., Long, A.E. & Rankin, G.I.B. 1986, 'The influence of compressive membrane action on serviceability and slab bridge decks

', *Structural Engineer* vol. Vo164b, no. No.1 ,Mar 1986 pp. 6-9.

Kirkpatrick , J., Long, A.E. & Thompson , A. 1984, 'Load distribution characteristics of Spaced M-beam bridge deck', *Structural Engineer* vol. Vo1 .62b, no. 4, p. 68—88.

Kirkpatrick, J., Rankin, G.I.B. & Long, A.E. 1984, 'Strength evaluation of M-beam bridge deck slabs', *Structural Engineer,* vol. 62B, no. 3, pp. 60-8.

Klowak, C., Memon, A.H. & Mufti, A.A. 2006, 'Static and fatigue investigation of second generation steel-free bridge decks', *Cement and Concrete Composites*, vol. 28, no. 10, pp. 890-7.

Klowak, C., Mufti, A.A. & Bakht, B. 2014, 'Examining the presence of arching action in edge-stiffened bridge deck cantilever overhangs subjected to a wheel load', *Journal of Composites for Construction*, vol. 18, no. 3.

Kuang, J.S. & Morley, C.T. 1992, 'Punching shear behavior of restrained reinforced concrete slabs', *ACI Structural Journal*, vol. 89, no. 1, pp. 13-9.

Kuang, J.S. & Morley , C.T. 1993, 'A plasticity model for punching shear of laterally restrained slabs with compressive membrane action', *Journal of Mechanic and Science* vol. 35, no. 5, pp. 371-85.

Kupfer, H., Hilsdorf, H.K. & Rusch, H. 1969, 'Behaviour of concrete under biaxial stress', *ACI Journal*, vol. 66, no. 8, pp. 656-66.

Kwak, Y.K., Eberhard, M.O., Kim, W.S. & Kim, J. 2002, 'Shear strength of steel fiber-reinforced concrete beams without stirrups', *ACI Structural Journal*, vol. 99, no. 4, pp. 530-8.

Kwon, G., Engelhardt, M.D. & Klinger, R.E. 2011, 'Experimental behavior of bridge beams retrofitted with post-installed shear connectors', *ASCE, Journal of Bridge Engineering*, vol. 16, no. 4, pp. 536-45.

Lahlouh, E.H. & Waldron, P. 1992, 'Membrane action in one-way slab strips', *Proceedings of the Institution of Civil Engineers, Structs & Bldgs*, vol. 94, no. 4, pp. 419-28.

Lawson, W.D., Wood, T.A., Newhouse, C.D. & Jayawickrama, P.W. 2010, *Evaluating existing culverts for load capacity allowing for soil structure interaction*, FHWA/TX-10/0-5849-01, TechMRT: Multidisciplinary Research in Transportation, Texas Tech University, Lubbock, TX.

Lee, J. & Fenves, G.L. 1998, 'Plastic-damage concrete model for earthquake analysis of dams', *Earthquake Engineering & Structural Dynamics*, vol. 27, no. 9, pp. 937-56.

Liu, X., Bradford, M.A., Chen, Q.J. & Ban, H. 2016, 'Finite element modelling of steel–concrete composite beams with high- strength friction-grip bolt shear connectors', vol. 108, no. January, pp. 54-65.

Liu, X., Bradford, M.A. & Lee, M.S.S. 2014, 'Behavior of high-strength friction-grip bolted shear connectors in sustainable composite beams', *ASCE, Journal of Structural Engineering (Published online)*.

Liu, X., Bradford, M.A. & Lee, M.S.S. 2015, 'Behaviour of high-strength friction-grip bolted shear connectors in sustainable composite beams. Journal of Structural Engineering', *ASCE, Journal of Structural Engineering*, vol. 141, no. 6.

Long, A.E. 1975, 'A two-phase approach to the prediction of the punching strength of slabs', *Journal Proceedings*, vol. 72, no. 2.

Luccioni, B., Ruano, G., Isla, F., Zerbino, R. & Giaccio, G. 2012, 'A simple approach to model SFRC', *Construction and Building Materials*, vol. 37, pp. 111-24.

Makhlouf, M.H. & Malhas, F.A. 1996, ' The effect of thick concrete cover on the maximum flexural crack width under service load', *ACI Structural Journal*, vol. 93, no. 3, pp. 257–65.

Marti, P., Alvarez, M., Kaufmann, W. & Sigrist, V. 1998, 'Tension chord model for strutural concrete', *Structural Engineering International* vol. 8, no. 4, pp. 287-98.

Massonet, C. 1968, 'General theory of elastic-plastic membrane plates. ', paper presented to the *Conference concerning Engineering Plasticity*, University of Cambridge.

Matsui, S. 1994, 'New weigh method of axle loads of vehicles and axle weigh characteristics of truck in Japan', paper presented to the *4th international conference on short and medium span bridges*, Halifax.

Maximos, H., Erdogmus, E. & Tadros, M.K. 2010, 'Fatigue evaluation for reinforced concrete box culverts', *ACI Structural Journal*, vol. 107, no. 1, pp. 13-20.

Maya, L.F., Ruiz, M.F., Muttoni, A. & Foster, S.J. 2012, 'Punching shear strength of steel fibre reinforced concrete slabs', *Engineering Structures*, vol. 40, no. 0, pp. 83-94.

McDowell, E.L., Mckee, K.E. & Sevin, E. 1956, 'Arching action theory of masonry walls', *J. Struct. Div. ASCE*, vol. 82(ST2).

McGrath, T.J., Liepins, A.A., Beaver, J.L. & Strohman, B.P. 2004, *Live load distribution width for reinforced concrete box culverts*, Pennsylvania Department of Transportation.

McGrath, T.J. & Mastroianni, E.P. 2002, 'Finite element modeling of reinforced concrete arch under live load ', *Transportation Research Record: Journal of the Transportation Research Board*, vol. 1814, pp. 203-10.

Meda, A., Minelli, F., Plizzari, G.A. & Riva, P. 2005, 'Shear behaviour of steel fibre reinforced concrete beams', *Materials and Structures/Materiaux et Constructions*, vol. 38, no. 277, pp. 343-51.

Michels, J., Waldmann, D., Maas, S. & Zürbes, A. 2012, 'Steel fibers as only reinforcement for flat slab construction - Experimental investigation and design', *Construction and Building Materials*, vol. 26, no. 1, pp. 145-55.

Mohammadi, Y., Carkon-Azad, R., Singh, S.P. & Kaushik, S.K. 2009, 'Impact resistance of steel fibrous concrete containing fibres of mixed aspect ratio', *Construction and Building Materials*, vol. 23, no. 1, pp. 183-9.

Morley, C.T. 1967, 'Yield line theory for reinforced concrete slabs at moderately large deflections.', *Magazine of Concrete Research*, vol. 19, pp. 211-21.

Morley, C.T. & Olonisakin, A.A. 1995, 'The galerkin method applied to compressive membrane action', *Developments in Computational Techniques for Structural Engineering* ed. B.H.V. Topping, Civil-Comp Press, Edinburgh, UK, pp. 15-20.

Moy, S.J. & Mayfield, B. 1972, ' Load deflection characteristics of reinforced concrete slabs', *Magazine of Concrete Research*, vol. 24, no. 81, pp. 209-18.

Mufti, A.A., Bakht, B. & Jaeger, L.G. 1991, 'Fibre RC deck slabs with diminished steel reinforcement', *BRIDGES: Interaction between construction technology and design*, vol. 64, pp. 388-9.

Mufti, A.A., Bakht, B. & Jaeger, L.G. 1993, 'Moments in deck slabs due to cantilever loads', *Struct. Eng.*, vol. 119, no. 6, pp. 1761-77.

Mufti, A.A., Bakht, B. & Jaeger, L.G. 2008, 'Recent advances in bridge engineering,' vol. Research, Scarborough, JMBT Structures

Mufti, A.A., Bakht, B. & Newhook, J.P. 2004, 'Precast concrete decks for slab-on-girder systems: A new approach', *ACI Structural Journal*, vol. 101, no. 3, pp. 395-402.

Mufti, A.A., Jaeger, L.G. & Bakht, B. 1997, 'Field performance of Steel-free Deck slab of Girder bridges.', *Proceedings, US-Canada-Europe Workshop on Bridge Engineering*, Zurich, Switzerland, pp. 236-46.

Mufti, A.A., Jaeger, L.G., Bakht, B. & Wegner, L.D. 1993, 'Experimental investigation of FRC slabs without internal steel reinforcement', *Canadian Journal of Civil Engineering*, vol. 20, no. 3, pp. 398-406.

Mufti, A.A., Memon, A.H., Bakht, B. & Banthia, N. 2002, 'Fatigue investigation of the steel-free bridge deck slabs', *Special Publication*, vol. 206.

Mufti, A.A. & Newhook, J.P. 1998, 'Punching shear strength of restrained concrete bridge deck slabs', *ACI Structural Journal*, vol. 95, no. 4, pp. 375-81.

Mufti, A.A. & Newhook, J.P. 1999, 'On the use of steel-free concrete bridge decks in continuous span bridges', *Canadian Journal of Civil Engineering*, vol. 26, no. 5, pp. 667-72.

Mufti, A.A., Newhook, J.P. & Jalali, S.J. 1999, ' Investigation of the flange splitting stresses in composite bridge beams. ', *General Conference, Structural Engineering*, vol. 1, Canadian Society for Civil Engineering Canada, pp. 41-50.

Mufti, A.A., Newhook, J.P. & Tadros, G. 1996, 'Deformability versus ductility in concrete beams with FRP reinforcement', *Proceeding of the second international conference on advanced composite materials in bridges and structures*, Montreal, Quebec, pp. 189-99.

Natário, F., Ruiz, M.F. & Muttoni, A. 2015, 'Experimental investigation on fatigue of concrete cantilever bridge deck slabs subjected to concentrated loads', *Engineering Structures*, vol. 89, pp. 191-203.

Neto, B.N.M., Barros, J.A.O. & Melo, G.S.S.A. 2013, 'A model for the prediction of the punching resistance of steel fibre reinforced concrete slabs centrically loaded', *Construction and Building Materials*, vol. 46, pp. 211-23.

Neto, B.N.M., Barros, J.A.O. & Melo, G.S.S.A. 2014, 'Model to simulate the contribution of fiber reinforcement for the punching resistance of RC slabs', *Journal of Materials in Civil Engineering*, vol. 26, no. 7.

Newhook, J., Mufti, A., Bakht, B. & Tadros, G. 2002, 'Application of steel-free concrete deck slabs to rehabilitation projects', *Rehabilitating and Repairing the Buildings and Bridges of Americas*, pp. 129-40.

Newhook, J.P., Jaeger, L.G. & Mufti, A.A. 1996, 'Steel-free concrete deck- the Salmon River project – design and construction', *1 st Structural Speciality Conference*, Canadian Society for Civil Engineering, Edmonton, Alberta, Canada., pp. 203-14.

Newhook, J.P., John, P. & Mufti, A.A. 1996, 'Reinforcing steel-free concrete deck slab for the Salmon River bridge', *Concrete International*, vol. 18, no. 6, pp. 30-4.

Newhook, J.P. & Mufti, A.A. 1995, 'Rational method for predicting the behavior of laterally restrained concrete bridge deck without internal reinforcement', paper presented to the *CSCE annual conference*, Ottawa Canada.

Newhook, J.P., Mufti, A.A. & Jaeger, L.G. 1996, 'Steel-free concrete deck- the Salmon River project – experimental verification. ', *1st Structural speciality*, Canadian Society for Civil Engineering,, Edmonton, Alberta, Canada

pp. 123-33.

Nielsen, M.P. 1984, 'Limit Analysis and Concrete Plasticity

', *Prentice Hall*, pp. 364-77.

Ockleston, A.J. 1958, 'Arching action in reinforced concrete slabs', *Structural Engineer*, vol. 36, no. 6, pp. 197-201.

OHBDC 1983, *Ontario Highway Bridge Design Code*, Ontario Ministry of Transportation and Communications.

OHBDC 1995, *Canadian Highway Bridge Design Code*, Ministry of Transportation of Ontario, , Ontario, Canada.

Orton, S., Loehr, E., Boeckmann, A. & Havens, G. 2013, *Live load effect in reinforced concrete box culverts under soil fill*, cmr14-009, University of Missouri, Columbia, US.

Orton, S.L. 2007, 'Development of a CFRP system to provide continuity in existing reinforced concrete buildings vulnerable to progressive collapse', University of Texas at Austin, Austin, TX.

Ouyang, C.S., W. 1987, ' RC Rectabgular Slabs With Edge Restraints', *Journal of Structural Division, ASCE,*, no. 113, pp. 2146-65.

Pantelides, C.P., Garfield, T.T., Richins, W.D., Larson, T.K. & Blakeley, J.E. 2014, 'Reinforced concrete and fiber reinforced concrete panels subjected to blast detonations and post-blast static tests', *Engineering Structures*, vol. 76, pp. 24-33.

Park, R. 1964 -a, 'The ultimate strength and long term behaviour of uniformly loaded two-way concrete slabs with partial lateral restraint at all edges', *Magazine of Concrete Research*, vol. 16, no. 48, pp. 139-52.

Park, R. 1964 -b, 'Ultimate strength of rectangular concrete slabs under short-term uniformloading with edges resrained against lateral movement', *Proceedings of the Institution of Civil Engineers*, vol. 28, pp. 125-50.

Park, R. 1965, 'The lateral stiffness and strength required to ensure membrane action at the ultimate load of a reinforced concrete slab and beam floor.', *Magazine of Concrete Research*.

Park, R. 1971, ' Further tets on a reinforced concrete floor designed by limit procedures. , ' *ACI STRUCTURAL JOURNAL*, no. SP-30, pp. 251-69.

Park, R. & Gamble, W.L. 1980, *Reinforced concrete slabs*, John Wiley & Sons, New York, USA.

Parvez, A. & Foster, S.J. 2014, 'Fatigue behavior of steel-fiber-reinforced concrete beams', *Journal of Structural Engineering (United States)*, vol. 141, no. 4.

Peel–Cross, R.J., Rankin, G.I.B., Gilbert , S.G. & Long , A.E. 2001, ' Compressive membrane Action in composite floor slabs in the Cardington LBTf , ' *Proceedings of the Instruction of Civil Engineers* vol. Structures and Buildings Journal 146, no. 2, pp. 217-26.

Perdikaris, P.C. & Beim, S. 1986, 'Fatigue strength of R/C bridge decks', paper presented to the *Physical Models in Engineering Education and Practice*, Baltimore, Md.

Perdikaris, P.C. & Beim, S. 1988, 'RC bridge decks under pulsating and moving load', *ASCE, Journal of structural engineering*, vol. 114, no. 3, pp. 591-607.

Perdikaris, P.C., Beim, S. & Bousias, S.N. 1989, 'Slab continuity effect on ultimate and fatigue strength of reinforced concrete bridge decks', *ACI Structural Journal*, vol. 86, no. 4, pp. 483-91.

Pimentel, M., Costa, P., Félix, C. & Figueiras, J. 2009, 'Behavior of reinforced concrete box culverts under high embankments', *Journal of Structural Engineering*, vol. 135, no. 4, pp. 366-75.

Powell, D.S. 1956, 'The ultimate strength of concrete panels subjected to uniformly distributed loads', Cambridge University.

Rankin, G.I.B. 1982, 'Punching failure and compressive membrane action in reinforced concrete slabs', Queen`s University of Belfast

Rankin , G.I.B. & Long , A.E. 1987, 'Predicting punching strength of conventional slab column specimens', *ICE Proceedings*, vol. Structures and Building, no. No 82, pp. 327-46.

Rankin, G.I.B. & Long, A.E. 1987, 'Predicting the enhanced punching strength of interior slab-column connection', *ICE Proceeding*, vol. Structures and Buildings, no. No. 82,, pp. 1165- 86.

Rankin, G.I.B. & Long, A.E. 1997, 'Arching action strength enhancement in laterally-restrained slab strips', *Proceedings of the Institution of Civil Engineers, Structs & Bldgs* vol. 122, no. 4, pp. 461-7.

Rankin, G.I.B., Niblock, R.A., Skates, A.S. & Long, A.E. 1991, 'Compressive membrane action strength enhancement in uniformly loaded, laterally restrained slabs', *The structural Engineer*, vol. 69, no. 16.

Rankine, W. 1857, 'On the stability of loose earth', *Philosophical Transactions of the Royal Society of London, Vol. 147.*, vol. 147.

Regan, P.E. 1975, 'Catenary action in damaged concrete structures', *American Society of Mechanical Engineers (Paper)*, pp. 191-226.

Rots, J.G. & Blaauwendraad, J. 1989, 'Crack models for concrete: discrete or smeared? Fixed multi-directional or rotating?', *Heron*, vol. 34, no. 1, pp. 3-59.

Rowe, M. & Bradford, M.A. 2013, 'Partial shear interaction in deconstructable composite steel-concrete composite beams with bolted shear connectors', paper presented to the *International Conference on Design, Fabrication and Economy of Welded Structures*, Miskolc, Hungary.

Ruddle, M.E., Rankin, G.I.B. & Long, A.E. 2002, 'Arching action—flexural and shear strength enhancements in rectangular and Tee beams', *Proceedings of the Institution of Civil Engineers, Structures and Buildings*, vol. 156, pp. 63-74.

Ryua, H.K., Changa, S.P., Kimb, Y.J. & Kimb, B.S. 2005, 'Crack control of a steel and concrete composite plate girder with prefabricated slabs under hogging moments', *Engineering Structures* vol. 27, pp. 1613–24.

Salim, W. & Sebastian, W.M. 2003, 'Punching shear failure in reinforced concrete slabs with compressive membrane action', *ACI Structural Journal*, vol. 100, no. 4, pp. 471-9.

Sanjayan, J.G., Nazari, A. & Pouraliakbar, H. 2015, 'FEA modelling of fracture toughness of steel fibre-reinforced geopolymer composites', *Materials & Design*, vol. 76, pp. 215-22.

Sargant, D.D., Mufti, A.A. & Bakht, B. 1999, ' Design, construction and field testing of steel-free arch panel bridge deck for forestry bridges. Proceedings, ' *Annual Conference, General Conference, Structural Engineering,*

, vol. 1, Canadian Society for Civil Engineering pp. . 95-104.

Sasani, M. & Kropelnicki, J. 2008, 'Progressive collapse analysis of an RC structure', *Structural Design of Tall and Special Buildings*, vol. 17, no. 4, pp. 757-71.

Sawczuk, A. 1965, 'Membrane action in flexure of rectangular plates with restrained edges. Flexural mechanics of reinforced concrete', *ACI/ASCE, SP. 12*, pp. 347-58.

Sawczuk, A. & Winnicki, L. 1965, 'Plastic behaviour of simply supported plates at moderately large deflections', *International Journal of Solids and Structures*, vol. 1, no. 1, pp. 97-111.

Schlafli, M. & Bruhwiler, E. 1998, 'Fatigue of existing reinforced concrete bridge deck slabs', *Engineering Structures*, vol. 20, no. 11, pp. 991-8.

Schumacher, P., Uijl, J.D., Walraven, J.C. & Bigaj-Van Vliet, A.J. 2004, 'Bond of reinforcing bars in steel fiber reinforced concrete', *5th International PhD Symposium in Civil Engineering - Proceedings of the 5th International PhD Symposium in Civil Engineering*, vol. 2, pp. 1205-12.

Selvadurai, A. & Bakht, B. 1995, 'Simulation of rolling wheel loads on an FRC deck,

' paper presented to the *University and Industry workshop in FRC*, Toronto , Canada

Shah, B.N., Sennah, K., Kianoush, M.R., Tu, S. & Lam, C. 2007, 'Experimental study on prefabricated concrete bridge girder-to-girder intermittent bolted connections system', *JOURNAL OF BRIDGE ENGINEERING*, vol. 12, no. 5, pp. 570-84.

Shim, C., Ryua, H.K., Chung, C., Youn, S. & Changa, S.P. 2006, 'Inelastic behavoiur of a continuous composite box-girder bridge with prefabricated slabs', paper presented to the *Composite Construction in Steel and Concrete*.

Shim, C.S. & Chang, S.P. 2003, 'Cracking of continuous composite beams with precast decks', *Journal of Constructional Steel Research*, vol. 59, pp. 201-14.

Shim, C.S., Lee, P.G. & Chang, S.P. 2001, 'Design of shear connection in composite steel and concrete bridges with precast decks', *Journal of Constructional Steel Research*, vol. 57, pp. 203–19.

Smeltzer, P. & Bentz, E. 2005, 'Research suggests conservative design of concrete box culverts', paper presented to the *First Canadain Conference on Effective Design of Structures: Transferring Research into Practice*, Canada, 2005.

Spadea, G., Swamy, R.N. & Bencardino, F. 2001, 'Strength and ductility of RC beams repaired with bonded CFRP laminates', *Journal of Bridge Engineering*, vol. 6, no. 5, pp. 349-55.

Standard, B. 1978, 'Steel, concrete and composite bridges: Specification for loads

', British Standard BS5400, London, United Kingdam.

Su, H., Xu, J. & Ren, W. 2014, 'Mechanical properties of ceramic fiber-reinforced concrete under quasi-static and dynamic compression', *Materials & Design*, vol. 57, pp. 426-34.

Su, Y., Tian, Y. & Song, X. 2009, 'Progressive collapse resistance of axially-restrained frame beams', *ACI Structural Journal*, vol. 106, no. 5, pp. 600-7.

Suthiwarapirak, P. & Matsumoto, T. 2006, 'Fatigue analysis of RC slabs and repaired RC slabs based on crack bridging degradation concept', *Journal of Structural Engineering*, vol. 132, no. 6, pp. 939-48.

Tadros, G., Tromposch, E. & Mufti, A.A. 1998, 'Superstructure replacement of the crowchild Trail bridge., ' *Development in Short and Medium Span Bridge Engineering, Advanced Materials in Bridges*, Calgary, Alberta, Canada, pp. CD-Proceedings.

Tadros, M.K., Benak, J.V. & Gilliland, M.K. 1989, 'Soil pressure on box culverts', *ACI Structural Journal*, vol. 86, no. 4, pp. 439-50.

Tahmasebinia, F., Ranzi, G. & Zona, A. 2012, 'Beam tests of composite steel-concrete members: A three-dimensional finite element model', *International Journal of Steel Structures* vol. 12, no. 1, pp. 37-45.

Tahmasebinia, F., Ranzi, G. & Zona, A. 2013, 'Probabilistic three-dimensional finite element study on composite beams with steel trapezoidal decking', *Journal of Constructional Steel Research*, vol. 80, no. January, pp. 394-411.

Taylor 2000, ' Compressive Membrane Action in High strength Concrete Bridge Deck Slabs', Queen’s University of Belfast.

Taylor S.E, R.G.I.a.C.D.J. 2003, 'Real strength of high-performance concrete bridge deck slabs ·', *ACI Structural Journal*, vol. Bridge Engineering 156 no. ssue BE2, pp. 81-90.

Taylor, S.E. & Mullin, B. 2006, 'Arching action in FRP reinforced concrete slabs', *Construction and Building Materials*, vol. 20, no. 1-2, pp. 71-80.

Taylor, S.E., Rankin, B., Cleland, D.J. & Kirkpatrick, J. 2007, 'Serviceability of bridge deck slabs with arching action', *ACI Structural Journal*, vol. 104, no. 1, pp. 39-48.

Taylor, S.E., Rankin, G.I.B. & Cleland, D.J. 2001, 'Arching action in high-strength concrete slabs', *Proceedings of the Institution of Civil Engineers: Structures and Buildings*, vol. 146, no. 4, pp. 353-62.

Taylor, S.E., Rankin, G.I.B. & Cleland, D.J. 2002, *A guide to compressive membrane action in concrete bridge decks*, Technical Paper, Queen's University of Belfast, UK

Taylor, S.E., Rankin, G.I.B. & Cleland, D.J. 2005, 'Arching action in concrete bridge deck slabs for increased durability and sustainability', pp. 306-13.

Tingley, D.D. & Davison, J.B. 2012,. 'Developing an LCA methodology to account for the environmental benefits of design for deconstruction'. *Building and Environment*, vol. 57, pp. 387-395. DOI: 10.1016/j.buildenv.2012.06.005.

Thorburn, J. & Mufti, A.A. 1995, 'Full-scale testing of externally reinforced FRC bridge deck on steel girders', paper presented to the *Annual Conference for the Canadian Society of Civil Engineers*, Canada, June 1995.

Thorburn, J. & Mufti, A.A. 2001, 'Design recommendations for externally restrained highway bridge decks', *JOURNAL OF BRIDGE ENGINEERING*, vol. 6, no. 4, pp. 243-9.

Tong, P.Y. 1971, 'Compressive membrane enhancement in two-way bridge slabs', *Special Publication*, vol. 30.

Transportation Officials 1977, 'Standard specifications for highway bridges', American Assn. of State Highway and Transportation Officials, Washington,DC.

Trapko, T. 2014, 'Behaviour of fibre reinforced cementitious matrix strengthened concrete columns under eccentric compression loading', *Materials & Design*, vol. 54, pp. 947-54.

Tsui, C.K., Burns, N. H., and Klingner, R. E. 1986, *Behavior of Ontario-type bridge deck on steel girders: Negative moment region and load capacity*, Center for Transportation Research, University of Texas at Austin, Austin, Texas.

Valipour, H., Farhangvesali, N. & Foster, S. 2013, 'A generic model for investigation of arching action in reinforced concrete members', *Construction and Building Materials*, vol. 38, pp. 742-50.

Valipour, H., Rajabi, A., Foster, S. & Bradford, M.A. 2015, 'Arching behaviour of precast concrete slabs in a deconstructable composite bridge deck', *Construction and Building Materials (Accepted April 2015)*.

Van Erp, G.M. 2001, 'Robustness of fibre composite structures loaded in flexure', *Proceeding of international conference on FRP composites in civil engineering (CICE)*, vol. 2, Hong Kong, China, pp. 1421-6.

Vaslestad, J., Johansen, T.H. & Holm, W. 1993, *Load reduction on rigid culverts beneath high fills: long-term behavior*.

Wang, H. & Belarbi, A. 2011, 'Ductility characteristics of fiber-reinforced-concrete beams reinforced with FRP rebars', *Construction and Building Materials*, vol. 25, no. 5, pp. 2391-401.

Wegner, L.D. & Mufti, A.A. 1994, 'Finite element investigation of fibre-reinforced concrete deck slabs without internal steel reinforcement', *Canadian Journal of Civil Engineering*, vol. 21 no. 2, pp. 231-6.

Welch, R.W., Hall, W.J. & Gamble, W.L. 2008, 'Specializing Park's compressive membrane theory', *Journal of Structural Engineering*, vol. 134, no. 5, pp. 854-8.

Westergaard, H.M. & Slater, W.A. 1921, 'Moments and stresses in slabs', *J. Am. Conc. Inst.*, vol. 17, pp. 415-538.

Wood, R.H. 1961, *Plastic and elastic design of slabs and plates*, Thames and Hudson, London.

Woodson, S.C. 1985, *Effects of shear stirrup details on ultimate capacity and tensile membrane behavior of reinforced concrete slabs*, SL-85-4, U.S. Army Engineer Waterways Experiment Station, Vicksburg, MS.

Woodson, S.C. & Garner, S.B. 1985, *Effects of reinforcement configuration on reserve capacity of concrete slabs*, SL-85-5, U.S. Army Engineer Waterways Experiment Station, Vicksburg, MS.

Wu, Z., Wang, X. & Wu, G. 2012, 'Advancement of structural safety and sustainability with basalt fiber reinforced polymers ', *FRP Composites in Civil Engineering (CICE) 6th Int.*, International Institute for FRP in Construction, Kingston, ON, Canada.

Xu, Z., Hao, H. & Li, H.N. 2012, 'Dynamic tensile behaviour of fibre reinforced concrete with spiral fibres', *Materials & Design*, vol. 42, pp. 72-88.

Yang, M.Z. 2000, 'Evaluation of factors affecting earth pressures on buried box culverts', University of Tennessee, Knoxville, University of Tennessee, Knoxville, Tenn.

Yap, S.P., Bu, C.H., Alengaram, U.J., Mo, K.H. & Jumaat, M.Z. 2014, 'Flexural toughness characteristics of steel–polypropylene hybrid fibre-reinforced oil palm shell concrete', *Materials & Design*, vol. 57, pp. 652-9.

Yeau, K.Y. & Sezen, H. 2012, 'load-rating procedures and performance evaluation of metal culverts', *ASCE, Journal of Bridge Engineering*, vol. 17, no. 1, pp. 71-80.

Yee, R.A., Bentz, E.C. & Collins, M.P. 2004, *Shear behaviour of concrete box culverts: A preliminary study*, Department of Civil Engineering, University of Toronto, Toronto,Canada.

Yi, W.J., He, Q.F., Xiao, Y. & Kunnath, S.K. 2008, 'Experimental study on progressive collapse-resistant behavior of reinforced concrete frame structures', *ACI Structural Journal*, vol. 105, no. 4, pp. 433-9.

Yu, J. & Tan, K.H. 2013a, 'Experimental and numerical investigation on progressive collapse resistance of reinforced concrete beam column sub-assemblages', *Engineering Structures*, vol. 55, no. 0, pp. 90-106.

Yu, J. & Tan, K.H. 2013b, 'Structural behavior of RC beam-column subassemblages under a middle column removal scenario', *ASCE, Journal of structural engineering*, vol. 139, no. 2, pp. 233-50.

Yu, J. & Tan, K.H. 2014, 'Analytical model for the capacity of compressive arch action of reinforced concrete sub-assemblages', *Magazine of Concrete Research*, vol. 66, no. 3, pp. 109-26.

Yu Zheng, S.T., Des Robinson, David Cleland 2010, 'Investigation of Ultimate Strength of Deck Slabs in Steel Concrete Bridges', *ACI Structural Journal*, Technical Paper, vol. 107, no S09, pp. 82-90.

Zanuy, C., Maya, L.F., Albajar, L. & De la Fuente, P. 2011, 'Transverse fatigue behaviour of lightly reinforced concrete bridge decks', *Engineering Structures* vol. 33, pp. 2839–49.

Zheng, Y., Fu, X., Lu, Z. & Pan, Y. 2013, 'Investigation of structural behaviour of GFRP reinforced concrete deck slabs through NLFEA', *Construction and Building Materials*, vol. 45, pp. 60-77.

Zheng, Y., Li, C. & Yu, G. 2012, 'Investigation of structural behaviours of laterally restrained GFRP reinforced concrete slabs', *J. Comp. Part B*, vol. 43, p. 1586.

Zheng, Y., Robinson, D., Taylor, S., Cleland, D. & Shaat, A. 2008, 'Analysis of compressive membrane action in concrete slabs', *Proceedings of the Institution of Civil Engineers: Bridge Engineering*, vol. 161, no. 1, pp. 21-31.

Zheng, Y., Taylor, S., Robinson, D. & Cleland, D. 2010, 'Investigation of ultimate strength of deck slabs in steel concrete bridges', *ACI Structural Journal*, Technical Paper, vol. 107, no S09, pp. 82-90.

Zheng, Y., Yu, G. & Pan, Y. 2012, 'Investigation of ultimate strengths of concrete bridge deck slabs reinforced with GFRP bars', *Construction and Building Materials*, vol. 28, no. 1, pp. 482-92.